AGRICULTURAL WATER SECURITY THROUGH SUSTAINABLE USE OF THE FLORIDAN AQUIFER: AN INTEGRATED STUDY OF WATER QUANTITY AND WATER QUALITY IMPACTS

By

SAGARIKA RATH

A DISSERTATION PRESENTED TO THE GRADUATE SCHOOL
OF THE UNIVERSITY OF FLORIDA IN PARTIAL FULFILLMENT
OF THE REQUIREMENTS FOR THE DEGREE OF
DOCTOR OF PHILOSOPHY

UNIVERSITY OF FLORIDA

2021

To my parents

ACKNOWLEDGMENTS

I thank my entire family for encouraging me to always put my best foot forward and for instilling in me the desire to get an advanced education. I am grateful to my Baba and Nana for teaching me to read and strive for greatness. I thank my husband Sibabrata Mohanty for keeping me encouraged and supporting me through this process. I thank my advisor Wendy Graham for her helpful guidance every step of the way developing this research and for her critical evaluations of my scientific methods and arguments. She always was willing to give me a piece of her valuable time to keep me on track and moving forward. I thank my co-advisor David Kaplan for giving me perspective on how to effectively write and analyze data to make clear arguments. I am also grateful to the faculty members who served on my committee Kenneth Boote, Michael Dukes, and Michael Annable for giving me the opportunity to learn about the research topic in depth. I am thankful to Rob DeRooij, who assisted me in numerical methods, model development and was a willing mentor throughout the process. I would like to thank my Water Institute Graduate Fellow Faculty and Student Cohort for giving me a new interdisciplinary lens through which the relevance of my work was made clear. I am very thankful to my very dear friends Patricia Spellman and Maria Zamora for their constant support throughout this journey. Finally, I want to thank the staff of the Water Institute for providing research support and always being willing to address administrative tasks so I could focus on my research.

TABLE OF CONTENTS

LIST OF TABLES

LIST OF FIGURES

Abstract of Dissertation Presented to the Graduate School
of the University of Florida in Partial Fulfillment of the
Requirements for the Degree of Doctor of Philosophy

AGRICULTURAL WATER SECURITY THROUGH SUSTAINABLE USE OF THE FLORIDAN AQUIFER: AN INTEGRATED STUDY OF WATER QUANTITY AND WATER QUALITY IMPACTS

By

Sagarika Rath

August 2021

Chair: Wendy Graham
Cochair: David Kaplan
Major: Agricultural and Biological Engineering

The Upper Floridan Aquifer (UFA) is a primary source of potable water supply for the state of Florida. The Santa Fe River Basin (SFRB), located in north central Florida, relies exclusively on the UFA for irrigation and public water supply. The unconfined portion of the SFRB is vulnerable to contamination from agricultural activities and, as a result, the Nitrate-Nitrogen (NO_3-N) concentration in springs discharging from the aquifer have increased substantially from background concentrations of <0.1 mg/L to 5 mg/L over the past 40-50 years. Most springs in the SFRB violate the State of Florida Numeric Nutrient Criteria (NNC) of 0.35 mg/L.

This research leveraged available experimental and observational data in the SFRB to develop field-scale and watershed scale hydrologic models to quantify the nitrate leaching reductions that can be expected from the adoption of improved agricultural nutrient and irrigation management practices in the SFRB, and to estimate the impact of these leaching reductions on nitrate concentrations in the Santa Fe River. Results showed that leaching from existing agricultural land uses in SFRB such as

grazed pasture, row crops, forests and hay currently contribute approximately 55%, 22%, 10% and 8% of the total NO_3-N stream load, respectively. Results also showed that adoption of agricultural best management practices that are considered economically feasible with currently available technology throughout the watershed has the potential to reduce total NO_3-N load to the Santa Fe River by approximately 31%.

However, model results suggest that these reductions are not adequate to meet the NO_3-N NNC established to protect springs and rivers in the basin if current land use patterns are maintained. Simulations indicated that if in the year 2020 current row crop and hay land uses were converted from conventional to best management practices, and all pasture was converted to native grassland, the NNC could be met by 2080. If all row crops, hay and pasture were converted to forest in 2020, simulations indicated the NNC could be met in 2055.

Results of this study should be useful for incorporation into investigations economic-environmental tradeoffs of changes in land use and land management practices in the Santa Fe River Basin. Ultimately these studies should provide a framework for developing effective, socially acceptable strategies for achieving stringent water quality regulations while maintaining a robust agricultural economy that is transferrable to other agricultural watersheds throughout the world.

CHAPTER 1
INTRODUCTION

Providing adequate clean water to future generations from finite water resources is a driving factor for research and development work on sustainable watershed management practices (Environmental Protection Agency (EPA), 2012). The rising demand for clean water, food and energy encourages increased application of fertilizers (Akhavan et al., 2010), development of various best management practices for different land uses (Srinivasan et al., 2010; Gao et al., 2017), and changes in land uses (Scanlon et al., 2007; Dosdogru et al., 2020) which pose substantial threats to the surface and groundwater resources (Scanlon et al., 2007). Improved watershed management is imperative to protect water resources and aquatic flora and fauna. Many watershed studies have emphasized water quantity rather than quality, although water quality is closely coupled to water quantity and cannot be overlooked in sustainable water resource management planning. Holistic study of the water system along with all factors affecting its long-term availability is of utmost importance for watershed management (Zhang et al., 2016; Trang et al., 2017). Water quality can be directly affected through several mechanisms such as contaminants transported from land into the water bodies through surface runoff and groundwater leaching (Arheimer et al., 2005).

Among many factors affecting the sustainable use of groundwater resources, non-point source (NPS) pollutants are an important component due to the large spatial extent of these sources and their long-term impact on the deterioration of groundwater quality (Takamatsu et al., 2014). The most common NPS pollutants such as synthetic nitrogen fertilizer, organic manure and sewage sludge have been of widespread concern due to the challenges associated with their quantification and remediation.

Moreover, because NPS pollutants such as Nitrate-Nitrogen (NO_3-N) are spread over large areas in relatively low concentrations, their detrimental environmental and health related effects are chronic rather than acute (Mitsch et al., 1999; Bowen et al., 2007; De la Monte et al., 2009), and the task of cleanup is difficult to accomplish (Loague et al., 1998). Karst aquifers are highly susceptible to NO_3-N loading from various sources because of rapid water infiltration through the epikarst or sinkholes which often provide direct connections between the surface and aquifer (Peterson et al., 2002; Ravbar and Goldscheider, 2009).The adverse effect of elevated NO_3-N in aquifer connected ecosystems such as springs, rivers, lakes, and estuaries prompted regulators such as Florida Department of Environmental Protection (FDEP) to establish limits of allowable Total Maximum Daily Loads (TMDL) of NO_3-N to surface waters and maximum allowable NO_3-N concentrations in groundwater and surface waters. This research aims to utilize a combination of field-scale and watershed scale hydrologic models, with available experimental and observational data, to quantity the NO_3-N leaching reductions as well as groundwater, spring and river NO_3-N concentration reductions that can be expected from widespread adoption of improved agricultural nutrient and irrigation management practices in karst watersheds overlying the Upper Floridan Aquifer.

Floridan Aquifer System

The Floridan Aquifer System (FAS), located in the southeast United States and extending over 260,000 km^2, is one of the most productive aquifer systems in the USA (Van Beynen et al., 2012; Maupin et al., 2014). It is the major source of public water supply and irrigation in north and central Florida (Bush and Johnson, 1988), supporting a productive agricultural economy and supplying more than 10 million people with

drinking water (Marella, 2014). The FAS is a karst system, and thus presents unique challenges to land use planners because of inherent vulnerabilities to contamination through direct connections between the aquifer and the surface.

The Upper Floridan Aquifer (UFA) in north Florida is mainly comprised of Ocala Limestone, ranges in thickness from 0 to 54 meter, and is underlain by a lower permeable limestone called the Avon Park Formation that is 243-335 meter thick (Figure 1-1). Where the Ocala Limestone is not exposed at the surface, it is covered by the Hawthorn Formation and a surficial aquifer of Plio-Pleistocene sands (Scott et al., 2004). Spatially variable erosion of the Hawthorn Formation has led to variations in UFA confinement throughout North Florida. The erosional boundary of the Hawthorn Formation is known as the Cody Escarpment, and defines a critical boundary for defining FAS vulnerability to contamination. Downgradient from the Cody Escarpment limestone is exposed and vulnerability is increased by enhanced surface-to-aquifer connectivity. The geologically unique Santa Fe River Basin (SFRB) (Figure 1-1), situated overlying the FAS, provides an excellent study area for this research. The SFRB is a well instrumented basin with various state and federal government agencies collecting hydrologic and water quality data at daily to monthly temporal scales, and it has been the focus of numerous field scale studies. Thus, there is a wealth of information available which can be used to develop and validate integrated hydrologic-water quality models.

Santa Fe River Basin

Over the past several decades, with the intensification of agricultural activities, population growth, socioeconomic development, and climate change ecological and environment problems associated with the SFRB water quality have escalated (Santa

Fe River Basin, Basin Management action Plan, 2012). Previous studies have shown the increase of NO_3-N in some springs in the region from background concentrations (≤0.1 mg/L NO_3-N) to above 5 mg/L NO_3-N over the last 40 years (Katz et al., 1999; Katz, 2004). These springs violate the State of Florida Numeric Nutrient Criteria (NNC) of 0.35 mg/L NO_3-N. Increasing NO_3-N concentrations have been found in several springs within the SFRB in Florida (e.g., Devil's Complex springs, Hornsby, Ichetuknee, Ginnie springs with >0.35 mg/L NO_3-N) (Upchurch et al., 2007; FDEP, 2018; Santa Fe River and Springs Environmental Analysis, 2020).

Potential nutrient sources in the Santa Fe River Basin are diverse and include various point and nonpoint sources like agricultural lands, wastewater spray fields, areas with dense concentrations of septic tanks, and storm-water runoff to sinkholes (FDEP, 2012). However, agricultural activities like cropland farming, fertilization and animal farming have contributed large quantities of nitrogen to groundwater in the Santa Fe River Basin in northern Florida (Katz et al., 1999). Studies in the SFRB area report evidence that most NO_3-N pollution found in the lower basin comes from fertilizer sources (Katz et al., 2009).

Assessment of the pollutant load from non-point sources such as agriculture lands to water systems is a challenge compared to the contributions from point sources like industries and wastewater treatment plants due to the difficulty of accurate estimation of NO_3-N leaching from spatially variable soils, land uses and nutrient and water management practices (Eller et al., 2017).

In response to the increasing NO_3-N concentrations and spring ecosystem degradation, the Florida Department of Environmental Protection (FDEP) set a Numeric

Nutrient Criteria (NNC) of 0.35 mg/L NO_3-N, as an annual geometric mean, for water emanating from UFA springs (62-302.530 (47) (b), F.A.C.; FDEP, 2013). Total Maximum Daily Loads (TMDLs; US Environmental Protection Agency, 2016) estimated to achieve the NNC, and Basin Management Action Plans (BMAPs) required to meet the TMDL, have been established for UFA springs not meeting the NNC. BMAPs specify a suite of projects/actions that are collectively intended to achieve the TMDL. For agricultural operations, adoption of Best Management Practices (BMPs) is required in spring BMAP areas. In Florida BMPs are defined as technically and economically feasible research-based practices developed to conserve water supply, as well as to maintain or improve surface and groundwater quality by reducing or treating pollutant discharges entering water resources (FDACS, 2015).

Nitrogen Research Needs

BMAPs for the SFRB estimate that synthetic fertilizer is the largest source of NO_3-N load to springs and specify that NO_3-N load reductions of approximately 65% (FDEP, 2018) are required to meet the NNC. A quantitative assessment of the effects of alternative water and nutrient management practices on crop yield, irrigation water requirements and NO_3-N leaching in the SFRB is needed to determine whether adoption of agricultural BMPs can achieve the reduction in loads mandated to achieve the NNC. This dissertation utilizes a combination of field-scale and watershed scale hydrologic models to 1) leverage the available experimental and observational data in the SFRB to quantity the nitrate leaching reductions that can be expected from the adoption of improved agricultural nutrient and irrigation management practices in the SFRB; 2) estimate the impact of these leaching reductions on nitrate concentrations in the Santa Fe River; and 3) determine the most vulnerable regions of the SFRB where

changes in practices could be targeted, and estimate the lag times required to observe reductions in river NO_3-N concentrations as a result of potential changes in practices in these vulnerable regions.

Organization of the Dissertation

This research is focused on the evaluation of NO_3-N load from different land uses and different water and fertilizer management practices across different soil types over long term weather conditions in the SFRB. The challenges associated with predicting spatial and temporal variation in hydrology and NO3-N fate and transport are investigated through experimental data and hydrological modeling efforts. Chapter 2: "*Quantifying nitrate leaching to groundwater from a corn-peanut rotation under a variety of irrigation and nutrient management practices in the Suwannee River Basin, Florida"* includes a detailed SWAT modeling study of the field-scale NO_3-N leaching, nitrogen (N) uptake, soil NO_3-N storage and yield from a corn-peanut rotation using data from a three-year irrigation and N fertilizer rate management experiment conducted in Live Oak, Florida (Zamora Re et al., 2018). In addition, the effect of planting a cover crop in between corn-peanut growing seasons on crop yield and NO_3-N leaching was simulated as an additional management practice to investigate further reduction in leaching during the fallow period. This work provides a framework for developing effective strategies for achieving stringent water quality regulations while maintaining a robust agricultural economy that is transferrable to other agricultural watersheds throughout the world.

Chapter 3: "*Impact of land use and land management practices on nitrate loading to groundwater in Santa Fe River Basin (SFRB)"* develops a watershed scale SWAT model to quantify the water and nitrogen budgets for current land uses and water and nutrient practices throughout the SFRB; predict the spatiotemporal pattern of water flux,

NO_3-N loading, transport and transformation from the root zone, through the aquifer, to the Santa Fe River for different management practices; and evaluate the potential for alternative land use and water and nutrient management practices to achieve the 65% reduction in NO_3-N load estimated to be required to achieve the NNC in streams in the SFRB.

Chapter 4: *"Estimation of groundwater contributing area and travel time to springs in Santa Fe River Basin"* analyzes hydrogeologic factors affecting the contributing area and travel time distribution for groundwater emerging in the Santa Fe River near Ft. White. Recharge from the watershed SWAT model was used to drive the North Florida-Southeast Georgia (NFSEG) MODFLOW model. The resulting groundwater fluxes were used in MODPATH to perform a backward particle tracking to estimate the groundwater travel time distribution and groundwater contributing area for for the reach of the Santa Fe River containing the Devil's complex springshed. Travel time based particle transport simulations were carried out to estimate the fate and transport of NO_3-N from the groundwater contributing area to the Santa Fe River to investigate alternative scenarios for meeting the numeric nutrient criteria (NNC) using land-use and management system specific nitrate loadings from the watershed SWAT model.

Chapter 5 summarizes the key findings of Chapters 2 through 4, discusses implications of key findings, and makes recommendations for continued efforts to improve watershed-scale prediction of sources, fate, and transport of nitrate in agricultural watersheds for alternative land use and management practices.

CHAPTER 2
QUANTIFYING NITRATE LEACHING TO GROUNDWATER FROM A CORN-PEANUT ROTATION UNDER A VARIETY OF IRRIGATION AND NUTRIENT MANAGEMENT PRACTICES IN THE SUWANNEE RIVER BASIN, FLORIDA

Background

Agricultural intensification and extensification to meet the food demand of a growing global population has led to elevated groundwater pumping and nitrogen (N) fertilizer usage worldwide (Spalding and Exner, 1993; Vitousek et al., 1997). Synthetic and animal waste-based N fertilizers are used in most agricultural operations to enhance plant growth (Motavalli et al., 2008), but excessive application may increase the risk of nitrate loading to groundwater (Singh et al., 1995; Nolan et al., 1996; Erisman et al.,2008). The adverse effects of elevated nitrate concentrations on human health (De la Monte et al., 2009) and the environment (Mitsch et al., 1999; Bowen et al., 2007) have prompted regulators to establish limits of allowable nitrate concentration in groundwater and surface water. Meeting these criteria can be challenging since they often require widespread changes in water and nutrient management practices and the effects of these changes can take decades to manifest in receiving waters (Vero et al., 2017; Van Meter et al., 2018). Local assessment and modeling of management practice changes that provide for agricultural sustainability while maintaining groundwater quality are thus necessary to develop informed and effective watershed management strategies.

Connectivity between agricultural lands and the underlying aquifer plays a significant role in the mass of nitrate leaching to groundwater (Kellman and Marcel , 2003). Important factors include soil drainage characteristics, depth to water table, crop type and mass of N in applied fertilizer. Nitrate concentrations are typically higher under

agricultural fields with well-drained soils overlying highly permeable aquifers (Nolan 2001). For example, high concentrations of nitrate are often found in karst aquifers, where discrete fractures and conduits can rapidly transmit large volumes of nitrate-enriched water with little attenuation (Vesper et al., 2001; Doerfliger et al., 1999). The vulnerability of karst aquifers to nutrients from agriculture has been well-documented (Boyer and Pasquerall, 1995; Boyer et al., 1996; Panno et al., 2001; Peterson et al., 2002). However, effective management strategies to minimize the nitrate loading to karst aquifers must be developed considering local economies and hydrogeologic settings (Coxon, 2011). Development and application of robust models to support decision-making is especially important in karstic regions, where wide variation in travel times can cause lags of years to decades between practice implementation and surface water quality improvement (Meals et al., 2010; Amin et al., 2017; Fenton et al., 2017).

The karstic Upper Floridan aquifer (UFA) is one of the most productive aquifers in the world. It is the major source of public water supply and irrigation in north and central Florida (Bush and Johnson, 1988), supporting a productive agricultural economy and supplying more than 10 million people with drinking water. Large portions of the UFA are characterized by unconfined, hydraulically connected carbonate rocks with high permeability and transmissivities, which allow nutrients to leach into the aquifer and quickly travel long distances (Bush and Johnson, 1988; Arthur et al., 2007). Agriculture and silviculture are the predominant land uses in the Suwanee River Basin (SRB) that overlies the UFA in north Florida. Increases in population and changes in land use across Florida have shifted the SRB toward more intensive agriculture practices such as row crops, cow-calf operations, dairy and poultry farms (FDEP, 2012), which has

resulted in increased nitrate-nitrogen (NO_3-N) concentrations in the UFA (FDACS 2015a; Harrington et al., 2010; Hochmuth et al., 2014). The region also has a high density of large freshwater springs, supplied with water from the UFA. Nitrate-N concentrations in UFA springs have increased over the last 40 years from background concentrations of ≤0.1 mg/L NO_3-N to above 5 mg/L NO_3-N in some springs (Katz et al., 1999; Katz, 2004).

In response to increasing NO_3-N concentrations and spring ecosystem degradation, a Numeric Nutrient Criteria (NNC) of 0.35 mg/L NO_3-N was set for water emanating from UFA springs (62-302.530 (47) (b), F.A.C.; FDEP, 2013). Total Maximum Daily Loads (TMDLs; US Environmental Protection Agency, 2016) required to achieve the NNC were then estimated, and Basin Management Action Plans (BMAPs) required to meet the TMDL have been established for UFA springs not meeting the NNC. Current BMAPs for the SRB estimate that synthetic fertilizer is the largest NO_3-N source to springs and specify load reductions ranging from 35% (FDEP, 2012) to 88% (FDEP, 2018) to meet the NNC. In this regulatory setting, a quantitative assessment of the effects of alternative water and nutrient management practices on crop yield, irrigation water requirements, and NO_3-N leaching is needed to determine whether adoption of agricultural BMPs can achieve the load reductions mandated to achieve the NNC. Critically, NNC have been partially or fully developed for 29 US states and territories (EPA, n.d.) and are widely adopted across Europe as part of the European Water Framework Directive (Poikane et al., 2019). Across regions, developing effective nutrient mitigation approaches to meet these environmental standards while also

meeting human food demand is a grand global challenge (Robertson et al., 2005; Davidson et al., 2015) with agricultural water management at its core.

Agricultural BMPs have been widely proposed to reduce adverse water quality impacts both globally (Liu et al., 2017) and in the SRB (FDEP, 2012). However, determining the effectiveness of these practices for reducing N leaching and meeting regional water quality goals is an on-going challenge due to difficulties in quantifying nutrient fate and transport processes (Chaubey et.al, 2010). For instance, measuring N fertilizer transformations and losses (e.g., leaching, volatilization, and denitrification) is expensive, time-consuming, and difficult due to variability in weather, soil properties and agricultural management practices across fields (Mulla et.al., 2004). Given these challenges, computer simulation models are commonly used to leverage field observations and improve estimates of the fate and transport of water and nutrients (Xie et al., 2015). However, data-intensive model calibration and validation for the specific soil, climate and agricultural management conditions being modeled must be performed for models to be effective (Ramos and Carbonell, 1991) and trusted by stakeholders (Karki et al., 2020).

This work leverages a uniquely robust experimental dataset (Zamora et al., 2018, 2020) to provide quantitative estimates of long-term changes in crop yield, water use, and NO_3-N leaching under alternate management scenarios. This effort is part of longer-term project that is bringing together scientists, regulators, agricultural producers, and non-governmental organizations to collaboratively evaluate tradeoffs among crop production, water quality, and water quantity associated with alternative land use and land and water management strategies. The coupled SWAT-MODFLOW model (Aliyari

et al., 2019; Wei et al., 2019) was selected as the platform for this analysis because complex surface-groundwater interactions in the karst watershed require explicit modeling of the groundwater system and its interaction with surface waters, which are not rigorously represented in typical agricultural watershed models such as SWAT (Arabi et al., 2008; Bieger et al., 2014; Cerro et al., 2014; Gassman et al., 2014; Francesconi et al., 2016), AGNPS (Young et al., 1989) or EPIC (Williams, 1989). Thus, the immediate goal of this study was to assess whether SWAT can provide reliable groundwater recharge and nutrient leaching fluxes to MODFLOW, while also producing accurate crop yields for subsequent economic-environmental tradeoff analyses. While other field-scale agricultural models (e.g., DSSAT [Jones et al., 2003]; HYDRUS 1-D [Simunek et al., 2008]; Leaching Estimation and Chemistry Model [Hutson and Wagenet, 1992]; and Root Zone Water Quality Model [RZWQM, USDA-ARS, 1990]) may be more biophysically rigorous than SWAT, none of these models are integrated with hydrologic models that can simulate the complex watershed-scale surface water-groundwater interactions that are important in the study area.

The overall goal of this study was to use SWAT to simulate the long-term response of crop yield, crop N uptake, irrigation requirements, and NO_3-N leaching under different irrigation, N fertilization, and cover crop management practices for a corn-peanut rotation, the most common row crop rotation in the SRB (USDA 2012). Specific objectives were to: (1) calibrate SWAT using observations from a three-year irrigation and N fertilizer rate management experiment for a corn-peanut rotation conducted in Live Oak, Florida (Zamora et al., 2018, 2020); (2) evaluate the long-term effects of the experimental irrigation and fertilization treatments on annual yield, N

uptake, irrigation applied, and NO_3-N leaching using calibrated parameters over a 39-year (1980-2018) historic weather record; and (3) estimate the effect of planting a rye cover crop on NO_3-N leaching, irrigation water use, and yield in corn-peanut rotations. Future studies will aggregate these practices to the watershed scale to determine the ability of changes in agricultural management practices to achieve the NO_3-N loading reductions required to meet the federally mandated NNC in the SRB. This work provides a framework for developing effective, socially acceptable strategies for achieving stringent water quality regulations while maintaining a robust agricultural economy that is transferrable to other agricultural watersheds throughout the world.

Materials and Methods

Study Area and Experimental Design

The experimental field site is located at the North Florida Research and Education Center – Suwannee Valley (NFREC-SV), near Live Oak, Florida (30.31 N, -82.90 W, Figure 2-1). The field is at an elevation of 49-50 m above mean sea level and has flat topography with an average slope of less than 0.5%. The site consists of three types of well-drained soil: Chipley, Hurricane and Blanton sand (SSURGO (Soil Survey Geographic database), NRCS 2016). Soils in the southern portion of the site are mostly Chipley, while those in the northern portion are mostly Hurricane (Figure 2-1). The site was divided into two systems based on the timing of rotation. System 1 (southern portion of the site) was a corn-peanut-corn rotation planted during 2015-17, and System 2 (northern portion) was a peanut-corn-peanut rotation grown during the same period. In this manuscript results and analysis from System 1 are presented in detail; results from System 2 were very similar and are thus summarized in the body of the paper and fully documented in the Appendix.

Systems 1 and 2 were divided into four blocks (i.e., replicates B1-B4), each containing fifteen 12.2 m x 6.1 m (74.4 m^2) plots (Figure 2-1). Each plot received a different irrigation management strategy (*n*=5) and N fertilizer rate (*n*=3) resulting in 15 treatments, each with 4 replicates. In this study, the subset of these plots that had most field observations were selected to develop the model. This subset included 9 treatments (3 irrigation methods and 3 fertilizer rates; Table 2-1). Complete documentation of the field experiment can be found in Zamora et al., (2018).

The three irrigation methods consisted of calendar-based irrigation, soil moisture sensor-based irrigation and no irrigation (rainfed). Calendar-based irrigation for corn consisted of no irrigation for the first 30 days after planting (DAP), unless severely windy conditions caused blowing sand to burn the plants. Beginning on 31 DAP, a target amount of 25 mm/week was established that could be made up of rain or irrigation, if rain events were > 13 mm. For 40-59 DAP, a 41 mm/week target was established. One irrigation event was skipped if 13-20 mm rainfall occurred, and two irrigation events were skipped if >20 mm of rain occurred. For 60-105 DAP a 61mm/week irrigation target was used. One irrigation event was skipped if 13-25 mm of rain occurred the day prior to a scheduled irrigation, and two irrigation events were skipped if >25 mm of rain occurred. Finally, around 105 DAP at full dent stage, weekly irrigation targets were reduced to 41 mm/week for one week and 20 mm/week for another week until finally irrigation was terminated at 115 DAP. Individual irrigation events were 13 mm.

A similar calendar-based irrigation schedule was applied during the peanut growing season. This consisted of no irrigation from 0 to 30 DAP; from 31 to 44 DAP 25 mm/wk was applied unless rainfall provided target irrigation amount; from 45 to 64 DAP

38 mm/wk was applied, however if rainfall between 13 to 19 mm occurred one irrigation event was skipped and if rainfall >19 mm occurred two events were skipped. Finally, from 65 to 135 DAP 51 mm/wk was applied, one irrigation event was skipped if 13 to 25 mm of rain occurred, and two irrigation events were skipped if >25 mm of rain occurred. Individual irrigation events were 10 mm.

For the soil moisture sensor (SMS)-based irrigation scheduling, the volumetric soil water content (VWC) was monitored continuously using sensors. Irrigation was triggered when the maximum allowable depletion (MAD) was 50% of the difference between field capacity (FC) and permanent wilting point (PWP). The irrigation volume required to refill the active root depth to field capacity was estimated according to guidelines proposed by Zotarelli et al., (2013). Active root depth was varied throughout the season based on root development.

The three N fertilizer treatments consisted of high, medium, and low application rates (336, 246 and 157 kg N/ha for corn, respectively). The high fertilizer application rate of 336 kg N/ha for corn and 17 kg N/ha peanut, is a common grower practice in the region (Zamora et al., 2018). The medium rate closely follows the University of Florida Institute for Food and Agricultural Sciences (UF-IFAS) recommendations (235 kg N /ha for irrigated corn and 0 kg/ha for peanut; Hochmuth et al., 1992; Mylavarapu et al., 2015). The low N represents the minimum N required to establish the corn crop in the low water holding capacity, low organic matter, and low cation exchange capacity sandy soils at the field site. For corn an extra application of up to 17 kg N /ha was made within the first four weeks after planting if 76 to 100 mm of rainfall occurred in a week (FDACS

2015). The fertilizer composition and application schedule are presented in Appendix Table A-1.

Data Collection and Processing

Table A-2 in Appendix summarizes the type, location and frequency of data collected from each plot. Soil moisture content was obtained from Sentek drill and drop capacitance probes (Sentek Pty Ltd 2003) installed in three replicates (blocks 2, 3 and 4) in each of the nine treatments (Figure 2-1). Each probe consists of nine sensors placed every 100 mm interval up to 900 mm. Probes recorded data every 30 min, which were averaged to daily values of soil moisture storage for comparison with SWAT daily output. The Sentek probes were calibrated at the factory. After installation at the field site the Sentek soil moisture measurements were checked against observed volumetric water content (estimated using gravimetric water content measured from soil cores within the same replicate and bulk density measured at the field site) to verify the factory calibration and establish their reliability for use in model calibration and validation. Soil Nitrate-N was collected from all plots at four depths (0-150, 150-300, 300-600 and 600-900 mm) throughout the rotation. Aboveground biomass and nitrogen uptake were collected at key growth stages from all plots under SMS-based irrigation. Detailed information about the data collection procedures is provided in Zamora et. al., (2018). Soil properties measured at the site are summarized in Appendix Table A-3.

Model Description

SWAT is a semi-distributed, continuous, process-based watershed-scale model used to evaluate the impact of different land management practices on surface and subsurface water quality and quantity, sediment, and agricultural yields (Arnold et at., 1998; Neitsch et al., 2004; Gassman et al., 2014). For spatial representation, SWAT

delineates a watershed into hydrological response units (HRUs), which are homogenous regions with similar slope, land use and soil type (Neitsch et al., 2011; Winchell et al., 2012). HRUs can be used for field or plot-level estimation of nitrate leaching, crop yield, evapotranspiration, and other management practice assessments (Neitsch et al., 2004; Anand et al., 2007; Gitau et al., 2008; Sinnathamby et al., 2017; Moloney et al.,2015; Cibin et al., 2017; Karki et al., 2019).

SWAT has two infiltration schemes: The Curve Number (CN) method at daily intervals and the Green-Ampt method when hourly precipitation data are available; CN-based infiltration was used in this study. SWAT simulates the movement of infiltrated flow between soil layers using a storage routing (tipping bucket) method, which allows downward movement or percolation of saturated flow when field capacity of a soil layer is exceeded and the underlying layer is not saturated (Arnold et al., 2004; Mapfumo et al., 2004). Soil moisture distribution below field capacity is governed by plant water uptake and soil water evaporation through two parameters, the soil evaporation compensation coefficient (ESCO) and the plant uptake compensation factor (EPCO), respectively (Vazquez-Amabile and Engel, 2005; Neitsch et al., 2011). The crop growth algorithm in SWAT is based on the Environmental Impact Policy Climate (EPIC) crop growth model (Williams et.al., 1989; Neitsch et.al., 2004). SWAT calculates the potential growth of the plant for each day as a function of solar radiation and leaf area index (LAI). Actual growth and LAI are dependent on stress factors including water, temperature, and nutrient stress. SWAT computes the accumulation of heat units until the crop attains maturity, after which crop growth ceases (Nair et al., 2011).

Model Setup

In this study, SWAT (version 2012/Rev664) was applied at the plot scale for the calibration and validation of soil and crop parameters following the approaches of Annand et al., (2007); Maski et al., (2008); Marek et al., (2016,2017) and Chen et al., (2017). The experimental area (Figure 2-1) was auto delineated into one basin with three HRUs (one per irrigation treatment) using the USGS 30 m DEM (Digital Elevation Map), USDA NRCS SSURGO soil map and USDA NASS Cropland Data Layer (CDL). These HRUs were converted to plots of equal size (74.4 m^2) by adjusting the area in the sub basin input file and the fraction of area of HRU in the HRU input file (Marek et al., 2016; Moloney et al., 2015; Karki et al., 2019). Each HRU was provided with information regarding management practices conducted in the experimental study period (e.g., planting date, irrigation and fertilizer schedules and harvest date). The default SSURGO soil data of soil bulk density, soil texture and organic carbon (%) were replaced with field measurements (Zamora et al., 2018) for each HRU (AppendixTable A-3). The total root zone depth in each HRU was set to 900 mm, with four layers (0-150 mm, 150-300 mm, 300-600 mm, and 600-900 mm) for consistency with measured soil nitrate depth resolution.

The source of irrigation water at the experimental site is the Upper Floridian Aquifer, which is approximately 3 m below land surface (USGS, 1983), with no interaction with the root zone. Surface runoff was never observed during the experiment at this well-drained site (Zamora et al., 2018). Thus, the irrigation source was set to an unlimited source outside of the field scale model domain. SWAT daily weather data (i.e., rainfall, temperature, solar radiation, relative humidity, and wind speed) required for the Penman-Monteith evapotranspiration module were obtained from the Live Oak Florida

Automated Weather Network (FAWN) located at the experimental site (30.305 lat, -82.898 long, https://fawn.ifas.ufl.edu/). Missing data were filled using the SWAT weather generator (Neitsch et al., 2011).

Calibration Methodology

Crop growth simulation depends on both crop biophysical processes as well as soil moisture dynamics, so model calibration and validation followed an integrated approach to predict both processes reasonably (Wang et al., 2016; Sinnathamby et al., 2017; Yang et al., 2017). The data used for calibration versus validation is summarized in Table 2-3. The calibration procedure is detailed below.

Soil moisture was the first variable to be calibrated with default SWAT crop parameters. The Sequential Uncertainty Fitting (SUFI-2) algorithm in SWAT Calibration and Uncertainty Procedures (SWAT-CUP 2012) was used to calibrate and validate the model and the Nash-Sutcliffe model efficiency (NSE) was chosen as the objective function (Abbaspour et al., 2018). The SUFI-2 algorithm has been extensively used in the calibration of the SWAT model due to its easy implementation, high flexibility in selecting parameters and the range for calibration, and the reduced number of model runs needed to achieve good prediction (Yang et al., 2008; Malago et al., 2015). For this study, the methodology recommended in the SWAT-CUP user manual (Abbaspour (2013) and several SWAT-CUP calibration papers (Yang et al., 2008; Abbaspour et al., 2015; Kamali et al., 2017; Abbaspour et al., 2018) were followed.

The initial range of soil parameters were selected based on literature values (Arnold et al., 2012) and prior experiments conducted on similar soils in the region (Zotarelli et al., 2007; Prasad et al., 2015). Sensitivity analysis was carried out within SWAT-CUP to determine sensitive parameters to be included in the calibration. Sentek

soil moisture sensor data was used to calibrate total soil moisture storage in the entire root zone (900 mm) at the daily scale during the cropping season because currently SWAT-CUP has no provision to calibrate the soil moisture storage for individual soil layers. SWAT provides a simulated soil moisture only for the whole soil column (output file) which is utilized by SWAT-CUP for the auto-calibration process.

Soil and hydrological parameters were calibrated using daily soil moisture storage (total soil moisture from 0 to 900mm) averaged across replicates for each high N irrigation treatment (i.e., Calendar, SMS and Rain fed) from 2015 to 2017 (Figure 2-1), after a three-year warm up period to stabilize the initial hydrological condition. The three high N irrigation treatments were selected for calibration to account for spatial variability in soil properties across a variety of moisture regimes under the assumption of plant growth under no N stress. The calibrated soil parameters were then validated for each irrigation treatment in the medium and low N fertilizer treatments. The three calibrated HRUs with the high N management schedule were replaced with the medium and the low N fertilizer schedule for validation.

After best-fit soil and hydrological parameters were identified, crop parameters were calibrated using the above ground biomass data averaged across replicates of the SMS high N treatments (note that biomass was measured at key growth stages only for SMS treatments (AppendixTable A-2)). Sensitivity analysis of seasonal biomass growth to SWAT crop parameters was conducted to determine the most sensitive parameters, after which the sensitive parameters were adjusted to reproduce the observed trend of crop growth in the high N fertilizer SMS treatment. Calibrated parameter values were validated using data from the low- and medium-N fertility SMS treatments. The

calibrated soil moisture parameters were further verified by re-simulating with the final crop parameters.

Field-measured harvest indices (i.e., average fraction of final biomass removed from the field across the treatment replicates) for the SMS and Calendar High N treatments were used to estimate yield for both corn and peanut, assuming yields were optimum (without any water and nutrient stress (Neitsch et al., 2004)) for those treatments. The default SWAT nitrogen uptake parameters, PLTNFR-1 (N uptake at emergence), PLTNFR-2 (N uptake at 50% maturity), and PLTNFR-3 (N uptake at full maturity), and default Nitrogen transformation parameters were used in all simulations. The adequacy of these parameters in simulating the N balance for the experiment was assessed by comparing measured and predicted N uptake by the crop and NO_3-N soil concentrations soil over time for each treatment. System 1 calibrated crop parameters were also validated using system 2 data.

For all comparisons, statistical indices such as Nash Sutcliffe efficiency (NSE), Root Mean Squared Error (RMSE) and percent bias (PBIAS) were used. NSE and RMSE were estimated accounting for replicate measurement variability (Harmel et al., 2007; Harmel et al., 2010) using the software “FITVAL” (https://abe.ufl.edu/faculty/carpena/software/FITEVAL) developed by Ritter and Muñoz-Carpena, 2013. These modified statistical indices are denoted here as NSE_M, and $RMSE_M$. PBIAS was estimated without measurement variability (Moriasi et al., 2012). The performance indices were judged based on the criteria of satisfactory (NSE_M>0.50) to very good (NSE_M >0.75) set by Moriasi et al., (2007, 2012).

Development of Long-term Scenarios

In order to estimate irrigation requirements, nitrate leaching and crop yield over the wider range of historical weather conditions, the corn-peanut rotation was simulated for the nine experimental treatments using 39 years of North American Land Data Assimilation System (NLDAS) historical weather data (1980 to 2018, using 1980 and 1981 as warmup period). In addition, scenarios were developed to estimate the potential reduction in nitrate leaching if a rye winter cover crop were planted instead of letting the land remain fallow between two subsequent crops. SWAT default parameters of rye crop was used for long term scenario. While many studies have shown that winter cover crops have benefits such as preventing soil erosion, improving long term soil quality, and enhancing carbon sequestration (Basche et al., 2016; Kaspar and Singer, 2011; Moore et al., 2014), the impact of cover crops on reducing nitrate leaching has not been fully established (Martinez-Feria et al., 2016; Dabney et al., 2010; Thorup-Kristensen et al., 2010).

A calendar irrigation schedule was developed from the historic rainfall data following an approach suggested by University of Florida Extension Specialists (Appendix Table A-4). Sensor-based irrigation was simulated with the SWAT auto irrigation option based on plant water demand, which triggers irrigation when the ratio of actual transpiration to potential transpiration becomes less than the user-defined threshold (Arnold et al., 2013). After multiple simulation trials and comparison with the experimental soil moisture scheduling irrigation amounts, and recommendations from stakeholders, a 0.65 threshold was used for both corn and peanut with an irrigation application of 12.7 mm/day for corn and 10.16 mm/day for peanut.

Split application of the three N fertilizer rates used in the field experiment (Table 2-1, Appendix Figure A-1) were applied using ammonium nitrate fertilizer as it is a common source of N fertilizer in the region. For simplicity, fixed planting and harvesting dates were adopted throughout the simulation period (Table 2-2). Based on local practices and communication with Extension Specialists, a rye cover crop planting and herbicide application schedule was incorporated into the simulations. The agricultural management schedule for the corn and peanut rotation with and without the cover crop is presented in Table 2-2.

Results and Discussion

Model Calibration and Validation

Table 2-3 presents final calibrated values, ranges, and *p*-values to indicate the sensitivity of parameters ($p<0.05$ indicates a sensitive parameter). Available water content (AWC), Soil Evaporation Compensation Factor (ESCO) and Plant Uptake Compensation Factor (EPCO) were the most sensitive soil and hydrological parameters. Notably, saturated hydraulic conductivity and curve number were not sensitive parameters. Best-fit parameters were similar, though not identical, between systems (Table 2-4).

Total heat units required to reach maturity (HEAT_UNITS) (in this experiment maturity for corn was 135 days after planting) and biomass-to-energy ratio (BIO_E) were the sensitive crop parameters, which is in accordance with previous studies (Faramarzi et al., 2009; Kiniry et al., 2002; Abbaspour et al., 2015; Almeida et al., 2017). Maximum potential leaf area index (BLAI) for corn and peanut were assigned to be 3 and 4 respectively, as specified in the SWAT database (Kiniry et al., 2002; Almeida et al., 2017). The final ranges of BIO_E for corn and peanut were close to ranges included

in the SWAT manual (BIO_E corn: 39-45 and BIO_E peanut: 20-25). The calibrated HEAT_UNITS value for peanut (1800) was close to that for Georgia green peanut variety (1900) estimated from previous experiments (Bennett et.al., 1993; Kiniry et.al., 2005). The optimal harvest index parameter (HVSTI) was set to the measured harvest index (the average quantity of biomass removed from field as yield) for the SMS and Calendar High N treatments, which was 0.60 for corn and 0.55 for peanut. The minimum harvest index parameter (WSYF) was kept at the default value of 0.3 for both corn and peanut.

Soil Moisture Storage

Figure 2-2 shows modeled and observed soil moisture storage for the three treatments used for calibration (SMS, Calendar and Rain fed irrigation, all under high N fertilization). The range of the observed measurements represents the spatial variability of soil moisture across replicates for each treatment. Soil moisture validation for the remaining six treatments (SMS, Calendar and Rain fed irrigation under medium and low N fertilization) for System 1 are shown in Appendix Figure. A-1 and A-2. Plots of modeled versus observed soil moisture for System 2 are presented in Appendix Figure A-6 to A-8.

Overall, soil moisture predictions showed satisfactory to very good fits ($0.67 < NSE_M < 0.97$) in both calibration and validation treatments for both systems (Table 2-5). However, observed soil moisture peaks during high rainfall events were under-predicted in System 1 Calendar and SMS treatments across all fertilization rates. These results indicate that, although SWAT was able to capture general patterns of soil moisture variation across the three growing seasons for both systems, soil water drained too rapidly when soil moisture was above field capacity. Discrepancies between simulated

and observed soil moisture, particularly during high rainfall events, due to simplified runoff and percolation process in SWAT were also reported by Rajiv et al., (2016), Yang et al., (2017), and Zhang et al., (2017). SWAT has a simplified approach for estimating soil moisture percolation that assumes soil water above field capacity in a particular layer percolates to the next layer at a rate governed by the saturated hydraulic conductivity (Neitsch et al., 2011).

Due to this SWAT model structure and its high sensitivity to available water content and low sensitivity to hydraulic conductivity (Table 2-4), the calibrated soil parameters were unable to reproduce some of the transient soil moisture peaks measured by the Sentek probes during large (particularly multi-day) rainfall events (Figure 2-2). However, manually increasing available water content and lowering hydraulic conductivity of the soil from the calibrated parameters to try to match the peaks resulted in long periods of time where the soil moisture remained much higher than the observations, deteriorating the overall model fit statistics significantly. In the sandy soils at the experimental site (and throughout much of the SRB region), the transient high soil moisture drains back to field capacity more slowly than SWAT predicts, but typically within a few days, causing this excess water (and any nitrate it contains) to eventually leach past the root zone. The fact that nitrogen uptake and biomass accumulation by the crop as well as soil nitrate storage were adequately predicted by the model (described in following sections) provides some reassurance that the transient inaccuracies around large-rainfall events do not affect the seasonal water and nitrogen mass balances.

With the calibrated Soil Conservation Service Curve Number (SCS-CN), the total overland runoff volume generated for the highest runoff generating treatment (calendar based irrigation with high N) was 0.77% of applied water (precipitation plus irrigation), compared to 54% for ET and 46% for percolation below the root zone, generally in conformance with the observation of no surface runoff at the field site. The small amount of runoff generated by SWAT occurred during large events such as Hurricane Irma in September 2017.

Crop Biomass and Yield

Crop growth dynamics for corn and peanut were very well predicted (NSE_M> 0.95) for the SMS irrigation treatments across both calibrated (high-N) and validated (medium- and low-N) fertilizer rates in System 1 (Table 2-6, Figure 2-3). Validation results for yield for all treatments in System 1 (Figure 2-4) were generally consistent with measured values (all NSE_M>0.75); however, in 2017 the model over-predicted both total aboveground biomass and yield for rainfed corn under all fertilization rates. This may indicate that water stress is under-predicted by the SWAT crop parameters that were calibrated using SMS-high N treatments. Validation results for crop growth dynamics for System 2 also showed very good results for 2015 peanut and 2016 corn (0.86<NSE_M<0.99; Table 2-6, Appendix Figure A-9), but total aboveground biomass and yields were not well predicted for any peanut treatments in 2017 (Appendix Figure A-10). Low observed peanut biomass and yield in 2017 were associated with crop loss caused by Hurricane Irma that hit the region in September 2017. These effects were not captured in SWAT simulations that were calibrated under limited stress conditions (Mittelstet et al., 2015).

Crop Nitrogen Uptake

Modeled N uptake dynamics followed the observed trends well for System 1 SMS treatments using default nitrogen uptake parameters (Figure 2-5 and Table 2-7). While observed total nitrogen uptake had high variability within treatments (last column Figure 2-4), System 1 total N uptake predictions reproduced mean observed values quite well (NSE_M 0.48 - 0.96, PBIAS -0.1-9.7%; Figure 2-4). Note that although there was no difference in N applied to the System 1 peanut treatments in 2016 both the observed and simulated peanut nitrogen uptake in 2016 were influenced by different irrigation treatments, primarily because irrigation treatments affected biomass production, hence affecting crop demand for N.

Modeled N uptake dynamics followed well the observed trends for System 2 SMS treatments in 2015 and 2016, but N uptake for peanut was significantly overpredicted in 2017. This was a result of overprediction of biomass and yield since SWAT was not able to correctly predict the crop loss that occurred as a result of Hurricane Irma in 2017 (Appendix Figure A-11 and Table 2-7). For System 2, total N uptake for corn was adequately predicted (NSE_M 0.63, PBAIS -8.8%); however, for peanut (N fixation plus N uptake from soil) was slightly underpredicted in 2015 (NSE_M -9.23, PBIAS 25%) and overpredicted in 2017 (NSE_M -11.44, PBIAS -89.7%) (Appendix Figure A-12).

Overall, SWAT predictions of final biomass, N uptake and yield for both systems agreed with the Zamora et al., (2018, 2020) experimental results in which the calendar-based and SMS irrigation management practices produced statistically higher final biomass, N uptake and yield than the rainfed practices. Zamora et al., (2018) found no statistically significant differences in final corn biomass across N rates, but differences

in total N uptake were found between the low and the high N rates. SWAT predicted both lower biomass and N uptake for the low N fertilizer rate.

Soil Nitrate-N

Time series of System 1 simulated and measured soil nitrate-N in the entire root zone (0-900 mm) for Calendar, SMS and Rainfed irrigation with high N treatments are shown in Figure 2-6. The remainder of the System 1 treatments are shown in Appendix Figure A-3 and A-4, and similar results for System 2 are shown in Appendix Figure A-13 – A-15. For both systems, soil nitrate-N simulated using default soil nitrate parameters followed the trend of the observed data with NSE_M values ranging from 0.55 (satisfactory) to 0.95 (very good) for all treatments except the rainfed high fertilizer treatment. The Rainfed high fertilizer treatment over-predicted soil nitrate-N for both Systems, primarily during the fallow season following corn production (NSE_M 0.16 and 0.25, respectively; Table 2-8). As mentioned earlier, SWAT overestimated the corn biomass and N uptake for the rainfed case, most likely because the SWAT corn parameters used for calibration had no water or N stress (i.e., SMS-high treatment). The erroneously low corn N uptake may have led to the erroneously high soil N in the fallow periods due to mineralization of plant residues after harvest, in part because water deficit reduces harvest index, thus leaving more non-grain residue with higher N content for later mineralization.

Nitrate-N Leaching

Based on satisfactory to very good prediction of simulated crop N uptake and soil nitrate-N storage (the only measured components of N balance in this study), simulated nitrate-N leaching was compared across treatments for the corn-peanut-corn rotation including the fallow periods between cropping seasons (System 1, Figure 2-7). As

expected, the high N fertilizer practice (336 kg N/ha) caused more nitrate-N leaching to groundwater than the medium and low fertilizer practices (246 and 157 kg N/ha) in all irrigation management systems. Similarly, the medium N rate caused more nitrate leaching to groundwater than the low fertilization practice. Interstingly, more nitrate leaching occurred during the fallow periods between crops than during the crop growing seasons across treatments.

Within the high N fertilizer practice, calendar irrigation caused more nitrate leaching to groundwater than SMS and rainfed practices during the 2015 corn growing season (Figure 2-7). However, the highest nitrate leaching occurred during the 2015-16 fallow period after the 2015 rainfed-high corn. Across all treatments the corn and peanut biomass left in the field after harvest (40 and 45%, respectively) apparently decayed and mineralized to N that contributed to nitrate-N leaching ranging from 15 to 70 kg N/ha and from 10 to 20 kg N /ha during the 2015-16 and 2016-17 fallow periods, respectively. Compared to 2015, corn grown in 2017 exhibited more leaching due to extreme weather conditions and the extra 17 kg/ha of N fertilizer that was added to compensate the loss of N due to leaching rain. Results show a ~40% (70 kg N/ha) reduction in nitrate leaching for the SMS-medium fertilizer treatment compared to the calendar irrigation and high N fertilizer practices that are common in the region.

Long-term Simulation Results

Crop Yield

The long-term simulations (1980-2018) showed no significant difference in average crop yields for the high and medium N fertilizer treatments when using Calendar or SMS irrigation scheduling methods. The rainfed and low fertility treatments showed statistically lower average yields (Figure 2-8). These results are consistent with

the field experiment results reported by Zamora et al., (2018). The incorporation of rye as a cover crop did not show any statistically significant effect on average corn yield for the high and medium N treatments. However, the Calendar and SMS low fertility corn treatments showed an average of 12% and 9% increase in corn yield following cover crops, respectively. For these low fertilizer treatments, the incorporation and mineralization of cover crop biomass provided additional nutrients beneficial for corn production (Krueger et al., 2011). Similar field results were reported by Zotarelli et al., (2009) where at lowest supplemental N rates, cover crops added benefits to sweet corn yields in Florida, USA. No statistically significant effects of cover crops on average peanut yields were observed. The wide variation in predicted rainfed corn and peanut yields across all N fertility rates represents variations in water stress due to variations in annual rainfall.

Nitrate-N Leaching

Figure 2-9 shows long term leaching simulated over the crop rotation including fallow and cover crops between growing seasons (corn – fallow/cover crop – peanut – fallow/cover crop). As expected, high N fertilization rates resulted in more nitrate-N leaching than medium fertilization rates, which in turn resulted in greater leaching than low fertilization rates. Long-term simulations showed that SMS irrigation resulted in statistically significant less leaching than calendar irrigation across all fertilization rates. Furthermore, introducing cover crops during the fallow periods reduced nitrate-N leaching by a statistically significant average of approximately 50 kg N/ha across all treatments. The calendar-based irrigation with high fertilizer and no cover crop practice resulted in ~65% more leaching (~120 kg N/ ha) in comparison to the SMS-based irrigation with medium fertilizer and cover crop practice. Moreover, the extra 100 kg/ha

fertilizer and 45% more irrigation water applied by this common practice did not provide any statistically difference in average corn or peanut yields (Figure 2-8). Long-term irrigation applied by the Calendar treatment averaged 506 and 309 mm during corn and peanut, respectively, whereas the SMS treatment (using auto-irrigation) applied an average of 290 and 160 mm, respectively. Thus, average irrigation reductions of 43% and 48% were achieved by using a sensor-based instead of calendar-based irrigation scheduling method in corn and peanut production, respectively.

Further analysis of N leaching patterns showed that on average the calendar-based irrigation with high N fertilizer practice resulted in an average of ~100 kg N /ha leaching within the corn growing season followed by an average of ~50 kg N /ha during the subsequent fallow season. In contrast, the rainfed – high N fertilizer practice resulted in an average of ~34 kg N/ha leaching during the corn season and an average of ~100 kg N /ha leaching during the subsequent fallow period (Appendix Figure A-5). For the rainfed corn, the fertilizer not taken up by the crop during the growing season along with the N mineralization from corn residue resulted in more leaching during the fallow period than either the calendar or SMS irrigation practices. Nitrogen leaching from peanut residue (average of ~ 50 kg/ha across all management practices) was significantly reduced (~80%) by planting rye as a cover crop compared to leaving the fields fallow between cropping seasons (Appendix Figure A-5).

Conclusions

Providing quantitative support for the efficacy and economic feasibility of agricultural best management practices is becoming more and more critical as communities around the globe seek to balance agricultural production and environmental protection. Coupling robust field experiments of specific management

practices with modeling approaches that allow inference to be drawn at larger spatiotemporal scales is particularly useful for exploring tradeoffs among alternative future scenarios and comparing results to regulatory requirements and the preferences of diverse stakeholders. In this study, it is shown that SWAT successfully estimated soil moisture, crop biomass, yield, crop N uptake and soil nitrate for corn-peanut rotations grown using a variety of irrigation and N fertilizer management practices in the Suwannee River Basin, Florida. Leveraging robust field measurements from a 3-year field study (Zamora et al., 2018, 2020) allowed us to predict likely long-term changes in crop yields, water use, and N leaching over a range of historical conditions. By expanding experimental results beyond the temporal limits of specific field seasons, these model results provide more widely applicable guidance for reductions in nutrient loads that can be expected from BMP implementation.

Specifically, we found that improving irrigation scheduling practices, reducing N fertilization rates and planting a cover crop during fallow periods have the potential to reduce NO_3-N leaching by ~65% over current commonly used corn-peanut rotation practices. Notably, this is within the 65% reduction in NO_3-N load that is estimated to be needed to achieve the NNC in spring ecosystems (FDEP, 2012, 2018). Furthermore, our results indicate that these load reductions can be achieved without adversely affecting crop yield. This suggests that an incentive program that cost-shares equipment purchases and protects producers from the risk of yield reductions may be an effective way to overcome barriers to the widespread adoption of SMS irrigation scheduling, reduced N fertilization rates and cover cropping practices in the region. Building from these results, we are currently engaging stakeholders to develop alternative land use-

land management scenarios at the watershed scale. These scenarios will be used to drive a SWAT-MODFLOW model to evaluate tradeoffs among the regional agricultural economy, surface water and groundwater quantity, and stream/aquifer water quality, and to determine whether improved management practices alone can achieve the NNC. Overall, the results of this study and our ongoing efforts provide a transferable framework for developing effective and economically feasible strategies for meeting water quality regulations while maintaining agricultural landscapes and livelihoods.

Table 2-1. Irrigation and N fertilizer treatments for the nine treatments in Systems 1&2.

Irrigation treatment	Irrigation applied (mm) 2015	2016	2017[1]	N fertilizer rate Rate	(kg N/ha)
Corn					
Calendar	330	490	546	High	336
				Medium	246
				Low	157
Soil Moisture Sensors (SMS)	151	291	302	High	336
				Medium	246
				Low	157
Rain fed	15	25	48	High	336
				Medium	246
				Low	157
Peanut					
Calendar	132	555	368		
SMS	25	205	122		17[2]
Rain fed	0	30	20		

[1] In 2017, due to leaching rainfall events occurring early in the season, an additional 17 kg N/ha were applied to each corn N fertility rate.
[2]No difference in N fertilizer rate for peanut.

Table 2-2. Irrigation and N fertilizer management schedule used to perform long-term simulations using historical weather data (1980-2018).

	Baseline Scenario[1]		Cover Crop Scenario[2]
	Corn	Peanut	Rye
Planting	20-Mar	12-May	01-Oct
Harvest	05-Aug	27-Sep	Chemically kill cover crop one month before planting corn and peanut [3]
Irrigation	Calendar Irrigation Schedule (Table 16) SWAT Auto irrigation (12.7 mm per event) Rain fed (No Irrigation)	Calendar Irrigation Schedule (Table 16) SWAT Auto irrigation (10.16 mm per event) Rain fed (No Irrigation)	None
Fertilizer	N Fertilization rates (low, med, high) schedule (Table 2).	None	None

[1] Baseline includes a fallow period between cropping seasons (i.e. corn-fallow-peanut-fallow).
[2] Cover crop scenario includes rye instead of fallow periods between cropping seasons (i.e. corn-rye-peanut-rye).
[3]Harvest and kill option 8 in SWAT, 100% biomass incorporated as residue

Table 2-3. Summary of data used for calibration versus validation.

Observation	Calibration Data	Validation Data
Soil moisture	Calendar Irrigation – High N, 2015-2017. SMS Irrigation – High N, 2015-2017. Rainfed – High N, 2015-2017.	Calendar Irrigation – Med & Low N, 2015-2017. SMS Irrigation – Med & Low N, 2015-2017. Rainfed – Med & Low N, 2015-2017.
Biomass dynamics	SMS Irrigation – High N, 2015-2017.	SMS Irrigation – Med & Low N, 2015-2017.
Final biomass	SMS Irrigation – High N, 2015-2017.	Calendar Irrigation – High, Med & Low N, 2015-2017. SMS Irrigation – Med & Low N, 2015-2017. Rainfed – High, Med & Low N, 2015-2017.
Final Yield	Calendar Irrigation – High N, 2015-2017. SMS Irrigation – High N, 2015-2017.	Calendar Irrigation – Med & Low N, 2015-2017. SMS Irrigation – Med & Low N, 2015-2017. Rainfed – High, Med & Low N, 2015-2017.
Crop N uptake	None (default parameters used)	Calendar Irrigation – High, Med & Low N, 2015-2017. SMS Irrigation – High, Med & Low N, 2015-2017. Rainfed – High, Med & Low N, 2015-2017.
Soil N	None (default parameters used)	Calendar Irrigation – High, Med & Low N, 2015-2017. SMS Irrigation – High, Med & Low N, 2015-2017. Rainfed – High, Med & Low N, 2015-2017.

Table 2- 4. Calibrated soil, hydrological and crop parameters including p-values for sensitivity and uncertainty range

		System 1			System 2		
Water Balance Parameters	Definition	Final Range	Used Value	P-Value	Final Range	Used Value	P-Value
r__CN2.mgt	SCS Curve Number	-0.04 - 0.137	-0.03(40*)	0.18	-0.17 - 0.13	-0.06(40*)	0.34
v__ESCO.hru	Soil evaporation compensation factor	0.49 - 0.60	0.52	$5.29x10^{-07}$	0.68 - 0.86	0.71	0.0003
v__EPCO.hru	Plant uptake compensation factor	0.15 - 0.26	0.21	0.01	0.15 - 0.26	0.16	$9.04x10^{-41}$
v__GW_DELAY.gw	Groundwater delay, days	2 - 10	8.35	0.8	2 - 10	7.9	0.45
v__SOL_AWC(1).sol	Soil available water storage capacity	0.07 - 0.12	0.09	$7.08x10^{-9}$	0.06 - 0.12	0.09	$2.21x10^{-43}$
v__SOL_AWC(2).sol		0.07 - 0.13	0.08	$9.37x10^{-60}$	0.030 - 0.10	0.05	$5.13x10^{-83}$
v__SOL_AWC(3).sol		0.07 - 0.10	0.08	$7.65x10^{-14}$	0.10 - 0.15	0.12	$4.19x10^{-29}$
v__SOL_AWC(4).sol		0.13 - 0.16	0.16	$2.20x10^{-34}$	0.14 - 0.16	0.15	$8.9x10^{-20}$
r__SOL_K(1).sol	Saturated hydraulic conductivity (mm/hr)	0.010 -0.028	0.017(204*)	0.8	0.02 - 0.03	0.022	0.41
r__SOL_K(2).sol		-0.002 - 0.014	0.005(205*)	0.59	0.008 - 0.013	0.010	0.29
r__SOL_K(3).sol		0.007 - 0.024	0.021(202*)	0.7	0.027 - 0.037	0.034	0.29
r__SOL_K(4).sol		-0.014 - 0.008	0.007(198*)	0.78	-0.12 - 0.026	-0.047	0.59
		Crop Parameters (Corn)			Crop Parameters (Peanut)		
BIO_E.plant.dat	Biomass/Energy	39 - 48	46	$6.9x10^{-7}$	20 -35	26	$2.18x10^{-5}$
HEAT_UNITS.mgt	Total heat units for plant to mature	2000 - 2500	2400	0.03	1700- 2500	1800	$2.63x10^{-23}$
HVSTI	Harvest Index for optimal growing condition		60[a]			55[a]	

r = relative changes in parameter values, v = absolute changes in parameter values, * = absolute value used in the model, a = manual adjustment based on experiment and suggestion from stakeholders, 1, 2, 3 and 4 denote the four soil layers 0-150, 150-300, 300-600 and 600-900mm.

Table 2-5. Goodness-of-fit indicators (NSE_M, PBIAS (%) and $RMSE_M$ (mm)) for calibration and validation of total soil moisture.

	System 1 Calibration				*System 2* Calibration		
	NSE_M	*PBIAS (%)*	*$RMSE_M$*		*NSE_M*	*PBIAS (%)*	*$RMSE_M$*
SMS-High	0.88	-0.9	6.37	SMS-High	0.94	7	3.64
Calendar-High	0.72	3.4	9.63	Calendar-High	0.84	0.8	5.86
Rainfed-High	0.82	-7.7	8.76	Rainfed-High	0.92	5.3	4.71
	Validation				Validation		
SMS-Medium	0.82	-1	9.62	SMS-Medium	0.86	3.5	7.16
Calendar-Medium	0.67	-1.7	12.43	Calendar-Medium	0.96	2.2	3.43
Rainfed-Medium	0.82	-12	8.15	Rainfed-Medium	0.93	-1.8	6.33
SMS-Low	0.69	-1.8	12.83	SMS-Low	0.77	5.6	7.87
Calendar-Low	0.76	-0.9	9.39	Calendar-Low	0.89	1.6	5.58
Rainfed-Low	0.83	-16.1	8.49	Rain fed-Low	0.97	-0.2	4.73

Table 2-6. Modified goodness-of-fit indicators for biomass trend with measurement uncertainty.

	System 1 Biomass trend									
	Treatments	Corn 2015			Peanut 2016			Corn 2017		
		NSE_M	PBIAS (%)	$RMSE_M$ (kg/ha)	NSE_M	PBIAS (%)	$RMSE_M$ (kg/ha)	NSE_M	PBIAS (%)	$RMSE_M$ (kg/ha)
Calibration	SMS-High	0.99	14.1	820	0.99	-5.4	182	0.99	-4.2	733
Validation	SMS-Medium	0.99	17.2	709	0.99	-10.8	321	0.97	-4	1440
	SMS-Low	0.99	11	472	0.99	-10.7	391	0.99	8.3	599
	System 2 Biomass trend									
	Treatments	Peanut 2015			Corn 2016			Peanut 2017		
Validation	SMS-High	0.99	8.8	157	0.86	-35	3544	-1.34	-74.9	3884
	SMS-Medium	0.96	5.3	1109	0.91	-31	2802	0.17	-60.6	3230
	SMS-Low	0.99	6.3	0	0.93	-10.5	2362	-0.34	-69.4	3696

Table 2-7. Modified goodness-of-fit indicators for total aboveground N uptake trend with measurement uncertainty. PBIAS is in %.

System 1 Nitrogen Uptake trend									
Treatments	Corn 2015			Peanut 2016			Corn 2017		
	NSE_M	PBIAS	$RMSE_M$ (kg/ha)	NSE_M	PBIAS	$RMSE_M$(kg/ha)	NSE_M	PBIAS	$RMSE_M$ (kg/ha)
SMS-High	0.99	-5	7	0.99	8.3	8	0.56	-42	58
SMS-Medium	0.99	3.1	11	0.99	-4.7	14	0.89	-13.6	29
SMS-Low	0.99	15.6	8	0.99	-3.8	4	0.97	8.7	12
System 2 Nitrogen Uptake trend									
Treatments	Peanut 2015			Corn 2016			Peanut 2017		
SMS-High	0.97	17	25	0.74	-36.3	53	0.77	-41.4	43
SMS-Medium	0.95	17.8	39	0.97	-2.1	18	0.95	-12.5	20
SMS-Low	0.99	8.9	7	0.76	24.1	47	0.88	-17.1	29

Table 2-8. Modified goodness-of-fit indicators for simulated soil nitrate-N for both systems

	System 1			System 2		
	NSE_M	PBIAS (%)	$RMSE_M$(mg/kg)	NSE_M	PBIAS (%)	$RMSE_M$(mg/kg)
SMS-High	0.81	-6.1	4.8	0.58	-6.4	9.46
Calendar-High	0.70	-16.7	4.2	0.80	-11.7	4.40
Rainfed-High	0.16	-66.8	8.45	0.25	-18.4	12.73
SMS-Medium	0.64	9.8	2.83	0.93	14	2.24
Calendar-Medium	0.74	20.6	3.33	0.90	17.9	3.30
Rain fed-Medium	0.76	-5.3	3.52	0.75	-1.9	6.56
SMS-Low	0.55	35.6	2.79	0.79	37.9	4.51
Calendar-Low	0.61	43.4	4.05	0.86	36.2	2.67
Rainfed-Low	0.65	43.1	3.22	0.84	26.1	4.08

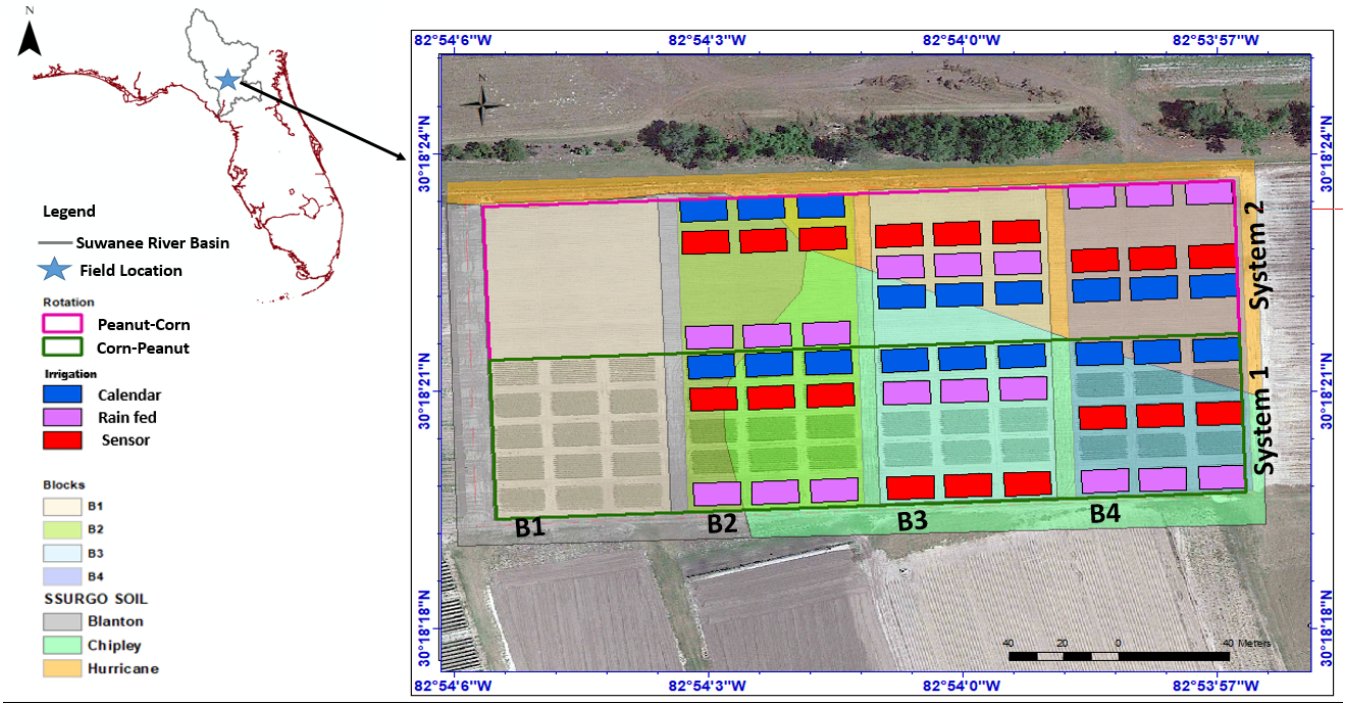

Figure 2-1. Site map showing layout of the experimental site with highlighted (blue, red, and purple) plots considered in this study.

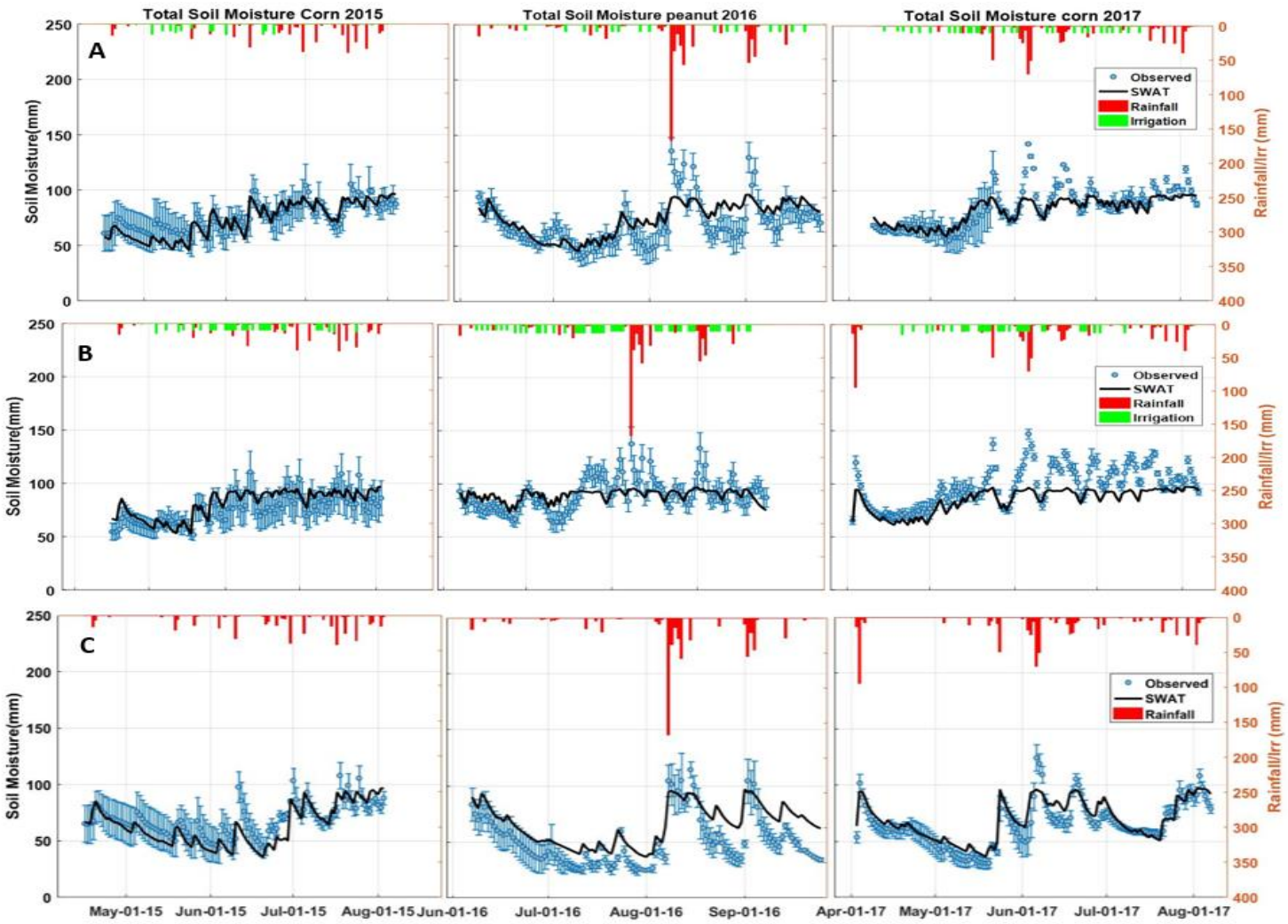

Figure 2-2. Observed and simulated total soil moisture (mm) in root zone (900 mm) during corn-peanut-corn growing seasons. (A) SMS-High, (B) Calendar-High, and (C) Rain fed-High for System 1. Vertical error bars correspond to the standard deviation of measured data.

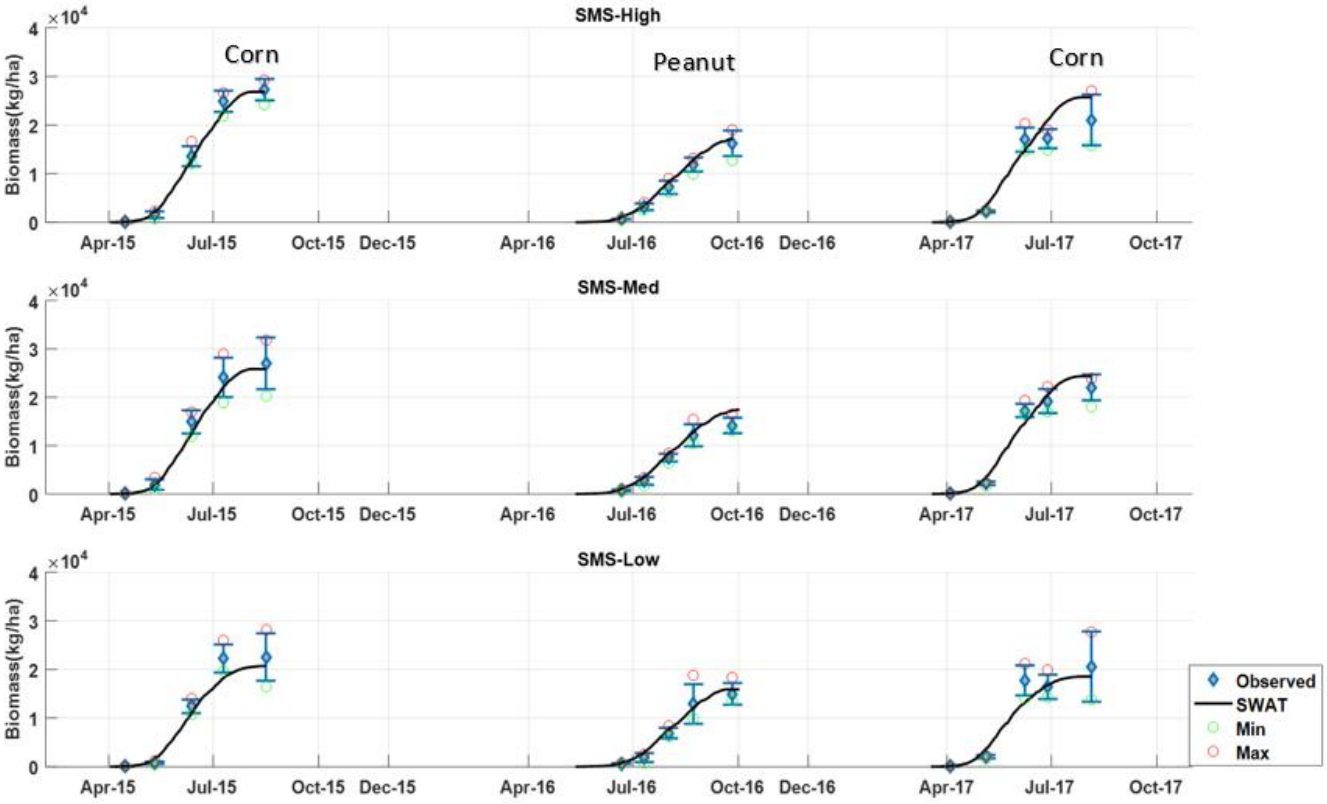

Figure 2-3. Simulated (lines) vs observed (dots) aboveground biomass dynamics for calibrated SMS-High and validated SMS-Medium and SMS-Low for System1.The experimental variation shown is the minimum and maximum of the field measurements (error bars).

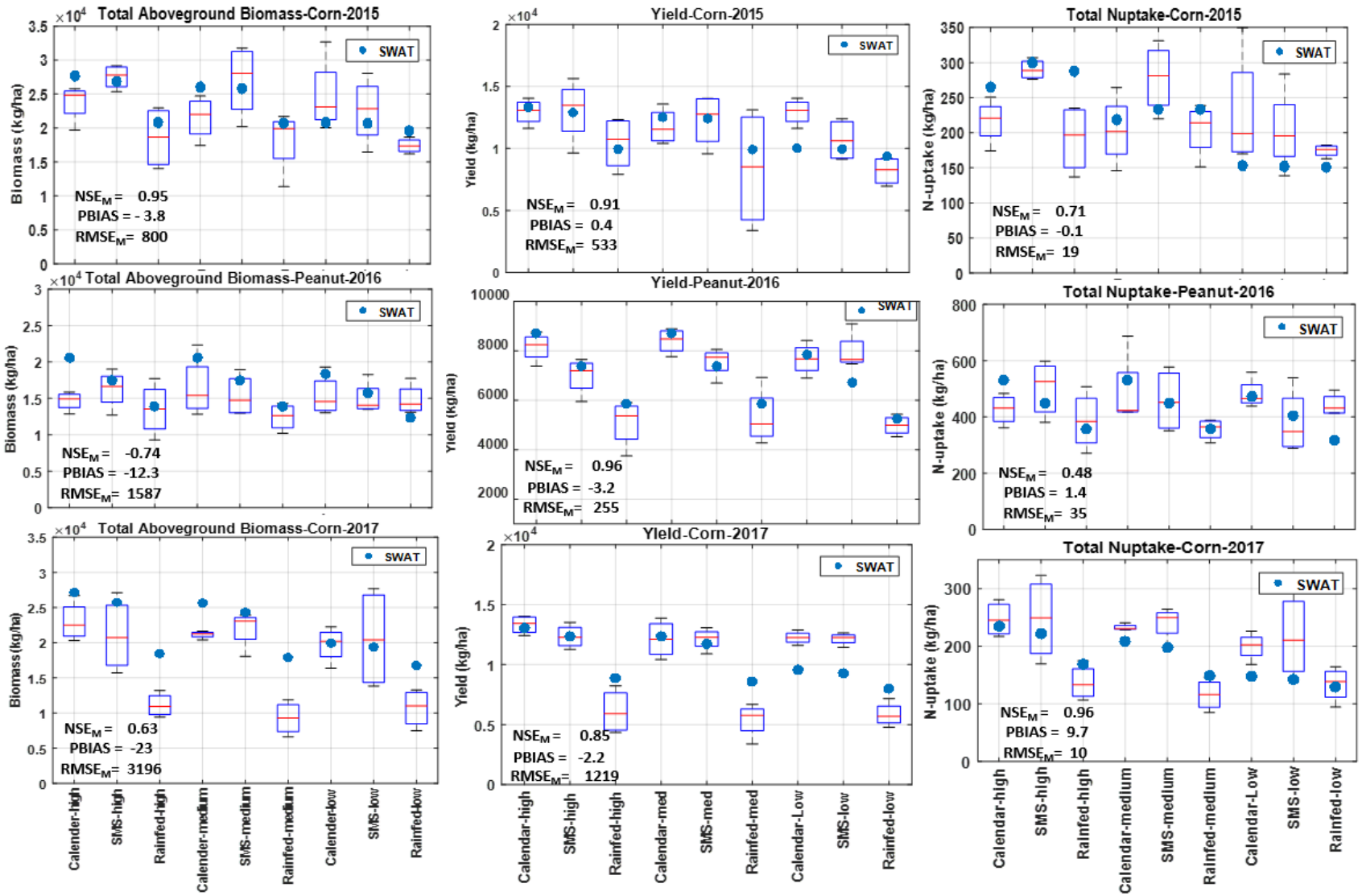

Figure 2-4. Simulated (dots) vs observed (boxplots) aboveground biomass, yield, and N uptake for corn 2015-peanut 2016-corn 2017 for System 1. Model performance statistics evaluated were NSEM, PBIAS (%) and RMSEM (kg/ha).

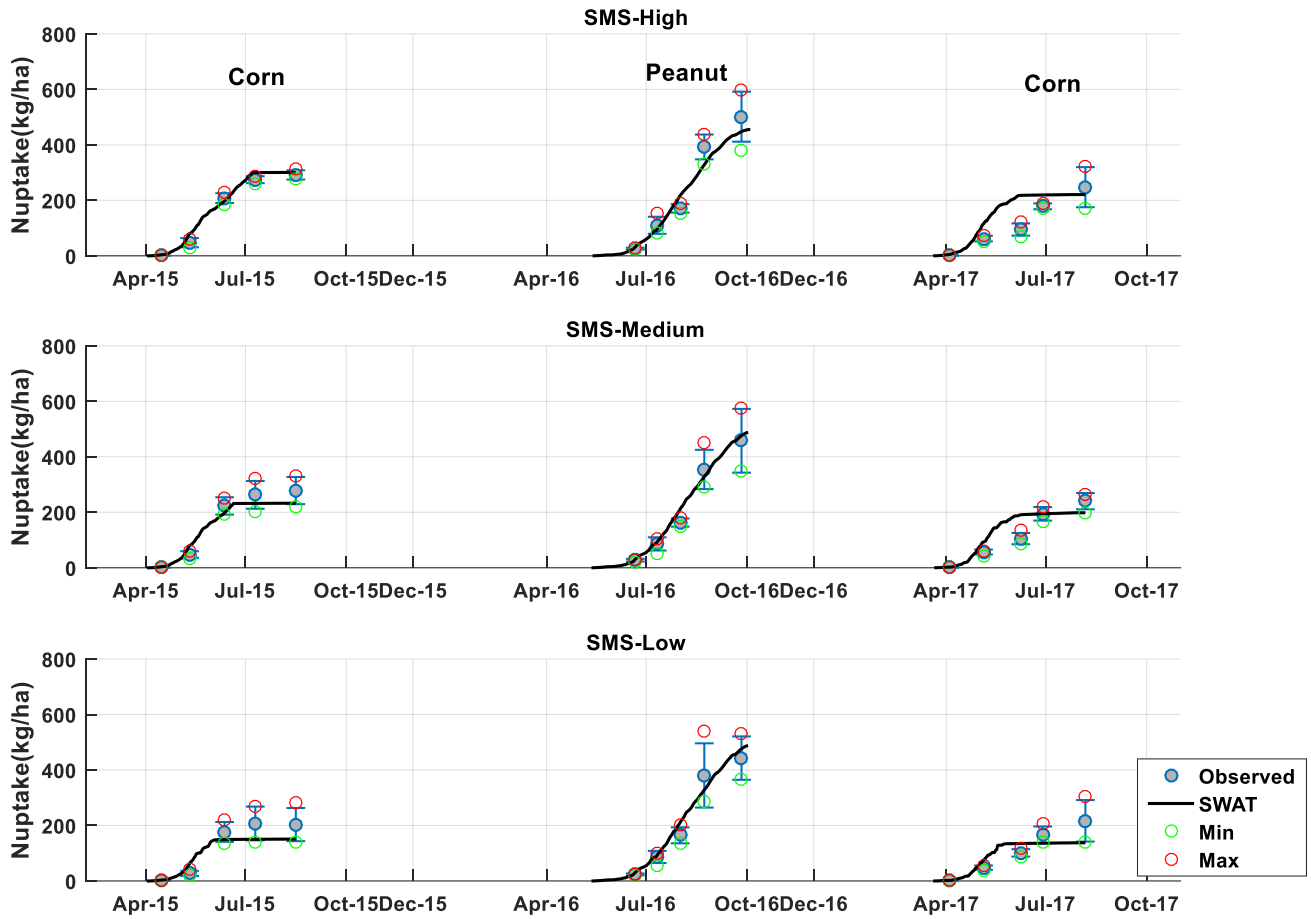

Figure 2-5. Simulated (line) vs observed (dots) N uptake during crop growing seasons for SMS-high, medium, and low in System 1. The experimental variation shown is the minimum and maximum of the field measurements (error bars).

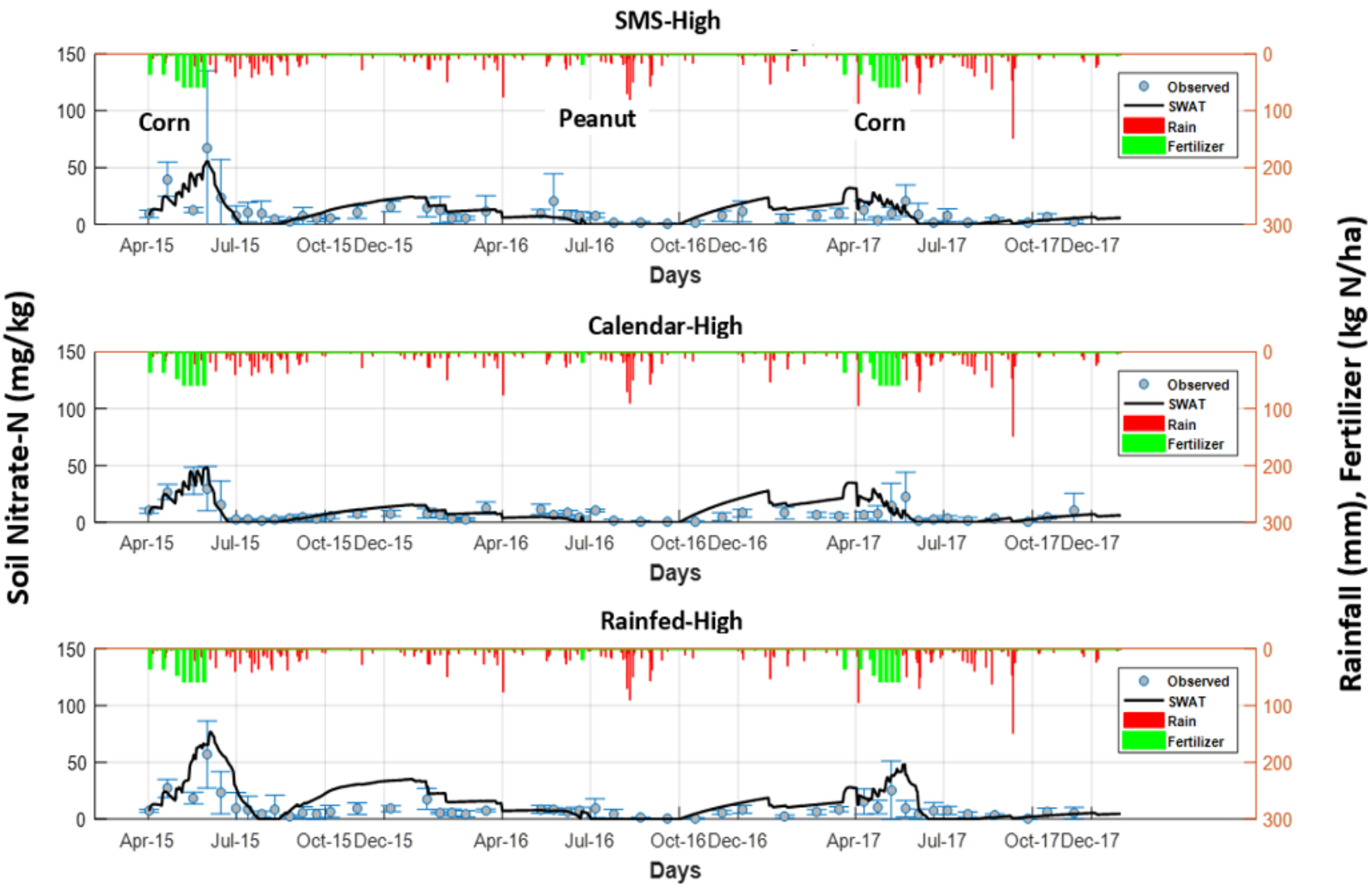

Figure 2-6. Observed (dots) vs simulated (lines) soil nitrate-N in root zone (0-900 mm) for SMS, Calendar and Rain fed -High treatments for System 1. Red and green bars denote daily rainfall and fertilizer applications. Vertical error bars correspond to the standard deviation of measured data.

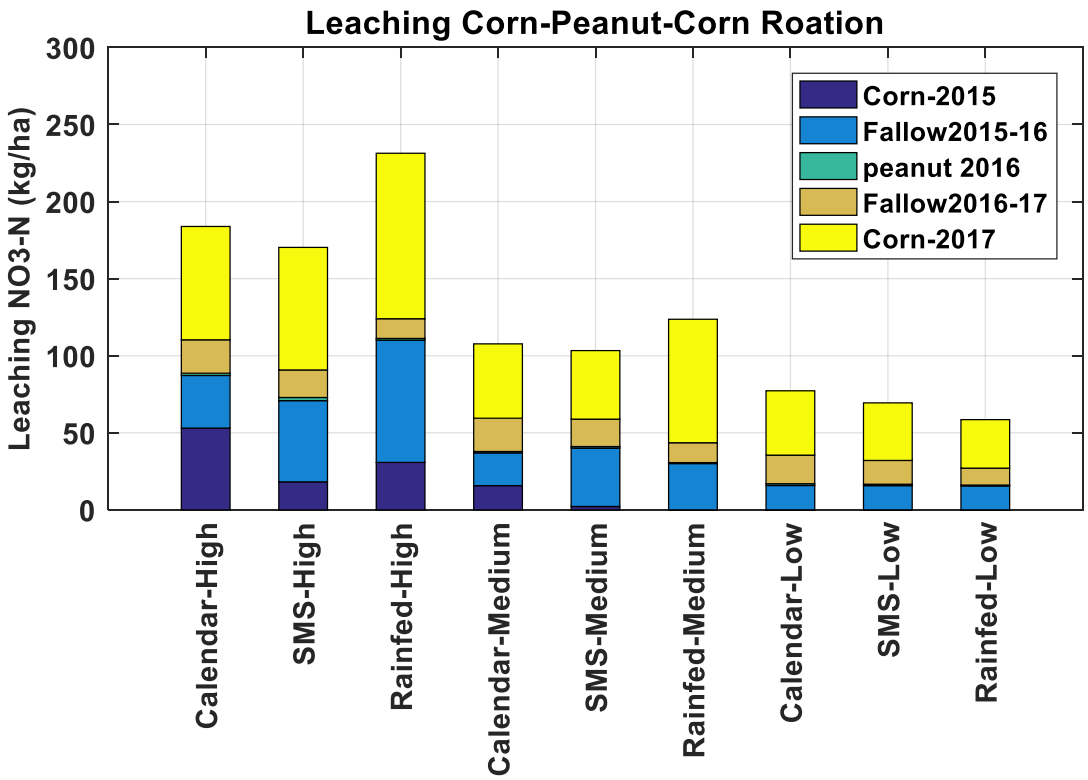

Figure 2-7. Simulated nitrate-N leaching during complete crop rotation for System 1 (corn 2015-peanut 2016-corn 2017) including intercropping bare fallow periods (2015-16 and 2016-17).

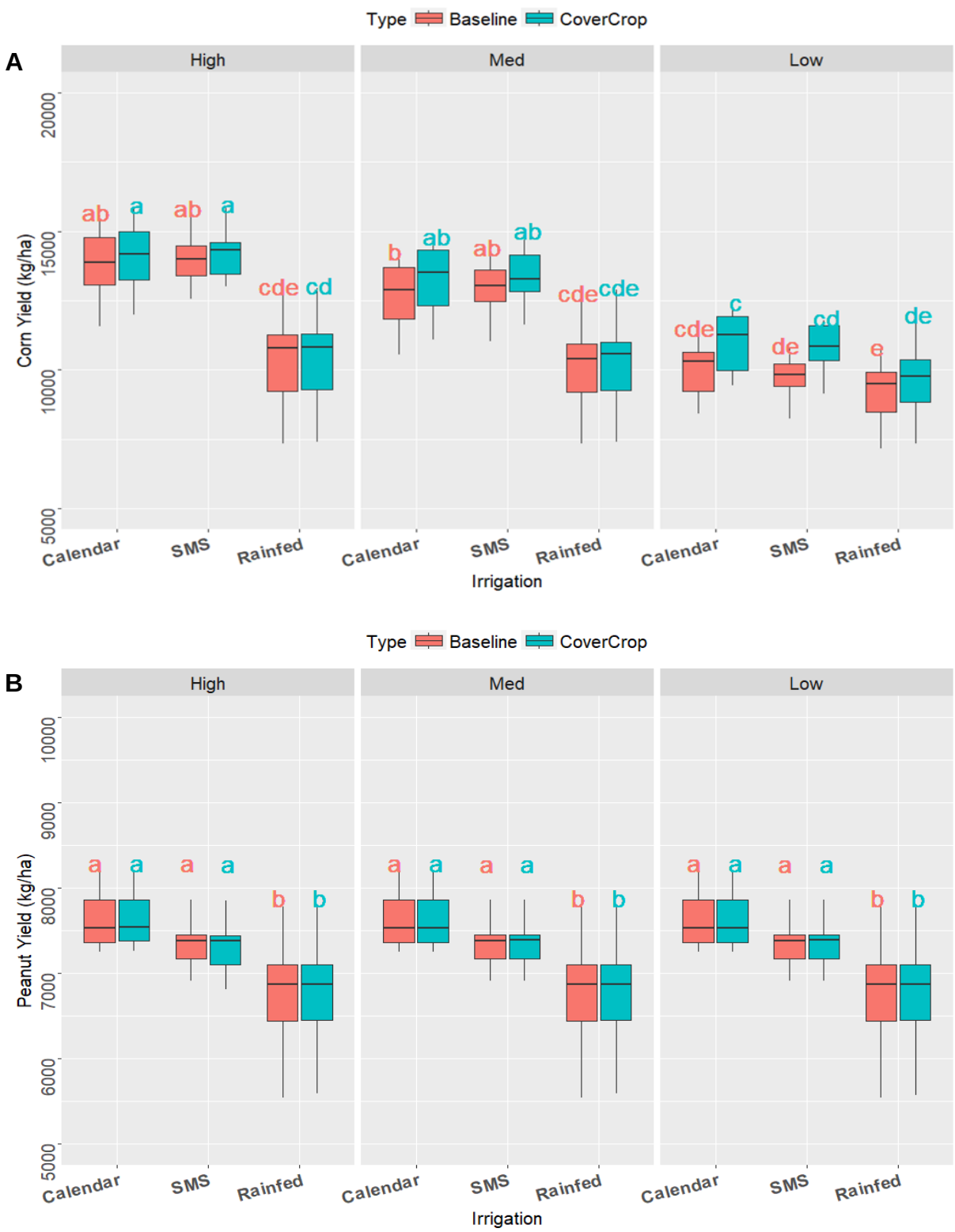

Figure 2-8. Long-term corn and peanut yield simulations with fallow (baseline) and with rye cover crop between cropping seasons across irrigation treatments (Calendar, SMS, and Rain fed) and N fertility rates (low, medium, and high). (A) Corn. (B) Peanut. Different letters indicate significant difference at α = 0.05 level.

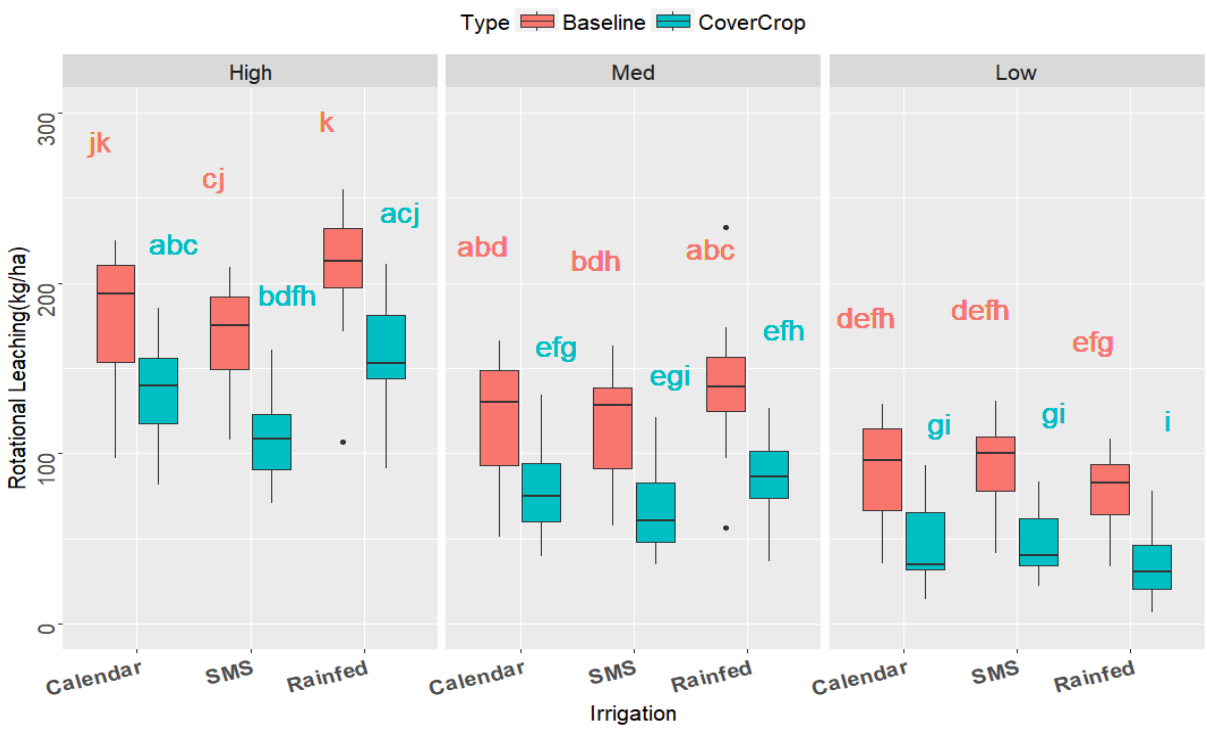

Figure 2-9. Long-term simulated N leaching over the crop rotation with fallow and rye cover crop between cropping seasons (corn-fallow/rye-peanut-fallow/rye). Different letters indicate significant difference at α = 0.05 level.

CHAPTER 3
IMPACT OF LAND USE AND LAND MANAGEMENT PRACTICES ON NITRATE LOADING TO GROUNDWATER IN SANTA FE RIVER BASIN

Background

Nitrate-nitrogen (NO_3-N) loading to groundwater is a chronic problem worldwide (Akhavan et al., 2010) due to its detrimental effects on the ecological health of springs, streams, and lakes (Mitsch et al., 1999; Bowen et al., 2007), as well as on human health (De la Monte et al., 2009). Multiple point and non-point sources contribute NO_3-N to groundwater, and agricultural land uses are recognized as a primary non-point source of groundwater NO_3-N pollution (Humenik et al., 1987; Spalding and Exner, 1993; Bower, 2000; Van Drecht et al., 2003; Vitousek et al., 2010). Application of synthetic fertilizer and manure to irrigated agricultural crops increases crop yields, however it can also result in NO_3-N leaching to aquifers, especially when applied in excess (Allaire-leung et al., 2001; Harter et al., 2002; Burow et al., 2010; Dahan et al.,2014). The problem of NO_3-N loading from non-point sources is particularly pronounced for karstic aquifers, which are characterized by discrete fractures conduits and carbonate rocks with high permeability and transmissivity (Vesper et al., 2001, Doerfliger et al., 1999).

The Upper Floridan aquifer (UFA), one of the most productive karstic aquifers in the world, is a major source of public water supply and irrigation in north and central Florida (Bush and Johnson 1988). The Santa Fe River, a tributary of Suwanee River located in north central Florida, overlies the UFA. The Santa Fe River Basin (SFRB) spans a transition zone between confined and unconfined regions of the Floridan aquifer system (Hunn and Slack 1983; Upchurch et al., 2008; Srivastava et al., 2014). The unconfined karst region has numerous springs that feed the Santa Fe River, supporting an important ecological and economic resource (Borisova et al., 2014;

Rosneau et al., 1977). Over the past several decades, the degradation of spring water quality has become a serious environmental concern (Nolan and Stone, 2000; Kingsbury, 2008; Obeidat et al., 2008; Siliang et al., 2010), as NO_3-N concentrations in UFA springs and rivers have increased from background concentrations of ≤0.1 mg/L NO_3-N to above 5 mg/L NO_3-N in some springs over the last 40 years (Katz et al., 1999; Katz, 2004). In response to increasing NO_3-N concentrations and spring ecosystem degradation, a Numeric Nutrient Criteria (NNC) of 0.35 mg/L NO_3-N as an annual geometric mean has been set by Florida Department of Environment Protection (FDEP) for groundwater emanating from UFA springs (62- 302.530 (47) (b), F.A.C.; FDEP, 2013). Total Maximum Daily Loads (TMDLs; US Environmental Protection Agency, 2016) estimated to achieve the NNC have been established for UFA springs, and Basin Management Action Plans (BMAPs) have been (or are being) established for waterbodies not meeting the NNC. Overall, NO_3-N load reductions required to meet the NNC in Santa Fe River Basin range from 35% (FDEP, 2012) to 65% (FDEP, 2018).

Agriculture and silviculture are the predominant land uses that overlie the UFA in north Florida and increasing NO3-N in surface and groundwater in the region has been attributed to agricultural land uses such as row crops, cow-calf operations, dairy, and poultry farms (FDEP, 2012; Marella, 2014; FDACS, 2015a; Harrington et al., 2010; Hochmuth et al., 2014). Isotope studies (Katz, 2004; Henson et al., 2019) have determined that synthetic fertilizer is the dominant NO_3-N source in SFRB springs, indicating that changes in agricultural practices will be required to meet environmental standards. Land use and land management influence hydrological processes such as runoff, evapotranspiration, and groundwater recharge (Ghaffari et al., 2010; Parajuli et

al., 2013; Lin et al., 2015), as well as nutrient cycle processes such as crop N uptake, soil NO_3-N storage, denitrification, and leaching (Costa et al, 2002; Bossa et al., 2012; Shrestha et al., 2018). Several studies of row crops, hay, and grazing pasture operations have been conducted at the field scale in the SFRB to quantify interactions among water and nutrient management, crop yields, water use, crop N uptake, and environmental N losses (Zamora-Re et al., 2018; Vendramini et al., 2006; Mylavarapu et al., 2016). Generally, these studies have found that targeted best management practices (BMPs) can reduce both irrigations applied, and NO_3-N leached to groundwater relative to conventional methods (Zamora-Re et al., 2018; Rath et al., 2020). However, developing improved land use and management practices that protect groundwater quantity and quality while maximizing agricultural production requires that these studies be scaled up to consider the temporal and spatial variability of NO_3-N load, fate, and transport across the watershed.

Accurate assessment of NO_3-N load to groundwater from different land uses is a critical step in developing effective N control programs (Lindgren et al., 2007; Carpenter, 2008; Eller et al., 2017). However, the spatial variation of soil and aquifer properties, topography, land use, and water and nutrient management practices add uncertainty to the estimation of NO_3-N load and its subsequent fate and transport at the watershed scale (Shen et al., 2014, Liu et al., 2016). Previous field experiments and modeling studies have made efforts to precisely estimate the relative contribution of NO_3-N load from various land uses to karst spring systems in Florida. Eller et al. (2017) developed “The Nitrogen Source Inventory and Loading Tool” (NSILT), a simple spreadsheet-based tool that estimates NO_3-N load from different point and non-point sources

considering N applied to the land surface and subsurface N attenuation. Application of NSILT to the SFRB indicated that inorganic fertilizer sources from agriculture land are the dominant NO_3-N load to receiving waters. NSILT subsurface NO_3-N attenuation through N uptake, denitrification and other gaseous losses were estimated from the literature to be approximately 50%-85% for row crops (Hochmuth, 2000; He et al., 2011; Liu et al., 2013), 80%-95% for livestock operations (Woodard et al., 2006; White-Leech et al., 2013), and 40%-75% for septic systems (EPA, 2002; Costa et al., 2002; Katz et al., 2009). While useful for first-order approximation, these attenuation factors do not consider the spatiotemporally variable hydrological and biochemical processes governing migration and transformation of NO_3-N from the root zone to its arrival in receiving water bodies. The NSILT approach also does not account for legacy NO3-N load resident in soils and groundwater from past decades of agricultural operations. Another similar catchment-scale N budget model study for the Silver Springs springshed in central Florida conducted by Jawitz et al., (2020) estimated that ~90% of N input to the landscape was removed before reaching the spring (64% removed by plant uptake and denitrification in surface soils, 20% by denitrification in the vadose zone, and 6% by denitrification in the aquifer). Prasad et al., (2016) and Desormeaux et al., (2019) assessed N attenuation by denitrification in the soil zone using *in-situ* measurements, however none of these studies examined the spatiotemporal variability of attenuation across the watershed. The spatial distributions of weather, soils, landuse, management practices, and water table depth play an important role in driving the hydrology and biogeochemical conditions that govern NO_3-N transport and transformation (Wang et al., 2020). Due to these complexities, distributed watershed scale hydrological -water

quality models are often employed to quantify nutrient loads to receiving waterbodies and to predict the effects of land-use and management changes (Chen et al., 2013; Liu et al., 2013; Shen et al., 2013; Wang et al., 2019).

Physically based, watershed-scale hydrology and water quality models such as the Soil and Water Assessment Tool (SWAT; Arnold et al.,1998), Agricultural Nonpoint Source model (AGNPS; Young et al.,1988), and Hydrological Simulation Program-FORTRAN (HSPF; Bicknell et al., 2001) have been employed to evaluate land use and management practices in watersheds around the world (Niraula et al., 2012; Chen et al., 2018; Wang et al., 2019). SWAT was selected for this study because it is a processed-based watershed-scale agro-hydrological model that has been applied throughout the world to simulate plant growth processes, agricultural production (Ullrich and Volk, 2009), hydrologic and water quality processes (Pisinaras et al., 2010), land use and climate change impacts on water resources (Varanou et al., 2002) and water-related ecosystem services (Psaris et al., 2012), and to identify critical pollution source areas (Panagopoulos et al., 2011). SWAT has been used to simulate nitrogen loads to receiving water bodies at time scales ranging from daily to annual (Jha et al., 2007; Ficklin et al., 2013; Boithias et al., 2014).

The objectives of this study are to: 1) quantify the water and nitrogen budgets for current land uses and water and nutrient practices throughout the SFRB to to help identify priorities for load reduction, 2) predict the spatiotemporal pattern of water flux , NO_3-N loading, transport and transformation from the root zone, through the aquifer, to the Santa Fe River for different land uses and water and nutrient management practices and 3) evaluate the potential for alternative land use and water and nutrient

management practices to achieve the approximately 65% reduction in NO_3-N load estimated to be required to achieve the NNC in streams in the SFRB. This work provides a framework for developing and evaluating strategies for achieving stringent water quality regulations while maintaining a robust agricultural economy that is transferrable to other agricultural watersheds throughout the world.

Materials and Methods

Study Area

The Santa Fe River Basin (SFRB) is a 3584 km^2 tributary basin of the Suwanee River (Figure 3-1. A) located in north central Florida, USA. Hydrogeomorphic characteristics of the SFRB vary from upstream to downstream. The upstream portion of the watershed is 30-86 meters above mean sea level (masl), with poorly drained soils that are separated from the underlying Floridan aquifer by a confining clay layer (Figure 1B) (Arthur et al., 2005). The downstream portion ranges from 2-30 masl, with well drained sandy soils directly overlying karstic topography (Figure 3-1.C). The area has a hot, humid climate, with average annual rainfall of 1356 mm (most rain occurs from May through October) and a mean annual temperature of 24^0 C (Frisbee, 2007; Srivastava et al., 2014). Regional groundwater movement in SFRB is generally from higher elevations in the east toward the Suwanee River in the west (Figure 3-1. B). Notably, the upstream (confined) portion of the watershed has a distinct stream network, while surface drainage in the downstream (unconfined) portion of the basin is primarily limited to the main Santa Fe River. Poorly drained soils in the confined zone result in a high surficial water table and considerable surface runoff, while fine sandy soils in the unconfined region result in rapid infiltration and are vulnerable to NO_3-N leaching (Upchurch, 2007).

Primary economic activities in the study area are silviculture and agriculture (Grubbs et al., 2007). Forest plantations (36% of basin area) and agricultural lands including row crops, hay, and pasture (21%) account for most of the land use in the study area, although wetlands (16%) and natural grass and shrublands (19%) also cover a large part of the study area (Figure 4). In addition to agricultural and silvicultural lands, NO_3-N sources in this watershed include septic tanks and atmospheric deposition.

SWAT Model

The Soil and Water Assessment Tool (SWAT) (Arnold et al., 1998) is a physically based, semi-distributed, multi-scale model developed by the Agricultural Research Service of United States Department of Agriculture (USDA-ARS) to simulate continuous hydrological and nutrient cycles (Gassman et al., 2007; Arnold et al., 1998; 2015). SWAT has been widely used to predict long-term impacts of changes in land use and management practices on water availability and quality by simulating different crop rotations with a variety of irrigation and fertility practices (Arabi et al., 2008; Srinivasan et al., 2010; Parajuli et al., 2013; Gao et al., 2017) and simulating alternative grazing operations (Zadsar et al., 2016; Park et al., 2017). To represent spatial heterogeneity, a watershed is divided into sub-basins, which are further subdivided into hydrologic response units (HRUs), where each HRU contains a single soil, slope range, and land use producing unique hydrological characteristics (Neitsch et al., 2009). An HRU is the basic calculation unit within the SWAT model. Different hydrological and biogeochemical processes are aggregated to the subbasin level by calculating area-weighted averages from all HRUs within a subbasin. Major hydrological processes including evapotranspiration, canopy storage, infiltration, surface runoff, lateral

subsurface flow and percolation are simulated at HRU scale. In this study, surface runoff and infiltration were estimated using the NRCS curve number (CN) procedure (SCS, 1972), and potential evapotranspiration was estimated using the Penman-Monteith method (SWAT, 2019). The crop growth model in SWAT is based on a simplification of the EPIC crop model (Williams et al., 1984) in which the phenological development of the crop is based on daily heat unit accumulation.

SWAT models nitrogen (N) in the vegetation, soil profile, surface water, and in the shallow aquifer (Arnold et al. 1998). Nitrogen may be added to the landscape by fertilizer, crop residue, animal waste, and atmospheric deposition, and it can be removed by plant uptake, volatilization, denitrification, and export in streams. NO_3-N mass in the soil results from five processes: (1) nitrification (conversion of NH_4-N to NO_3-N), (2) addition of manure and N fertilizer, (3) mineralization of soil organic N, (4) biological N fixation, and (5) mineralization of crop residue N (Neitsch et al., 2011). NO_3-N transport is modeled by first supplying available NO_3-N within the soil to plants. Remaining NO_3-N in the soil zone may then be denitrified or transported from the soil zone via runoff, lateral subsurface flow, or percolation (Santhi et al., 2006). NO_3-N losses in the aquifer due to denitrification are modeled as a first order process using a defined half-life (Neitsch et al., 2011).

Data Sources

ArcSWAT (Version 2012/Rev 664) was used to set up and parameterize the SFRB model. The key spatial input files included a digital elevation model (DEM), land cover, soil map and weather (Table 3-1). Daily discharge data from USGS gauging stations at Worthington Springs, Fort White, and Hildreth (Figure 3-1, Table 3-1) were used for calibration and validation of SWAT predicted streamflow. The USGS SSEBop

daily actual evapotranspiration (ET_a) product (Senay et al, 2013) was aggregated to monthly values (Table3-1) and used to validate SWAT-predicted ET_a at the watershed scale. Monthly stream NO_3-N concentrations measured at Worthington Springs and Fort White were used for stream NO_3-N load calibration (Table 3-1). Monthly NO_3-N load was calculated from observed monthly NO_3-N concentration and average monthly discharge. Due to insufficient discharge and NO_3-N concentration data, Hildreth was not included in the NO_3-N calibration process. Crop yield and N uptake data were validated against field experimental data (Zamora-Re et al., 2018, 2020; Kiniry et al., 2007).

Land Cover Dataset

The US Department of Agriculture National Agricultural Statistics Service (USDA-NASS) Cropland Data Layer (CDL) for 2017 was used as the base-year land cover for the SFRB. However, the 2017 CDL did not differentiate pastureland into either grazed or un-grazed. Therefore, an aggregate land cover classification was developed by combining the CDL with the Florida Statewide Agricultural Irrigation Demand (FSAID) 2017 land use map (www.fdacs-fsaid.com). Using FSAID, pastureland cover within the CDL was expanded into two classes: un-grazed land included in the deafult grass land of bermuda grass and grazed land as bermuda grass with livestock grazing and fertilizer application. Roads from the urban land cover were excluded and reassigned to neighboring land covers to eliminate a large number of very small HRUs (Teshager et al., 2016). Septic tanks were considered as a separate land use class to measure their standalone contribution to NO_3-N loading.

Septic tank point shape files were taken from the Florida Geographic Data Library (FGDL; https://www.fgdl.org/metadataexplorer/explorer.jsp) and converted to

rasters and combined with the CDL and FSAID coverage (Figure 3-2) following methods adopted by Jeong et al., (2011), Hoghooghi et al., (2017), and Paul et al., (2017).

Soil Map

A SSURGO soil map was created by aggregating detailed county scale maps, which consist of more than 100 types of soil (Figure 3-3).

Weather Data

Daily weather data (precipitation, minimum and maximum temperature, wind speed, and solar radiation) were obtained from the North American Land Data Assimilation System (NLDAS-2) climate forcing dataset. NLDAS-2 has a spatial resolution of 1/8th degree covering the continental United States and is available at 1-hour temporal resolution (Xia et al., 2012). A total of 24 weather grids are contained within the watershed.

Water and Nutrient Management Practices

Water and nutrient management practices must be specified for each land use to obtain accurate predictions of water quantity and quality at the watershed scale. However, collecting detailed spatiotemporal information regarding field-scale management across watersheds is difficult. Therefore, a range of practices representing different agricultural land uses in the SFRB (row crops, hay and pasture) were defined based on in-depth consultation with stakeholders and Extension agents as well as previous studies in this region (Zamora-Re et al., 2020; FDEP BMAP 2012; 2018). Table 3-2 summarizes the range of current management practices for agricultural land uses, ranging from high to low N fertilizer and irrigation application. Management System 3 (MS3) represents conventional, higher-input practices historically applied in the region; MS2 represents improved water and nutrient management approaches

adopted more recently (including soil moisture sensors for triggering irrigation); and MS1 represents the best management practices that are considered economically feasible with currently available technology. For production forests, we assumed slash pine forest management with no fertilization, no irrigation, no thinning, and a 36-year rotation length.

For calibration, it was assumed that conventional, higher-input practices (MS3) were applied for all agricultural land uses. This simplifying assumption was motivated by the timeframe for calibrating and validating modeled stream NO_3-N predictions to observations (2000-2018) and the fact that groundwater emerging from springs in the SFRB has been estimated to be approximately 20 years old (Katz et al., 1999; Katz, 2004) (i.e., having entered as recharge between 1980 and 1998). Taken together with the observation that peak fertilizer sales occurred in the region in the 1970s-1990s (Katz et al., 2001), it is thus reasonable to consider that surface water NO_3-N loads observed during our simulation period were dominated by aquifer loadings during periods of high-input management. The sensitivity of results to this assumption is discussed in water quality sections.

In addition to simulating conventional practices (MS3), three additional scenarios were analyzed to evaluate the impact of changes in land use and water and nutrient management on NO_3-N loads, fate, and transport in the SFRB: 1) application of MS2 for all existing agricultural land uses in the watershed; 2) application of MS1 for all agricultural land uses in the watershed; and 3) conversion of the entire watershed to slash pine forest production. The MS2 scenario reduced N fertilizer application by 15% for row crop rotations, 25% for hay, and 37% for pasture over MS3 and included an oat

cover crop in the row crop rotation. The MS1 scenario reduced N fertilizer application by 28% for row crop rotation, 68% for hay, and 50% for pasture over MS3 and included a rye cover crop in the row crop rotation. The slash pine scenario was used to verify that the calibrated model would accurately simulate stream NO_3-N concentrations of ≤0.1 mg/L that are currently observed in forested watersheds in the region (Maddox et al., 1992; Katz et al., 2009; FDEP, 2010) and to estimate the NO_3-N load reduction that would be realized by removing agriculture from the basin.

Previous studies have estimated that NO_3-N load from septic tanks is approximately 12% of total NO_3-N load in the SFRB (Eller et al., 2017; Katz et al., 2009), and septic tank loads were included in the MS1, MS2, and MS3 scenarios. An input factor of 4.08 kg-N per person per year (United States Environmental Protection Agency (EPA), 2002) and average of 2.5 people per household septic tank were assumed. Atmospheric N deposition was also considered as a NO_3-N source in the watershed (Katz et al., 2004) for all scenarios. Rainfall was assumed to contain 0.65 NO_3-N mg/L based on the annual average value (2000-2018) measured at the Bradford Forest National Atmospheric Deposition Program station in the SFRB (http://nadp.slh.wisc.edu/data/sites/; Schwede and Lear, 2014).

Model Setup and Calibration

Land use and soils maps were used along with a 30-m DEM to construct sub-basins and HRUs. SWAT delineated the watershed into 31 sub-basins and further divided each sub basin into HRUs based on similar land use, soil, and slope class (Figure 3-4). Five slope classes were defined (<5%, 5-15%, 15-25%, 25-50% and >50%) to create a total of 13,880 HRUs, using a 0% coverage threshold for land use, slope, and soil (Neitsch et al., 2011).

Since N fate and transport depends strongly on the accuracy of water flows (Pohlert et al., 2007; Ferrant et al., 2013; Epelde et al., 2016), a sequential method for watershed calibration (Santhi et al., 2006; Arnold et al., 2012; Daggupati et al., 2015) was followed by first calibrating stream flow and then nutrient load using both automatic and manual calibration (Arnold et al., 2012; Glavan et al., 2010). Before calibration, a sensitivity analysis was performed to identify model parameters that govern the important processes used for calibration and validation (Gassman et al., 2007; Ercan et al., 2014; Hamby ,1994; Lenhart et al., 2002). Sensitivity analysis, calibration, and validation were all conducted using the Sequential Uncertainty Fitting version 2 (SUFI-2) algorithm in the SWAT Calibration and Uncertainty Program (SWAT-CUP) program. The ranges of parameters governing streamflow were selected based on the SWAT-CUP manual (Abbaspour et al.,2015), peer-reviewed SWAT literature studies (Santhi et al., 2001; Gassman et al., 2007; Yang et al., 2016; Brighenti et al., 2019; Liang et al., 2020), and regional knowledge.

Given the distinct regional hydrogeological features across the SFRB (Figure 3-1), a spatially structured calibration procedure was followed (Mechal et al., 2015; Liu et al., 2019). Hydrogeologically, the watershed can be divided into three zones (Figure 3-1), and the three gauging stations along the Santa Fe River account for the cumulative water draining from each zone via surface flows. The model was calibrated and validated for daily streamflow beginning with the upstream station and moving toward the watershed outlet. Specifically, sub-watersheds contributing to flow at Worthington Springs (upstream) were calibrated first, and the resulting parameters were held constant while the sub-watersheds contributing to flow at Fort White were calibrated.

The same process was used then applied to calibrate sub-watersheds contributing to flow at Hildreth (downstream). Model parameters were adjusted separately for sub-watersheds in each hydrogeological region to improve the objective function, and streamflow calibration was considered satisfactory when measured and simulated values were within ±15 percent bias (PBIAS), coefficient of determination (R^2) > 0.60, and the Nash-Sutcliffe efficiency coefficient (NSE) was > 0.5 (Moriasi et al., 2015). After the three zones were sequentially calibrated, the complete watershed model was rerun to check the statistics of the objective function and the interaction of parameters across zones.

The land use and management systems were assumed to remain constant for the entire simulation period during calibration and validation. Crop (corn, peanut, Bermuda grass) and slash pine forest growth parameters were derived from field-scale SWAT models calibrated using experimental data from the region (Rath et al., 2020; Graetz et al., 2006; Kiniry et al., 2007; Haas, 2020). As an additional check on the calibrated hydrologic and crop parameters, simulated monthly actual evapotranspiration data (ETa) was validated against monthly USGS SSEBop ETa data (Table 3-1) aggregated over the watershed, and simulated crop yields were compared against experimental data. Reproducing streamflow, ETa, and crop yield increases confidence that the model is adequately representing plant biomass dynamics and the partitioning of water between soil storage, actual evapotranspiration, and aquifer recharge (Faramarzi et al., 2009, 2010). The calibration period was from 2000-2011, and validation period was from 2012-2018, with a warmup period of eight years (1992-1999; excluded from analysis) to stabilize the soil water and NO_3-N balance.

After streamflow calibration, monthly NO_3-N load was calibrated and validated at Worthington Springs and Fort White to estimate N parameters in the confined and unconfined regions, respectively. The evaluation of model performance on NO_3-N load calibration and validation was considered satisfactory when monthly statsistics of R^2>0.30, NSE > 0.35 and PBIAS ≤ ±30% were obtained (Moriasi et al., 2015). As an additional check on calibrated N parameters, and to assess compliance with the NNC, the annual geometric mean concentration NO_3-N concentrations were calculated from the simulated daily NO_3-N load and streamflow values and compared to the observed annual geometric mean NO_3-N concentrations measured at both stations.

Similar to the flow calibration strategy, NO_3-N calibration was carried out sequentially for the Worthington Springs and Ft. White stations. Sensitive parameters were first identified using SWAT-CUP, and then appropriate ranges of sensitive parameters were constrained to conform with local knowledge from available measurements and estimates of internal SFRB processes such as crop/tree N uptake, environmental losses in the soil zone (including denitrification and leaching), and denitrification in the aquifer (Yen et al., 2014; Sullivan et al., 2015; and Epelde et al., 2016). Specifically, the following constraints were imposed when determining appropriate parameter ranges: crop N uptake limited to 50-70% of total N inputs (Lassaletta et al., 2014; Dosermeaux et al., 2019; Jawitz et al., 2020; Zamora-Re et al., 2018; Rath et al., 2020) environmental N loss (denitrification and leaching) from the soil zone limited to 20-35% of total inputs (Prasad et al., 2016; Desormeaux et al., 2019) denitrification loss within the UFA limited to 30-40% (Heffernan et al., 2012; Henson et al, 2019); and total N input loss in the aquifer limited to ~6% (Jawitz et al., 2020).

Partitioning of environmental losses in the soil zone between denitrification and leaching depends on many factors such as soil moisture content, soil organic matter, soil carbon, rainfall, and temperature (Costa et al., 2002; Galloway et al., 2004; Tague et al., 2008; Epelde et al., 2016). Knowledge that conditions in the unconfined and semi-confined regions (well drained sandy soil with low organic carbon) favor leaching over denitrification, whereas conditions in the confined region (saturated soils, higher organic carbon) favor denitrification over leaching was also taken into account when determining parameter ranges. Finally, crop N uptake across the watershed was compared with measured field data (Zamora-Re et al., 2018, 2020; Rath et al., 2020) to build confidence in the proportion of environmental losses relative to total N inputs.

Results and Discussion

Water Quantity

Table 3-3 summarizes the parameters used for streamflow calibration and their calibrated ranges. Eight of sixteen parameters CN2, ESCO, SOL_AWC, GW_DELAY, GWQMN, ALPHA_BF, and GW_REVAP were found to be sensitive ($p<0.05$). Percentage-based variations (relative changes with respect to default SSURGO value) for Curve Number moisture condition II (CN2), available water capacity (SOL_AWC), and saturated hydraulic conductivity (SOL_K) were used to maintain their spatial variability. Calibrated parameters were broadly reflective of the spatial variation in hydrogeological setting described above. For example, in the confined region, calibrated CN2 and AWC were increased over their default SSURGO values, leading to high evapotranspiration and overland runoff potential. Low values of GW_ DELAY and ALPHA_BF and high values of GWQMIN in this region cause rapid recharge to the shallow aquifer but relatively small base flow contributions to the river. On the other

hand, in the semi-confined and unconfined regions, calibrated CN2 and AWC values were decreased with respect to SSURGO, leading to low surface runoff and high infiltration potential, while high GW_DELAY, ALPHA_BF, and low GWQMN result in a relatively steady and continuous base flow contribution to the river.

SWAT predicted daily as well as monthly streamflow dynamics at the three gauging stations with calibration and validation statistics in the satisfactory to good range (NSE≥ 0.5, R^2≥ 0.6, PBIAS ±15%) except for PBIAS at Worthington Springs (Table 3-4, Figure 3-5). Specifically, SWAT overestimated daily and monthly streamflow at Worthington Springs during the calibration period (PBIAS -53% and -49%, respectively) and slightly during the validation period (PBIAS -17% and -15%, respectively), and in particular overestimated times of very low flow (<1 m^3/s) (Appendix Figure B-1). Nevertheless, acceptable PBIAS (±15%) values were obtained at downstream stations Fort White and Hildreth, for both the calibration and validation periods. At Worthington Springs SWAT underestimated the peaks of extreme flow events due to tropical storm Debby in 2012 and hurricane Irma in 2017. However, peak flows from these events were predicted more accurately at Fort White and Hildreth. It should be noted that Borah et al., 2006; Arnold et al., 2012; Gassman et al., 2014 also found in their studies that SWAT underestimated peak flows during extreme events. Simulated monthly ETa accurately reproduced MODIS estimated monthly ETa (USGS SSEBop) when aggregated over the watershed (NSE=0.7, PBIAS= 14%, R^2=0.83; Figure 3-6). Simulated annual average evapotranspiration (~800 mm) and recharge (~436 mm/year) was approximately 65% and 33% of annual rainfall which is in

consistent with previous values estimated for the region (Hunn and Slack, 1983; Bush and Johnston, 1988; Srivastava et al., 2013).

Water Quality

The sensitivity analysis of watershed N parameters identified the denitrification threshold water content (SDNCO), soil denitrification rate (CDN), organic N mineralization rate CMN, and groundwater denitrification half-life (HLIFE_NGW) as the most sensitive water quality parameters ($p < 0.05$, Table 3-5); findings that are consistent with other studies (Akhavan et al., 2010; Yuan et al., 2015; Sullivan et al., 2016; Malik et al., 2020). SWAT's representation of the N cycle makes denitrification and leaching a competitive process in the soil zone (Pohlert et al., 2005; 2007; Yen et al; 2014). SWAT is a cascading percolation model, which moves water downward into an underlying soil layer, when field capacity is exceeded. If SDNCO is set below field capacity (AWC), denitrification will continue after water percolation ceases, which may lead to a complete depletion of NO_3-N in the soil zone (Pohlert et al., 2005; 2007; Epelde et al., 2016). To avoid excessive denitrification in the well-drained soils of the SFRB, SDNCO was set at field capacity and then a constrained manual calibration was carried out for other parameters to fit monthly NO_3-N load at measured stations. As dictated by SWAT model structure, all calibrated water quality parameters except for the groundwater NO_3-N half-life (HLIFE_NGW) were assumed to be constant across the watershed. Notably, the calibrated half-life for denitrification in groundwater was ~50 days for Worthington Springs versus ~1300 days for Fort White, reflecting the higher potential for aquifer denitrification in the confined region where the water table is near the land surface and dissolved organic carbon is high (Reed et al., 2018)

Overall, the dynamics of observed and simulated monthly NO_3-N loads were similar for the calibration and validation periods at both stations (Figure 3-8). The model performance statistics were satisfactory for calibration at both Fort White and at Worthington Springs (NSE=0.35 - 0.46, R^2 0.42-0.50, PBIAS< ±15%, Table 3-4). For validation, the NSE and R^2 statistics were unsatisfactory at both stations (NSE -1.5 - 0.16, R^2=0.15), even though the PBIAS remained very good (PBIAS< ±15%). The flashiness of the NO_3-N load at Worthington Springs is reflective of the flashiness of flow predictions. Overprediction of NO_3-N load at Worthington Springs occurred during months with peak storm events due to hurricanes and tropical storms (e.g. 2012, 2017; Figure 3-8) and resulted in unsatisfactory NSE values during validation. For Fort White the monthly load was over-predicted for years 2012 and 2013 in the validation period. The frequency of measured data after 2012 was limited, which made satisfactory validation challenging. Less-accurate SWAT estimation of NO_3-N load than stream discharge has been reported in many studies due to inadequate data availability (Chaplot et al., 2005), uncertainty in discharge and concentration measurements (Dakhlalla and Parajuli, 2019), and inaccuracy in the assumptions of land management operations (Malik et al., 2020).

In spite of the challenges in reproducing monthly NO_3-N loads, Tukey's HSD analysis showed that the annual geometric mean NO_3-N concentrations at Worthington Springs were not statistically different from measured values in any year at Worthington Springs and were only statistically different from the measured value in 2003 at Fort White (Figure 3-9). SWAT accurately predicts that the annual geometric mean NO_3-N NNC of 0.35 mg/L is met at Worthington Springs where water tables are high, surface

runoff predominates and conditions are favorable for denitrification, but it is violated at Fort White where water tables are lower, groundwater recharge predominates, and conditions are not as favorable for denitrification.

The simulated NO_3-N mass balance at the watershed scale showed that total annual average NO_3-N inputs to the SFRB (27,684 tons/year) consist of synthetic fertilizer (48%), mineralization of crop residues and manure (42%), and atmospheric deposition (10%) (Figure 3-10 A). Annual average NO_3-N output was dominated by plant uptake (~68%), with other components including denitrification in soil (10%), denitrification in shallow aquifer (5%), outflow from the river (6%), and storage in the soil (11%) (Figure3-10 C). Of the NO_3-N leached from soil into groundwater (Figure 3-10 B), 45% denitrified in aquifer, before emerging in the river. The simulated watershed scale NO_3-N mass balance distribution is consistent with observations in the SFRB reported by others. For example, the SFRB Basin Management Action Plan (FDEP, 2018) estimated that atmospheric deposition in the basin ranges from 8-15% of total N input. Corn and peanut NO_3-N uptake data from field experiments conducted in the area (Zamora-Re et al., 2020; Rath et al., 2020) were compared to SWAT predictions of NO_3-N uptake and fell within the 25-75 percentiles of the simulated N distribution from 1980-2018 (Appendix Figure B-3). Heffernan et al., (2010) and Henson et al., (2019) reported 30-40% loss of NO_3-N in the UFA beneath the SFRB.

The simplifying assumption that the conventional practices of high N fertilizer application (MS3) were used for agricultural landuses throughout the simulation period (2000-2018) impacts the values of the calibrated nitrogen cycle parameters. In the SWAT model, after plant uptake the excess N either dentrifies in the soil or leaches to

groundwater where denitrification can also occur. More N input to the surface will cause more loading to the aquifer and may require higher dentrification to match observed NO_3-N concentration values in the river. In this study the inclusion of processes measured at field scale such as environmental loss (leaching and denitrification), N uptake and N load to streamflow was used to reduce the uncertainty in parameter estimation as much as possible. However, the assumption of MS3 practices throughout the calibration period will result in higher loss of N through denitrification to match river nitrate concentrations than if lower N input practices were assumed.

Spatial Analysis

Recharge, actual evapotranspiration, overland flow, lateral subsurface flow and baseflow generated at the HRU scale were averaged over the simulation period (2000-2018) to visualize the spatial variability of water balance components across the watershed (Figure 3-7). These figures reveal clear spatial patterns that are consistent with previous studies (Grubbs, 1998; Srivastava et al., 2013, Hunn and Slack, 1983), including: 1) more recharge in the unconfined and semiconfined zones (> 300mm/year) than the confined zone (0-300 mm/year); 2) more ETa in the confined zone (700-1600 mm) than in the unconfined and semi-confined zones (300-700mm), with wetlands and water bodies showing highest ETa in all regions; 3) more baseflow to the stream from the unconfined and semi-confined zones; and 4) more overland flow to the streams from the confined zone. Overall, SWAT simulations show that the Santa Fe River gets approximately 85% of its annual water yield from base flow, which is consistent with the findings of Hunn and Slack (1983). Base flow contributions ranging from 200 mm to more than 750 mm in the unconfined region provide significant opportunity for NO_3-N leaching from the soil zone and transport through the aquifer to the stream by baseflow.

Figure 3-11A and B illustrate the wide spatial variability of leaching and denitrification losses across the watershed (i.e., from 0 to >100 kg N/ha/year), with considerably more leaching occurring in the unconfined zone. Denitrification occurred throughout the watershed, with the highest rates in the confined zone. Figure 3-12 A and B show the relative magnitudes of annual average denitrification in, and leaching from, the soil zone across HRUs by land use for the confined and unconfined zones, respectively. Row crops and pasture have the highest leaching and denitrification losses per unit area in both the confined and unconfined zones, with the unconfined zone having slightly higher average leaching losses and slightly lower average denitrification losses than the confined zone. In both zones, hay has higher leaching than denitrification losses, whereas septic tanks have higher denitrification than leaching losses. Forests, wetlands, and other land uses (shrubland, natural grasses and barren land) have low leaching and denitrification losses in both zones.

Estimated annual average denitrification of ~45 kg N/ha/year and ~52 Kg N/ha/year in the soil zone beneath row crops in the unconfined and confined zones, respectively, are consistent with values of 20-80 kg N /ha from irrigated agricultural land reported in the literature (Simone et al., 2005; Eplede et al., 2015, 2016). Estimated average denitrification rates for forests, wetlands, and other land uses (4.6, 7.2, and 5.6 kg N/ha) are slightly lower than the 13 to 49 kg N/ ha reported by Sullivan et al., (2016) and Yen et al., (2014) for unmanaged (non-fertilized, non-irrigated) land uses. The annual average leaching from septic tanks in the unconfined and confined zones were estimated to be 4.8 kg N/ha/year and 2.4 kg N/ha/year, respectively, which are in the

range of to the 2.9 kg/ha/year estimated for the Silver Springs region in Central Florida by Jawitz et al., (2020).

Over the entire SFRB, the total estimated NO_3-N load leached to the aquifer was estimated to be 2783 tons/year (Table 3-6). Pasture contributed the greatest load to the aquifer (1541 tons/year, 55%) due to the relatively large land area assigned to pasture (12%) and leaching rate of ~48 kg N/ha/year. Row crops were the next largest contributor (632 tons/year, 22%) with a smaller land area and leaching rate of ~45 kg N/ha/year, followed by forests (278 tons/year, 10%), which cover a large proportion of the basin (36%) but have low leaching rates of 4.8 kg N/ha/year. Of the agricultural land uses, hay contributed the smallest load (222 tons/year, 8%). The very high leaching rates for few pasture and row crop HRUs (Figure 3-11) are due to high recharge simulated from low soil available water content (Soil_AWC). However, the contributing area of these regions is less than 1% of the watershed, so there was negligible effect on the total leaching to the groundwater.

Scenario Analysis

Figure 3-13 A shows annual average leaching per unit area across HRUs for each land use across scenarios. The MS2 scenario reduced mean annual average leaching from row crops by ~40%, pastures by 44%, and hay by 15% compared to the conventional practices (MS3) used for calibration. The MS1 scenario reduced annual average leaching from row crops by 65%, pastures by 50% and hay by 15% compared to the MS3 conventional practices. When aggregated across the watershed, the MS1 and MS2 scenarios reduced total leaching to groundwater by ~43% and ~34%, respectively compared to MS3 (Figure 3-13 B). Moving from MS3 to MS1 reduced the pasture contribution of the total from 55% to 46%, the row crop contribution of the total

load from 22% to 14% and increased the forest contribution to total load from 10% to 16% (Figure 3-13 B). Converting the entire watershed to slash pine forest reduced the total leaching to groundwater to 492 tons/year, an ~80% reduction over the MS3 scenario. The surface water NO_3-N load in the river at Fort White was reduced from 755 tons/year for MS3, to 588 tons/year for MS2, to 522 tons/year for MS 1, and to 140 tons/year for the slash pine scenario. As a result, NO_3-N concentrations at Fort White were reduced from an average annual geometric mean of 0.79 mg/L (monthly concentration ranging from 0.45 to 1.4 mg/L) for MS3, to 0.57mg/L (0.32 to 0.96 mg/L) for MS2 and to 0.5mg/L (0.28 to 0.87 mg/L) for MS1, all of which are above the NNC criteria of 0.35 mg/L NO_3-N (Figure 3-14). In contrast, the slash pine-only scenario reduced simulated stream NO_3-N concentration to an annual average geometric mean of 0.11 mg/L (0.06 to 0.24 mg/L), consistent with concentrations currently observed in forested conservation lands in the region (Maddox et al., 1992; Katz et al., 2009; FDEP, 2010).

Conclusions

Accurate quantification of NO_3-N loading to springs and rivers in karst watersheds is a major challenge due to heterogeneity in soils, geology, land use and land management practices. In this study, a Soil and Water Assessment Tool (SWAT) model was calibrated and validated to predict the sources, fate and transport of NO_3-N in the karstic SFRB. Despite the watershed complexity, SWAT satisfactorily predicted monthly streamflow (NSE=0.62-0.78), monthly evapotranspiration (NSE=0.70), and annual geometric mean NO_3-N concentrations (no statistical difference in 17 of 18 years for the 2000-2018 time-period).

Model results estimated that of the total NO_3-N added to the SFRB through atmospheric deposition, fertilization and mineralization, approximately 68% is removed by plant uptake, 10% by denitrification in the soil and 5% by denitrification in groundwater before reaching the Santa Fe River. Furthermore, model results indicated that leaching from grazed pasture, row crops, forests and hay currently contribute approximately 55%, 22%, 10% and 8% of the total NO_3-N stream load respectively. Scenario analyses showed that adoption of agricultural best management practices that are considered economically feasible with currently available technology throughout the watershed has the potential to reduce total NO_3-N load to the Santa Fe River by approximately 31%, but that this would not be adequate to meet the NO_3-N Numeric Nutrient Criterion (NNC) that has been established to protect springs and rivers in the basin. If entire watershed was converted to slash pine forest, model results indicate that the total NO_3-N load to the Santa Fe River would be reduced by 80%, achieving the NNC and returning the river to background concentrations observed in other forested watersheds in the region.

Results from this study show the significance of the assessment of different watershed processes such as recharge, leaching, and denitrification influenced by crop management, soil characteristics and hydrometeorological conditions on the estimation of nitrate load. The deduced N fluxes such as denitrification and leaching were indirectly validated by comparing with general ranges available from the past experiments conducted in the region and other literature values. However, in the future field measurements of N fluxes from different soil and agricultural land use types in the

SFRB (particularly pasture and row crops) should be obtained to improve the calibration and validation of the regional model.

Despite its simplified groundwater flow algorithms, SWAT reproduced the in-stream nitrate concentration reasonably well, which provides confidence in the quantification of nitrate loads to the stream from different land management practices. However, the groundwater residence times, and groundwater nitrate half-life calibrated for SWAT are unreasonably short. Furthermore, the SWAT delineated SFRB surface drainage basin did not cover the entire groundwater contributing area to Fort White that is estimated from potentiometric maps. Thus, while the direction and relative magnitude of changes in SWAT stream nitrate concentration predictions that would result from changes in management practices are robust, the timing and precise value of changes in stream nitrate concentrations are less reliable.

In future work, the SWAT model should be coupled with MODFLOW, MODPATH and/or RT3D (Reactive Transport in 3- Dimensions) to more accurately simulate the source, fate and transport of NO3-N through the Upper Floridan aquifer to the Santa Fe River. This will allow scientists, governmental regulators, agricultural producers, and nongovernmental organizations to more accurately 1) evaluate the regional crop production – water quality – water quantity tradeoffs associated with alternative land use and land and water management strategies; and 2) determine the lag time required to see the impact of improved management practices on reducing groundwater, spring and stream NO_3-N concentrations. Results of these efforts would provide a framework for developing effective, socially acceptable strategies for achieving stringent water quality

regulations while maintaining a robust agricultural economy that is transferrable to other agricultural watersheds throughout the world.

Table 3-1. Input data for model set up, calibration, and validation.

Data	Scale/Extent	Source
	Model Setup	
DEM	30 m raster	National Elevation Dataset, USGS, http://ned.usgs.gov/
Land use/land cover (2017)	30 m raster	USDA-NASS Cropland Data Layer, FSAID
Septic Tanks	Point shape files	Florida Geographic Data Library
Soil types	1:12,000 to 1:63,360 (30 m to 52 m)	Soil Survey Geographic Database (SSURGO) (USDA-NRCS, 2018), http://soildatamart.nrcs.usda.gov
Weather	Daily	NLDAS https://ldas.gsfc.nasa.gov/nldas
Crop and Forest Growth Parameters	Farm/forest scale	Experimental data (Zamora-Re et al., 2018, 2020. Graetz et al., 2006; Kiniry et al., 2007; Haas, 2020)
	Other data	
Calibration, Validation and Comparison		
Discharge: Worthington Springs, Fort White, Hildreth [a]	2000-2011 (calibration, Daily) 2012-2018 (validation, Daily)	Suwannee River Water Management District (SWRMD).
ETa	2000-2015 (validation, Monthly)	USGS SSEBop https://earlywarning.usgs.gov/ssebop/modis/daily
Crop (Corn and Peanut) Yield and N uptake, Bermuda Grass	2015-2017 (validation, Annual)	Experimental data (Zamora-Re et al., 2018, 2020; Graetz et al., 2006; Kiniry et al., 2007)
NO_3-N load (Worthington Spring [b] and Fort White [c])	2000-2011 (calibration, monthly), 2012-2017(validation, monthly)	Suwannee River Water Management District SWRMD
NO_3-N concentation (Worthington Spring [b] and Fort White [c])	2000-2018 validation (geometric annual mean)	Suwannee River Water Management District SWRMD

[a] Hildreth data available from 2008-2018. Worthington Springs was missing data between May - July in 2005 and 2006.
[b] monthly data, 118 data points available (2000-2011) and 30 data points available (2012-2018)
[c]: monthly data, 137 data points available (2000-2011) and 24 data points available (2012-2017)

Table 3-2. Agronomic practices assumed for the three Management Systems for corn-peanut rotation, hay, and pasture.

Management Systems	Crops	N fertilizer (kg/ha)	Irrigation scheduling method	Planting date	Harvest
		AGRR (Row Crops) (Corn-Peanut Rotation)			
MS3	Corn	336	Calendar	March 20th	August 5th
	Peanut	11.2		May 12th	October 2nd
*MS2	Corn	290	SWAT Auto irrigation (0.65 plant water stress threshold)	March 20th	August 5th
	Peanut	6.73		May 12th	October 2nd
**MS1	Corn	240	SWAT Auto irrigation (0.65 plant water stress threshold)	March 20th	August 5th
	Peanut	0		May 12th	October 2nd
			Hay		
MS3	Bermuda	89.7 (4 times/yr)	No Irrigation	-	4 times/yr [a]
MS2	Bermuda	89.7 (3 times/yr)	No Irrigation	-	4 times/yr [a]
MS1	Bermuda	112 (1 time/yr)	No Irrigation	-	1 time/yr
			Pasture (Grazed)		
MS3	Bermuda	89.7 (2 times/yr)	No Irrigation	-	[b]
MS2	Bermuda	112 (1 time/yr)	No Irrigation	-	[b]
MS1	Bermuda	89.7 (1 time/yr)	No Irrigation	-	[b]
			Forest		
	Slash Pine	No fertilizer	No irrigation		Rotation length 36 years[c]

[a] 6-week harvest interval, 80% biomass removal per harvest.
[b] Grazing 1 cow/0.81 ha; Consumption=9.07 kg/day/cow dry matter; Excretion=5.66 kg/day/cow dry matter, 9.07 kg hay/day/cow supplied from Nov to Feb. The amount of biomass that is reduced by trampling is 9.07 kg/day/cow.
c Rotation length:36 years-35 years growth (plant -Jan 1st harvest -Dec31st), one-year fallow, no thinning. *Oat cover crop planted after corn and peanut harvest with no irrigation. 2 tons of chicken litter applied to oats after peanut harvest only. Kill (incorporating 100% biomass) one month before next crop planting. ** Rye cover crop plantation (post corn and peanut harvest) with no fertilizer and no irrigation and kill (incorporating 100% biomass) one month before next crop planting.

Table 3-3. Parameters used for streamflow calibration.

Parameter	Description	Initial Range	Final Values		
			Subbasins: confined zone (5-7,10-13,16,19,23-25,29)	Subbasins: semi-confined zone (5-7,10-13,16,19,23-25,29)	Subbasins: unconfined zone (1-4,14,18,20,22,27,28,31)
v_SURLAG.bsn	Surface runoff lag time(days)	1-10	3		
		Hydrologic parameters			
r_CN2.mgt *c	Initial SCS runoff curve number for moisture condition II	-0.5 -0.2	0.05	-0.45	-0.5
v__OV_N.hru*s	Manning´s “n” overland flow	0.1-0.5	0.33	0.35	0.35
v_EPCO.hru	Plant uptake compensation factor	0.01-1	0.8	0.8	0.8
v_ESCO.hru *c *s *u	Soil evaporation compensation factor	0.01 - 1	0.34	0.54	0.57
		Soil Parameters			
r_SOL_AWC.sol *c *s *u	Available water capacity (mm H_2O/ mm soil)	-0.7 - 0.5	0.44	-0.51	-0.53
r_SOL_K.sol	Saturated Hydraulic Conductivity (mm/hr)	-0.2 - 0.2	0.09	-0.09	-0.1
		Channel Parameters			
v_CH_N2.rte	Manning's "n" value channel	0.014 - 0.3	0.013	0.13	0.13
r_CH_W2.rte	Average width of main channel	-0.01 - 0.3	-0.033	0.175	0.175
r_CH_S2.rte	Average slope of main channel	-0.2 - 0.2	0.073	-0.16	-0.16
		Groundwater Parameters			
v_GWQMN.gw *s *u	Threshold depth of for return flow(mm)	0-4000	2486.57	349.18	360
v_ALPHA_BF*s *u	Alpha base flow factor	0-1	0.46	0.86	0.86
v_GW_DELAY.gw*s *u	Groundwater delay time (day)	1-500	5.18	263.75	265
r_GW_REVAP.gw *s *u	Groundwater “revap” coefficient	-0.01 - 0.2	0.02	0.11	0.11
r__REVAPMN.gw	Threshold depth of water for “revap”	-0.2 - 0.2	-0.028	-0.11	-0.137
r_RCHRG_DP.gw	Deep aquifer percolation fraction	-0.1 - 0.2	0.1	-0.003	-0.00025

v: indicates the existing parameter value is replaced by the calibrated value; r : indicates the existing parameter value is multiplied by (1+ the calibrated value); * indicates sensitive parameters ($p<0.05$) c: confined, s: semiconfined, u: unconfined

Table 3-4. Evaluation of the hydrological goodness of fit of the streamflow (daily and monthly scales) and NO_3-N load (monthly).

Category	Gauging site	Daily Calibration			Daily Validation		
		NSE	R^2	PBIAS (%)	NSE	R^2	PBIAS (%)
Streamflow	Worthington Spring	0.51(s)	0.71(g)	-53 (u)	0.60(s)	0.66(s)	-17.42(u)
	Fort White	0.66(s)	0.74(g)	6.70(g)	0.72(s)	0.83(g)	12.90 (g)
	Hildreth*	0.55 (s)	0.58(s)	-9.61(g)	0.77(s)	0.78(s)	10.58 (g)
		Monthly Calibration			Monthly Validation		
		NSE	R^2	PBIAS (%)	NSE	R^2	PBIAS (%)
Streamflow	Worthington Spring	0.64(s)	0.81(g)	-49.20(u)	0.72(g)	0.8 (g)	-15.40(s)
	Fort White	0.72(s)	0.77(s)	6.70(g)	0.62(g)	0.81(g)	12.90 (g)
	Hildreth*	0.6(s)	0.6(s)	-10.37(g)	0.66(s)	0.8(g)	5 (g)
		Monthly Calibration			Monthly Validation		
		NSE	R^2	PBIAS (%)	NSE	R^2	PBIAS (%)
Nitrate Load	Worthington Spring	0.35 (s)	0.42(s)	11(vg)	-1.50 (u)	0.15(u)	7.70(vg)
	Fort White	0.46(s)	0.50(s)	-9.61(vg)	-0.16 (u)	0.15(u)	-15.40(vg)

		Validation		
		NSE	R^2	PBIAS (%)
ETa	Watershed	0.70	0.83	14

* Hildreth has streamflow data from 2008-2018. s= satisfactory u=unsatisfactory g=good, vg=verygood (Moriasi et al., 2007, 2012, 2015).

Table 3-5. Parameters used for NO_3-N load calibration.

Parameter	Description	Final Range	Value Used
v_CDN*	Denitrification exponential rate coefficient	0.56-0.85	0.75
v_CMN*	Rate factor for humus mineralization of active organic N	0.0001-0.0002	0.0001
v_NPERCO*	Nitrogen percolation coefficient	0.18-0.25	0.2[a]
v_BIOMIX	Biological mixing efficiency	0.2-0.4	0.2[a]
v_RSDCO	Residue decomposition coefficient	0.05-0.08	0.05[a]
v_SDNCO*	Denitrification threshold water content	0.99-1.1	1[b]
v_HLIFE_NGW	Half-life of N in groundwater (days) (sub basins: contributing to Worthington Springs)	25-100	50
v_HLIFE_NGW*	Half-life of N in groundwater (days)(sub basins: contributing to Fort White)	1250-2000	1300

v_ indicates that the existing parameter value is replaced by a given value.
*Sensitive parameters ($p<0.05$)
[a] Default values used in the model
[b] Set at field capacity

Table 3-6. Total load and % of total load contribution from different land uses across watershed

Land uses	Row crops	Forest	Hay	Pasture	Wetland	septic tanks	Other
Load (Tons/year)	610	278	222	1541	27	27	78
% of Total Load	22	10	8	55	1	1	3

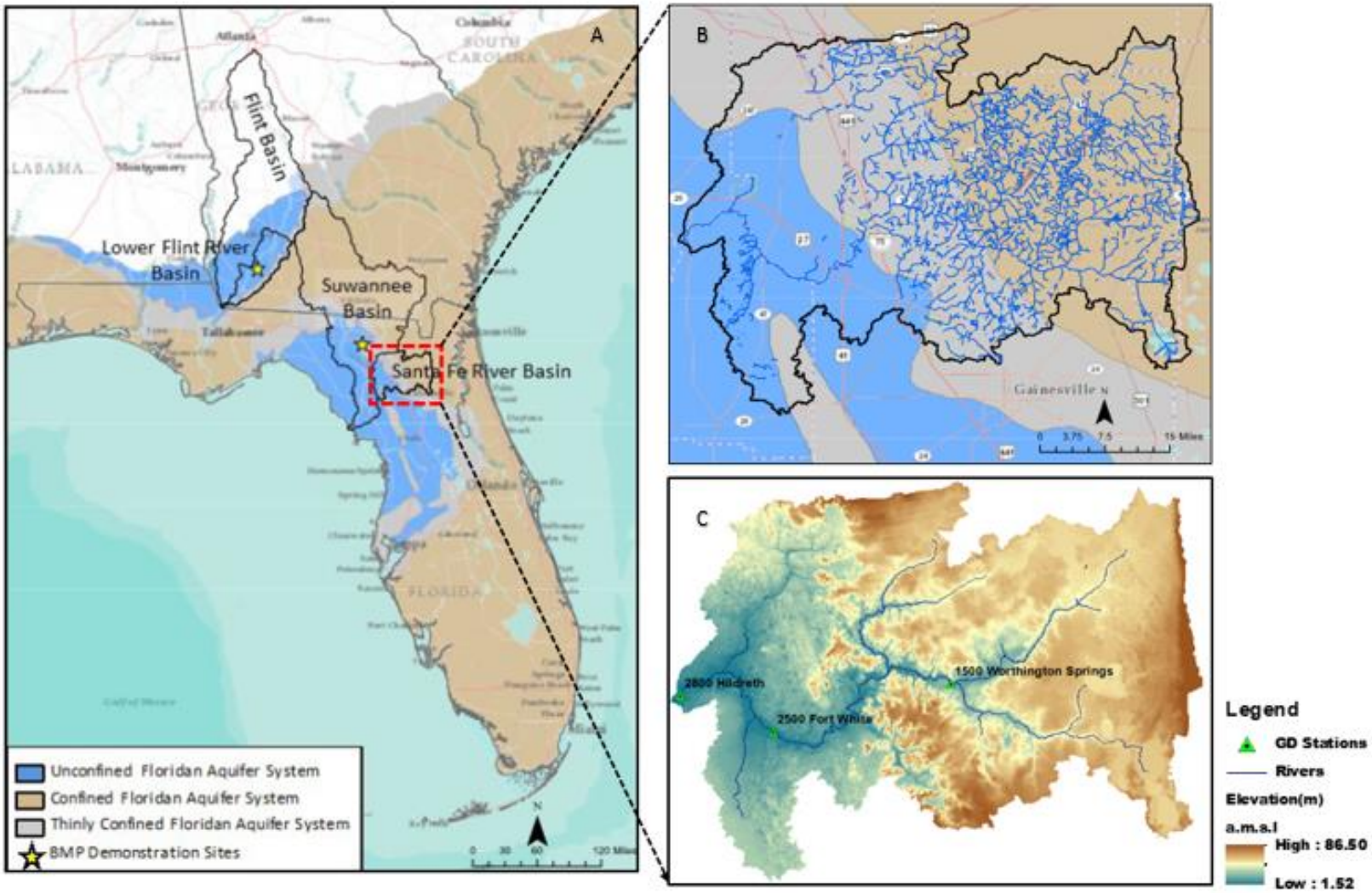

Figure 3-1. Floridan aquifer system (FAS) with location map of the Suwanee River Basin (SRB) and its tributary the Santa Fe River Basin (SFRB). (A) SRB and SFRB in Floridan aquifer system. (B) Hydrogeological features of Santa Fe River Basin. (C) Santa Fe River Basin topography, stream network and GD (gauge discharge) stations. http://floridanwater.org/issues/

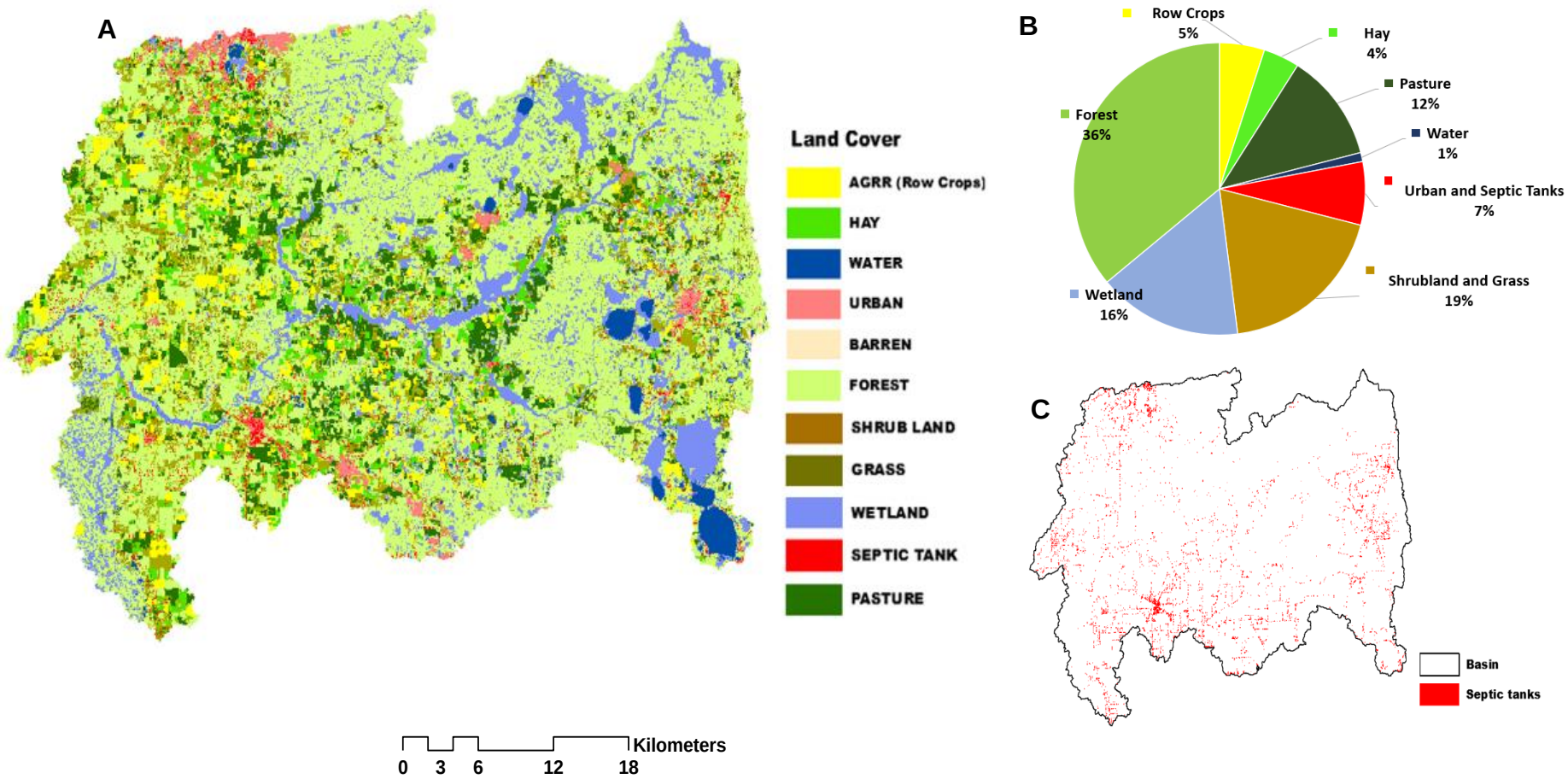

Figure 3-2. Land use classification with percentage of coverage in SFRB. (A) Land Use map. (B) Area percentage (septic tank area is included in urban percentage). (C) Spatial distribution of septic tanks in the SFRB.

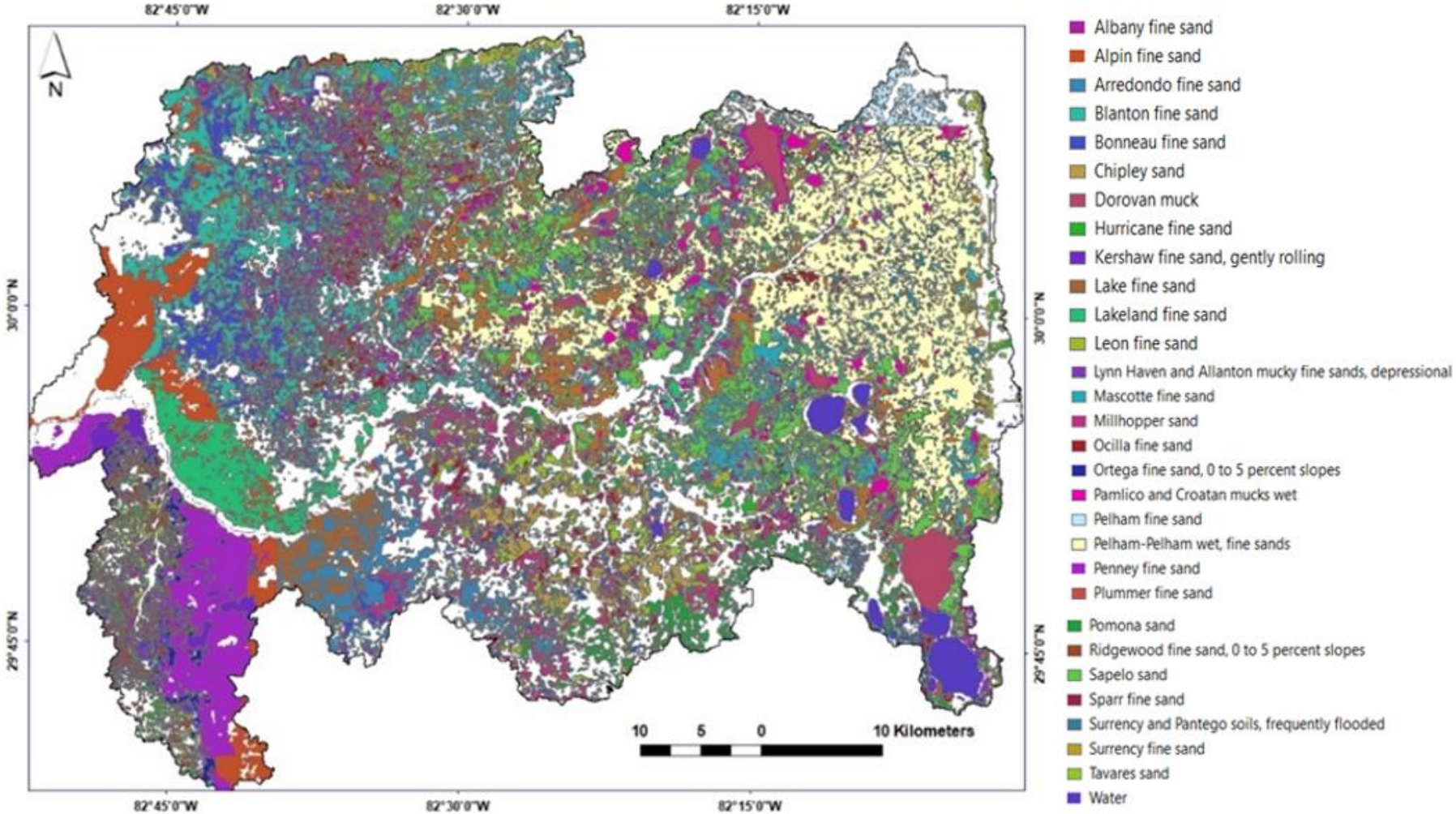

Figure 3-3. SSURGO soil classification. Only soil types covering more than 30 sq km in the watershed are shown in the map. http://soildatamart.nrcs.usda.gov.

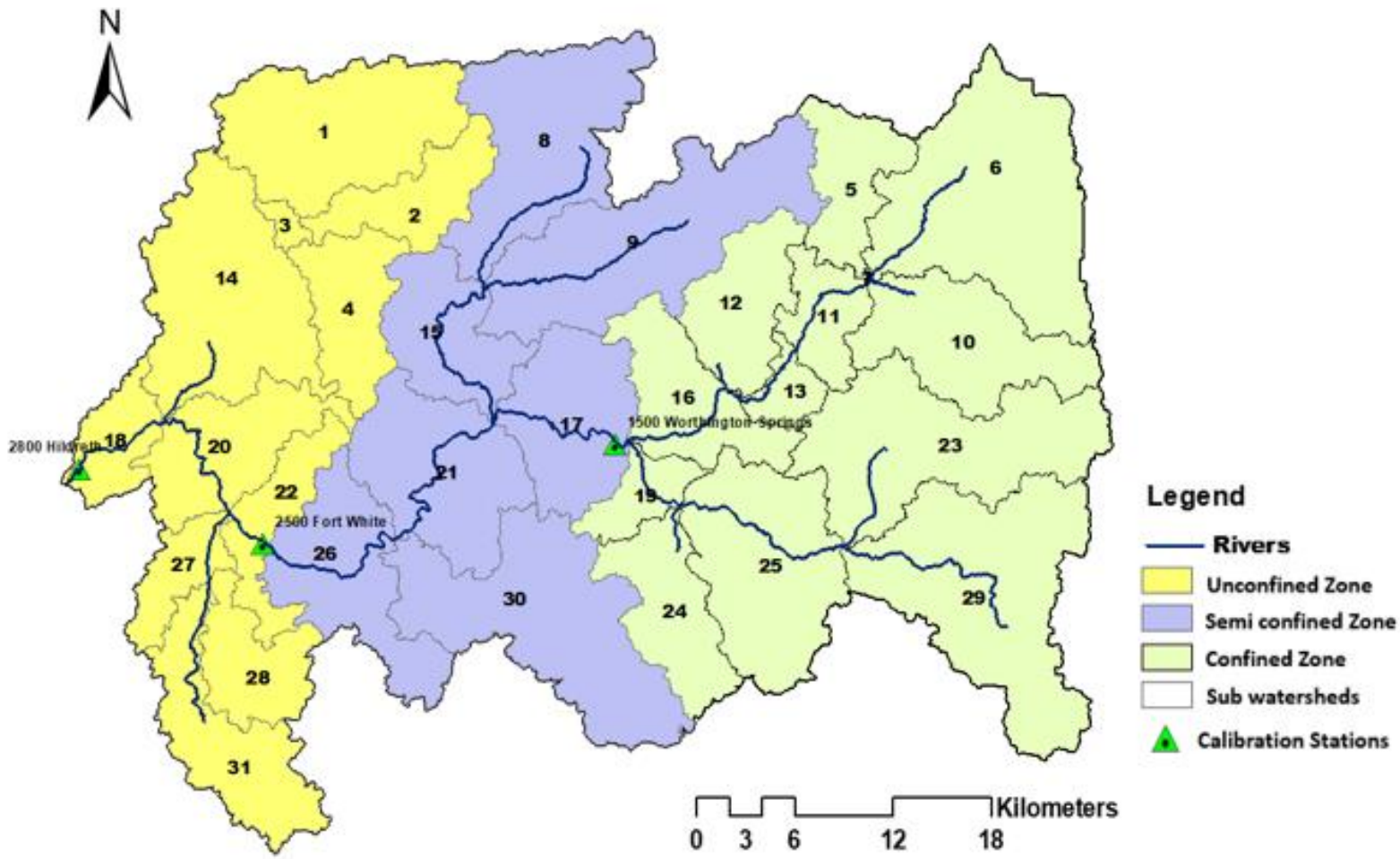

Figure 3-4. SFRB with streams, calibration gauge stations, sub basins and distinct hydrogeological zones for sequential calibration scheme. Confined zone encompass sub basins up to Worthington Spring, semi-confined Zone covers sub basins from Worthington springs to Fort White, and Unconfined zone includes sub basins from Fort White to Hildreth.

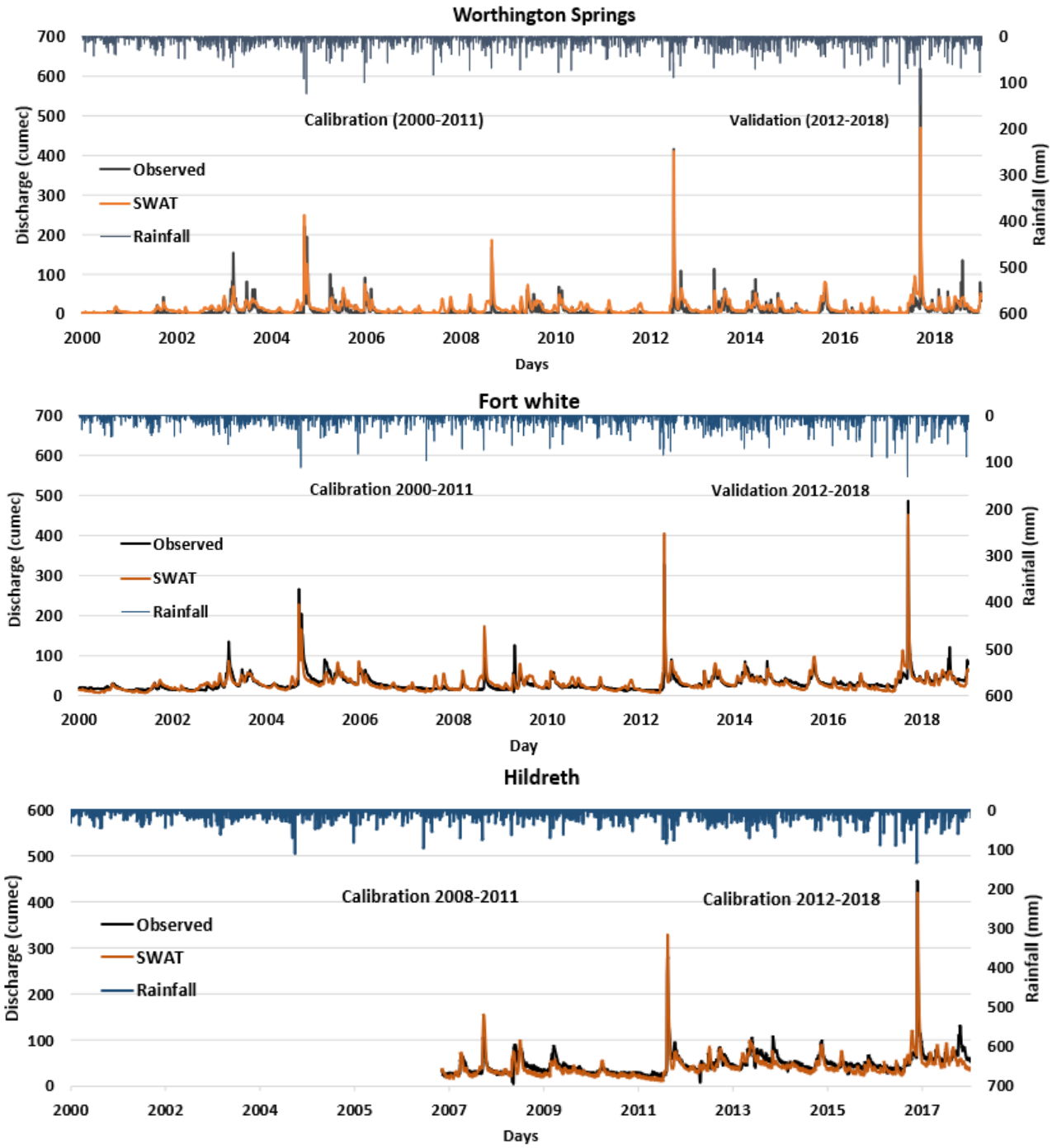

Figure 3-5. Observed and simulated hydrographs for Worthington spring, Fort White, Hildreth along with calibration and validation duration.

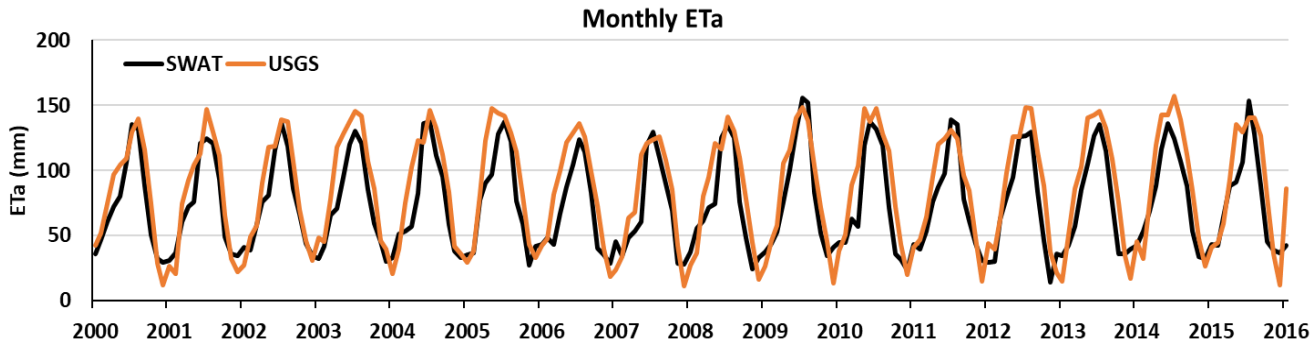

Figure 3-6. Monthly ETa comparison between USGS SSEBop data and SWAT predictions at the watershed scale.

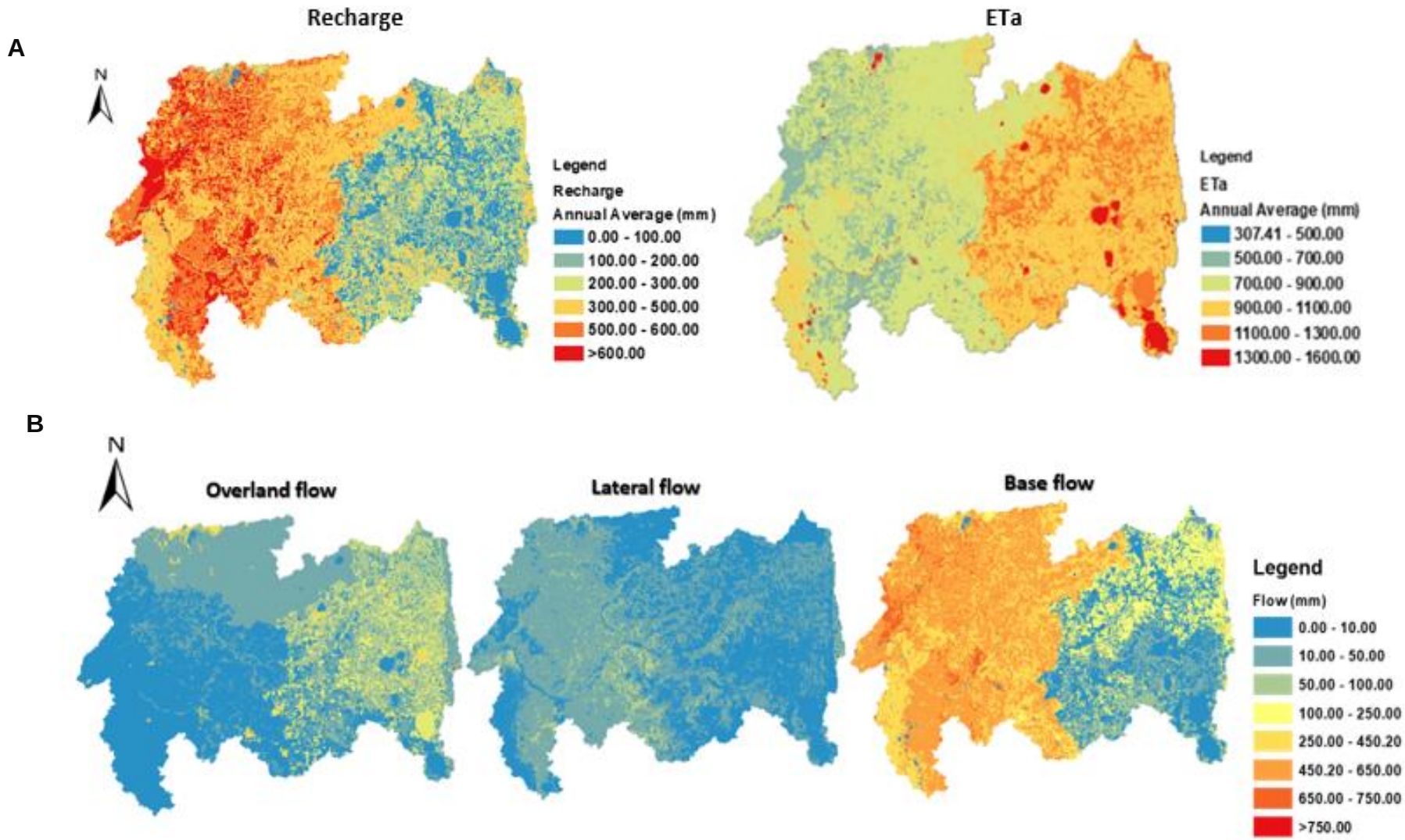

Figure 3-7. Spatial distribution of annual average (2000-2018) recharge, ETa and flow components. (A) Recharge and ETa. (B) overland flow, subsurface lateral flow, and base flow across watershed.

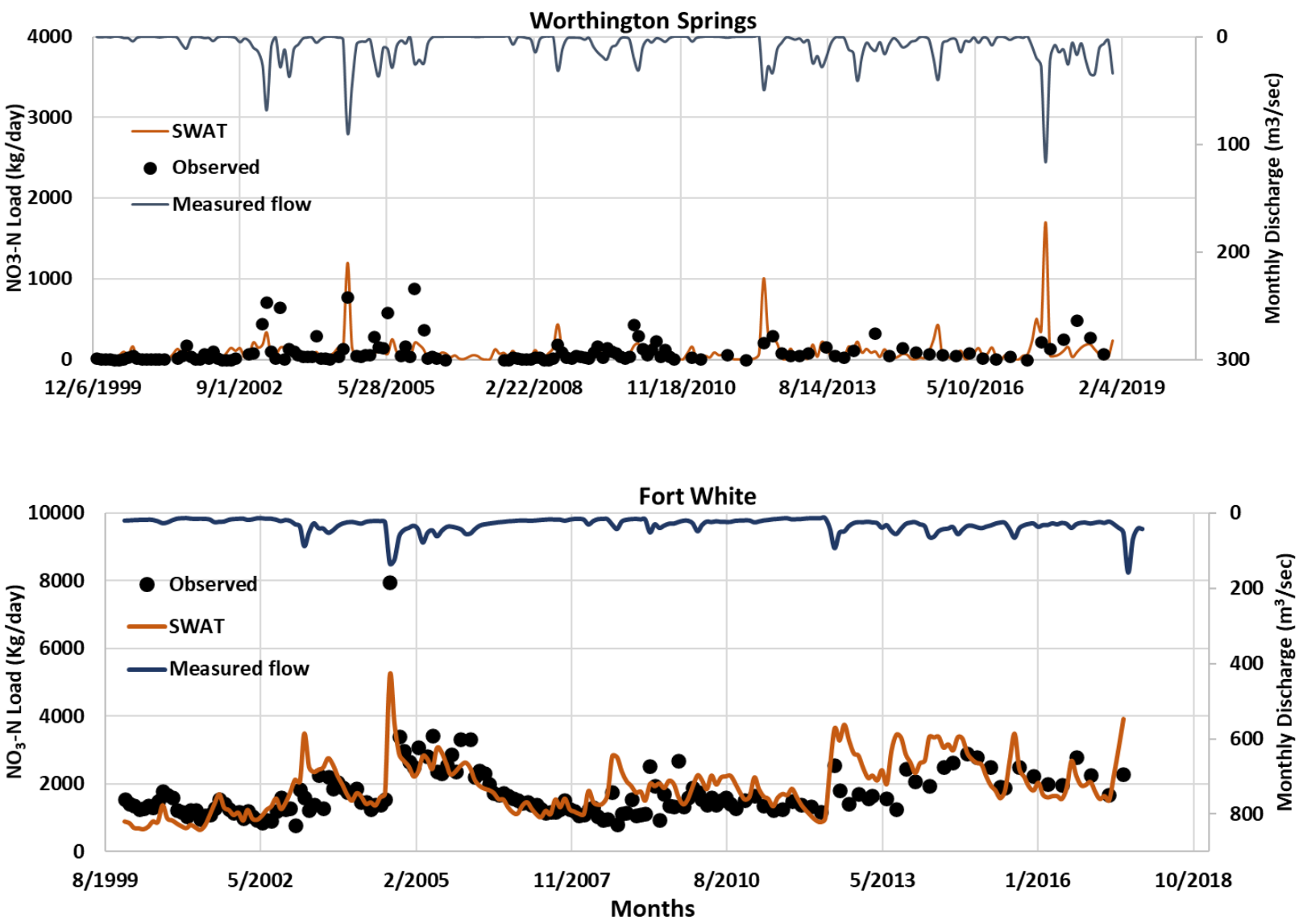

Figure 3-8. Calibration (2000-2011) and validation (2012-2018) of monthly NO_3-N load at Worthington Springs (top) and at Fort White (bottom).

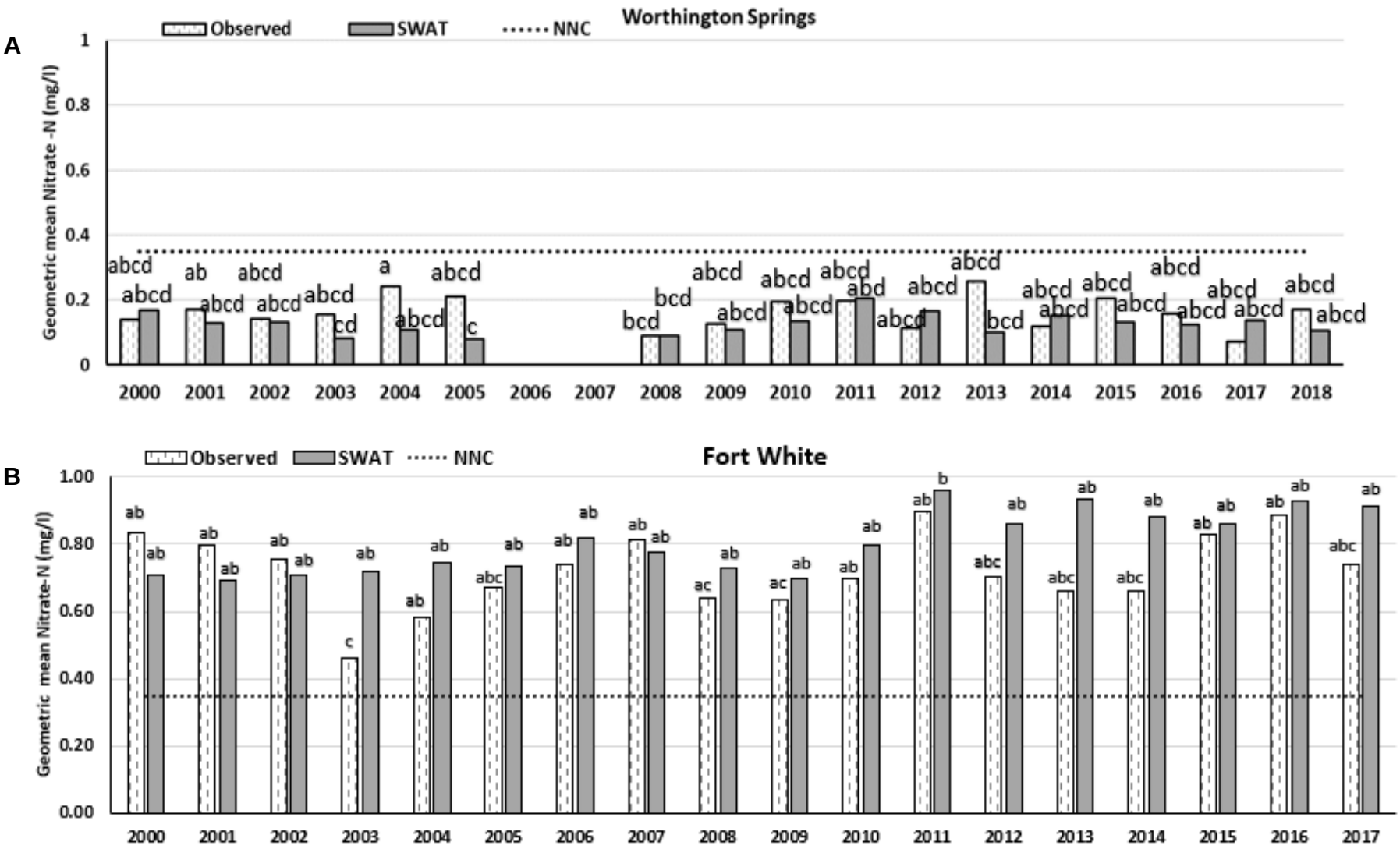

Figure 3-9. Annual NO_3-N geometric mean at Worthington Springs and at Fort White. (A) Worthington Springs (measured data for year 2006 and 2007 were not available). (B) Fort White. Different letters indicate significant difference at α = 0.05 (Tukey's HSD analysis).

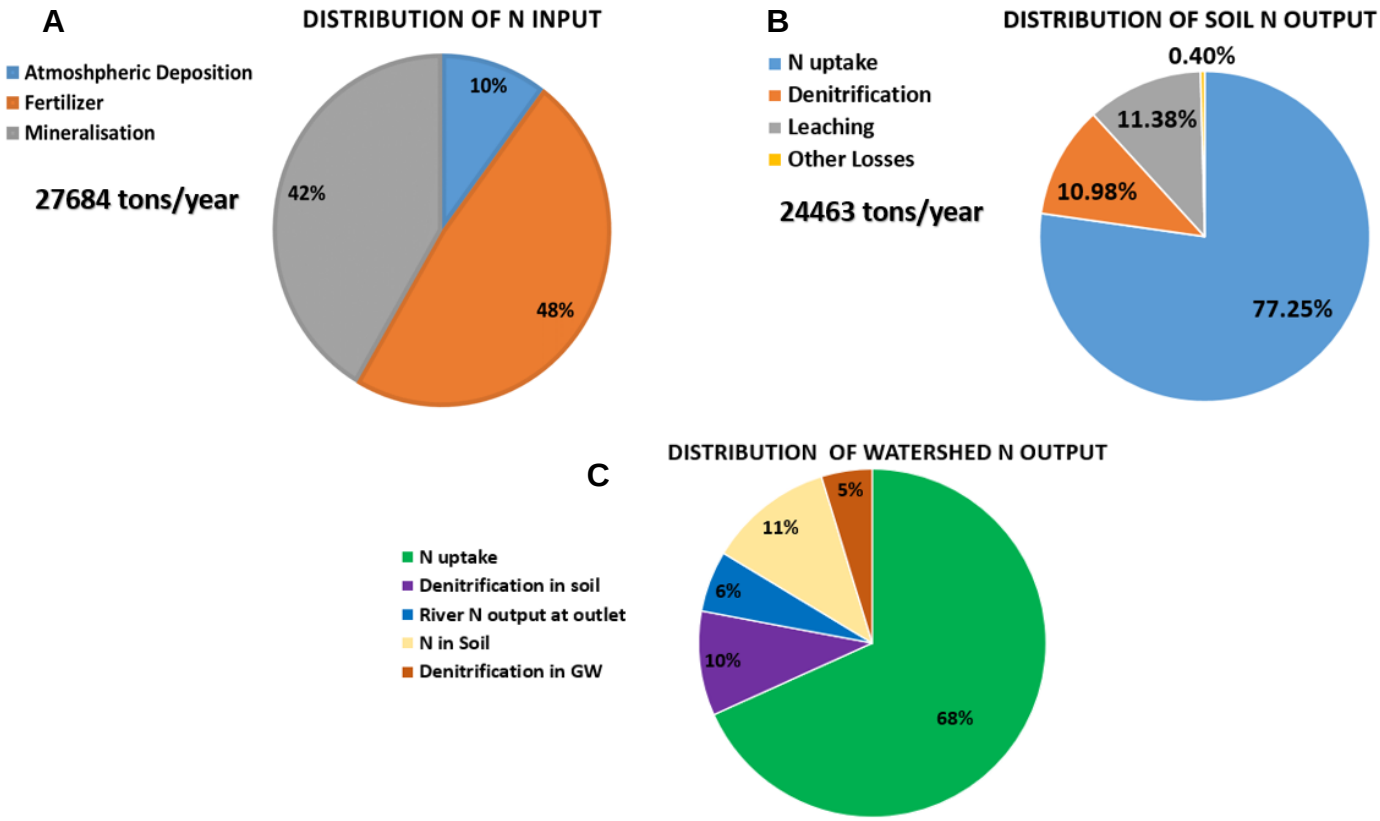

Figure 3-10. Watershed-scale average N annual mass balance (2000-2018). (A) Distribution of annual average N input components. (B) Distribution of annual average soil N outputs including uptake and environment losses including denitrification, leaching, surface runoff loss, and subsurface lateral flow loss. (C) Distribution of annual average watershed N output.

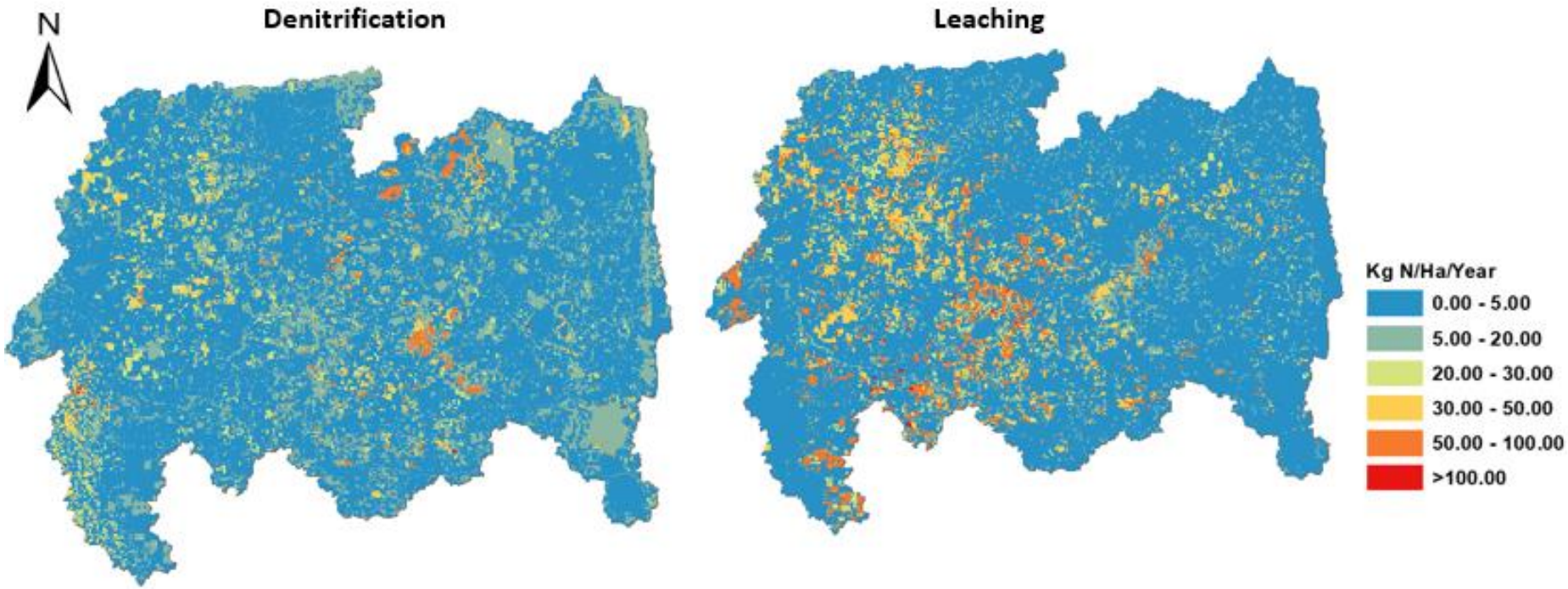

Figure 3-11. Spatial distribution of annual average denitrification and leaching (2000-2018).

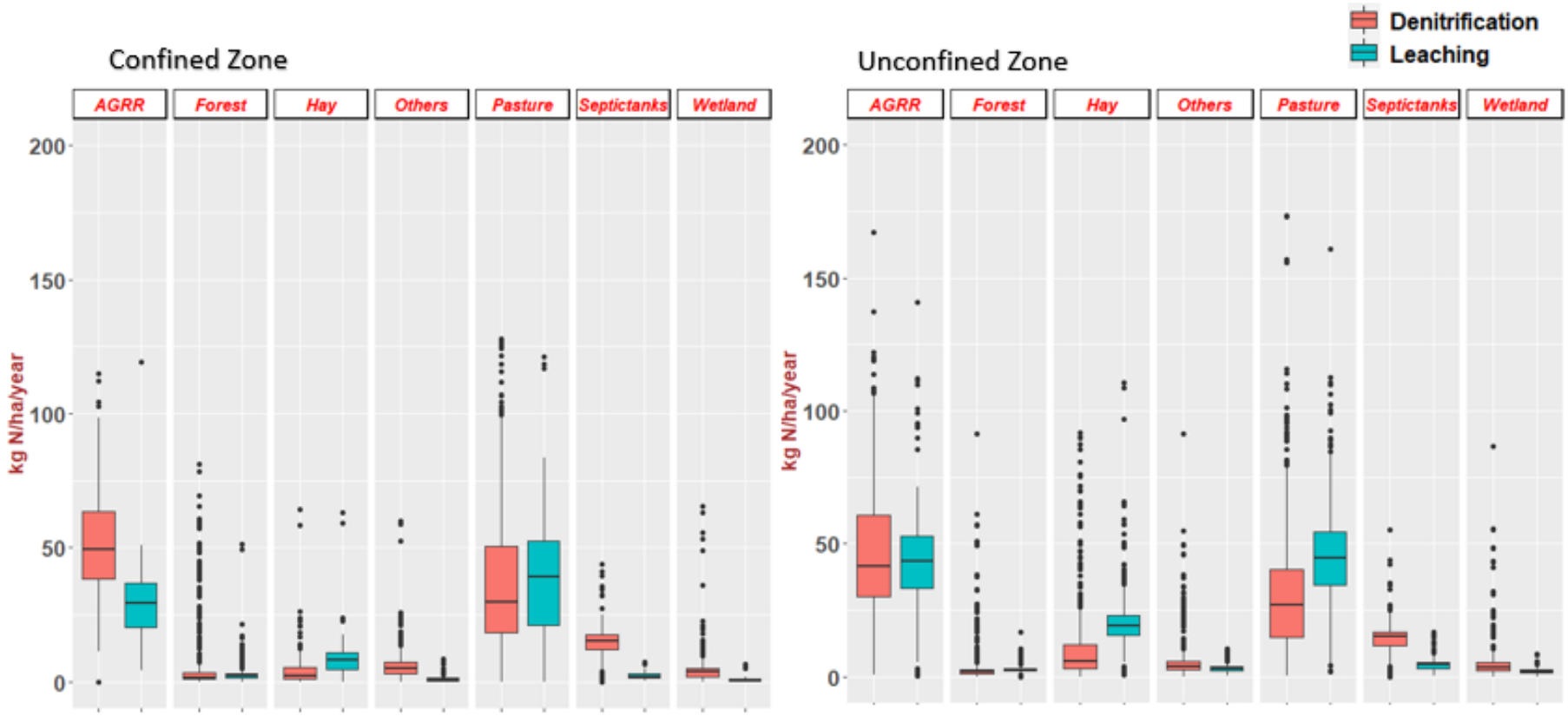

Figure 3-12. Denitrification and leaching from different land use across HRUs in confined and unconfined zone (semiconfined+unconfined) across the watershed. AGRR: Row crop rotation.

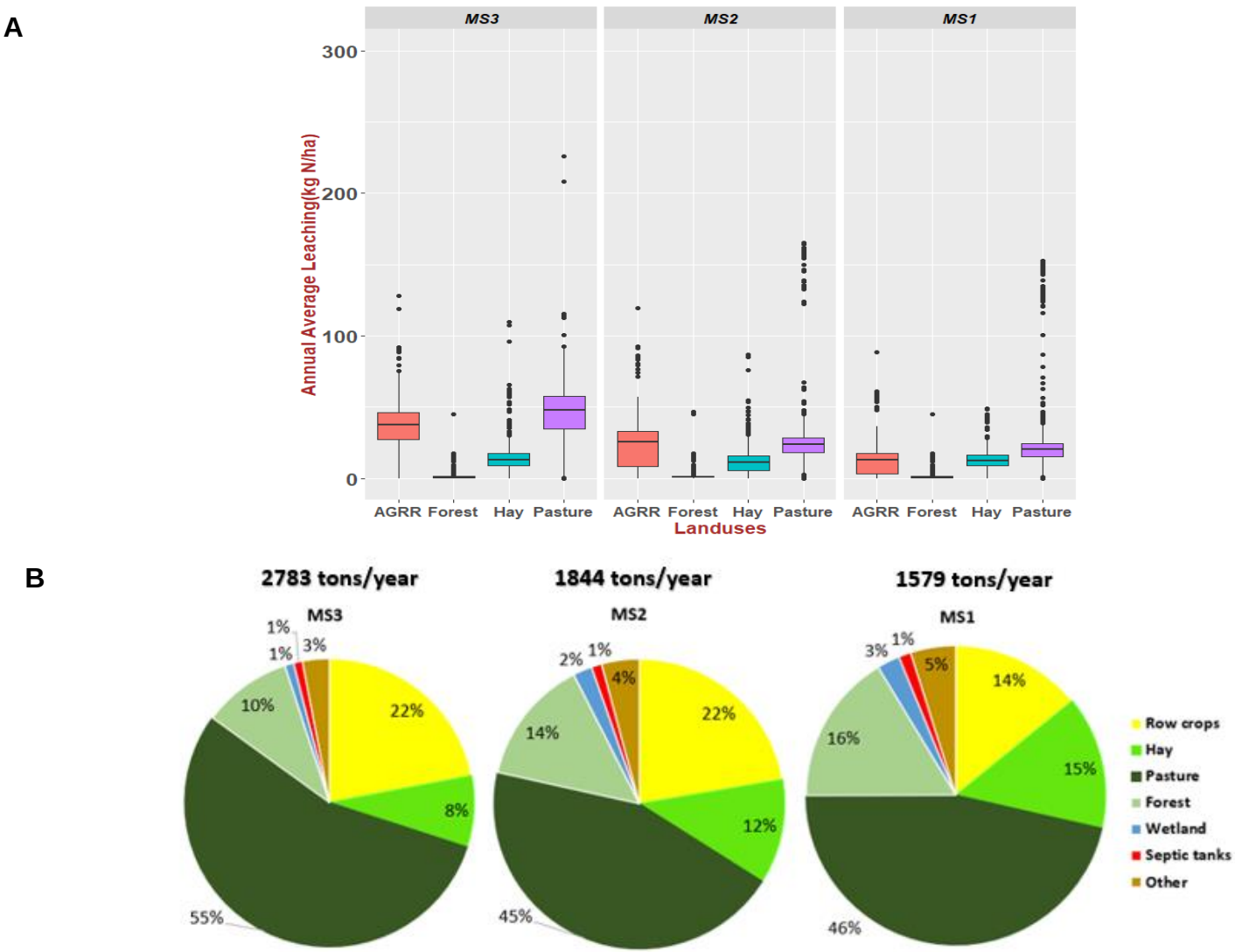

Figure 3-13. Annual average leaching and total load for each management system. (A) annual average leaching across HRUs for each land use and management system. (B) Percentage of total load contribution by management systems.

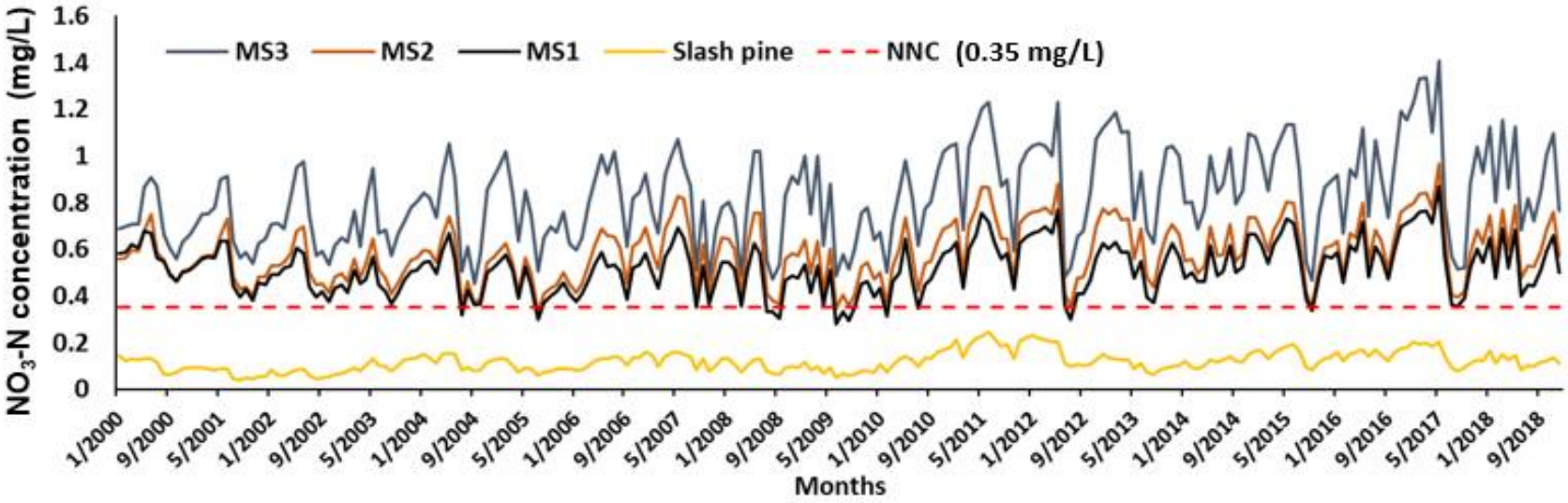

Figure 3-14. Monthly average NO_3-N concentration (mg/L) at Fort White from all scenarios.

CHAPTER 4
ESTIMATION OF GROUNDWATER CONTRIBUTING AREA AND TRAVEL TIME TO SPRINGS IN SANTA FE RIVER BASIN

Background

Nitrate-Nitrogen (NO_3-N) contamination of groundwater is a worldwide concern because of its detrimental effects on the environment (Bowen et al., 2007) and human health (De la Monte et al., 2009). NO_3-N contamination is of particular concern in karst aquifers because soil water enriched with NO_3-N can rapidly infiltrate to the aquifer and move through karst features, such as sinkholes, conduits, and fractures, leading to aquifer and spring contamination. The Upper Floridan aquifer (UFA), one of the most productive karstic aquifers in the world, is a major source of public water supply and irrigation in north and central Florida (Bush and Johnson, 1988). Increasing NO_3-N concentrations in the springs of Upper Floridan Aquifer (UFA) over the past 40 years (Upchurch et al., 2007; Heffernan et al., 2010) has been tied to anthropogenic activities such as fertilizer and manure application for agricultural production (Katz et al., 2004). Growing concern over the environmental impacts of elevated NO_3-N in the UFA has led to the development and implementation of environmental regulations and improved water and nutrient management practices (Maresch et al., 2008; Osmond et al., 2012). However, according to recent reports by the Florida Department of Environmental protection (FDEP, 2017, 2018) and the Florida Springs Institute (2020), little or no water quality improvement has been achieved in the springs in the Santa Fe River Basin (SFRB) overlying the UFA in North Florida. Furthermore, a project conducted by FDEP from 2012-2016 to quantify the effects of water and nutrient Best Management Practice (BMP) implementation in the SFRB Devil's Complex region (i.e., the Ginnie and Gilchrist Blue springsheds) showed no significant decrease in spring NO_3-N concentration

despite BMP adoption. Several possible reasons were hypothesized for this lack of observed response, including: 1) limitations of the effectiveness of BMPs; 2) presence of legacy nitrogen in the root zone and shallow aquifer; and 3) a time lag between when BMPs are implemented and when improvements in receiving water quality can be seen. Lag time is considered one of the most important reasons that watershed planning fails to meet water quality expectations (Meals et al., 2001, 2010).

Continuous long-term water quality monitoring of surface and groundwaters to track the effectiveness of BMPs implemented at the field scale is time consuming and expensive (Choubey et al., 2010; Geissen et al., 2015). In addition, uncertainty in the estimation of the time it will take to detect the impact of BMP adoption on receiving waters is associated with uncertainties in transport pathways, physical and biogeochemical processes, and complex flow in karst aquifers (Snider et al., 2010; Lindsay et al., 1991; Husic et al., 2019). Many simplified surface-groundwater models such as TOPMODEL (Beven ,1989); the Semi distributed Land Use-based Runoff Processes (SLURP; Kite, 1996); and the Soil and Water Assessment Tool (SWAT; Arnold et al., 1996) have been used to study the effectiveness of BMPs in terms of reducing NO_3-N load to surface and groundwaters. However, these simplified models have limited capabilities to accurately predict groundwater flowpaths and travel times (Refsgaard, 1996; Beven, 1989). Understanding groundwater travel time is important for evaluating the impacts of land use and management practices on receiving water bodies because it provides insights on when recovery of the receiving waterbody can be expected (McGuire and McDonnell, 2006).

In Chapter 3, a semi-distributed hydrological-water quality SWAT model was built for the SFRB to study the sources, fate, and transport of N from the land surface to the Santa Fe River. SWAT simulations indicated that NO_3-N transport to the river through base flow was the dominant pathway for the SFRB. However, in SWAT, water flow and solute transport in the subsurface is driven by a simplified storage routing technique with exponential delay parameters. The transport of NO_3-N applied on the land surface through the subsurface to streams is quantified by SWAT in three sequential processes: 1) transport through the soil zone, governed by an exponential percolation lag time parameter (TTperc); 2) transport through the vadose zone to the groundwater (shallow aquifer) governed by an exponential groundwater delay parameter (GW_DELAY); and 3) transport within the shallow aquifer to the stream through baseflow governed by an exponential groundwater recession parameter (ALPHA_BF). Each of these lag parameters are estimated by calibrating the model to observed streamflow data.

The simplified representation of subsurface processes in SWAT has been shown to lead to low performance in base flow simulation as well as inaccurate estimation of groundwater transport because it does not accurately characterize spatially distributed Darcy fluxes and pore water velocities needed for predicting travel paths and travel times (Bosch et al., 2010; Guse et al., 2014; Pfannerstill et al., 2014a; Nguyen et al., 2017). For example, groundwater emerging from springs in the SFRB has been estimated to have a median age of 20-40 years using isotopes and natural tracers (Pittman et al., 1997; Katz et al., 1999, 2004, 2009; Sepulveda et al., 2002; Scott et al., 2004; Planert et al., 2007; Srivastava, 2014; Martin et al., 2016). However, the parameters calibrated for the SFRB SWAT model (Chapter 3) simulate a maximum

travel time of about 3 years for water and NO_3-N to move from the soil zone through the aquifer to the river. Critically, the SFRB model domain, as delineated by SWAT, captures the surface drainage area based on topography but does not include the entire region that contributes groundwater to the river (i.e., the “groundwatershed” or “springshed”, which has been estimated from piezometric maps). Neglecting these recharge areas limits SWAT’s ability to accurately predict the magnitude and timing of water quality impacts resulting from land use and management practice changes in the SFRB.

Under the Florida Springs and Aquifer Protection Act (Chapter 373, Part VIII, Florida Statutes [F.S.]), the Florida Department of Environmental Protection (FDEP) identified 30 “Outstanding Florida Springs (OFS)” that required additional protections to ensure their conservation and restoration for future generations.Out of 30 springs, three springs in the SFRB are identified as impaired OFS that have NO_3-N concentrations above the Numeric Nutrient Criteria (NNC) of 0.35 mg/L NO_3-N: Devil’s Complex, Hornsby Spring, and the Ichetuknee Springs Group. To restore and protect these springs the Santa Fe Basin Management Action Plan (BMAP) delineated Primary Focus Areas (PFAs) within the springsheds. The PFAs are vulnerable areas for NO_3-N inputs to the UFA particularly due to the connectivity between groundwater pathways and the springs. These areas serve as focal points for implementing restoration strategies to reduce spring NO_3-N concentrations (FDEP, 2018). In particular the PFAs boundaries defined in the SFRB BMAP (FDEP, 2018) were developed by overlaying geographic information system (GIS) coverages of high groundwater recharge rates, presence of sinkholes and conduits, soil types, connectivity between groundwater pathways and

springs, aquifer vulnerability, and potential nitrogen source information. These characteristics are associated with increased pollutant loading from surface to the aquifer, but accurately mapping PFAs boundaries requires knowledge of groundwater contributing areas, flow paths and travel times through the aquifer to the springs. It was proposed by FDEP (2018) that tracer or modeling studies be used in the future to determine groundwater flow paths and travel times to improve the delineation of PFAs. These serves, in part, as the motivation to conduct this study.

Uncertainties in quantification of groundwater flow paths and travel time distributions (TTD) may result from uncertainties associated with external forcing such as recharge, internal hydrogeologic properties (conductivity, porosity, saturated aquifer thickness), the groundwater contributing area, the head within the aquifer, and the hydraulic gradient (Ajami et al., 2007; Darracq et al., 2010; Jing et al., 2019). This study aims to improve the prediction of groundwater flow and transport processes in the SFRB by coupling the SWAT model developed in Chapter 3 with a numerical groundwater model (MODFLOW 2005, Harbaugh, 2005) and particle tracking algorithm (MODPATH 7, Pollock, 2016). Devil's complex springs was selected for particle tracking analysis due to its proximity to the Fort White gauging station which was a focus for chapter 3 analyses. The resulting SWAT-MODFLOW-MODPATH model was used to 1) investigate the impact of external forcings such as recharge and aquifer properties (i.e., porosity and hydraulic conductivity) on the groundwater contributing area, flow paths and travel time distribution for the region of the Santa Fe River where the Devil's Complex springs emerge, and 2) estimate the effect of changes in land use and land

management practices on groundwater NO_3-N concentrations contributing to the Devils Complex springs, and the time it will take for these changes to appear in the springs.

Study Area

The Floridan Aquifer System (FAS) underlies an area of about 260,000 km^2 in the southeastern United States, including all of Florida and parts of Georgia, Alabama, and South Carolina (Figure 4-1).The FAS is composed of two main aquifers, the Upper Floridan aquifer (UFA) and the Lower Floridan aquifer (LFA) separated by a composite semiconfining unit which ranges from low-permeable clays, dolomites and gypsiferous anhydrite in west-central Florida to permeable limestone along the east coast of Florida and elsewhere (Knowles et al., 2002; Katz et al., 2004). Where these intervening sediments and rock are permeable, the UFA and LFA behave as a single unit (Knowles et al., 2002). Conversely, where the intervening sediments are less permeable, there is less hydraulic connection between the UFA and LFA. Regardless of rock type, wherever the middle confining unit is present, it restricts the movement of groundwater between the UFA and (LFA) (Miller, 1986). Portions of the FAS shown in blue (Figure 4-1) are unconfined where confining unit is breached, or absent providing optimal conditions for water to percolate rapidly into the Upper Floridan aquifer.

The UFA is of primary importance to the north and central Florida as a source of water for irrigation, domestic and industrial supply, and as a source of water that discharges to springs and streams providing recreational and tourist destinations and unique aquatic habitats. Due to extensive use of water from the UFA, the hydrogeological properties have been well-investigated and reported by United States Geological Survey (USGS, 2007). The transmissivity of the Upper Floridan aquifer varies over several orders of magnitude ranging from 120.77 m^2 /d to 120,773 m^2 /d

(Faulkner, 1973; Kuniansky et al., 2012). Almost 90 percent of the natural discharge to rivers and springs is estimated to come from the Upper Floridan aquifer in central Florida (Bush and Johnston, 1988; Sepulvada et al., 2012). The geologic characteristics and hydraulic properties of LFA, assessment of vertical flow between the UFA and the LFA and flow within the LFA itself are not well studied. There is a paucity of water-level and aquifer characterization measurements available as LFA is located at greater depth (Sepulvada et al., 2002). The Lower Floridan includes the lower part of the Avon Park Formation, the Oldsmar Limestone, and the upper part of the Cedar Keys Formation.

The SFRB study area, located over the north-central part of the FAS, consists of several hundred meters of limestone and dolostone but only the upper 0-54 m, the UFA comprised primarily of Ocala Limestone, yields potable water (Hunn and Slack, 1983). The stratigraphic units constituting the upper part of the aquifer are, from oldest to youngest: the Eocene Ocala Limestone, the Oligocene Suwannee Limestone, and the limestones at the base of the Miocene Hawthorn Group. Where the Ocala Limestone is not exposed at the surface, it is covered by the Hawthorn Formation and a surficial aquifer of Plio-Pleistocene sands (Scott et al., 2004). Spatially variable erosion of the Hawthorn Formation has led to variations in UFA confinement throughout North Florida. The erosional boundary of the Hawthorn Formation is known as the Cody Escarpment, and defines a critical boundary for defining UFA vulnerability to contamination. Down gradient from the Cody Escarpment, where limestone is exposed, and vulnerability is increased by enhanced surface-to-aquifer connectivity. UFA is underlain by a lower permeability limestone called the Avon Park Formation that is 54-225 m thick (Figure 4-2).

Methods

In this study the groundwater contributing area, flow paths and travel time distribution for the Devil's Complex springs were estimated by coupling the calibrated SWAT model (Rath, Chapter 3) with calibrated North Florida-Southeast Georgia (NFSEG 1.1) MODFLOW model (Durden et al., 2019) and using the coupled model to drive the advective transport code, MODPATH (version 7) (Pollock,1989,1994). Details of the integration/coupling process and particle tracking are provided below.

North Florida-Southeast Georgia (NFSEG1.1) MODFLOW Model

A fully distributed calibrated regional groundwater flow model, North Florida-Southeast Georgia (NFSEG1.1), developed by St Johns River Water Management District and Suwanee River Water Management District, was coupled with the SWAT SFRB model to improve the representation of groundwater flow and transport processes. NFSEG1.1 is a steady-state model developed to assess regional effects of groundwater withdrawals on groundwater levels, stream base flows and spring flows and provide a framework for water supply planning and establishment of minimum flows and minimum water levels (MFLs) (Durden et al., 2019). A brief description of the NFSEG1.1 model is presented here; further details about the conceptualization of model structure including data collection and calibration methods can be found at https://northfloridawater.com/groundwaterflowmodel.html.

The spatial domain of the NFSEG1.1 model covers about 155,400 square kilometers, encompassing a large area of the Floridan Aquifer System (FAS) in north Florida, Georgia, and South Carolina. The model was discretized uniformly in the horizontal direction using a 760 m x 760 m grid. The NFSEG1.1 model utilizes seven layers to represent the FAS. The hydro stratigraphy in the NFSEG model maps the

surficial aquifer (layer 1) and intermediate confining unit (layer 2) as continuous throughout the model domain (Figure 4-4). In places where the Floridan Aquifer System (FAS) is unconfined, layer 2 exists with a minimum thickness of 3 meters and is assigned the properties of the UFA (layer 3). The thickness of the UFA (layer 3) varies from 20 m to 140 m; the thickness of the composite semiconfining unit (layer 4) varies from 20 m to 180 m; and the thickness of the LFA (layer 5) varies from 50 m to 450 m for LFA (see Figure Appendix C-1). The spatial variation of calibrated horizontal hydraulic conductivity is shown in Figure 4-5.

The NFSEG1.1 model utilized annual average recharge and maximum saturated evapotranspiration (i.e. potential evapotranspiration remaining after actual surface and root zone evapotranspiration) from a catchment scale rainfall-runoff model HSPF (Hydrological Simulation Program—FORTRAN, Bicknell et al., 2001) as input forcing. Two years were used for steady-state model calibration: 2001(a dry year) and 2009 (a wet year). A third year, 2010, was used for model validation. NFSEG1.1 performed well in matching the observed head (2% error in 2001 and 1% error in 2009) in calibration years for SFRB region. The base flow prediction at Fort White was very good with 1% error for both the years 2001 and 2009.

SWAT-MODFLOW

The groundwater domain for the SFRB SWAT-MODFLOW model was delineated from the NFSEG1.1 model (Figure 4-4) based on the groundwater contributing area to the Santa Fe River that was estimated using the potentiometric surface of the UFA and previously estimated spring shed boundaries (FDEP 2018;2016; USGS 2011; Santa Fe River and Springs Environmental Analysis, Final Report 2020). The sub basins outside the topographically defined SFRB were manually delineated based on HUC-10 and

HUC-12 basin shape files (Figure 4-6). The SWAT SFRB model was calibrated and validated at the sub basin scale based on three stream gauge sites encompassing flow from the confined, semiconfined, and unconfined zones (Figure 3-4). For details regarding the calibration scheme for the three zones see Chapter 3.

The confined, semiconfined, and unconfined zones were extrapolated to SWAT-MODFLOW sub-basins beyond the topographically defined SFRB based on the presence/absence of the intermediate confining unit (Figure 4-6). The calibrated relative changes with respect to the default Soil Survey Geographic database (SSURGO) values for Curve Number moisture condition II (CN2) and for soil parameters such as available water capacity (SOL_AWC) and saturated hydraulic conductivity (SOL_K) for each zone within the topographically defined SFRB (Table 3-3) were extrapolated to the exterior sub-basins in the same zone and used with local default SSURGO values to generate appropriate local values. The calibrated absolute values used for the soil evaporation compensation factor (ESCO) plant uptake compensation factor (EPCO) and groundwater parameters such as groundwater delay parameter (GW_Delay), groundwater revap coefficient (GW_REVAP), groundwater recession constant (ALPHA_BF) (Table 3-3) were extrapolated directly to the exterior sub-basins by zone.

SWAT was coupled with NFSEG 1.1 following the procedure described by Bailey et al., 2017. To allow transient simulation a specific yield of 0.25 was specified for the surficial unconfined layer (Davis and Katz, 2007; Katz et al., 1999; Martin, 2006) and a specific storage of 0.00001 m^{-1} was specified for the remaining confined layers based on the literature values (Wong et al., 2012; Swain et al., 2016; Kuang et al., 2020). SWAT-MODFLOW was run using a daily time step from the year 2000 to 2018.

Streamflow and groundwater head from the coupled transient model were compared with the observed flow at the USGS Fort White gauging station and observed groundwater levels from observation wells within the SWAT-MODFLOW domain.

Particle Tracking

The advective particle-tracking scheme MODPATH (version 7; Pollock, 1989,1994) was used with SWAT-MODFLOW to compute the contributing area, flow paths and travel time distribution for groundwater emerging from the reach of the Santa Fe River containing the Devil's Complex springs system. Particles were tracked backwards through time from the river where the Devil's Complex springs emerge to the model boundaries by computing the pore water velocity vector based on the darcy flux across each face of a grid cell and the effective porosity (n_e) shown in equation 4-1.

$$v_i = \frac{-K_i}{n_e}\frac{dh}{dx_i} \qquad 4\text{-}1$$

Where v_i porewater velocity in ith direction is, K_i is hydraulic conductivity in ith direction, $\frac{dh}{dx_i}$ is the hydraulic gradient in ith direction and n_e is effective porosity. Effective porosity is the interconnected porespace of the total porosity that contributes significantly to fluid flow with a velocity greater than the average fluid velocity (Horton et al., 1987). MODPATH stores the travel time and final location for each particle as it crosses a model boundary. From these results the travel time distribution (TTD) for all particles and the source area encompassing all particles were determined.

Particle tracking was performed under steady state conditions in a wet and dry year for the Santa Fe River basin. Transient particle tracking requires fluxes to be stored in each cell at each time step for each stress period which can be computationally intensive. To avoid computationally intensive simulations, steady state

particle tracking for a wet (2009) and dry (2001) year were performed, which were the same years that were modeled for the NFSEG 1.1. The steady state particle tracking under two hydrologically different conditions was conducted to identify how travel time distributions and groundwater contributing areas may vary under different recharge conditions. To perform the steady state simulation, daily recharge from the transient simulation of SWAT-MODFLOW was averaged for each year.

The backward particle tracking through groundwater was performed by releasing 100,000 particles (i.e., sufficient particles to construct a smooth travel time distribution) in the river grid cells of the SWAT sub basin contributing to Fort White which contains the Devil's Complex springs (Figure 4-7). Particles were distributed among the river cells in proportion to the groundwater flux to the cells so that each particle represents an approximately equal volume of water.

Importantly, effective porosity and hydraulic conductivity have a profound influence on the estimation of groundwater travel paths and travel times (Basu et al., 2012). Groundwater travel time is directly proportional to effective porosity and distance and inversely proportional to permeability and hydraulic gradient (Horton et al., 1987; Stephens et al., 1998). The NFSEG 1.1 model parameterization and configuration did not specifically consider karst structures such as fractures and conduit networks located in UFA which result in preferential flow pathways with rapid groundwater flow that can greatly impact groundwater travel times. For equivalent porous media models, the preferntial pathways in karst systems are represented via lowering the effective porosity (Rayne et al., 2001) or increasing the hydraulic conductivity (Saller et al., 2013) to

increase the flow velocity. Both conditions were tested to assess the impact on travel time distribution analysis.

Because of the significant matrix porosity of the limestone, flow in the UFA occurs in both the rock matrix and in fractures and conduits (Thayer and Miller, 1984). Previous research estimated the effective porosity of the UFA to range from 25% to 35% (Davis and Katz, 2007; Katz et al., 1999; Budd et al., 2004; Martin, 2006). In this study particle tracking was initially simulated assuming a uniform effective porosity of 0.25 for each model layer and a travel time distribution was calculated and compared with the median travel time of ~20 years that has estimated from isotopic and natural tracer measurements (Katz et al., 2001; Katz,2004; Katz and Griffin, 2008) and further adjusted manualy if required.

Similarly, the spatial distribution of hydraulic conductivity has a substantial influence on groundwater head, flux, groundwater travel time, travel path and contributing area. Particle tracking was first simulated using the calibrated NSFEG1.1 model to analyze the groundwater median age and contribution of flow through each layer. The calibrated NFSEG 1.1 model does not specifically consider the preferential flow through karst structures in UFA. To represent the higher preferential flow pathways that have been observed in the UFA versus the composite semiconfining unit and the LFA, the hydraulic conductivity of layers 3 through 5 (the UFA, composite semi confining unit and LFA) were adjusted to produce a median travel time of ~20 years as well as allow majority of spring flow sourced from the UFA (Bush and Johnston ,1988; Sepulveda et al., 2012; Grubbs et al., 2007). Hydraulic conductivity adjustments in layers 3, 4 and 5 were constrained to maintain the calibrated effective conductivity

across these layers so that the ability of the model to simulate observed groundwater heads and baseflows was not compromised.

Estimating NO_3-N Concentrations at the River using Travel Time Distributions

The source, fate and transport of NO_3-N reaching the river in the Devil's Complex Springs area was analyzed by combining the SWAT-MODFLOW-MODPATH-estimated groundwater contributing area and travel time distribution, the SWAT predicted average NO_3-N concentration leaching to groundwater from each land use (Chapter 3), and a first order groundwater denitrification rate of 0.00005 day $^{-1}$ (~38 year half-life) estimated from observations made by Heffernan et al., 2011and Henson et al., 2017 (equation 4-2).

$$C_t = \frac{\int_A q(a) \int_{\tau=0}^{\infty} C_o(a,\tau) e^{-k\tau} \delta(t(a)-\tau) d\tau da}{\int_A q(a) dA} \qquad 4\text{-}2$$

where A is the groundwater contributing area, t(a) is the travel time from source area increment da to the river, q(a) is the darcy flux from source area increment da, $C_0(a,\tau)$) is the initial concentration from source area increment da τ years prior, k is the first order denitrification rate, and δ (.) is the dirac delta function representing piston flow along the path line (Desouni and Graham, 1995).

As indicated in chapter 3, a range of practices representing different agricultural land uses in the SFRB (row crops, hay, and pasture) were defined based on in-depth consultation with stakeholders and Extension agents as well as previous studies in this region. Table 3-2 summarizes the range of current management practices for agricultural land uses, ranging from high to low N fertilizer and irrigation application. Management System 3 (MS3) represents conventional, higher-input practices historically applied in the region; MS2 represents improved water and nutrient

management approaches adopted more recently (including soil moisture sensors for triggering row crop irrigation); and MS1 represents the best management practices that are considered economically feasible with currently available technology. For production forests, we assumed slash pine forest management with no fertilization, no irrigation, no thinning, and a 36-year rotation length. Natural grasses also had no fertilization or irrigation. Based on results presented in Chapter 3, the daily NO_3-N leaching concentration from row crops, pasture, hay, forest, and native grass lands were estimated by dividing the SWAT simulated daily mass of NO3-Nleaching from that land use (kg NO3-N/ha) by the SWAT simulated daily volume of water recharging the aquifer from that land use (mm), applying appropriate unit conversion factors and taking the long term average. The resulting average concentrations for all agricultural land uses (by management systems), natural grasses and forests are shown in Table 4-1.

With the SWAT-MODFLOW-MODPATH estimated travel time distributions and the SWAT-estimated leaching concentrations, several heuristic experiments were carried out to analyze the fate and transport of NO_3-N from different land use and land management systems to the Devils Springs Complex area in the SFRB (Table 4-2). All cases assumed that conventional higher input practices (MS3) were used for all agricultural land uses from 1970-2020. Case 1 assumed all agricultural land uses continued using MS3 into the future. Case 2 assumed all agricultural land uses shifted from MS3 to MS1 after 2020. Since pasture was found to be the highest NO_3-N load contributor among the agricultural land uses (Chapter 3, Figure 3-13) Case 3 assumed that after 2020 all pasture was converted to hay using MS1, and all other agricultural landuses shifted from MS3 to MS1. Case 4 assumed that after 2020 pasture was

converted to natural grassland to further decrease the NO_3-N load (Chapter 3, Figure 3-13), and all other agricultural landuses shifted from MS3 to MS1. Finally, Case 5 assumed that all agricultural land uses were converted to slash pine forest after 2020.

Results and Discussion

SWAT-MODFLOW Model Performance

SWAT-MODFLOW-simulated monthly flow at Fort White was in the satisfactory to good range Moriasi (2015) (R^2=0.68, NSE=0.62, and PBIAS=5.1%), which is approximately equivalent to the accuracy of the SWAT-only model presented in Chapter 3 (Table 3-4). SWAT-MODFLOW simulated daily flow was in the unsatisfactory to good range (R^2 =0.35, NSE =0.33, and PBIAS=5.1%) (Figure 4-8), which was significantly less accurate than the SWAT-only model. These results would likely improve by recalibrating the coupled SWAT-MODFLOW model simultaneously rather than directly coupling the two previously calibrated models.

Observed and simulated groundwater head were generally in in good agreement other (Figure 4-9) (R^2=0.86, PBIAS = -7%), however variation in observed heads were often greater than simulated heads, particularly in the confined region. This could be due to the absence of the confining unit in some well locations (or puncturing of this layer during well construction). Hydrographs for individual wells (Appendix Figures C-2, C-3 and C-4) show simulated head in the unconfined region has more variability than in the confined region, likely due to the absence of the confining layer and proximity to the river.

Analysis of the SWAT-MODFLOW recharge in comparison to the original NFSEG 1.1 recharge was carried out for the wet year 2009. SWAT estimated higher recharge (percolation from root zone) compared to HSPF, particularly in the unconfined region

(Figure 4-10). Both SWAT and the HSPF surface model used North American Land Data Assimilation System (NLDAS) historical rainfall data and partitioned rainfall into recharge and ET in the soil zone. Notably, SWAT-calibrated soil parameters produced high recharge and low ET in the unconfined zone in order to match streamflow at Fort White, likely a result of the fact that the SWAT-only model did not consider the entire groundwater domain contributing flow to SFRB.

Despite the difference in recharge, simulated heads between SWAT-MODFLOW and the original NFSEG 1.1 across all grids for year 2009 (wet year) were in good agreement (R^2=0.95, slope= 1.03, intercept= -0.02) (Figure 4-11) and SWAT-MODFLOW performed well in matching the observed head (R^2=0.83, slope=0.78, intercept= 2.06). Differences in head between NFSEG 1.1 and SWAT- MODFLOW varied from 5.98 m to -13 m. The range of positive and negative differences span the transition from confined to unconfined regions due to differences in recharge between HSPF and SWAT. The small differences between SWAT-MODFLOW and NFSEG1.1 simulated heads, in spite of differences in recharge, may be because MODFLOW uses any remaining (unsatisfied) potential evapotranspiration (PET) after evapotranspiration from the soil zone to calculate additional evapotranspiration from the aquifer, which could compensate for excess recharge in the unconfined region. Overall, the SWAT-MODFLOW model adequately reproduced observed stream flow and groundwater heads.

Groundwater Travel Time Distribution (TTD) in SWAT-MODFLOW

With a unifom effective porosity of 0.25 in all layers and the original NFSEG 1.1 calibrated hydraulic conductivities, the median value of the TTD was more than 200 years (Figure 4-12), which is nearly 10 times the estimated median age of ~ 20 years for

springs discharging to Santa Fe river near Fort White (Katz et al., 2001; Katz,2004; Katz and Griffin, 2008). Inspection of the length of time that particles spent in each layer (Figure 4-13) showed that more than 50% of particles in this simulation traveled into the LFA and stayed for long periods, indicating that the composite semi confining unit (4th layer) did not restrict flow between the UFA and LFA. As a result, particles followed a long flow path through the LFA before emerging in the springs. In contrast, previous tracer experiments (Ellins et al., 1991; Crandall et al., 1999) and modeling studies (Bush and Johnston, 1988; Grubbs et al., 2007; Sepulveda et al., 2012) estimated that approximately 90% of water contributed to springs comes from the UFA.

Reducing the effective porosity of the confining unit (2nd layer), UFA, composite semi confining unit and LFA to 0.02 (Davis et al., 2010; Yang et al., 2019) in SWAT-MODFLOW-MODPATH reduced the estimated median age to ~ 20 years (Figure 4-12). Groundwater heads and groundwater contributing area remained the same when only effective porosity was changed (Figure 4-14) because simulated Darcy fluxes remained unaffected. Flow path lines were predominantly from eastern areas of model domain for both cases. Hydraulic gradient plays a key role in determining the extent of groundwater contributing area (and source of pollutants) while the effective porosity determines how fast the pollutant reaches the discharge point. The effect of dry (2001) and wet (2009) simulation years had a negligible effect on travel time and the groundwater contributing area (Figure 4-15) as hydraulic gradient and flux were not substantially affected by differences effective recharge across these years.

Although the estimated median age of ~20 years was accurately represented by lowering the effective porosity to 0.02, ~60% of particles traveled through the LFA which

is likely unrealistic. On the other hand, keeping the the effective porosity at 0.25 and reducing the hydraulic conductivity of the composite semi-confining unit and LFA by 100-fold and increasing the hydraulic conductivity in the UFA, keeping the effective hydraulic conductivity the same across the layers, reduced median groundwater age to ~20 years (Figure 4-16) and resulted in no groundwater flowing through the LFA, which is in better agreement with previous studies (Figure 4-17). In this case the recharge sources contributing older water (>100 years) originate from the large low-gradient parts of the Northern Highlands confined region (Figure 4-18) due to travel through the confining unit, whereas younger water (<20 years) is from the unconfined region directly north and south of the river. The groundwater conributing area with travel time less than 100 years falls primarily within the unconfined zone of the SFRB (Figure 4-19).

Travel Time Distribution Based NO_3-N Transport

Using the estimated TTDs from SWAT-MODFLOW-MODPATH with the adjusted hydraulic conductivities in layers 3-5, the five heuristic experiments described in the methods section were carried out to analyze the fate and transport of NO_3-N from different land use and land management systems. Persistent use of conventional higher input agricultural practices (MS3) in the future (Case1) results in a steady state nitrate concentration for groundwater emerging from the Devils Springs complex near Fort White of ~1.18 mg /L (Figure 4-20) which is within the lower range of average measured NO_3-N concentrations in Devil's Complex springs from 2013-2020: Twin Spring 0.9-1.3 mg/L, Ginnie Springs 1.0-1.7 mg/L, Devil 's Eye 1.4 to 2.0 mg/L, Gilchrist Blue Spring 2.0 to 2.4 mg/L (FDEP,2017; Florida Springs Institute, 2020).

Changing the management systems for row crops, hay, and pasture from MS3 to MS1 (Case 2) lowered the NO_3-N concentration from approximately 1.1 mg/L in 2020, to

0.6 mg/L in 2100. However, this is not sufficient to meet the NNC criteria of 0.35 mg/L NO_3-N (Figure 4-20). Converting pasture to hay and shifting all management practices to MS1 (Case 3) reduced the NO_3-N concentration to approximately 0.5 mg/L, which is also above the NNC. However, changing pasture to natural grass (Case 4) was able to meet the NNC by 2080. Converting all agricultural land uses to forests (Case 5) reduced the NO_3-N concentration to the NNC by 2055, and to background concentrations of approximately 0.1 mg/L by 2100 (Figure 4-20).

These results are consistent with the SWAT model predictions from Chapter 3 that predicted that implementing best management practices on current agricultural lands would be insufficient to meet the NNC in the Santa Fe River at Fort White. Nevertheless, results indicate that a combination of land use change and improved agricultural water and nutrient management pactices shows good potential for meeting the NNC.

Conclusions

A SWAT-MODFLOW-MODPATH model was developed and used to investigate the groundwater contributing area, groundwater flow paths and groundwater travel time distribution for the Devil's Complex springs in the Santa Fe River Basin. Results indicated that hydraulic conductivity had a major influence on predicting groundwater contributing area, flow path and travel times, whereas effective porosity had primary influence on predicting travel times. Differences in mean recharge between a wet dry year (2001) and a wet year (2009) did not substantially change estimates of contributing area, flow path or travel times.

Using the original calibrated NFSEG1.1 hydraulic conductivity in the SWAT-MODFLOW-MODPATH model estimated that more than 50% of the groundwater

emerging from springs in the Devil's Complex area traveled through the LFA.This resulted in a median groundwater age of more than 200 years, which is not consistent with previous modeling and tracer studies (Ellins et al., 1991; Crandall et al., 1999; Sepulveda et al., 2012). Decreasing the hydraulic conductivity for the composite semi confining unit (layer 4) and the LFA (layer 5) and increasing the hydraulic conductivity for the UFA (layer 3), while keeping the effective hydraulic conductivity across the three layers the same as for the original calibrated model, eliminated groundwater traveling through the LFA and reduced the estimated median age of groundwater to ~20 years. This finding raises questions about how the original NFSEG 1.1 model parameterization represents the groundwater flow and travel paths through the FAS and suggests that further calibration and validation of the coupled SWAT-MODFLOW model should be conducted before combining with the USGS Reactive Transport Model (RT3D).

Using the predicted travel time distributions from the SWAT-MODFLOW-MODPATH model with the modified hydraulic conductivity field and an effective porosity of 0.25, and land use-specific annual average NO_3-N leaching concentrations from the SWAT model, the fate and transport of NO_3-N to the reach of the Santa Fe River containing the Devil's spring complex was analyzed for a set of land use- land management system scenarios. Results indicated that keeping the 2017 land use pattern but changing agricultural management systems from conventional practices to current best management practices in 2020 would not be sufficient to meet the NNC of 0.35 mg/L NO_3-N established by the Florida Department of Environmental Protection. Results showed that if in the year 2020 current row crop and hay land uses were converted from conventional to best management practices, and all pasture was

converted to native grassland, the NNC could be met by 2080. If all row crops, hay, and pasture were converted to forest in 2020, the NNC could be met in 2055.

The predictions of nitrate concentration emerging from the Devil's springs complex using SWAT-MODFLOW-MODPATH based TTDs were based on simplifying assumptions such as the spatially and temporally uniform nitrate concentration by land-use, steady state groundwater flows and spatially and temporally constant denitrification rate. Chapter 3 showed that nitrate concentrations and water recharging the aquifer vary over space and time according to soil type, weather, land use and management practices, and it is well known that denitrification rates are dependent on dissolved oxygen and organic matter concentrations in the aquifer. Therefore, relaxing these assumptions could improve model utility. Similar particle tracking studies to estimate groundwater travel time distribution, recharge source contributing area, and fate and transport of nitrate in the Ichetucknee and Hornsby springsheds should be conducted to extend the analysis to other impaired springs in the Santa Fe river basin.

Table 4-1. NO_3-N Concentration (mg/L) from various land uses by management systems

	MS3	MS2	MS1
Row Crops	8.3	5.5	2.5
Hay	4.5	3.4	2.8
Pasture	9.2	6.4	4.7
Slash Pine*		0.3	
Grass*		0.3	

*Denotes constant for all systems

Table 4-2. Summary of case studies representing assumed current and future practices.

Experiments	Current Practices (1970-2020)	Future Practices (2020-2100)
Case 1	Row crops: MS3 Hay: MS3 Pasture: MS3	Row crops: MS3 Hay: MS3 Pasture: MS3
Case 2	Row crops: MS3 Hay: MS3 Pasture: MS3	Row crops: MS1 Hay: MS1 Pasture: MS1
Case 3	Row crops: MS3 Hay: MS3 Pasture: MS3	Row crops: MS1 Hay: MS1 Pasture*: Hay MS1
Case 4	Row crops: MS3 Hay: MS3 Pasture: MS3	Row crops: MS1 Hay: MS1 Pasture*: Grass
Case 5	Row crops: MS3 Hay: MS3 Pasture: MS3	Row crops*: Slash Pine Hay*: Slash Pine Pasture*: Slash Pine

*Denotes changes in landuse along with land management practices.

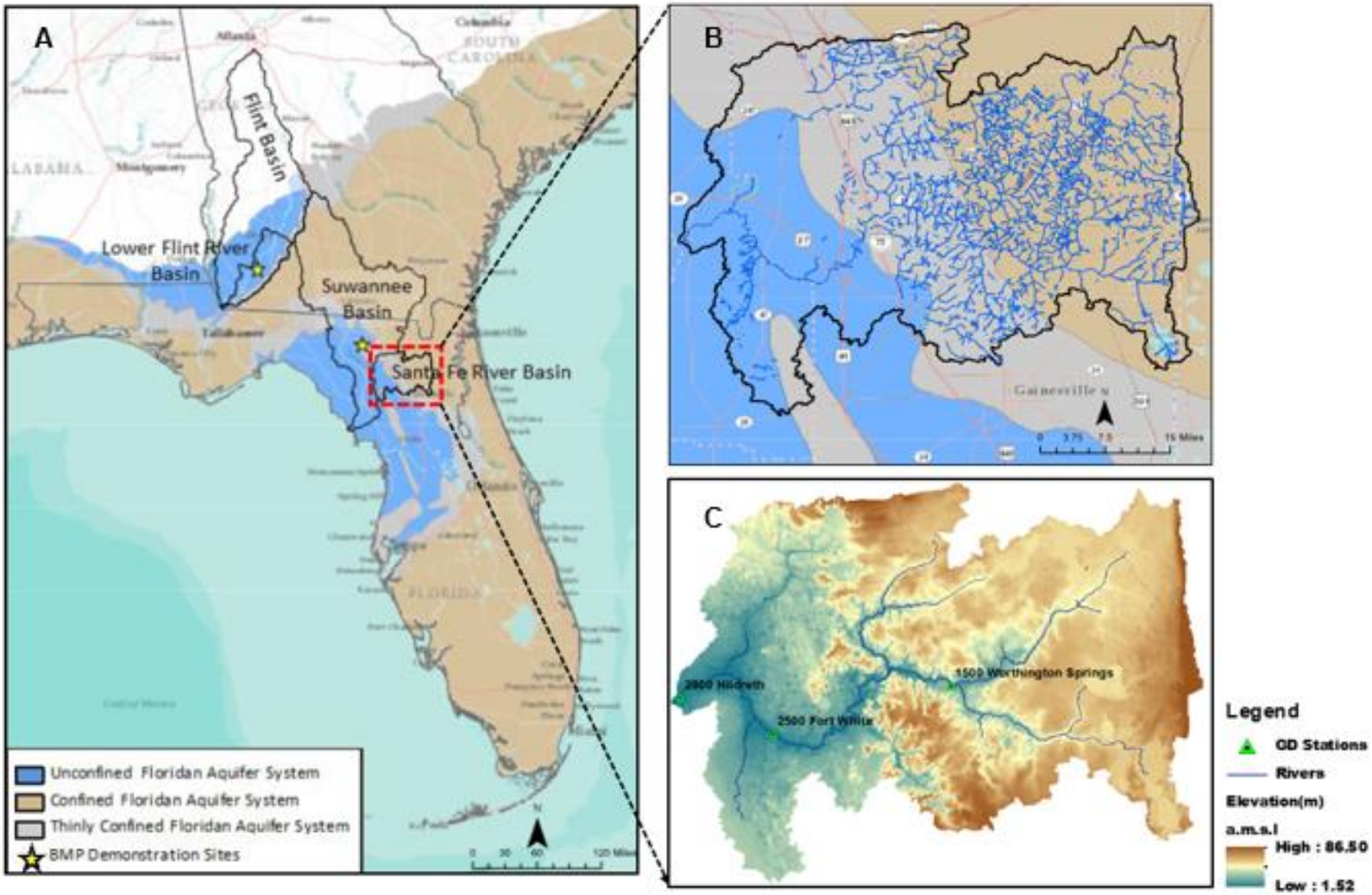

Figure 4-1. Location map for the Suwanee River Basin and its tributary Santa Fe River Basin with the underlying Floridan aquifer system. (A) Extent of Floridan Aquifer System. (B) Hydrogeological features of Santa Fe River Basin (SFRB). (C) Santa Fe River Basin (SFRB) with topography, stream network and GD (gauge discharge) sites. http://floridanwater.org/issues/

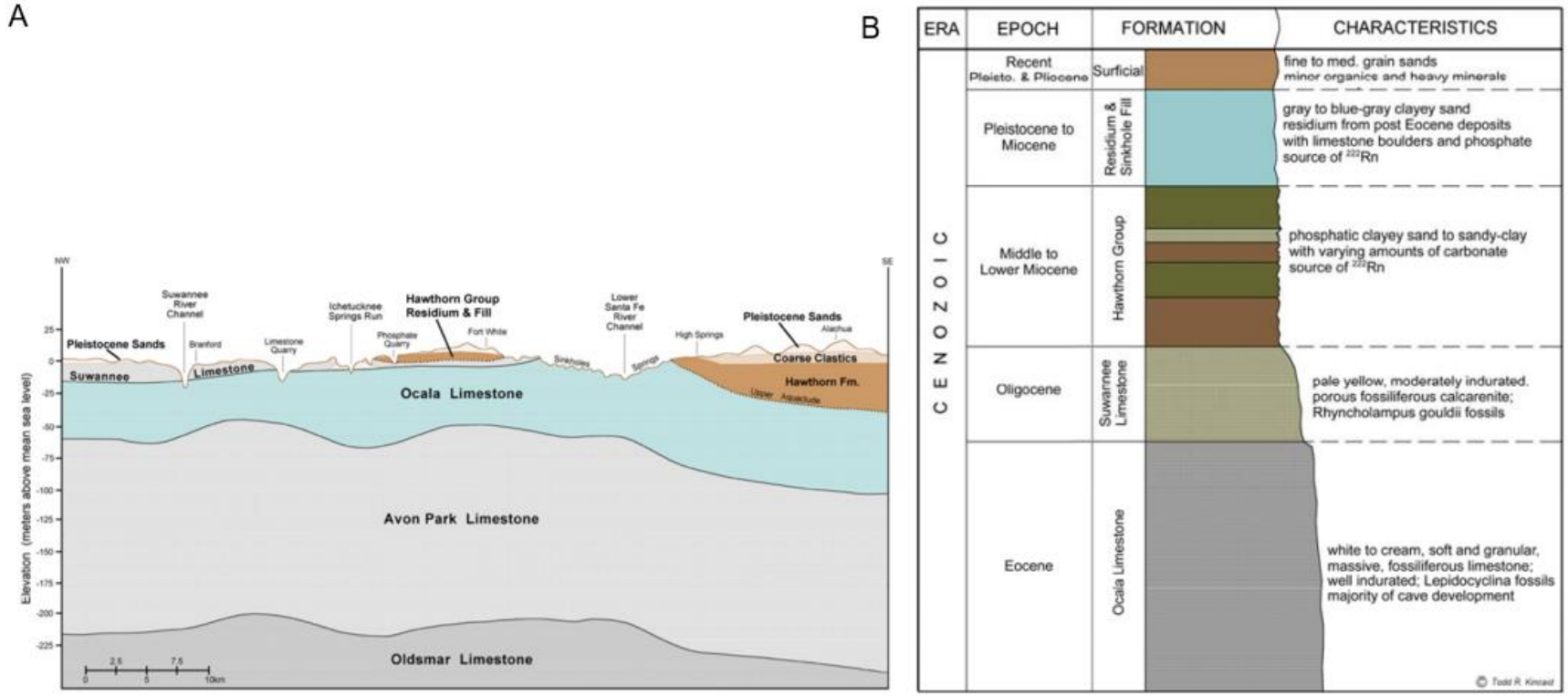

Figure 4-2. Geologic cross-section across the Santa Fe River Basin from northwest to south-east (Ref: Todd R. Kincaid, PhD, 2007). (A) Geologic cross-section across the Santa Fe River Basin. (B) Stratigraphic sequence underlying the Santa Fe River Basin, north-central Florida.

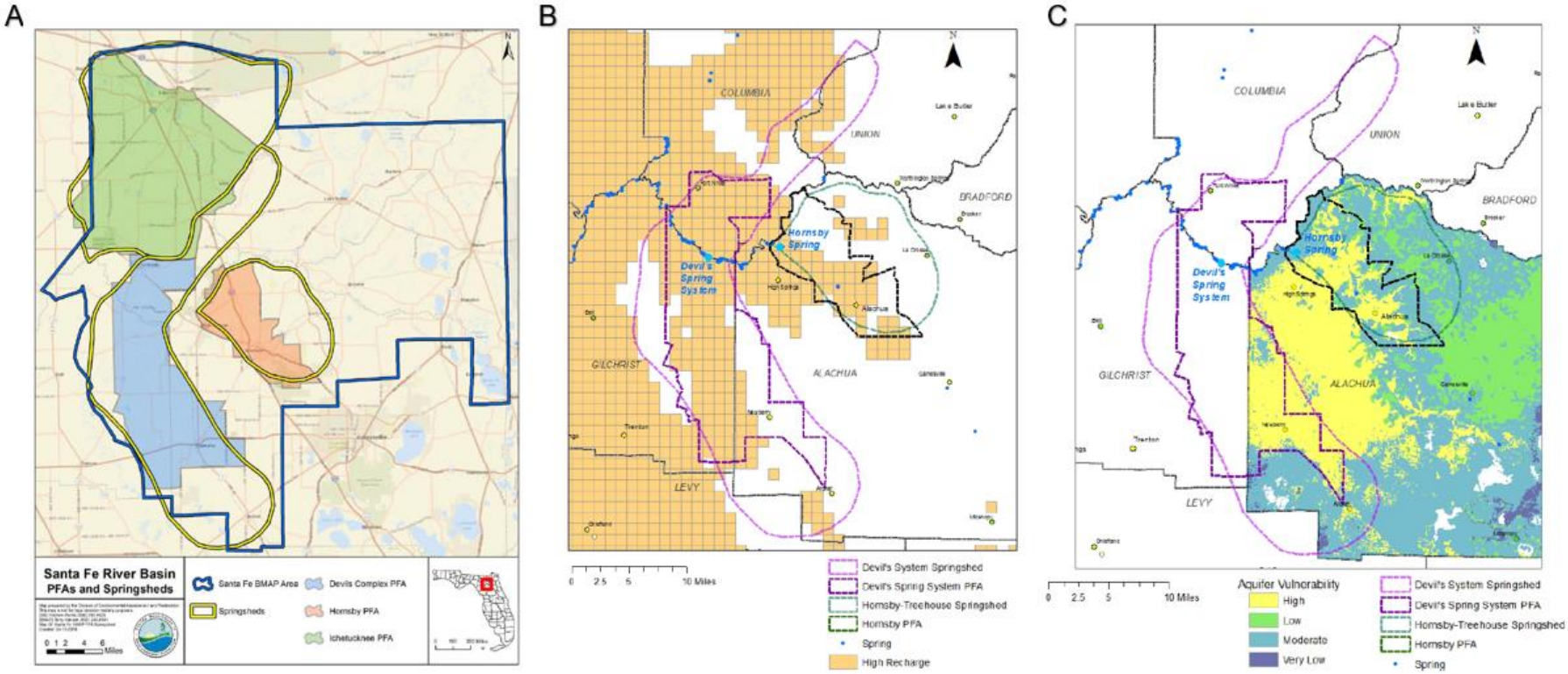

Figure 4-3. Santa Fe River BMAP and PFA boundaries. (A) PFA boundaries. B) High recharge area to the Floridan aquifer (≥10 in/yr) based on USGS 2002 methodology. (C) Aquifer vulnerability in Alachua County based on Florida Aquifer Vulnerability Assessment (FAVA) model. (Reference: FDEP, 2018)

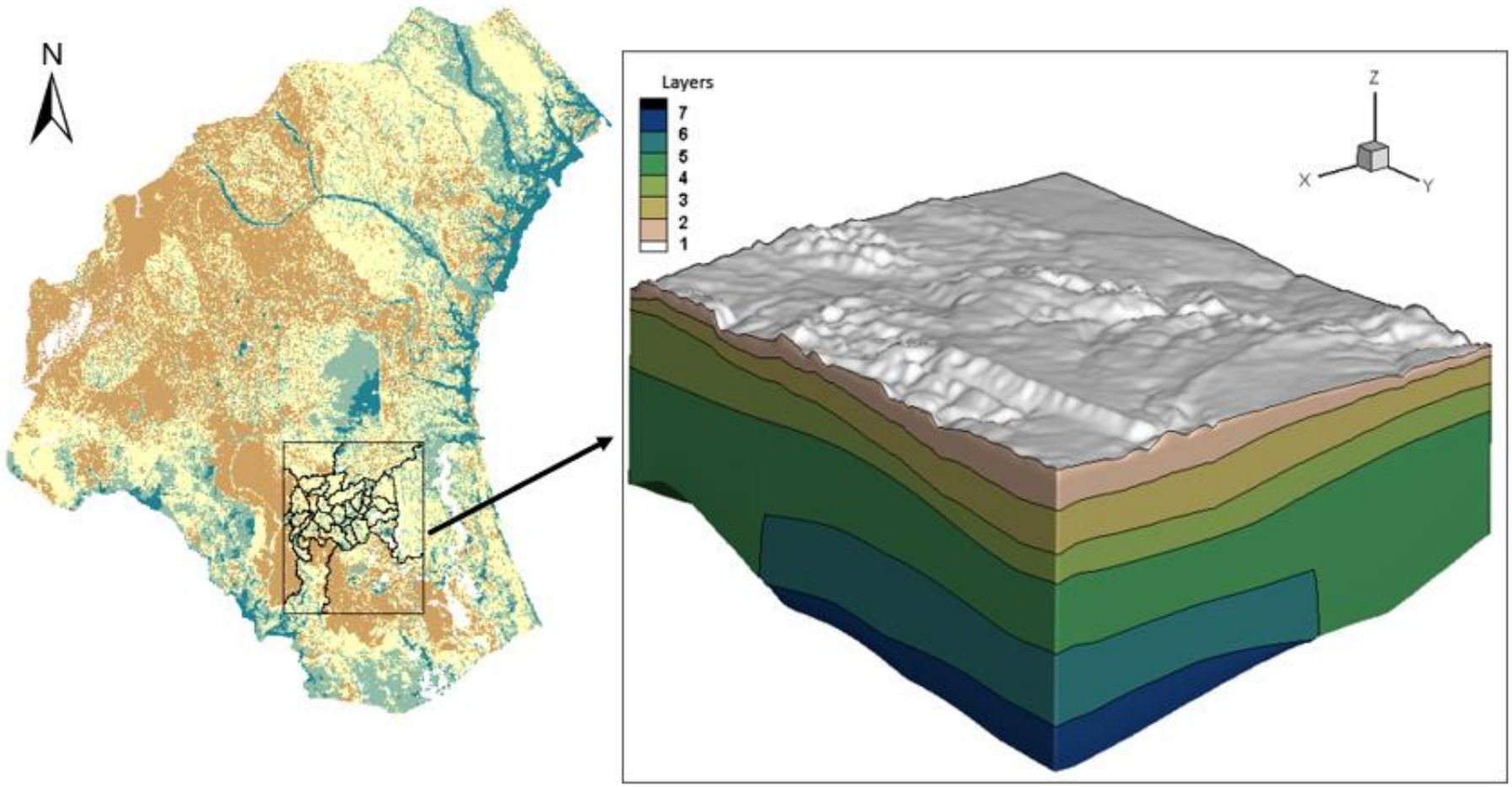

Figure 4-4. Santa Fe River Basin (SFRB) SWAT-MODFLOW domain (Left), 3D diagram of layers within the NFSEG model for SFRB region (Right), 3rd layer is Upper Floridan Aquifer (UFA), and 5th layer is Lower Floridan Aquifer (LFA).

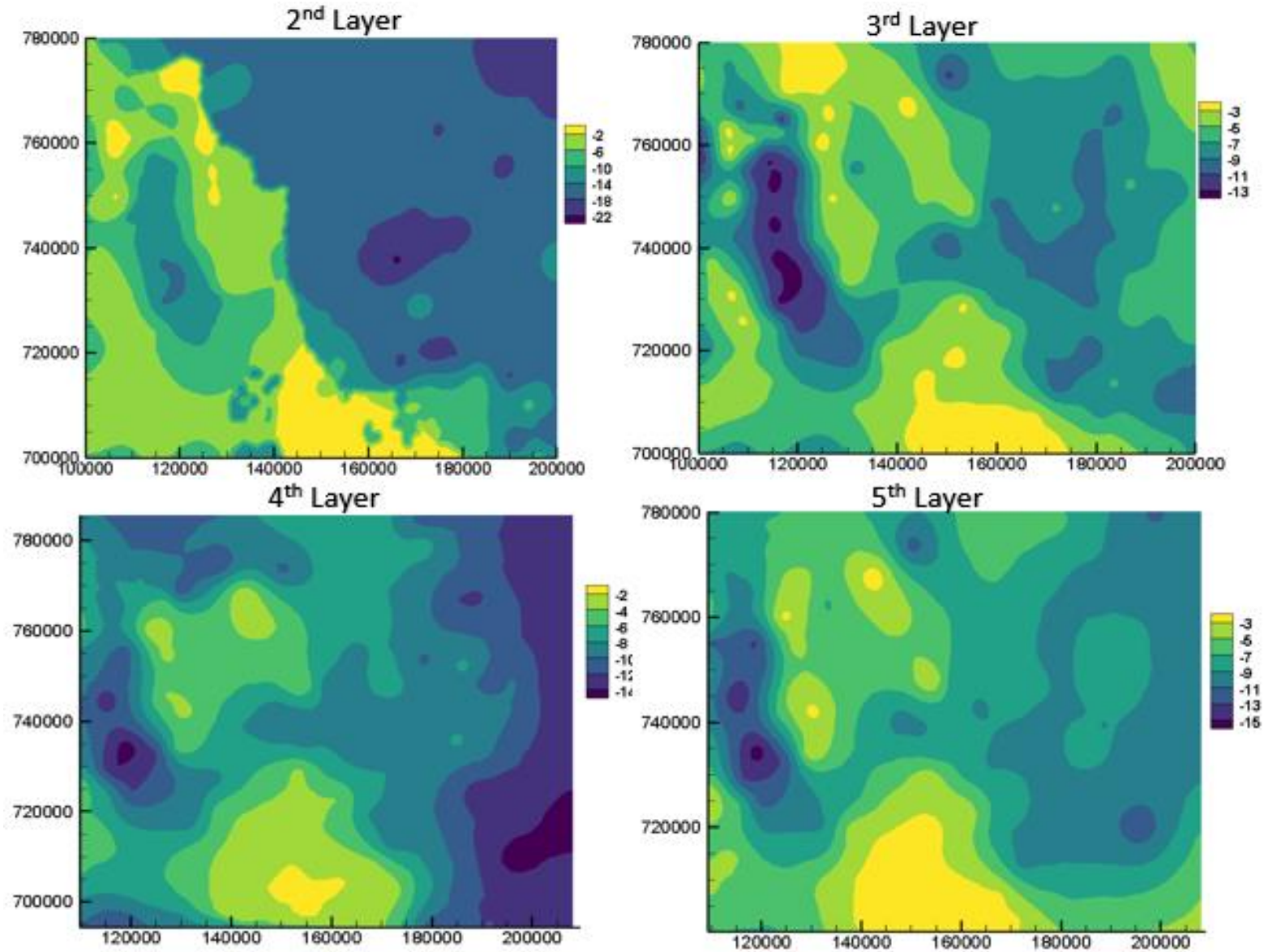

Figure 4-5. Spatial distribution of horizontal hydraulic conductivity (Kx (m/day)) for 2nd, 3rd, 4th, and 5th layer in log scale.

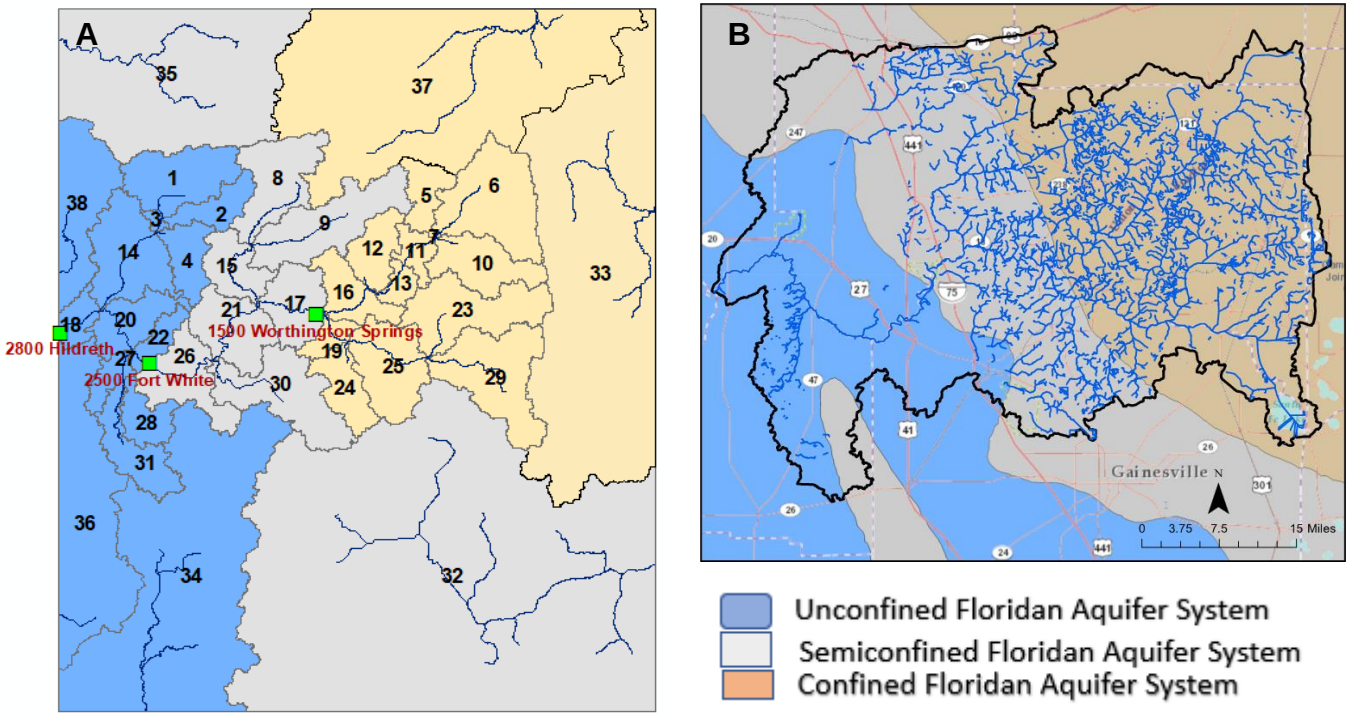

C

Zones	Santa Fe watershed subbasins	Subbasins outside Santa Fe watershed
Confined	5,6,10,11,12,13,16,19,23,24,25,29	37,33
Semi confined	8,9,15,17,21,26,30	32,35
Unconfined	1,2,3,4,14,18,20,22,27,28,31	34,36,38

Figure 4-6. Extended sub basins outside the Santa Fe River Basin. (A) Sub basins for entire domain. (B) Hydrogeological zone across Santa Fe River Basin. (C) Calibrated parameters of SFRB subbasins applied to the subbasins outside of SFRB.

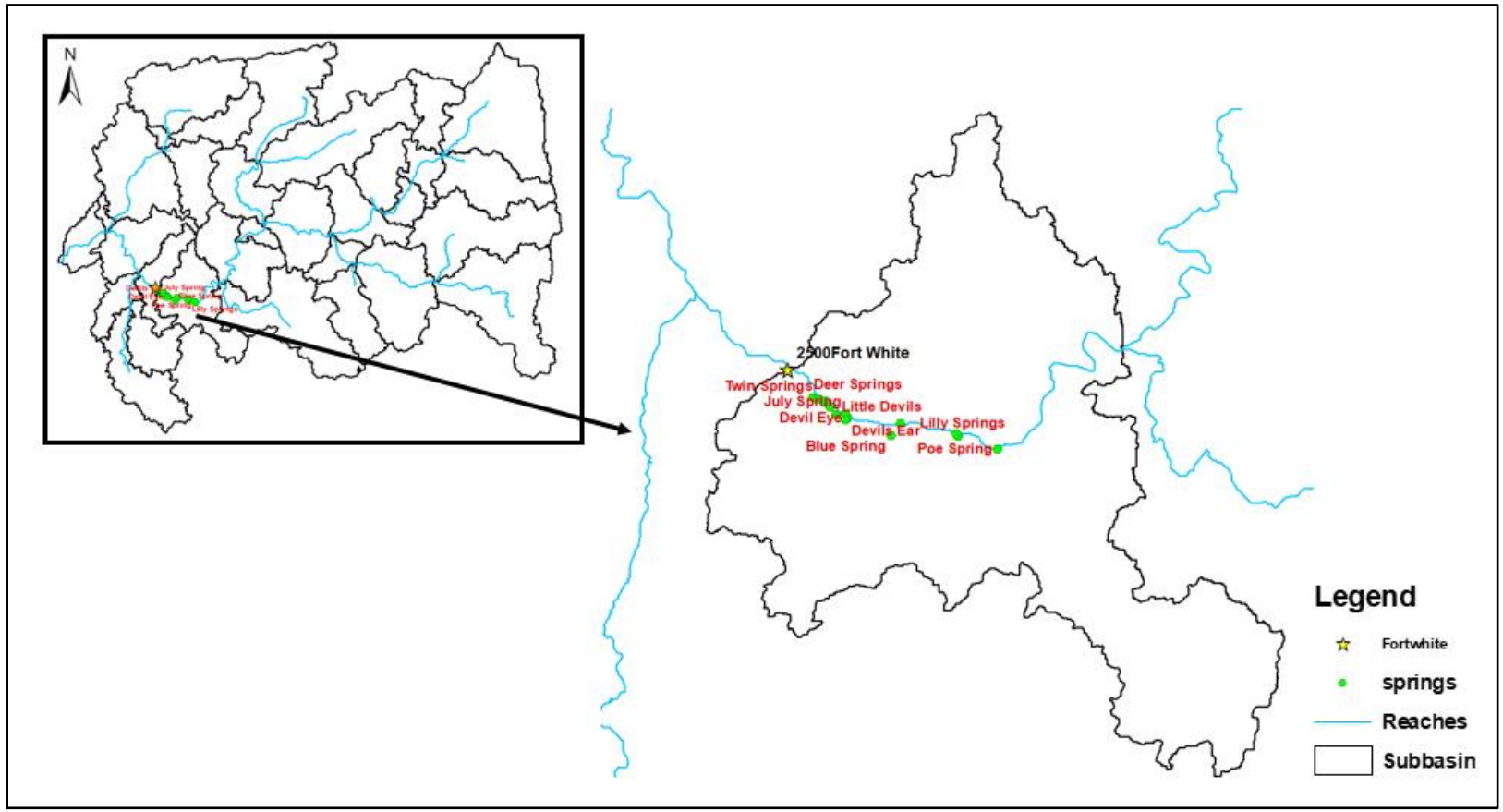

Figure 4-7. Santa Fe River within the Ft White subbasin where particles were released.

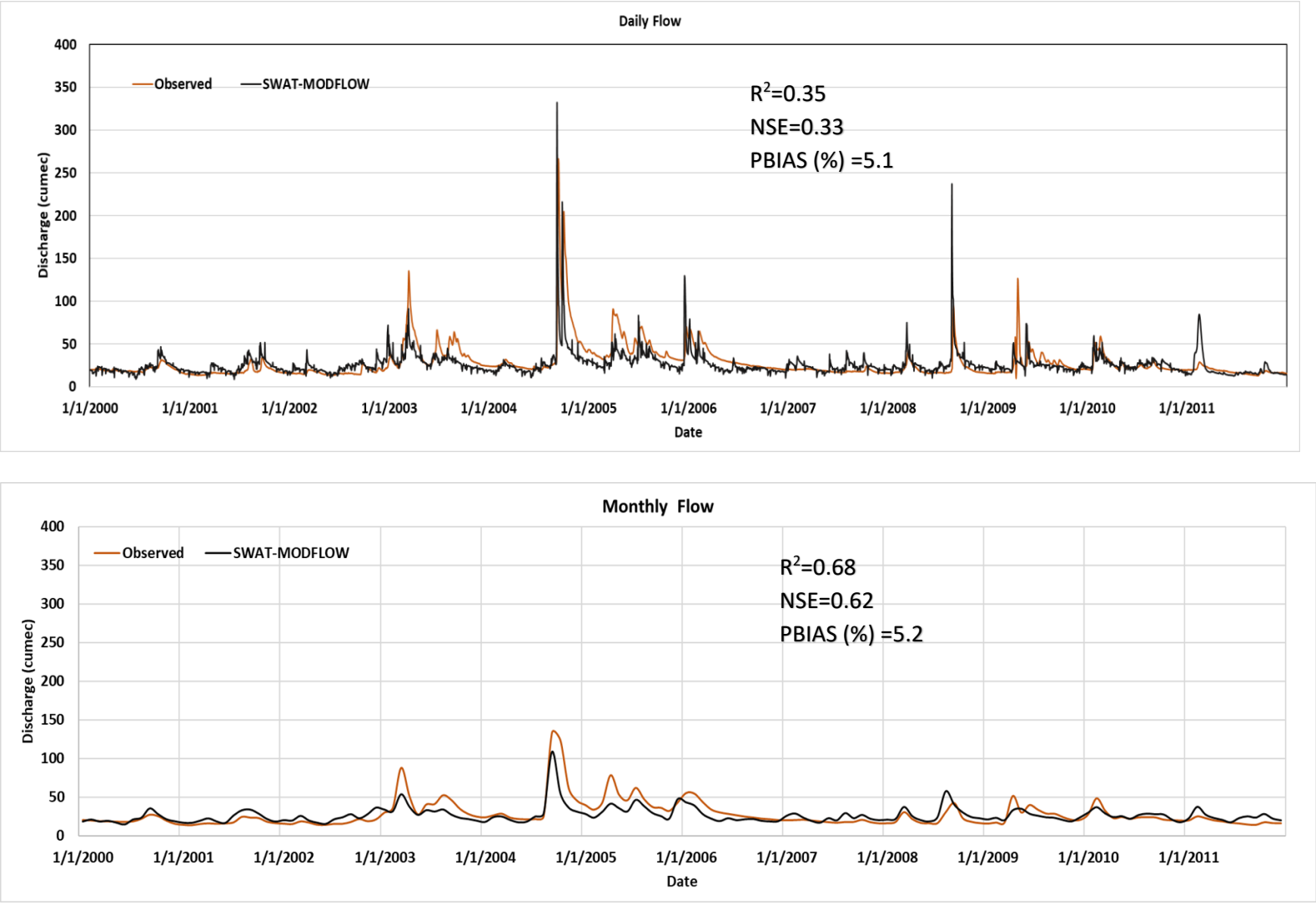

Figure 4-8. Comparison of the daily and monthly simulated vs. observed streamflow at Fort White For SWAT-MODFLOW.

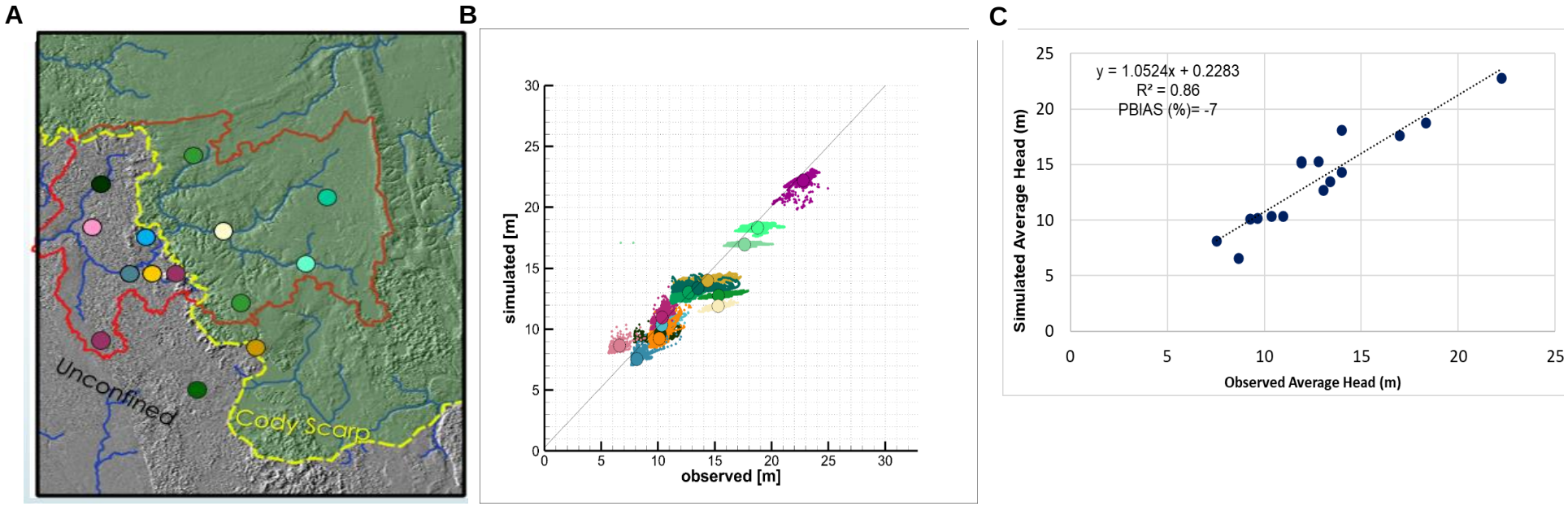

Figure 4-9. Comparison of simulated and observed hydraulic head in UFA for each observation well. (A) location of Cody scarp, observation wells and unconfined zone. (B)The big dots are the mean values over the time-period and the small dots represent all the values over time. (C) Observed vs simulated average head.

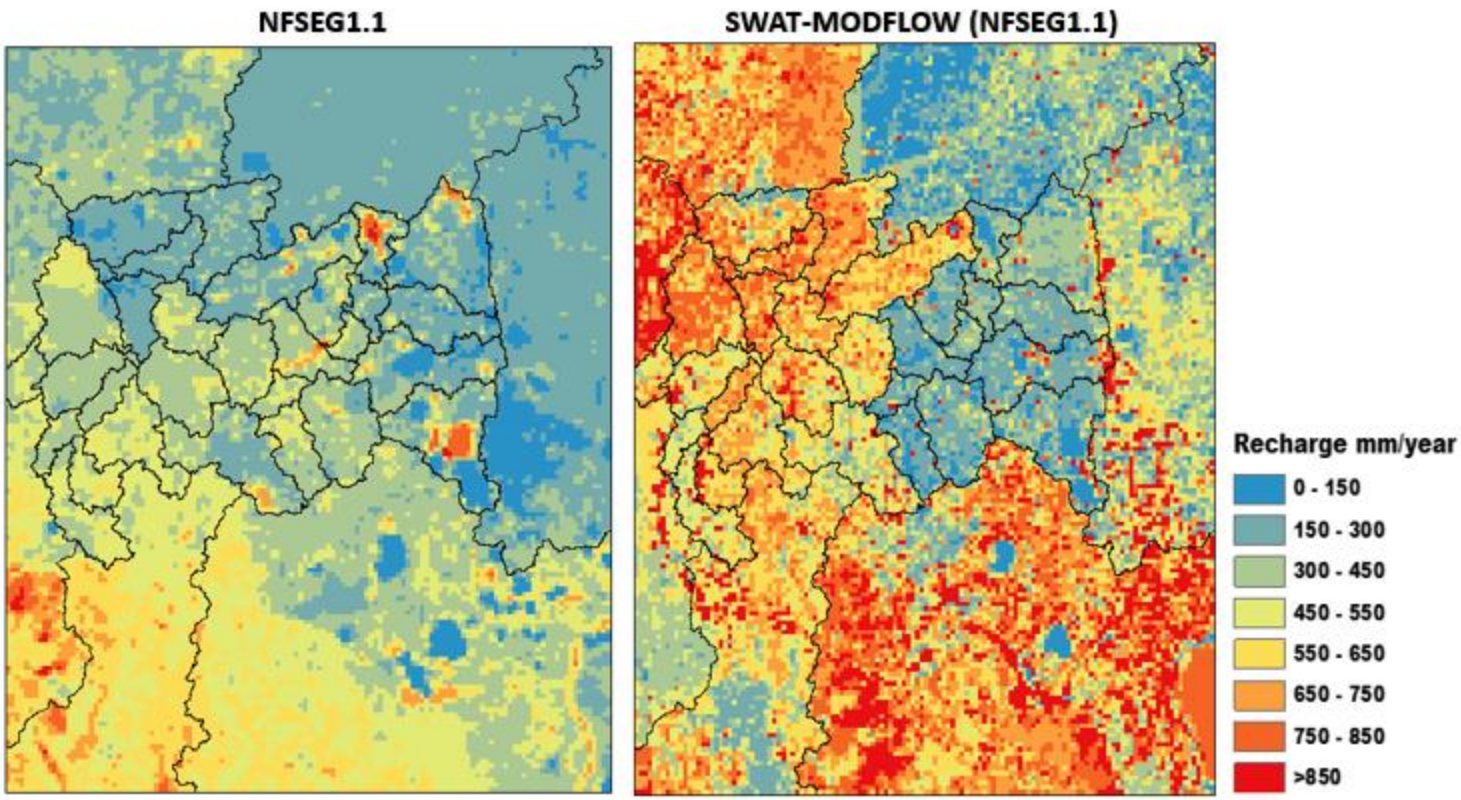

Figure 4-10. Recharge from SWAT-MODFLOW and NFSEG 1.1 for wet year 2009.

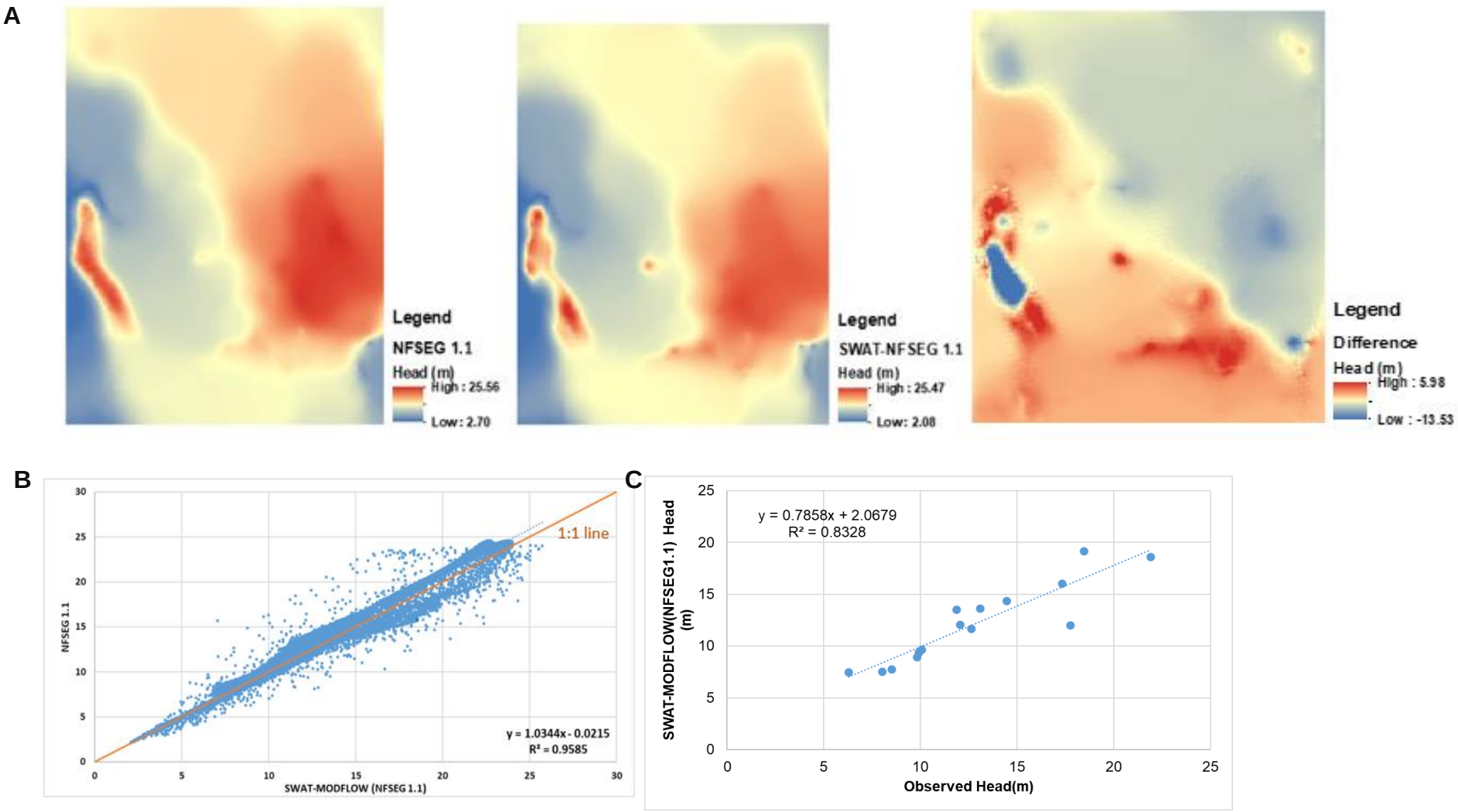

Figure 4-11. Simulated head of NFSEG 1.1 Vs SWAT-MODFLOW and the difference in head. (A) Simulated head SWAT-MODFLOW Vs NFSEG 1.1). (B) Simulated head (UFA) for SWAT-MODFLOW vs NFSEG1.1 across all model grids for year 2009. (C) Observed head vs simulated SWAT-MODFLOW for year 2009.

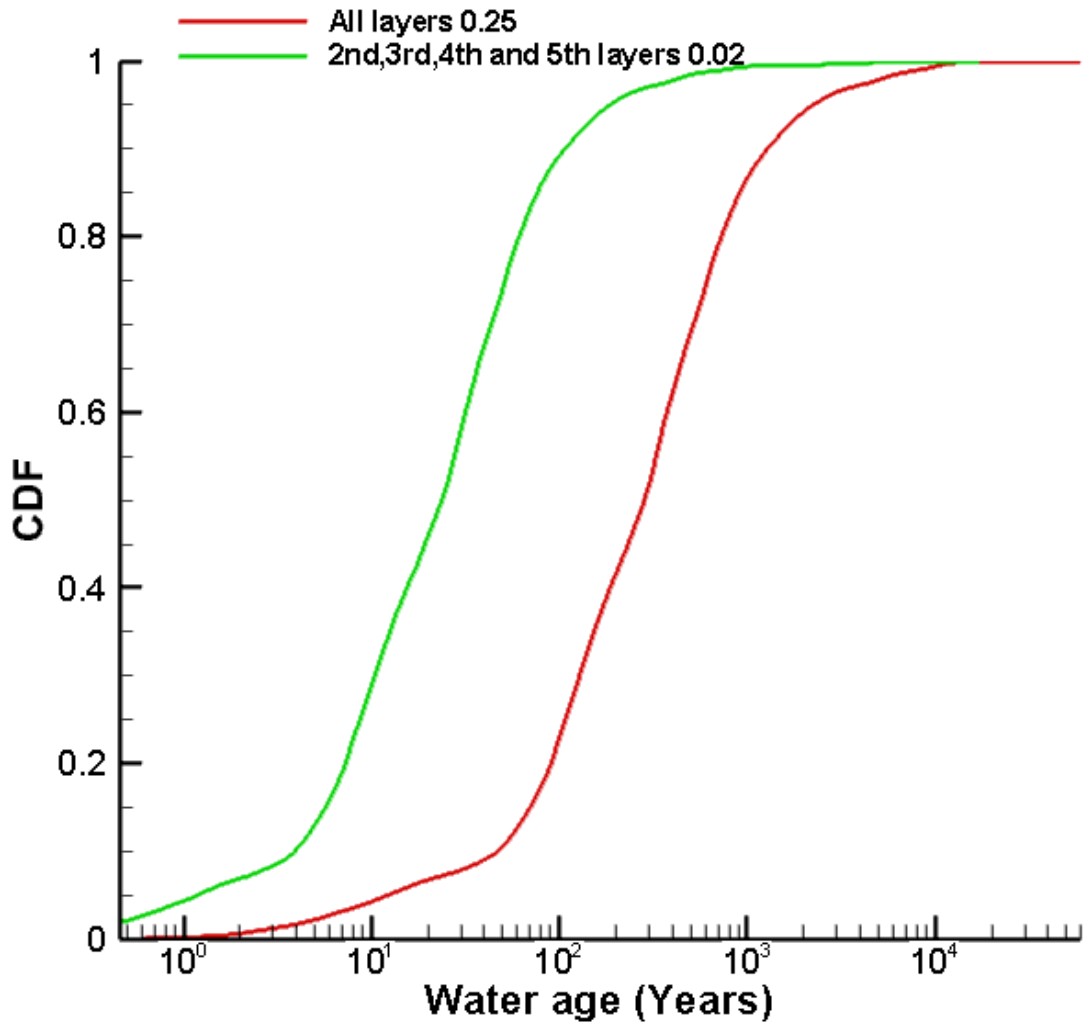

Figure 4-12. Travel time distribution (TTD) for different values of effective porosity for SWAT-MODFLOW-MODPATH.

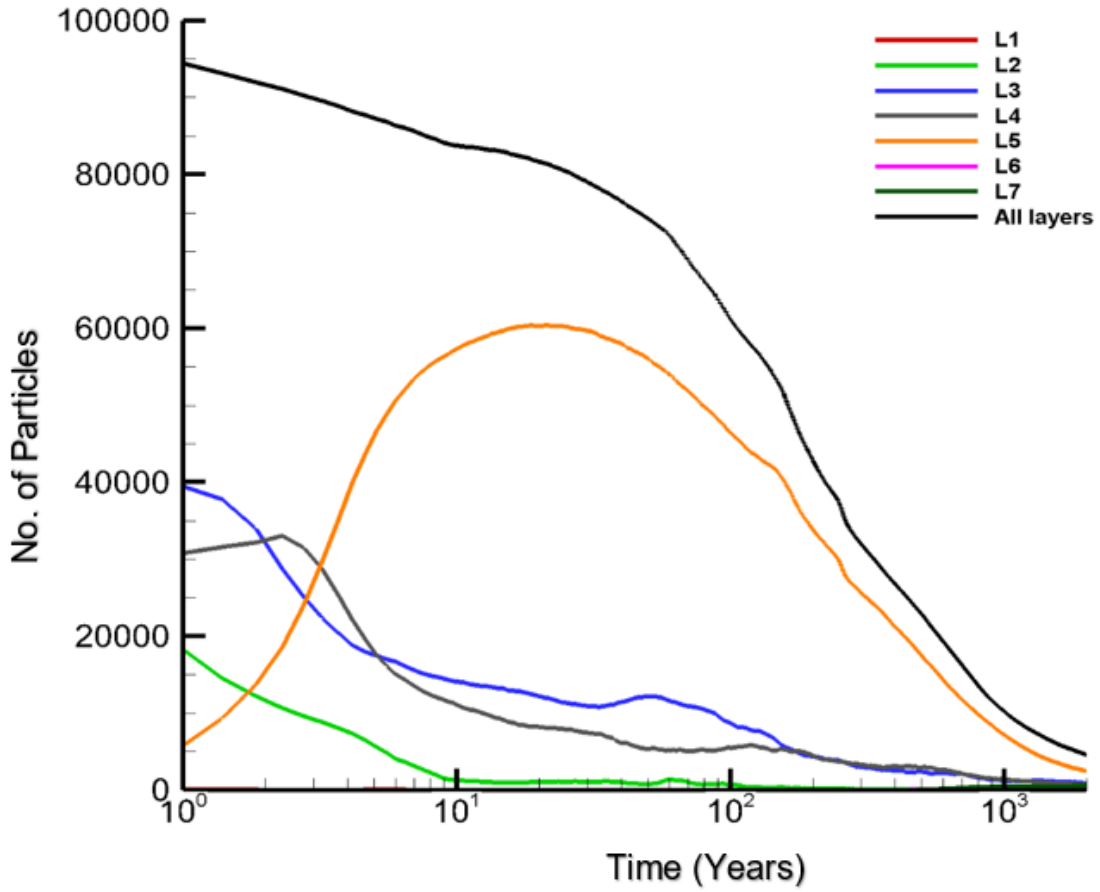

Figure 4-13. Number of particles per layer with respect to time for SWAT-MODFLOW-MODPATH for effective porosity 0.25 for each layer. Due to very small number of particles entering 6th and 7th layer the graphs for these two layers are not visible. Particles remain in 1st layer for a very short time so are not clearly visible.

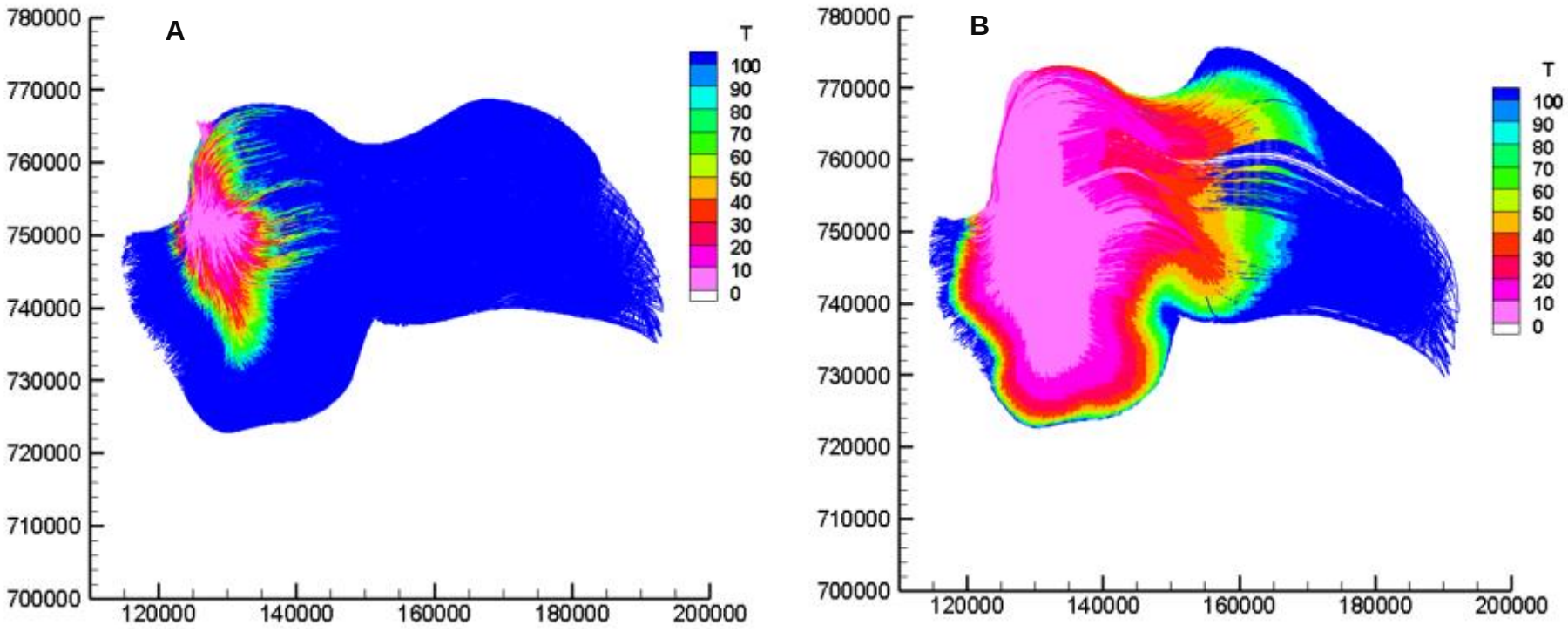

Figure 4-14. Groundwater contributing area map. A) all layers 0.25 effective porosity. B) 0.02 effective porosity for all layers except 1st (T= years).

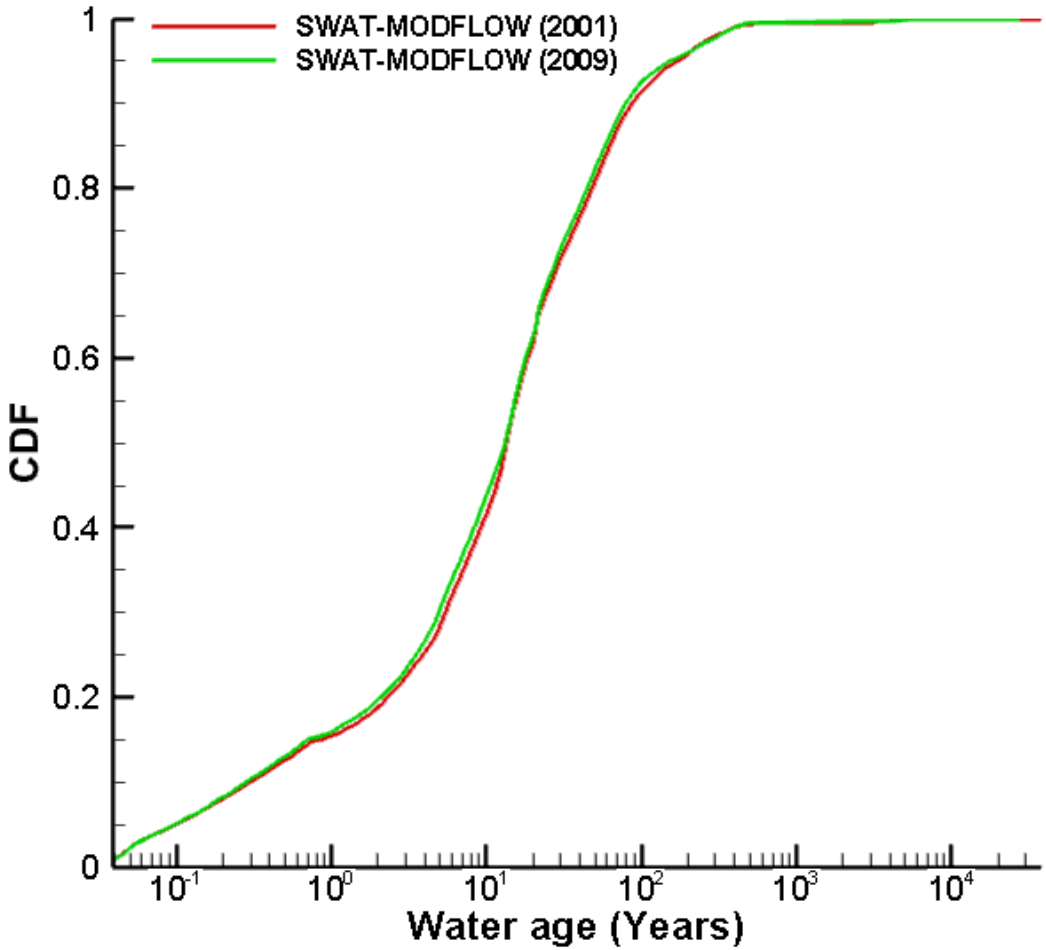

Figure 4-15. Travel time distribution (TTD) for SWAT- MODFLOW-MODPATH models for year 2001 and 2009 with effective porosity 0.02 for 2nd,3rd, 4th, and 5th layer.

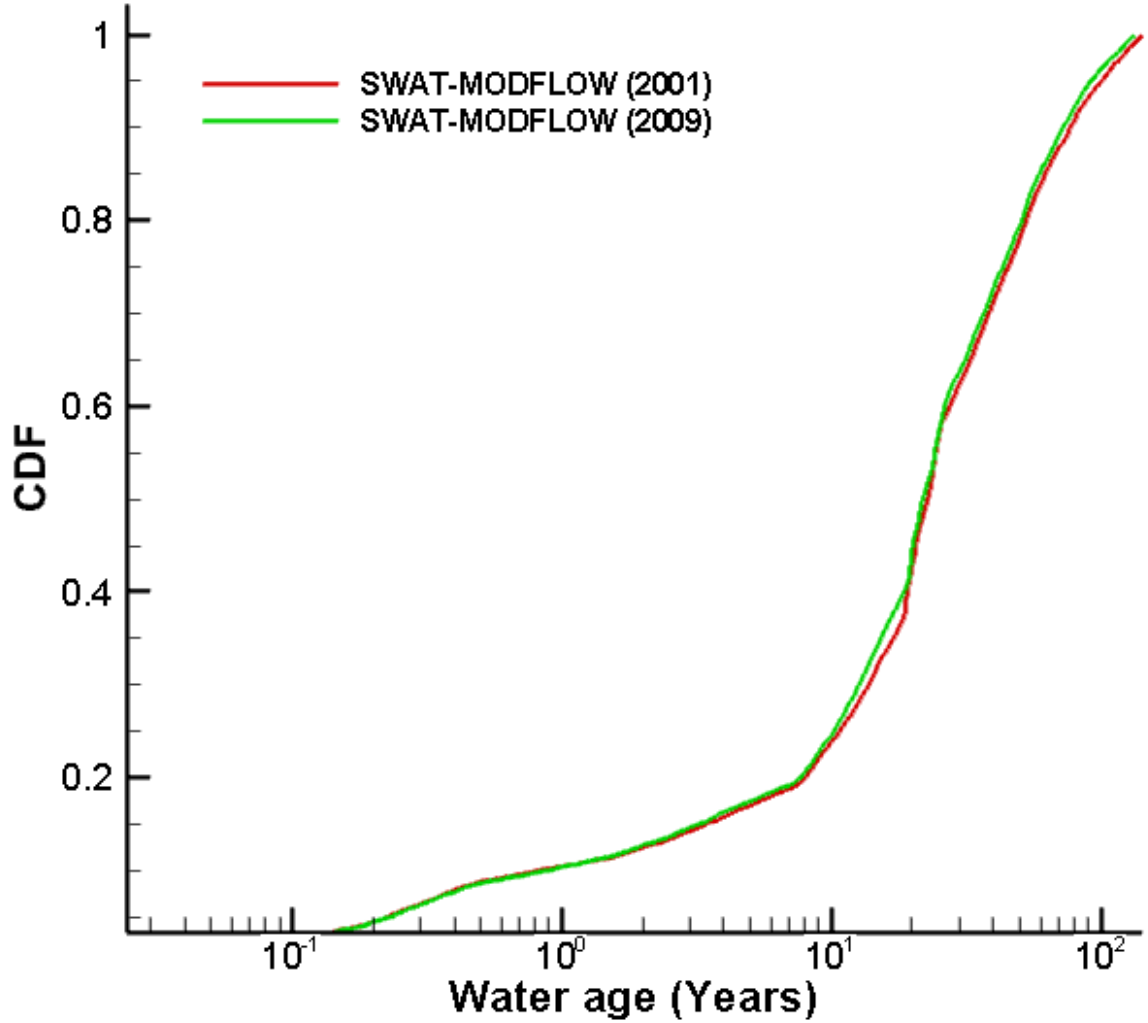

Figure 4-16. Travel time distribution (TTD) of SWAT-MODFLOW-MODPATH models with adjusted hydraulic conductivity in layers 3,4, and 5.

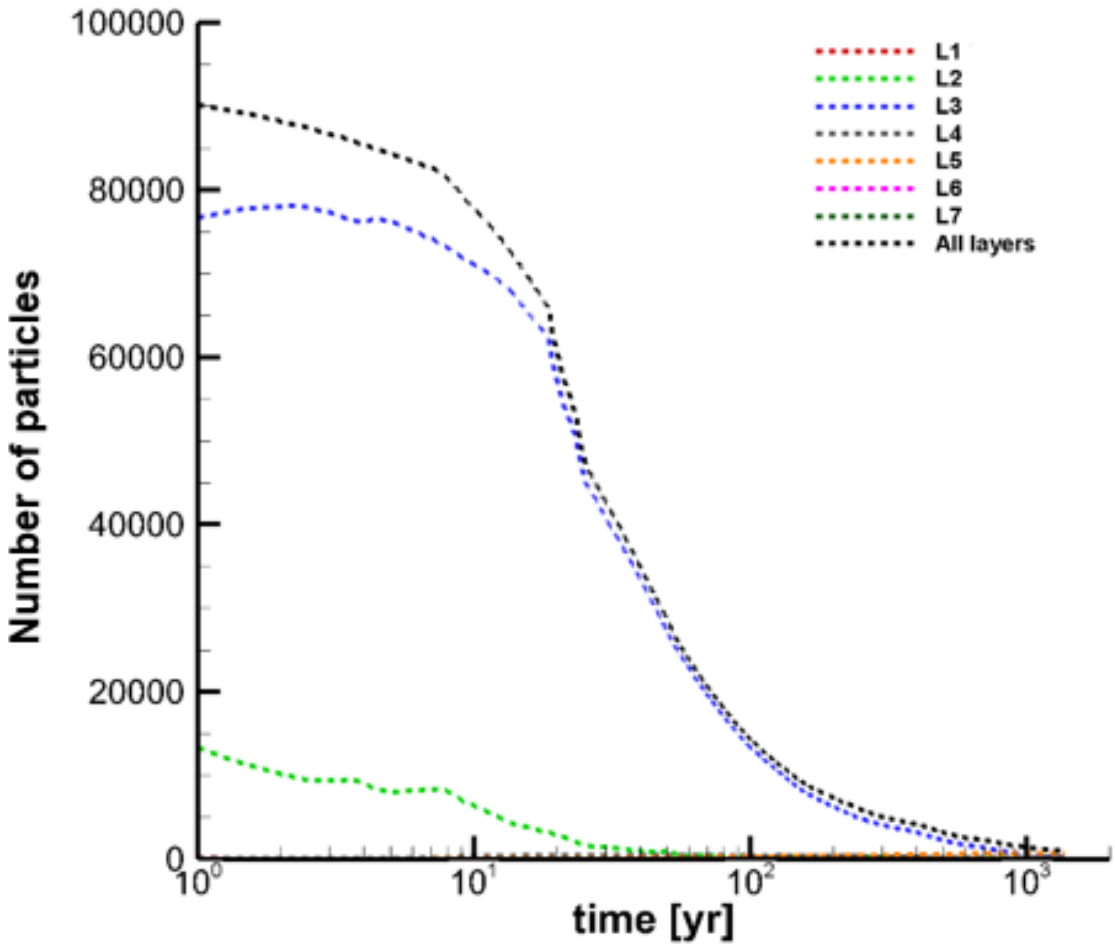

Figure 4-17. Number of particles per layer with respect to time for SWAT-MODFLOW-MODPATH with adjusted hydraulic conductivity.

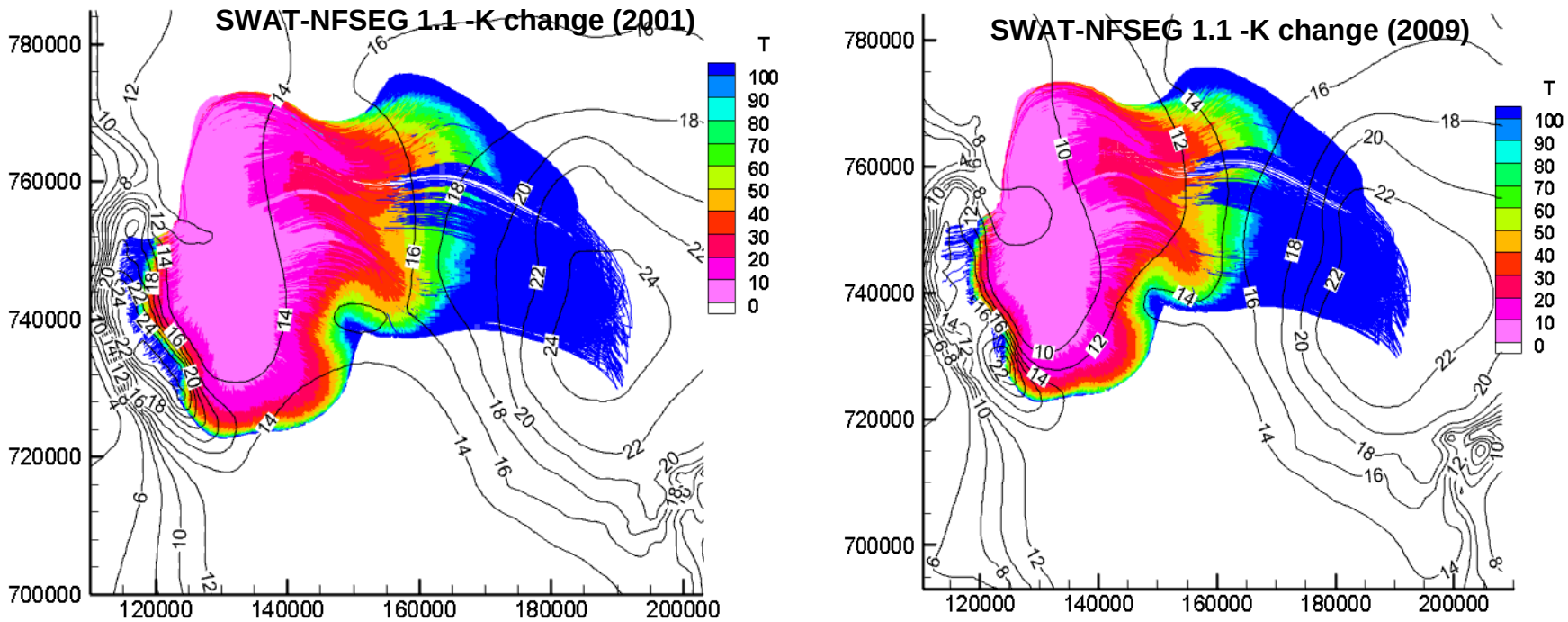

Figure 4-18. Spatial distribution of groundwater contributing area and simulated UFA head contour lines. (T=years)

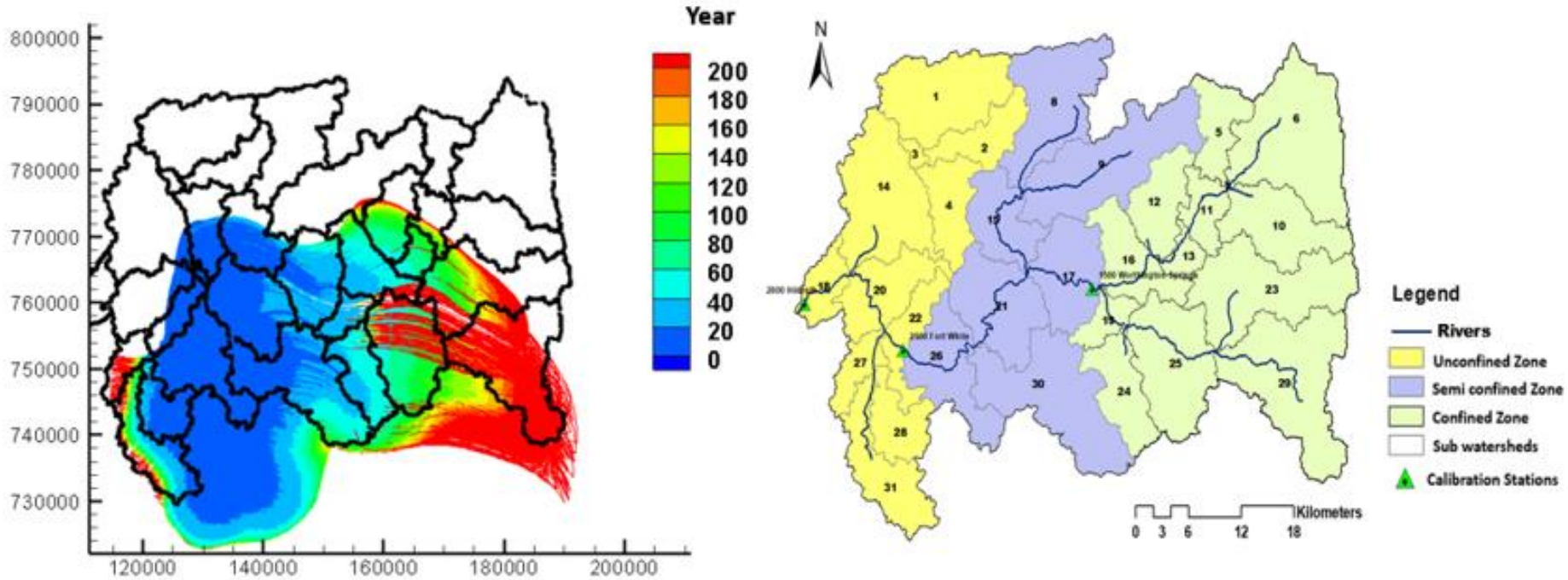

Figure 4-19. Flow path lines for SWAT-MODFLOW-MODPATH over SWAT SFRB sub basins (Left). Hydrogeologic zones of SFRB with gauge stations (Right).

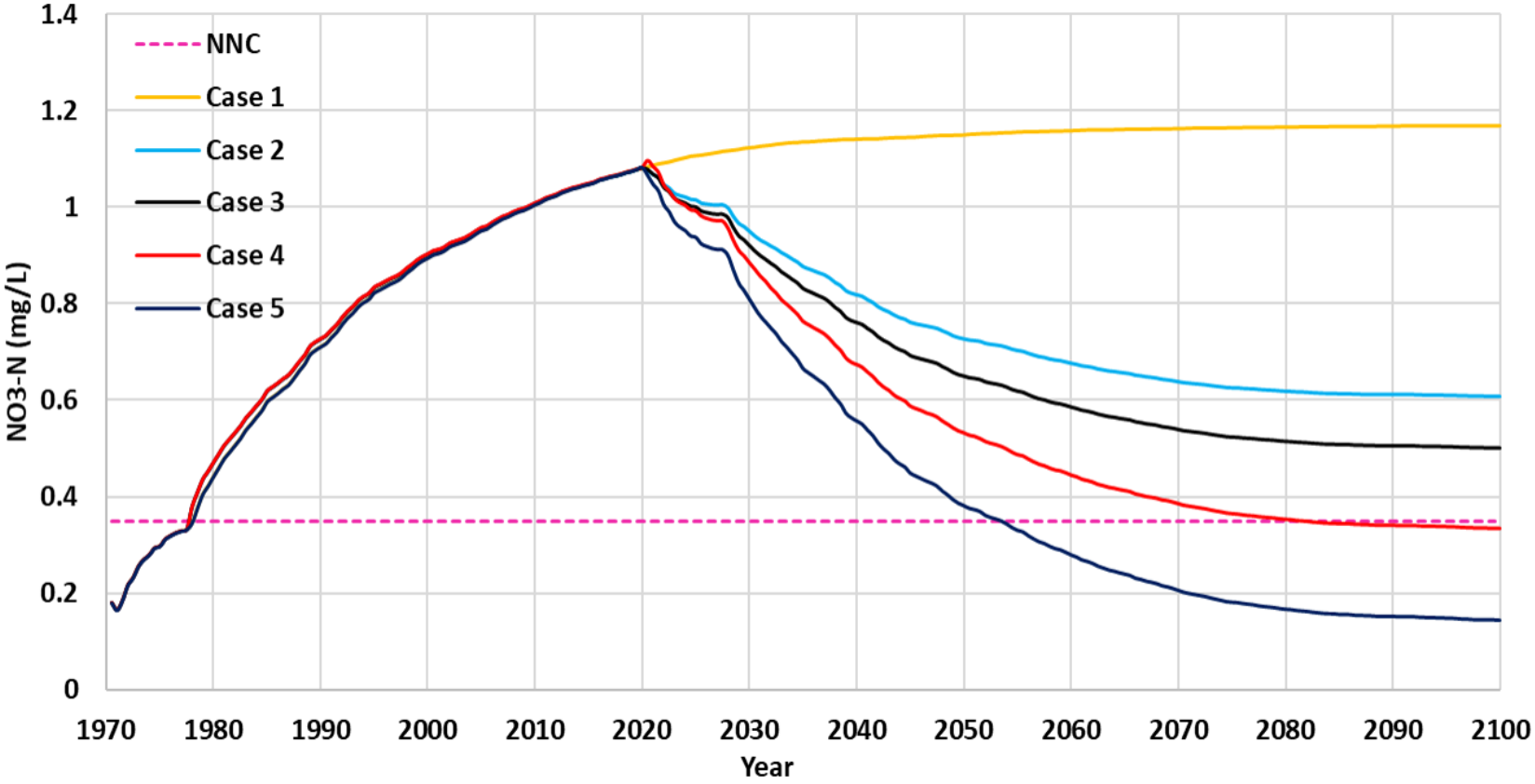

Figure 4-20. Break though curve of total NO_3-N concentration with denitrification for different case studies.

CHAPTER 5
CONCLUSIONS, CONTRIBUTIONS AND RECOMMENDATIONS FOR FUTURE REASEARCH

Nitrate-nitrogen (NO_3-N) loading to groundwater is a chronic problem worldwide due to its detrimental effects on the ecological health of springs, streams, and lakes as well as on human health. The NO_3-N pollution issue is especially critical in karst aquifers because of their susceptibility to leaching of contaminants from the land surface. The Upper Floridan aquifer (UFA), one of the most productive karst aquifers in the world, is a major source of public water supply and irrigation in north and central Florida and has experienced elevated nitrate concentrations in its groundwater and springs. In response to these increasing NO_3-N concentrations a Numeric Nutrient Criteria (NNC) of 0.35 mg/L NO_3-N has been set for groundwater emanating from UFA springs. Total Maximum Daily Loads (TMDLs) estimated to achieve the NNC, and Basin Management Action Plans (BMAPs) required to meet the TMDLs, have been established for UFA springs not meeting the NNC.

The Santa Fe River Basin (SFRB) overlying the UFA in north central Florida, USA provides an excellent location in which to investigate causes and potential solutions for the UFA nitrate enrichment problem. The SFRB spans a transition zone between confined and unconfined regions of the UFA. Numerous springs that feed the unconfined portion of the Santa Fe River have NO_3-N concentrations above the NNC. The Santa Fe River BMAP (FDEP, 2018) has estimated that a 65% reduction in NO_3-N load to groundwater will be required to achieve the NNC. The complex hydrogeological features of the SFRB, magnitude of the nitrate enrichment problem, and good

availability of hydrologic and water quality data, provided a good platform to conduct this study.

One of the key sources of NO_3-N pollution to the UFA in general, and the SFRB in particular, is the application of synthetic N fertilizer to enhance agricultural production. Many Best Management Practices (BMPs) for N fertilizer and irrigation have been tested at the field scale with the goal of maintaining yields while reducing leaching. However, these short duration experiments do not provide information on the effectiveness of the BMPs over a wide variety of weather conditions or soil types. In addition, these experiments often do not measure the reduction in leaching and other environment losses associated with BMP adoption and therefore cannot estimate the effectiveness of widespread adoption of BMPs on receiving water bodies such as aquifers, springs, and rivers

The objectives of this dissertation were to utilize a combination of field-scale and watershed scale hydrologic models to 1) leverage the available experimental and observational data in the SFRB to quantity the nitrate leaching reductions that can be expected from the adoption of improved agricultural nutrient and irrigation management practices in the SFRB; 2) estimate the impact of these leaching reductions on nitrate loads to and nitrate concentrations in the Santa Fe River; and 3) determine the most vulnerable regions of the SFRB where changes in practices could be targeted to improve spring and river concentrations, and estimate the time required to observe reductions in river nitrate concentrations as a result of potential changes in practices in these vulnerable regions.

Based on these objectives, major research findings and suggestions for further investigation are summarized below.

Objective 1. Quantify the nitrate leaching that can be expected from the adoption of improved agricultural nutrient and irrigation management practices in the SFRB.

- The agro-ecohydrological model, Soil and Water Assessment Tool (SWAT) was successfully used at the field scale to simulate impacts of alternative fertilizer and irrigation management practices on crop yield, irrigation demand and nitrate leaching for a three-year corn-peanut rotation BMP experiment conducted at the North Florida Research and Education Center – Suwannee Valley (NFREC-SV), near Live Oak, Florida.

- SWAT simulations showed that shifting from conventional calendar-based irrigation practices and high corn fertilizer rates (~336 kg N/ha) to Soil Moisture Sensor (SMS) based irrigation practices with fertilization rates of 246 kg N/ha, a rate close to the UF/IFAS N recommendation (235 kg N/ha), reduced nitrate leaching by an average 45% over the 1982-2018 weather record, with no reduction in yield for corn or peanut.

- SWAT simulations showed that cultivating a rye cover crop between corn and peanut cropping seasons could reduce leaching by an additional ~50kg N/ha compared to leaving the field fallow between cropping seasons, for a total 65% reduction.

- Successful use of SWAT to simulate the outcomes of field scale corn-peanut rotation experiment built confidence in its further application at the watershed scale.

- Future work should focus on long-term evaluation of the effectiveness of BMPs using future climate data for better predictions of yield, as well as field experiments that incorporate cover crops to confirm and measure reduction in N leaching during fallow periods.

Objective 2. Estimate nitrate leaching reductions across cropping systems, management practices and soil types in the SFRB, and resulting impacts on nitrate concentrations in the Santa Fe River.

- A SWAT model for the Santa Fe river basin was developed and successfully calibrated and validated for daily stream flow, monthly stream nitrate load, and annual geometric mean stream nitrate concentration.

- Leaching and denitrification losses across the watershed varied from 0 to >100 kg N/ha/year, with considerably more leaching occurring in the unconfined than the

confined region. Denitrification occurred throughout the watershed, with the highest rates in the confined region due to higher available water content.

- Row crops and pasture had the highest leaching and denitrification losses per unit area in both the confined and unconfined zones, with the unconfined region having slightly higher average leaching losses and slightly lower average denitrification losses than the confined region.

- Pasture contributed the greatest total load to the aquifer (1541 tons/year, 55%) due to the relatively large land area assigned to pasture (12%) and high leaching rates (~52 kg N/ha/year).

- Shifting the corn-peanut row crop rotation from conventional calendar-based irrigation practices with high corn fertilization (~336 kg N/ha) and no cover crops to SWAT based auto irrigation practices with fertilization rates of 246 kg N/ha, a rate close to the UF/IFAS N recommendation (235 kg N/ha) and a rye cover crop reduced nitrate load from row crops to the aquifer by 65% over the entire watershed, consistent with field scale simulation outcomes.

- Shifting all agricultural lands uses (row-crop, pasture, hay) from conventional practices to BMPs reduced the nitrate load in the Santa Fe River by 31%, but was insufficient to achieve the NNC of 0.35 mg/L NO_3-N.

- Converting the entire watershed into slash pine forest reduced the nitrate load to the river by ~80% over the current land uses with conventional practices, which was sufficient to achieve the NNC.

- A major limitation of this study is the fact the SWAT cannot simulate groundwater contributions to rivers that originate outside its surface watershed boundary, a phenomenon thought to occur in the unconfined region of the SFRB. As a result, calibrated soil parameters in the unconfined region of the SFRB had to be adjusted to reduce evapotranspiration and increase recharge to reproduce observed streamflow. Future validation of SWAT with satellite soil moisture data could evaluate the validity of these soil parameters. In addition, the groundwater residence times, and groundwater nitrate half-life calibrated for SWAT are unreasonably short. Coupling of SWAT with MODFLOW, MOPATH and/or RT3D to allow groundwater contributions from outside the surface watershed boundary, and to more rigorously simulate groundwater flow, transport and transformation processes, is recommended.

- Another limitation associated with this study was the lack of measured data to calibrate and validate the biogeochemical parameters controlling the competition between NO3-N leaching and denitrification in the soil zone, and denitrification within the aquifer. In this study constraints were imposed on these parameters based on prior knowledge of the biophysical processes occurring at the watershed scale, however these assumptions should be evaluated with new experiments and observations. For example, measured denitrification and leaching rates from

different land uses under different soil conditions could corroborate or improve parameter calibration.

Objective 3. Determine the most vulnerable regions of the SFRB where changes in practices could be targeted to reduce nitrate concentrations in springs and rivers in the unconfined region of the SFRB. Estimate the time required to observe reductions in river nitrate concentrations as a result of potential changes in practices in these vulnerable regions.

- SWAT recharge and NO3-Nloading were used to drive the calibrated North Florida-Southeast Georgia (NFSEG) MODFLOW model. The resulting groundwater fluxes were used in MODPATH to investigate the groundwater contributing area and groundwater travel time distribution (TTD) for the Santa Fe River near Fort White.

- The groundwater flow path and groundwater contributing area to the Santa Fe River near Fort White were sensitive to the spatial distribution of hydraulic conductivity in the NSFEG model. The groundwater TTD was sensitive to both the spatial distribution of hydraulic conductivity and effective porosity. The groundwater flow path, groundwater contributing area and TTD were less sensitive to the spatial distribution of recharge.

- The calibrated hydraulic conductivities in the NFSEG 1.1 model estimated that a large percentage (60 to 70%) of groundwater emerging in the Santa Fe River near Fort White travelled through the Lower Florida Aquifer (LFA), resulting in long median travel times (~100 years). These predictions are not consistent with published studies of spring travel paths or groundwater travel times (cite USGS, Katz, 2001; Katz et al., 2004). Reducing the hydraulic conductivity of the middle confining unit and the LFA, while increasing the hydraulic conductivity of the UFA to maintain the effective hydraulic conductivity of the three layers in the calibrated NFSEG model, decreased the percentage of water travelling through the LFA to 20%, increased the percentage of water traveling through the UFA to ~80%, and decreased the median groundwater travel time to ~200 years, findings that are more consistent with published studies.

- Scenario studies estimating the fate and transport of NO3-N from the groundwater contributing area to the Santa Fe River using travel-time based solute transport simulations showed that keeping the existing land use pattern but changing the agricultural management systems from conventional practices to current best management practices after 2020, would not be sufficient to meet the NNC of 0.35 mg/L NO_3-N established by FDEP. However, converting all pastureland to native grassland and changing the conventional practices of row crops and hay to current best management practices could meet the NNC by 2080. Furthermore, if all row

crops, hay, and pasture were converted to forest in 2020 the NNC could be met in 2055.

- NFSEG calibrated parameters need to be further evaluated with additional field data to improve the reliability of contaminant transport modeling using SWAT-MODFLOW-RT3D.

APPENDIX A
CHAPTER 2 ADDITIONAL FIGURES

Table A-1. Fertilizer composition applied at different corn growth stages for System 1 (corn grown in 2015 and 2017).

Corn Growth Stage	Fertilizer	Composition	Element (%)
At Planting ~0 DAP	Starter	16-0-0	N
		Ammoniacal N	8.6
		Nitrate N	2.47
		Urea N	4.93
V3 (3 leaves with visible collars) ~15 DAP	1st Granular	(33-0-0)	N
		Ammoniacal N	16.49
		Nitrate N	16.51
V6(6 leaves with visible collars) ~30DAP	2nd Granular	(33-0-0)	N
		Ammoniacal N	16.49
		Nitrate N	16.51
V8-VT (8 leaves with collars to tasseling stages) ~37 DAP to ~52 DAP	1st -4th Liq. Side-dress. *A total of 4 liquid side dress applications at week interval were performed between V8 and before tasseling	(28-0-0)	N
		Ammoniacal N/	8.73
		Nitrate N	6.42
		Urea N	12.85

*DAP (Days after planting).

Table A-2. Summary of data collection types and collection methods.

Soil data	Sampling location	Sampling frequency
Soil Texture: % clay, silt and sand Bulk density (gm/cm3)	A total of 9 samples were randomly selected across the field experiment	At the beginning of experiment, pre-planting
Soil moisture storage (mm)	Total soil moisture storage (0-900 mm) was collected using one capacitance probe per plot. Each probe has 9 sensors placed every 100 mm (from 50 mm to 850 mm) providing soil moisture storage for soil profile.	Every 30 min during crop growing seasons
Gravimetric water content	Every plot[1]	Biweekly during crop season and monthly after harvest
Soil NO_3-N	Every plot at four depths (0-150, 150-300, 300-600 and 600-900 mm). Total nitrate-N in the soil profile was summed across all depths	Biweekly during crop season and monthly after harvest
Crop Data	**Replicates per treatment**	**Sampling frequency**
In season aboveground biomass and N content	SMS irrigated plots	At crop key growth stages
Final aboveground biomass and N content	Every plot[1]	At the end of the crop growing season
Yield	Every plot[1]	Annual (at the end of crop season).

[1] Every plot means samplings were performed in all irrigation and N fertility rate treatments.

Table A-3. Soil properties collected from soil sampling across experimental site (system 2 & 1).

System 2 (Peanut-Corn Rotation)

Depth (mm)	Texture	Bulk Density(gm/cm^3)	Clay (weight %)	Silt (weight %)	Sand (weight %)	Organic Carbon (weight %)
0-150	Fine sandy	1.5	2.5	3	94.5	0.53
150-300	Fine sandy	1.5	2	2	96.0	0.41
300-600	Fine sandy	1.5	1.4	2.3	96.3	0.28
600-900	Fine sandy	1.5	1.7	2.3	96.0	0.22

System 1 (Corn-Peanut Rotation)

Depth (mm)	Texture	Bulk Density(gm/cm^3)	Clay (Weight %)	Silt (weight %)	Sand (weight %)	Organic Carbon (weight %)
0-150	Fine sandy	1.5	1.7	1.7	96.6	0.76
150-300	Fine sandy	1.5	1.4	1.7	97.0	0.67
300-600	Fine sandy	1.5	1.7	1.7	96.6	0.57
600-900	Fine sandy	1.5	1.4	1.3	97.0	0.34

Table A-4. Calendar irrigation schedule for corn and peanut.

Corn

DAP (Days After Planting)	Grower Irrigation Rules	Rainfall Condition
0-30 DAP	Consisted 12.7 mm/wk irrigation for the first 30 days after planting (DAP) with irrigation event of 12.7 mm in a day	Skip the irrigation if rainfall event is > 12.7 mm.
31-39 DAP	Beginning on 31 DAP, a target amount of 38 mm/wk with irrigation event of 12.7 mm in a day	One Irrigation skip if 12.7-19 mm rainfall occurs, and two irrigations skip if >19 mm of rain occurs
40-59 DAP	For 40-59 DAP a 50 mm/wk target with irrigation events of 12.7 mm/day.	One Irrigation skip if 12.7-19 mm rainfall occurs, and two irrigations skip if >19 mm of rain occurs
60-105 DAP	For 60-105 DAP a 50 mm/wk target with irrigation events of 12.7 mm/day.	One Irrigation skip if 12.7-25.4 mm rainfall occurs. Two irrigations skip if >25.4 mm of rain occurs.
106-115 DAP	Around 105 DAP at full dent stage, weekly irrigation targets of 41 mm/wk for one week with irrigation event 12.7 mm/day. 20mm/wk for another week until finally irrigation terminates approximately 115 DAP with irrigation event 12.7mm/day	One Irrigation skip if 12.7-25.4 mm rainfall occurs. Two irrigations skip if >25.4 mm of rain occurs.

Peanut	Irrigation Rules	Rainfall condition
0-30 DAP	Consisted of zero irrigation for the first 30 days after planting (DAP) unless severe windy conditions that caused blowing sand to burn the plants.	
30-45 DAP	Beginning on 31 DAP, a target amount of 25.4 mm/wk with irrigation event of 10.2 mm or larger (Growers apply 10.2mm/day)	One Irrigation skip if 10.2-19 mm rainfall occurs, and two irrigations skip if >19 mm of rain occurs.
45-65 DAP	A target amount of 41 mm/wk with event of 10.2 mm/day	One Irrigation skip if 10.2-19 mm rainfall occurs, and two irrigations skip if >19 mm of rain occurs.
65-80 DAP	A target amount of 41 mm/wk with event of 10.2 mm/day	One Irrigation skip if 10.2-19 mm rainfall occurs, and two irrigations skip if >19 mm of rain occurs.
80-115 DAP	A target amount of 50 mm/wk with event of 10.2 mm/day.	One Irrigation skip if 10.2-25.4 mm rainfall occurs. Two irrigations skip if >25.4 mm of rain occurs.

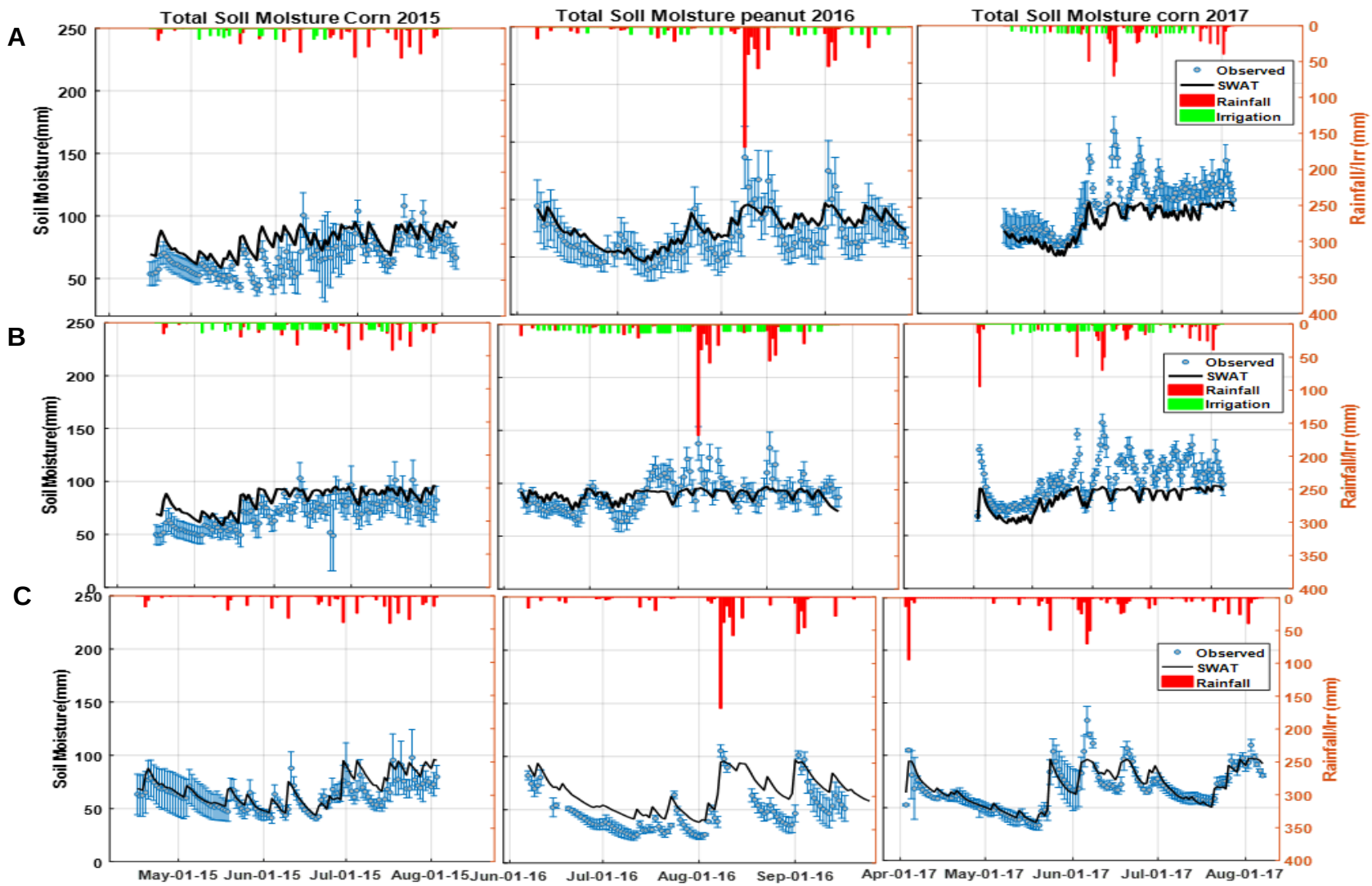

Figure A-1. Observed and simulated total soil moisture in root zone (900 mm) during corn-peanut-corn growing seasons. (A) SMS-Medium, (B) Calendar-Medium, and (C) Rainfed-Medium for System 1. Error bars correspond to the standard deviation of measured data.

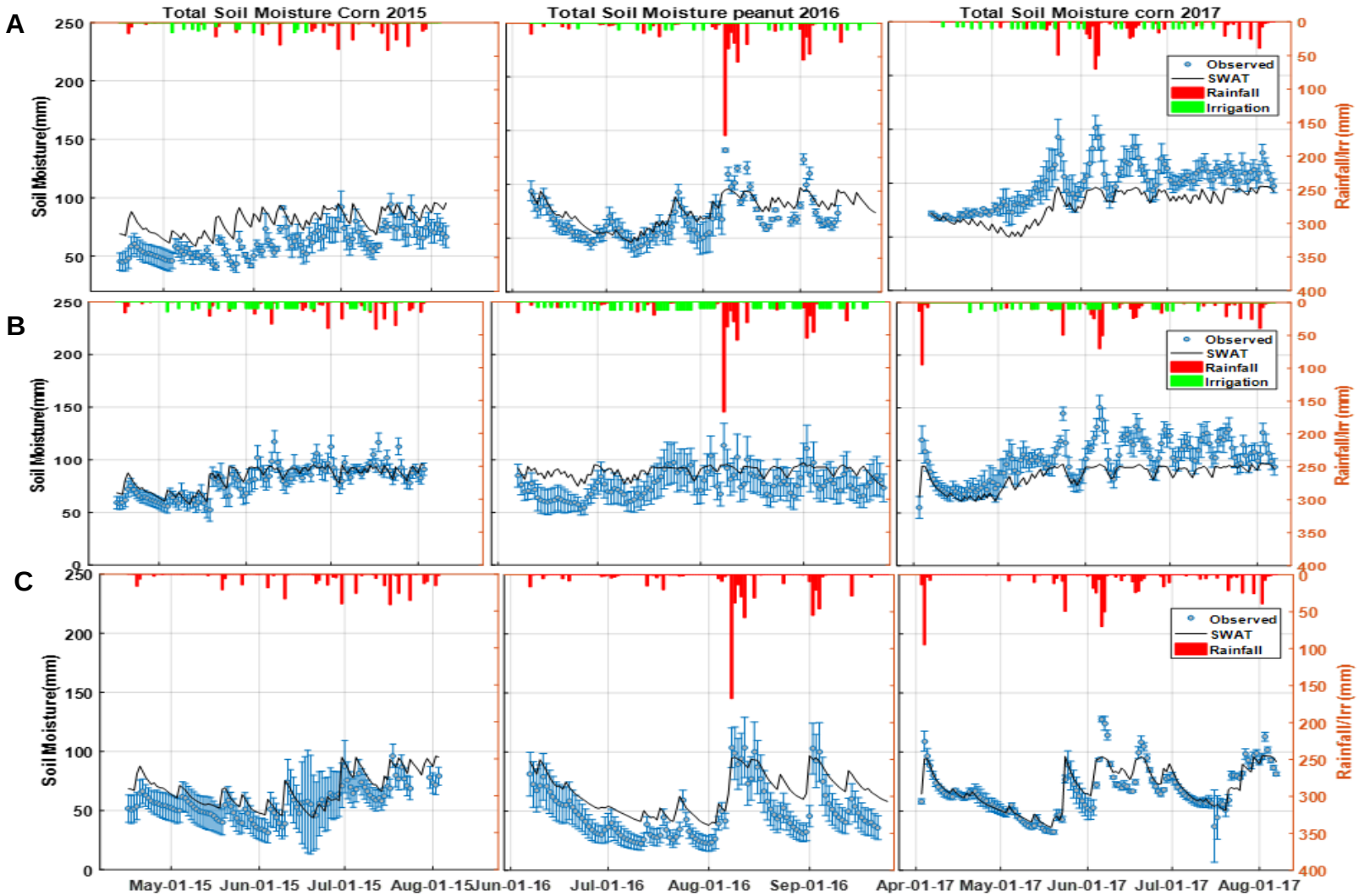

Figure A-2. Observed and simulated total soil moisture in root zone (900 mm) during crop seasons. (A) SMS-Low, (B) Calendar-Low, and (C) Rain fed-Low for system 1. Error bars correspond to the standard deviation of measured data.

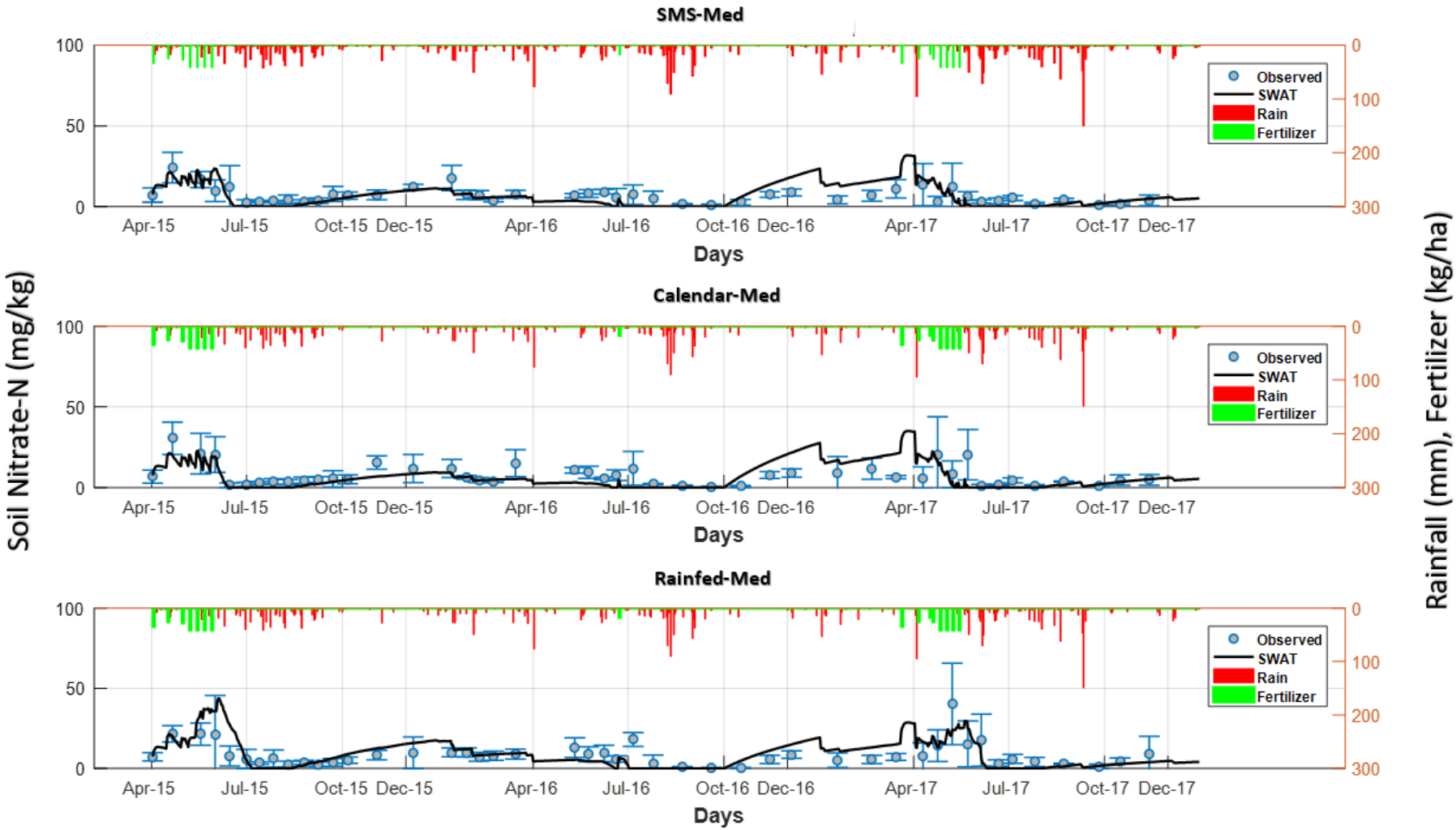

Figure A-3. System 1 observed vs simulated soil nitrate in entire root zone (900mm) for medium fertility treatments

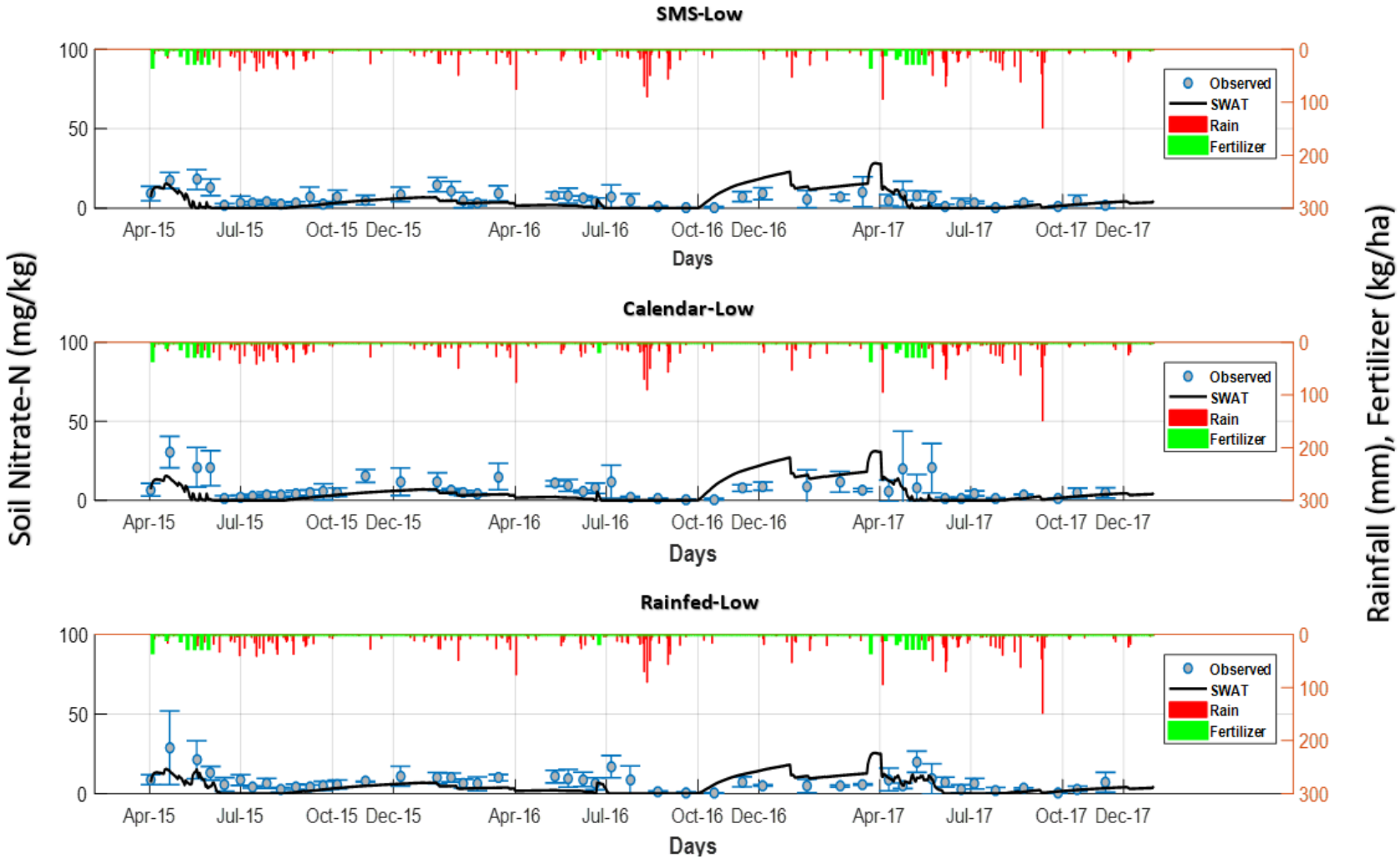

Figure A-4. System 1 observed vs simulated soil nitrate in entire root zone (900mm) for low fertility treatments.

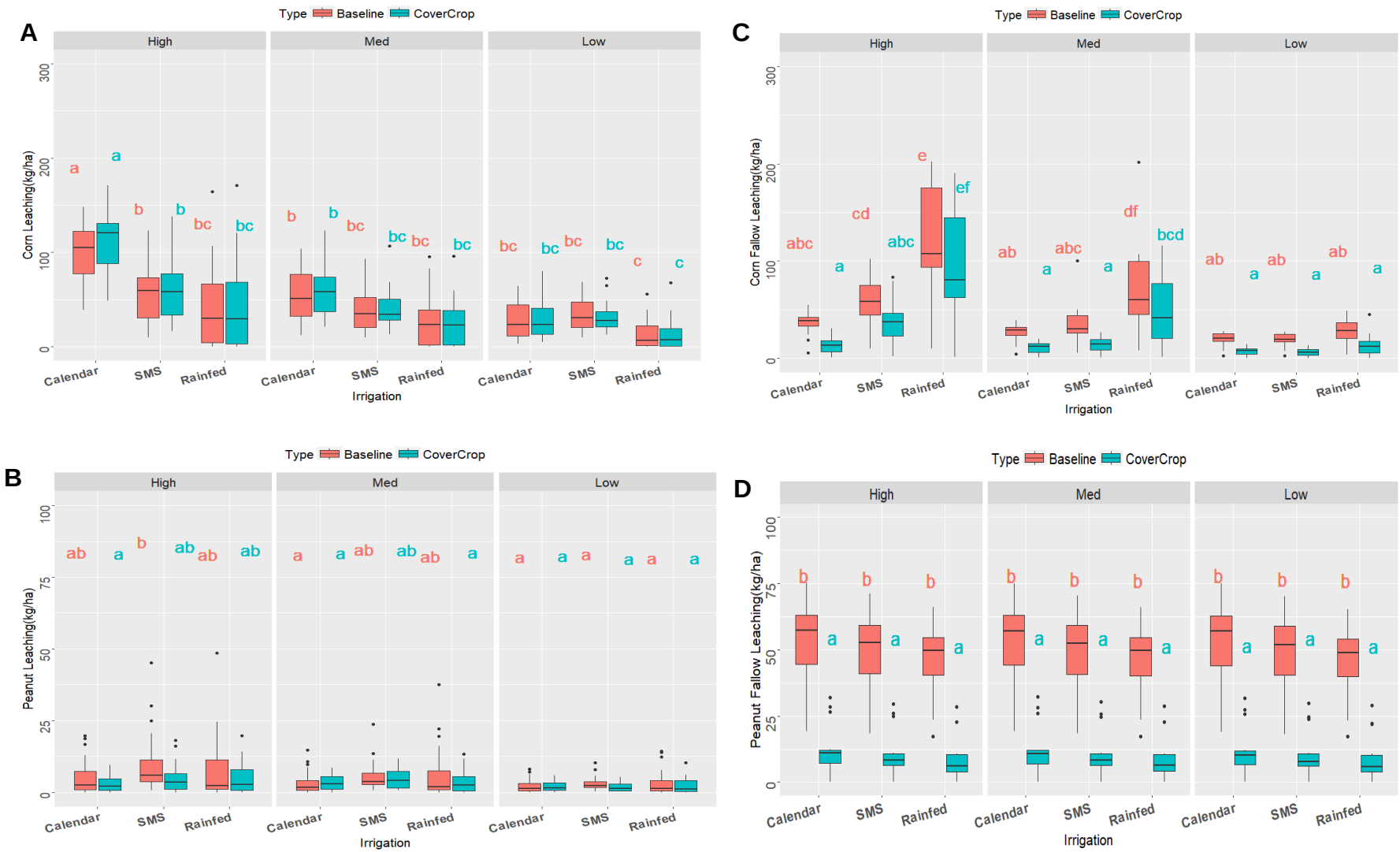

Figure A-5. Long term simulated seasonal leaching during crop rotation. (A) corn and (B) peanut growing seasons, and during main crops growing seasons with intercropping fallow or rye as cover crop (i.e. (C) corn-fallow/cover crop- and (D) peanut-fallow/cover crop). Different letters indicate significant difference at α = 0.05 level.

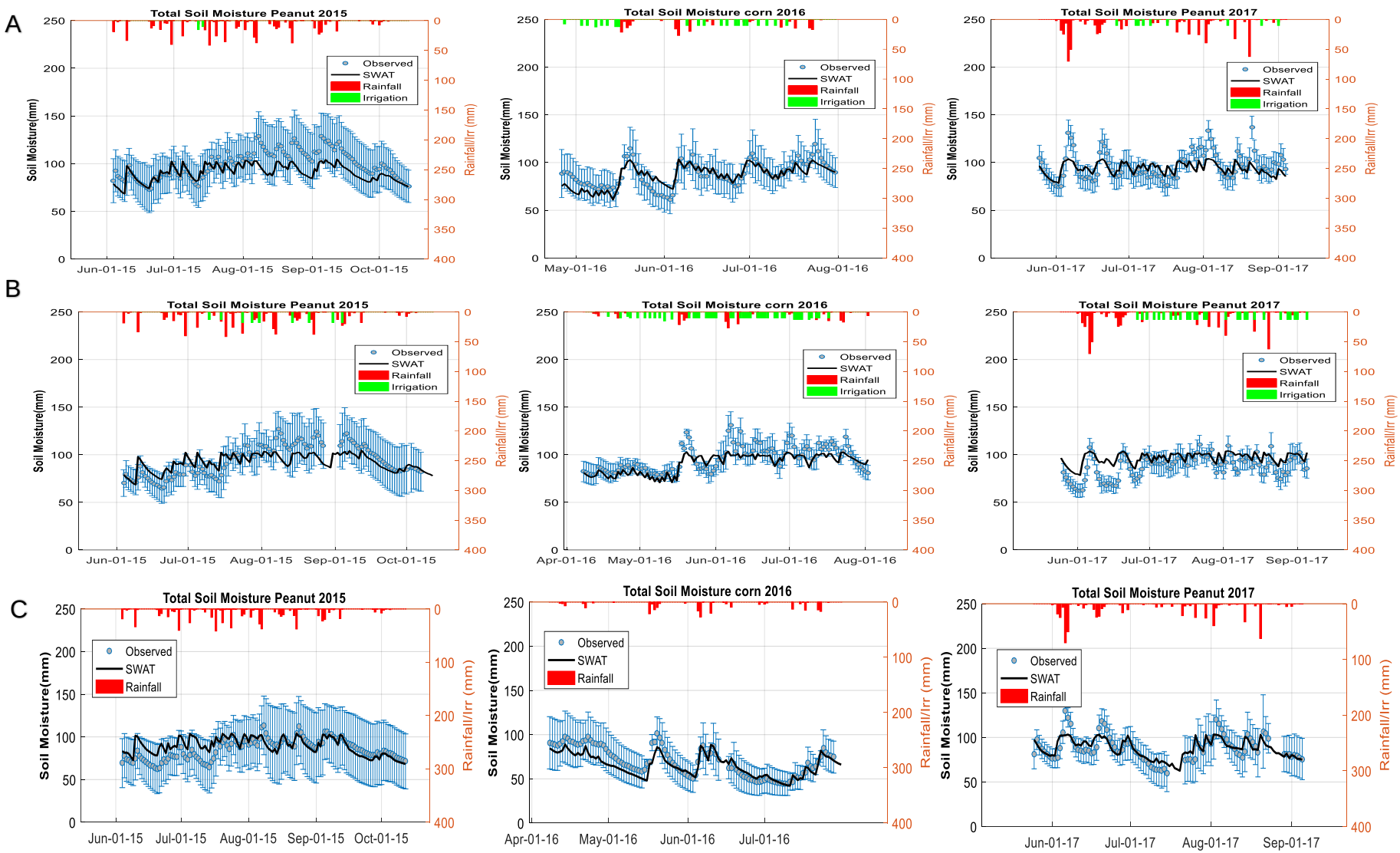

Figure A-6. Observed and simulated total soil moisture in root zone during crop seasons. (A) SMS-High, (B) Calendar-High, and (C) Rainfed-High for system 2. Vertical bars correspond to the standard deviation of measured data.

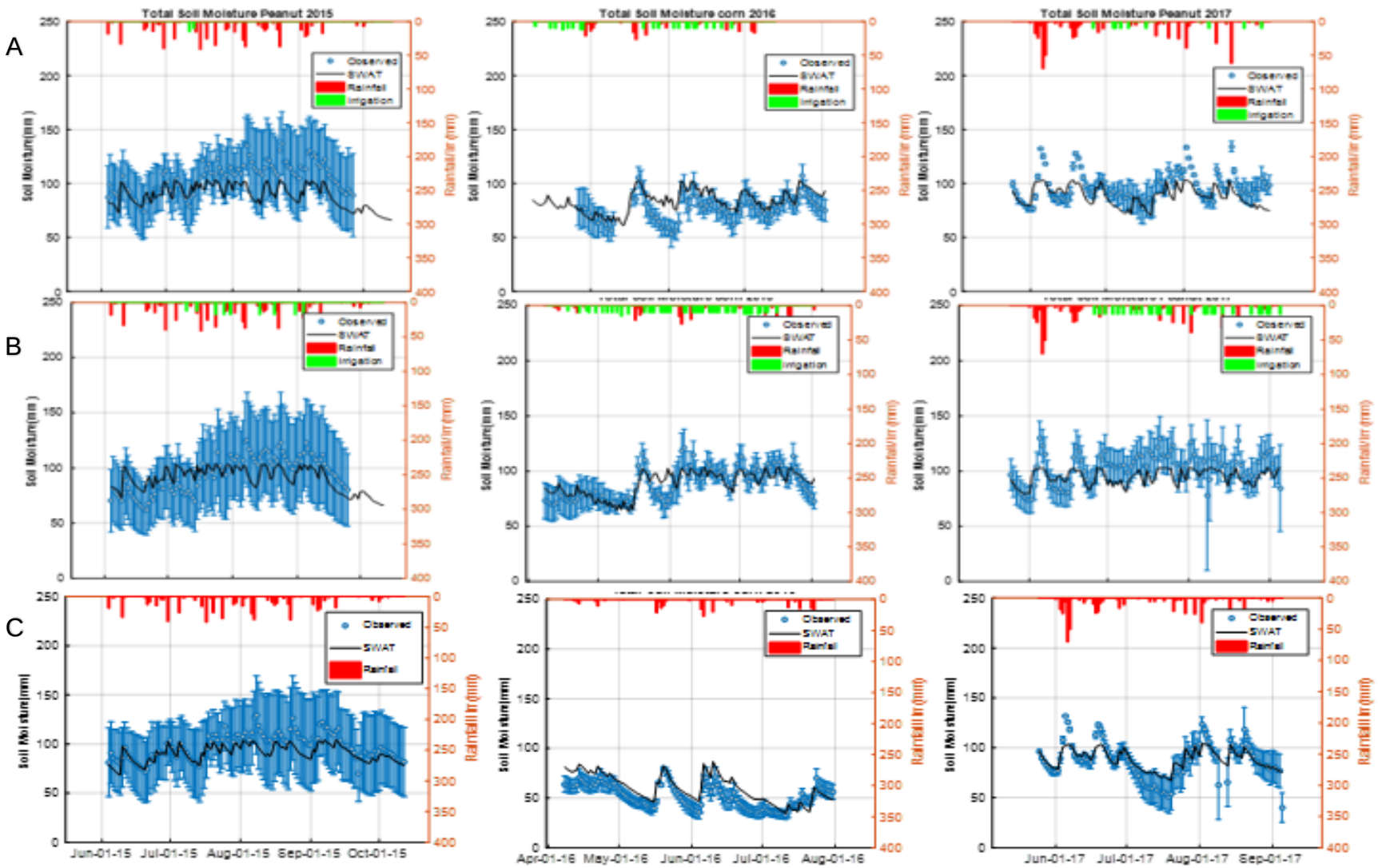

Figure A-7. Observed and simulated total soil moisture in root zone during crop seasons. (A) SMS-Medium, (B) Calendar-Medium, and (C) Rainfed-Medium for system 2. Vertical bars correspond to the standard deviation of measured data.

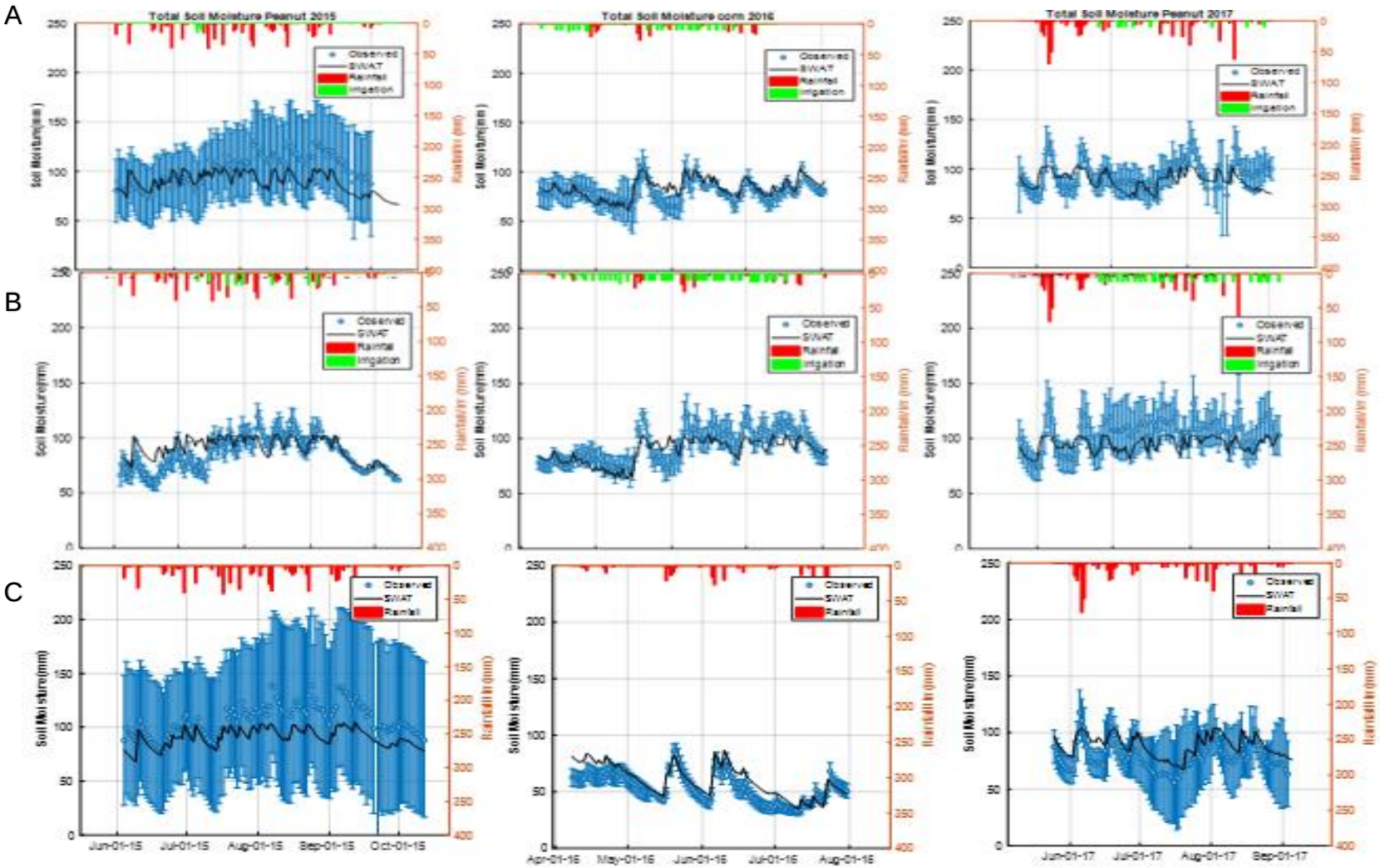

Figure A-8. Observed and simulated total soil moisture in root zone during crop seasons. (A) SMS-Low, Calendar-Low (b) and Rainfed-Low(c) for system 2. Vertical bars correspond to the standard deviation of measured data. Experimental variation is more in the year 2015 as compared to rest of the years.

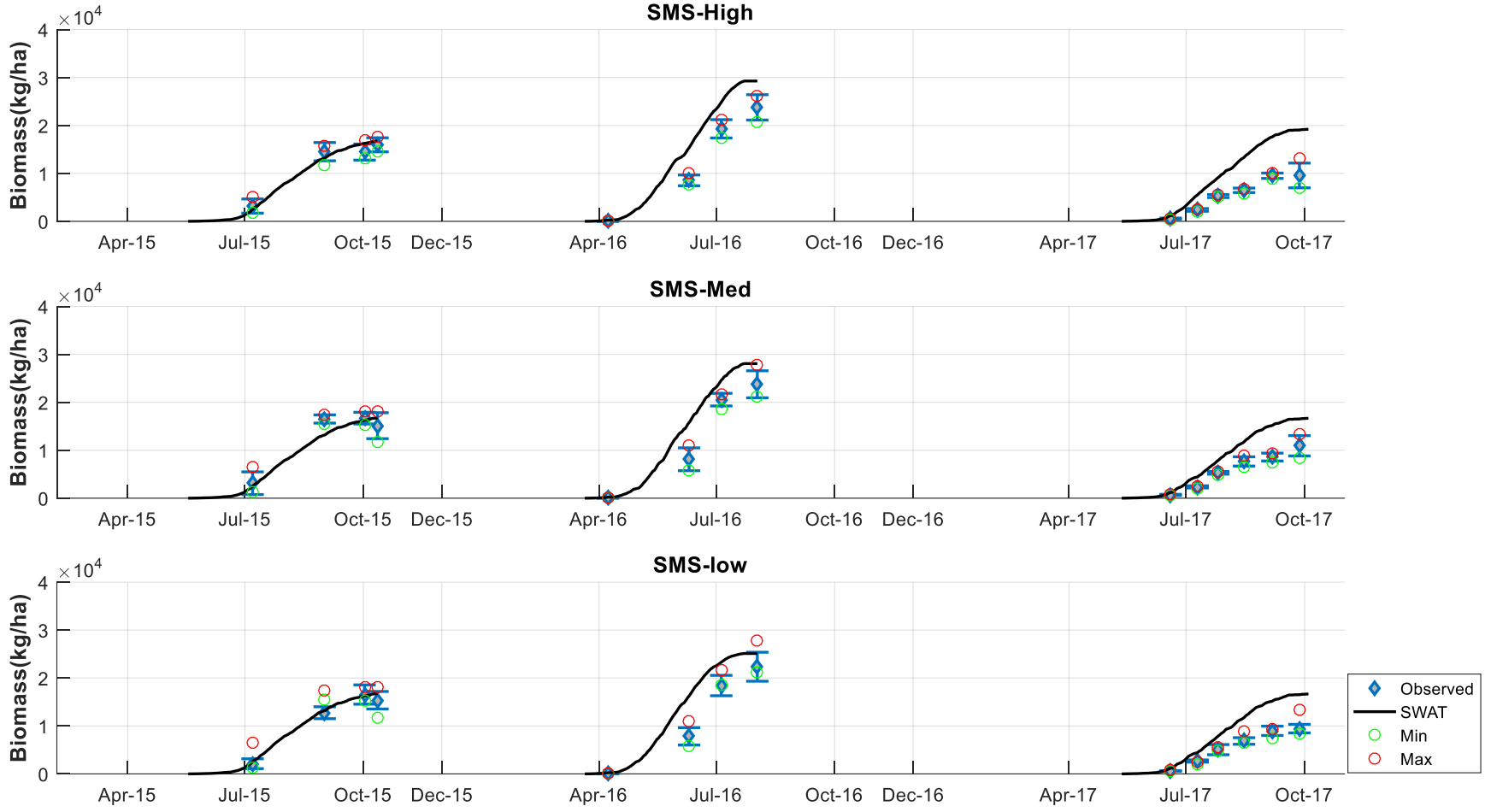

Figure A-9. Simulated Vs Observed above ground biomass dynamics for SMS-High, SMS-Medium, and SMS-Low (System 2). The experimental variation represented as min and max is within one standard variation.

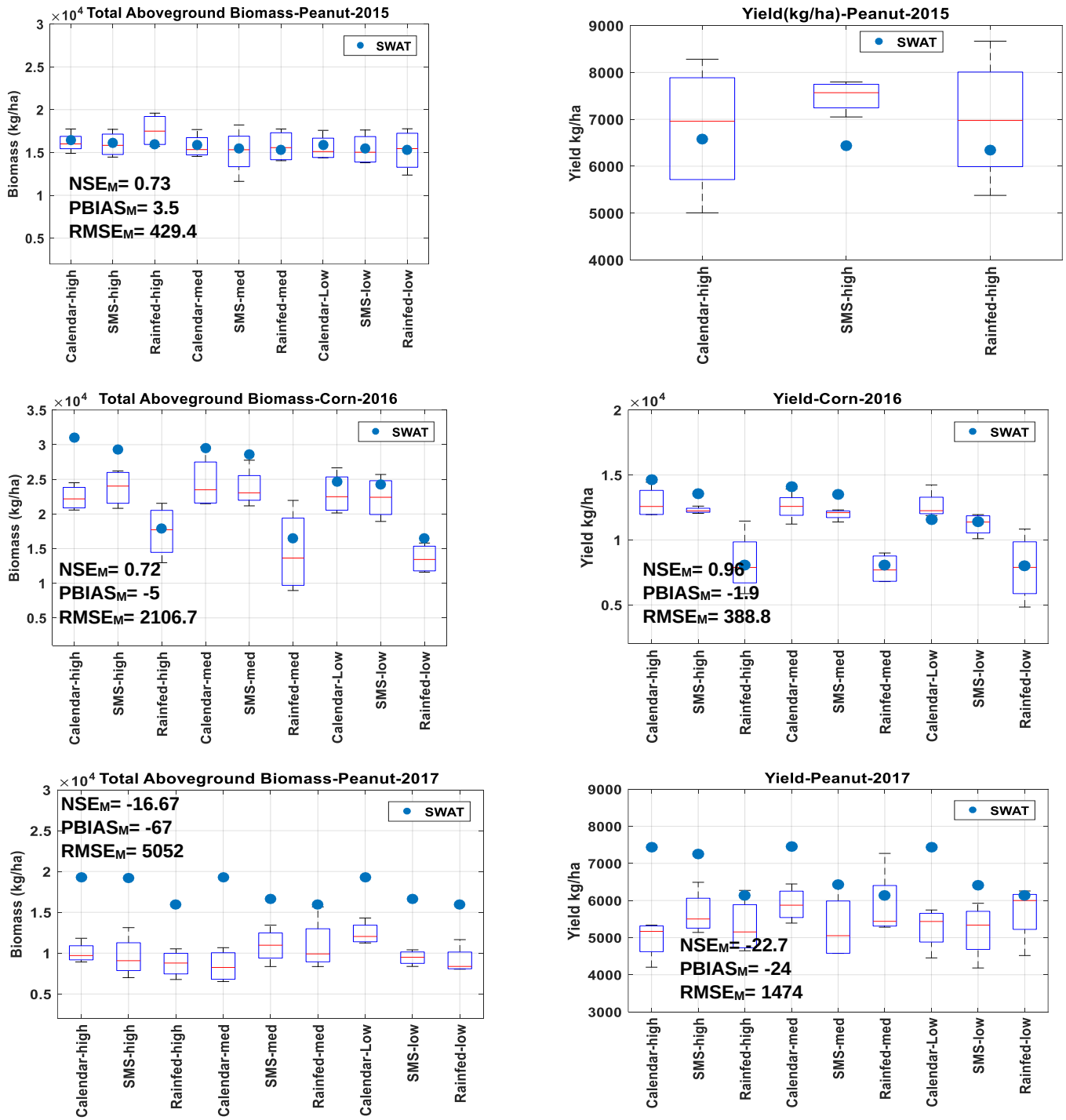

Figure A-10. Simulated Vs Experimental variation of System 2 biomass and yield. Model performance statistics evaluated were NSEM, PBIAS (%) and RMSEM (kg/ha). 2017 peanut biomass and yield collection had discrepancies due to hurricane. 2015 peanut yield was not measured for all plots (Zamora et al., 2018, 2020).

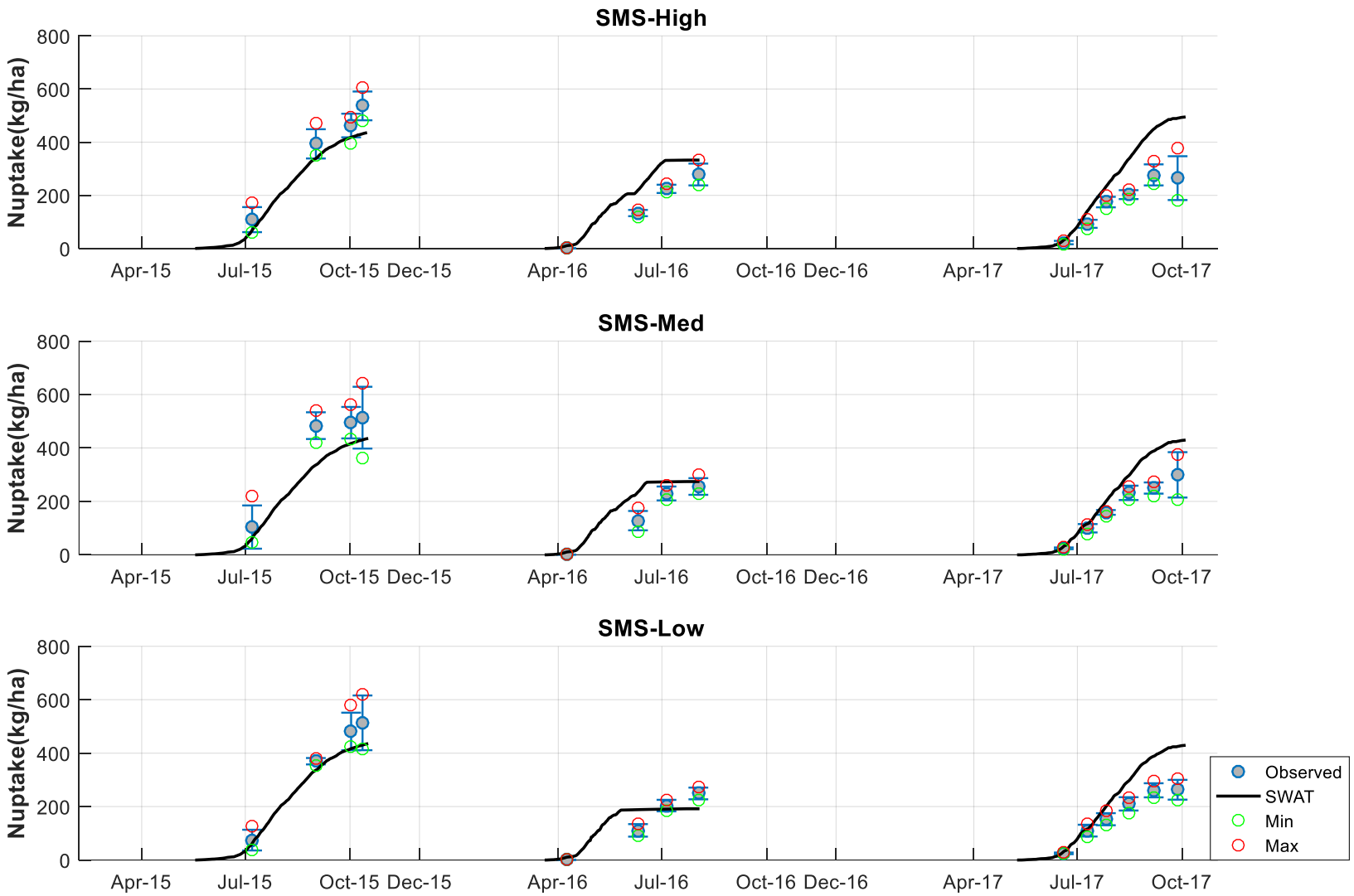

Figure A-11. Simulated Vs Experimental Nitrogen uptake trend for system2.

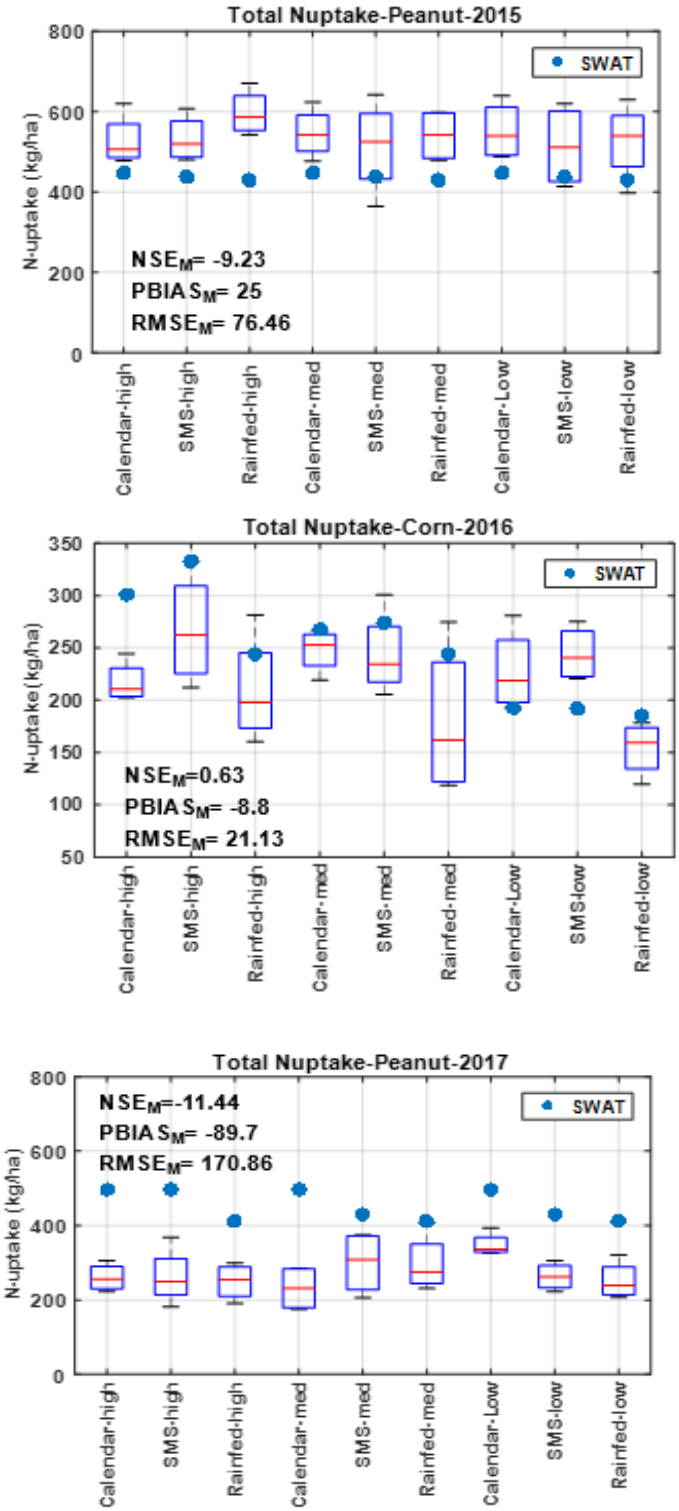

Figure A-12. Simulated Vs Experimental variation of System 2 Nitrogen uptake. Model performance statistics evaluated were NSEM, PBIAS (%) and RMSEM (kg/ha).

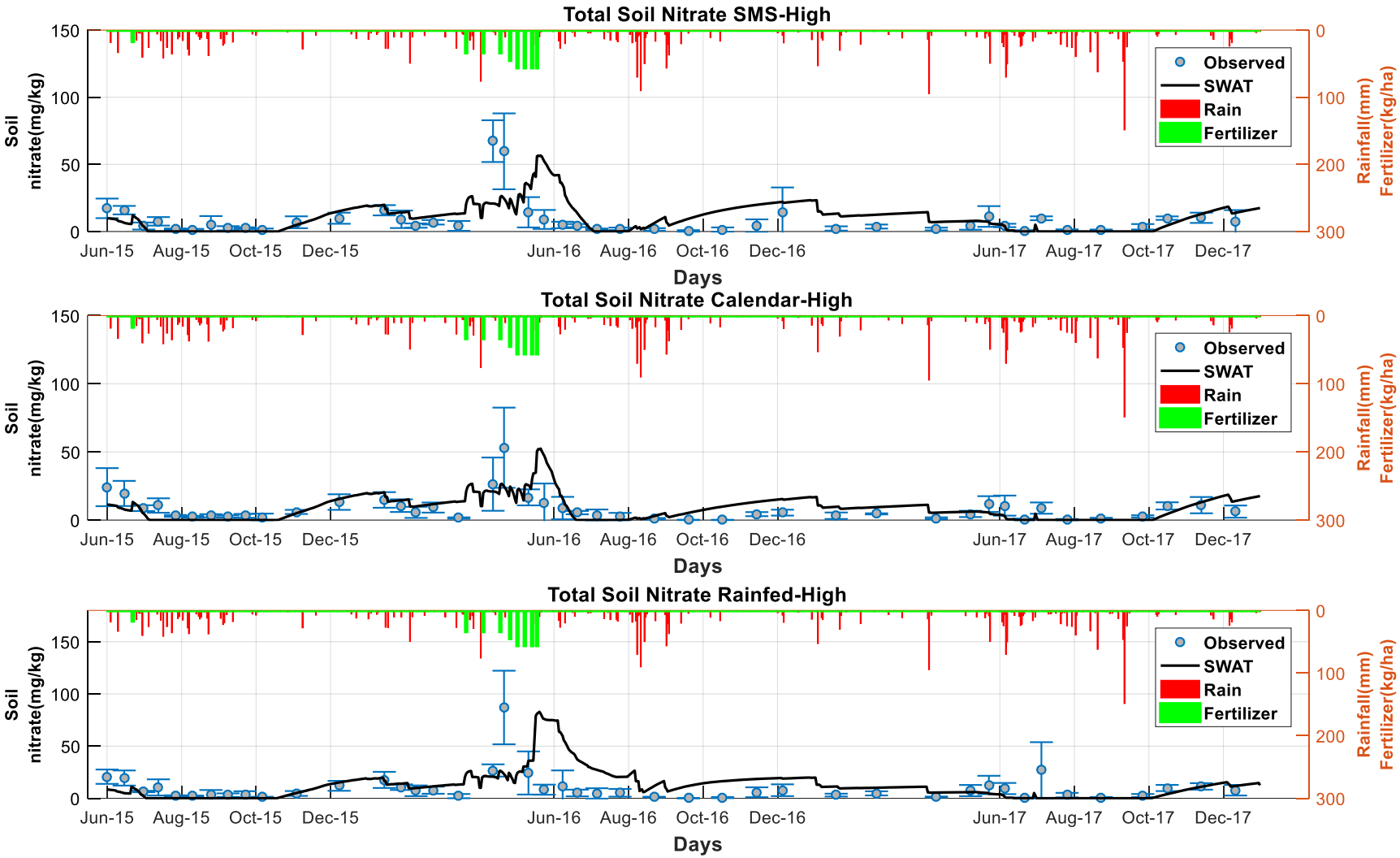

Figure A-13. System 2 simulated Vs observed soil nitrate in root zone (900 mm) for high fertility treatments.

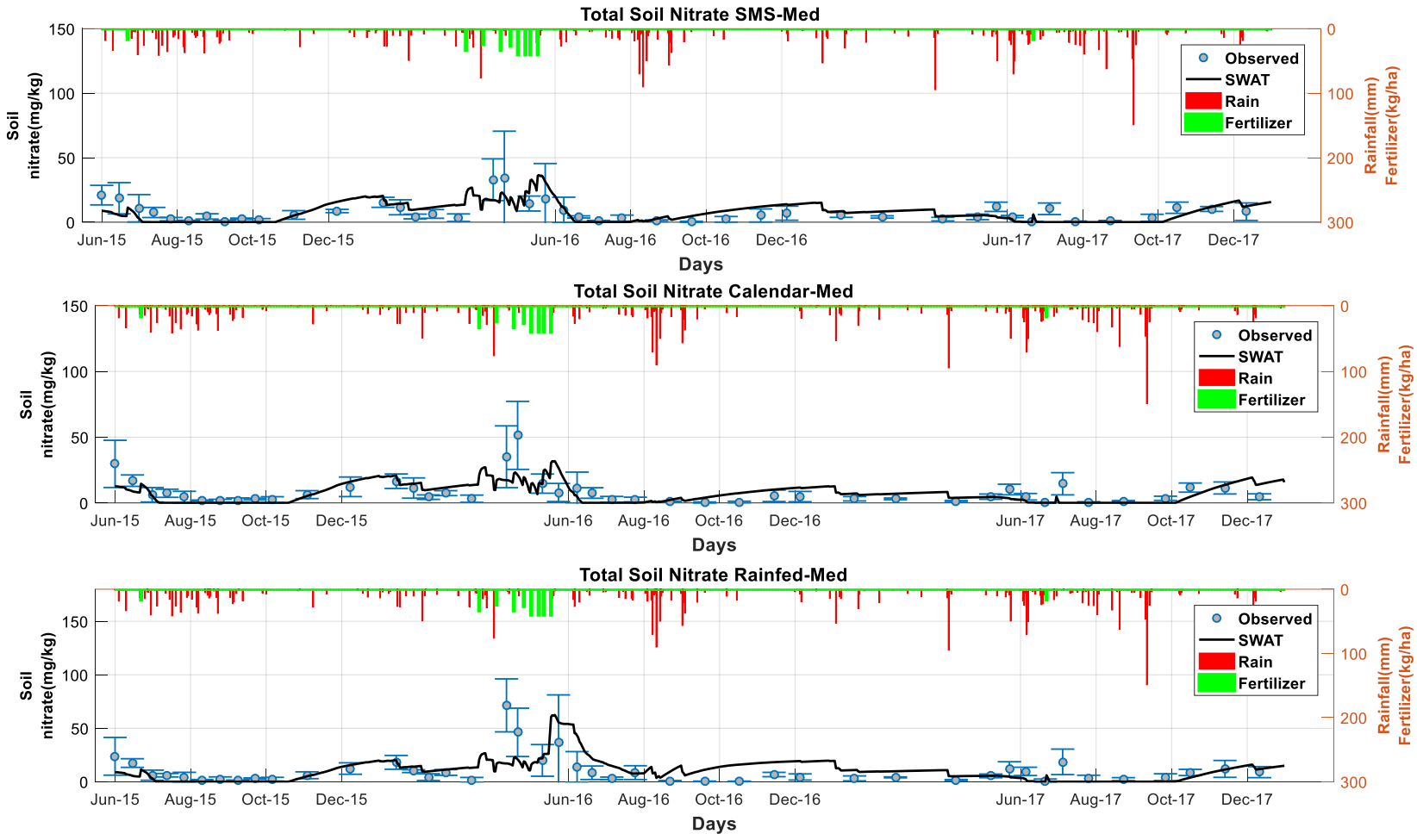

Figure A-14. System 2 simulated Vs observed soil nitrate in root zone (900 mm) for medium fertility treatments.

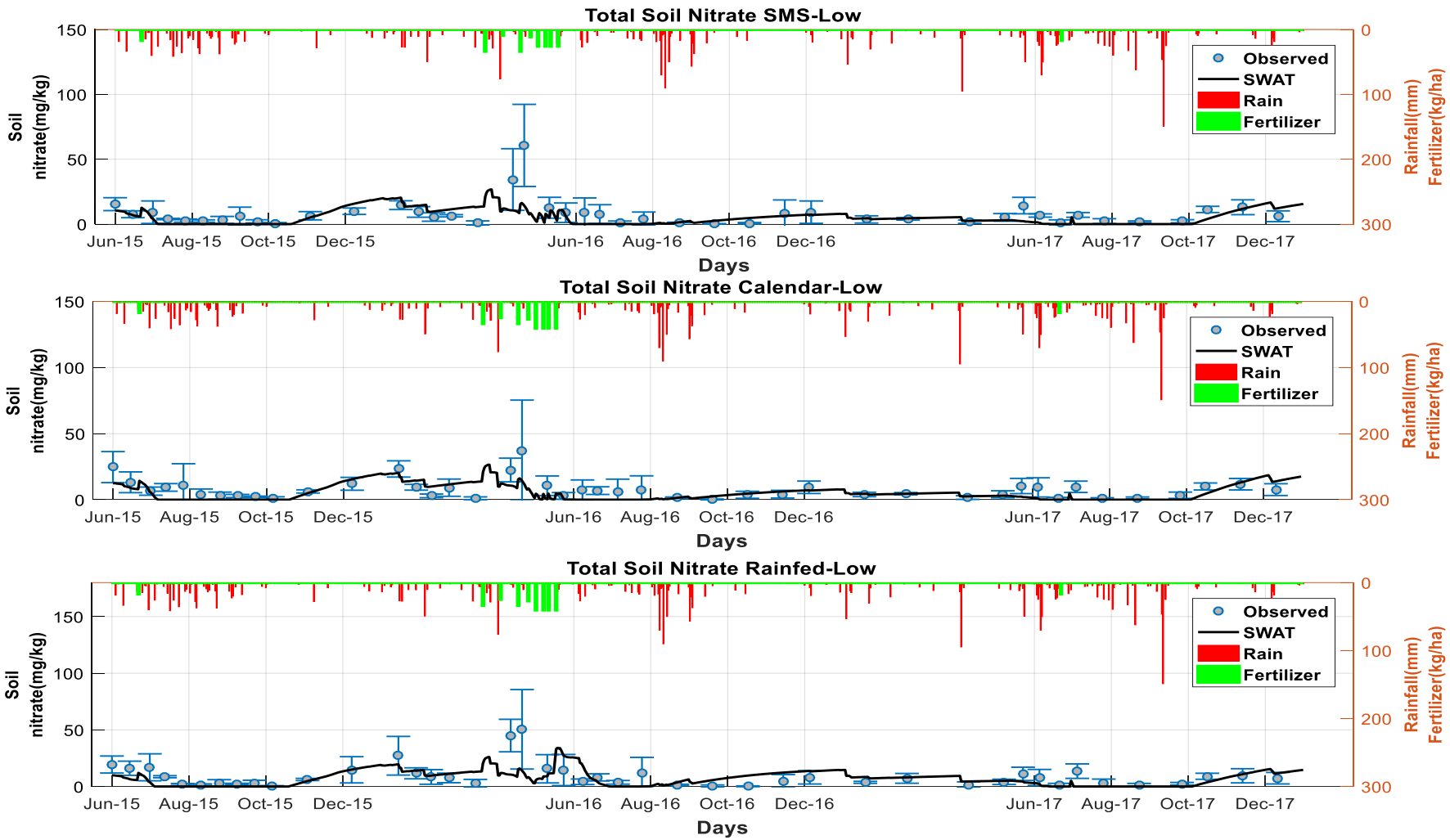

Figure A-15. System 2 simulated Vs observed soil nitrate in root zone (900 mm) for low fertility treatments.

APPENDIX B
CHAPTER 3 ADDITIONAL FIGURES

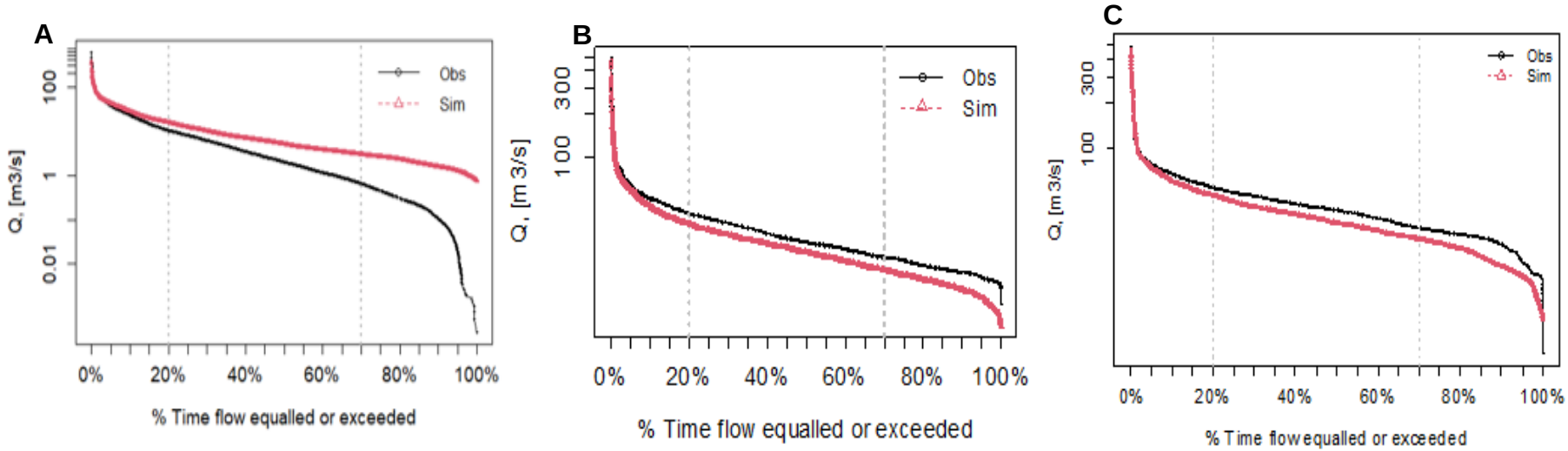

Figure B-1. Simulated and observed daily streamflow duration curve. A) Worthington Spring B) Fort White C) Hildreth.

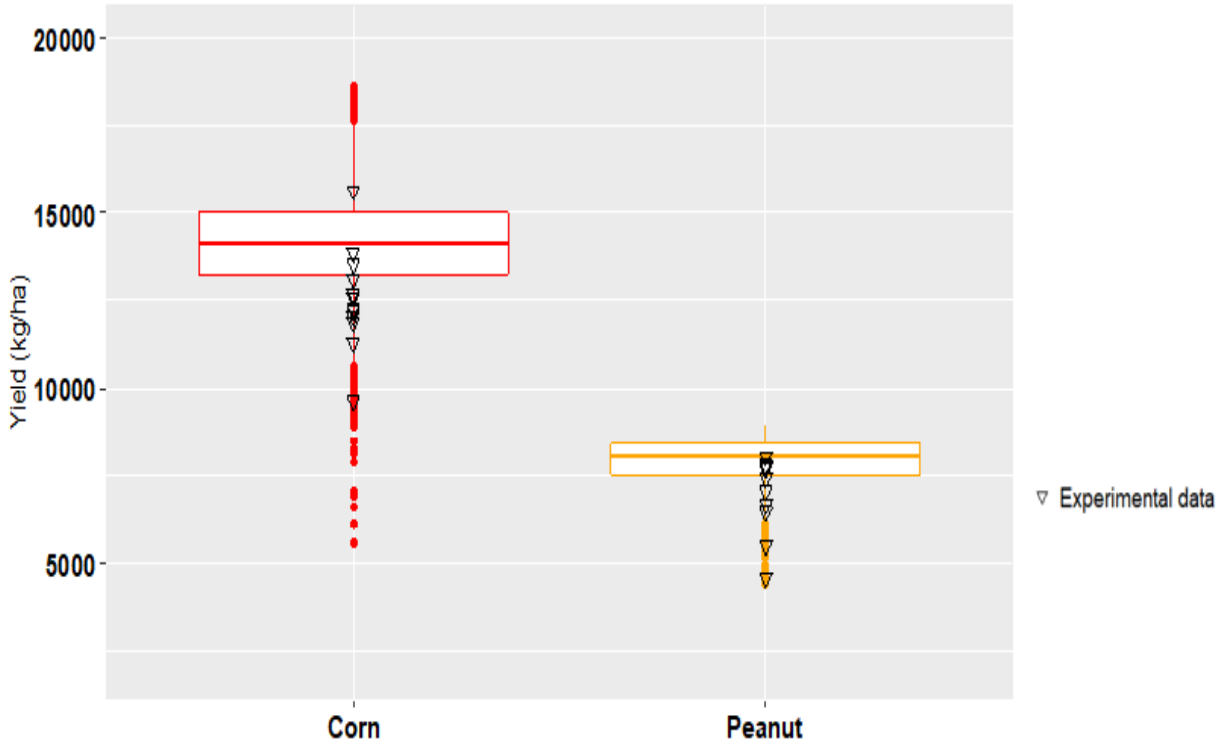

Figure B-2. Spatiotemporal (all row crop HRUs (2000-2018)) corn and peanut yield in comparison to experimental data (corn-peanut-corn rotation from 2015-17, Zamora-Re et al., 2018).

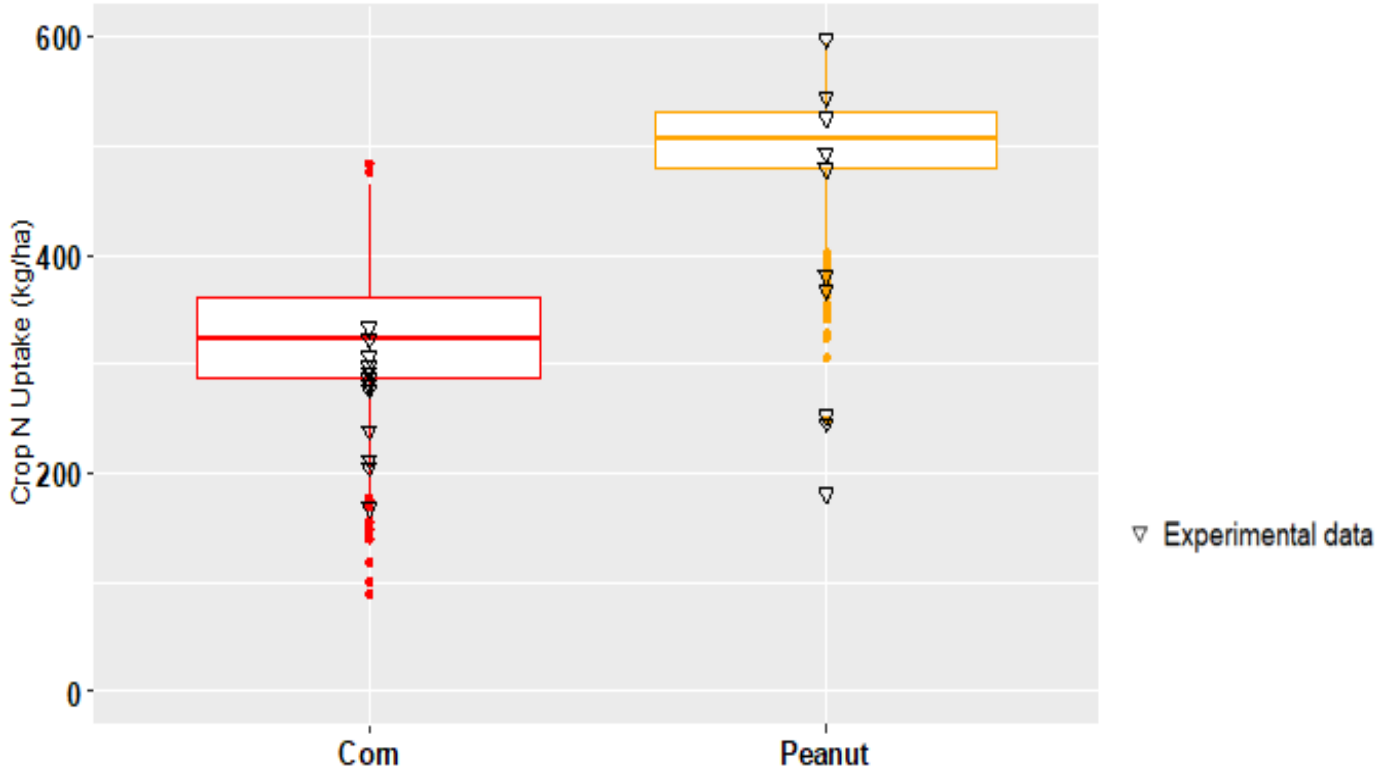

Figure B-3. Spatiotemporal (all row crop HRUs (2000-2018)) corn and peanut N uptake in comparison to experimental data (corn-peanut-corn rotation from 2015-17, Zamora-Re et al., 2018).

APPENDIX C
CHAPTER 4 ADDITIONAL FIGURES

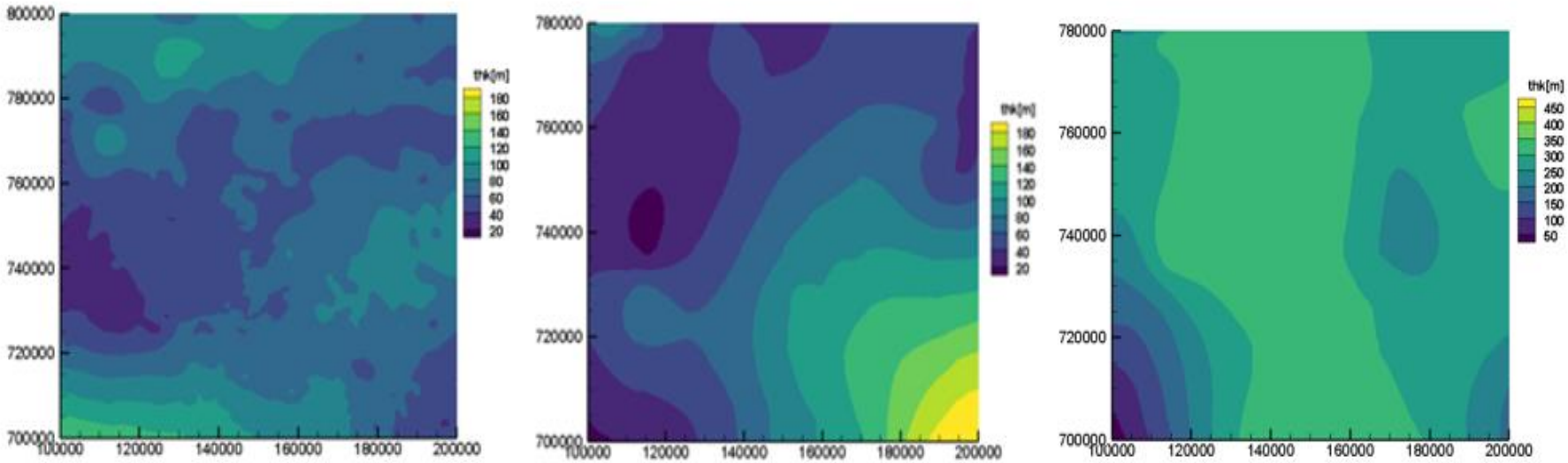

Figure C-1. Thickness of UFA (3rd layer), confining unit (4th layer) and LFA (5th layer) in NFSEG model.

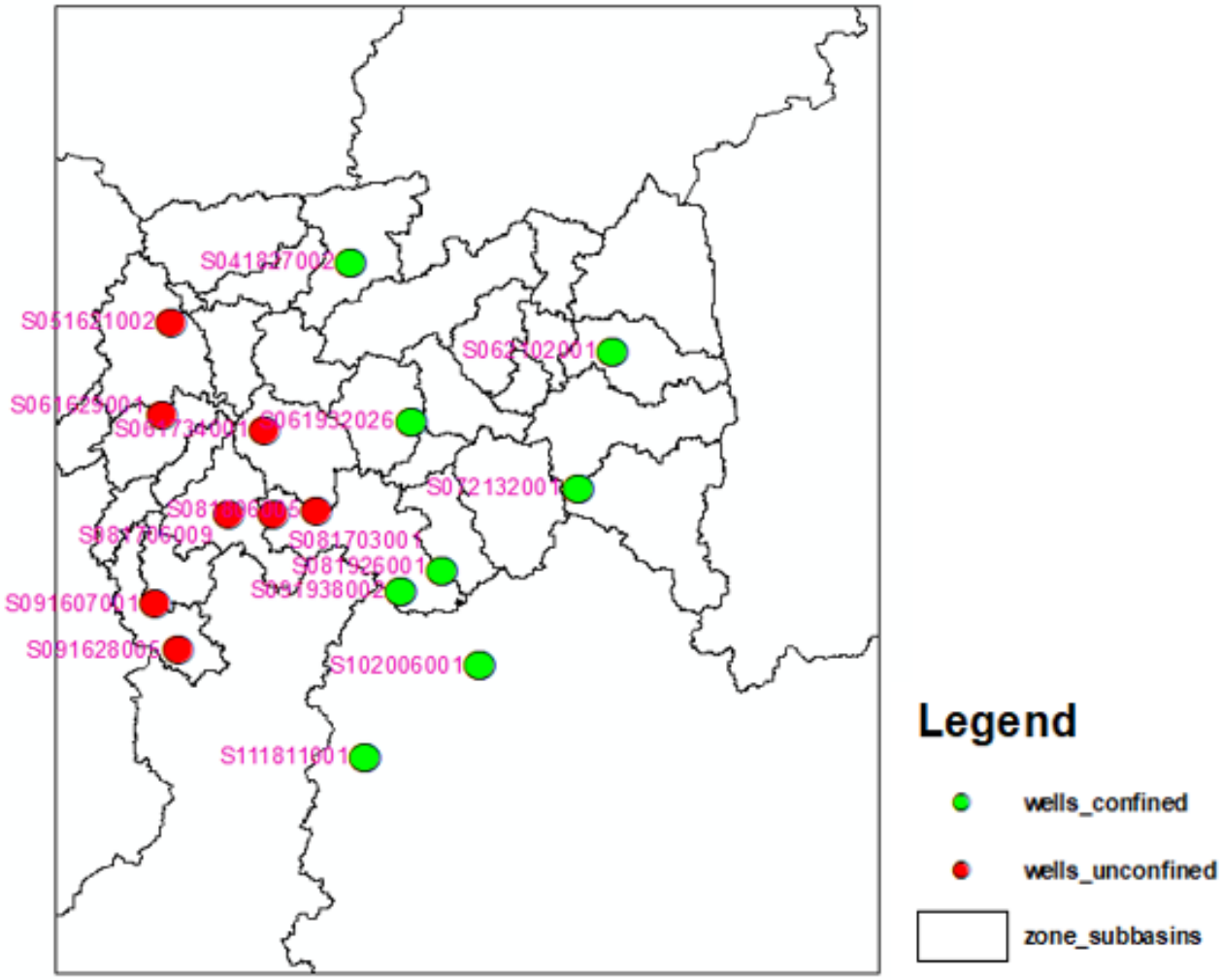

Figure C-2. Observation wells in confined and unconfined region with subbasins.

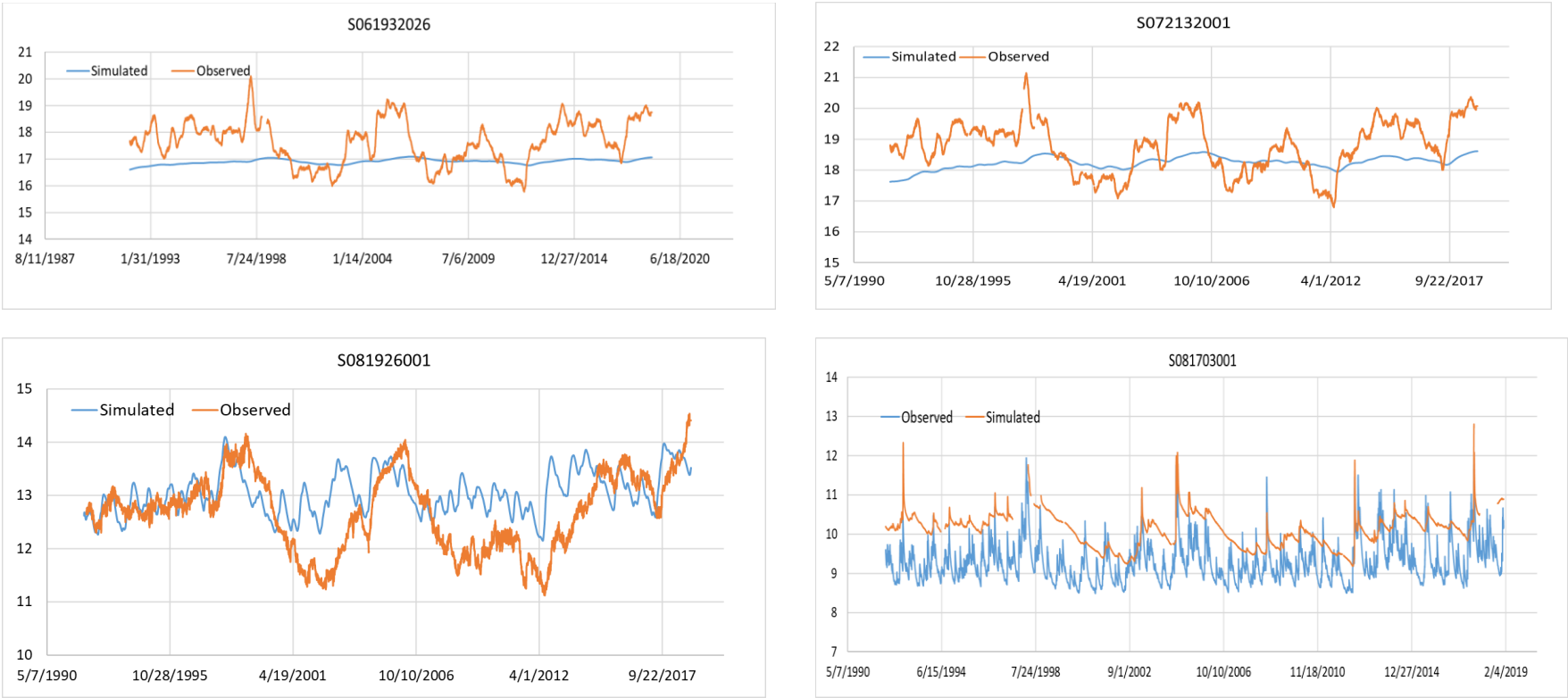

Figure C-3. Observation vs simulated groundwater head of wells in confined region.

Figure C-4. Observation vs simulated groundwater head of wells in unconfined region.

LIST OF REFERENCES

Abbaspour, K.C. 2013. SWAT-CUP 2012. SWAT Calibration and Uncertainty Program-A User Manual.

Abbaspour, K.C., Rouholahnejad, E., Vaghefi, S., Srinivasan, R., Yang, H., Kløve, B., 2015. A continental-scale hydrology and water quality model for Europe: Calibration and uncertainty of a high-resolution large-scale SWAT model. Journal of Hydrology 524 (2015) 733–752.

Abbaspour, K.C., Vaghefi, S., Srinivasan, R., 2018. A Guideline for Successful Calibration and Uncertainty Analysis for Soil and Water Assessment: A Review of Papers from the 2016 International SWAT Conference. Water 2018, 10, 6; doi:10.3390/w10010006.

Abusaada, M., Sauter, M., 2013. Studying the flow dynamics of a karst aquifer system with an equivalent porous medium model. Groundwater 51 (4), 641–650. https://doi.org/10.1111/j.1745-6584.2012.01003.x.

Akhavan, S., Abedi, K. J., Mousavi, S.F., Afyuni, M., Eslamian, S.S., Abbaspour, K.C., 2010. Application of SWAT model to investigate nitrate leaching in Hamadan–Bahar Watershed, Iran. Agric Ecosyst Environ 139:675–688.

Alam, S.M., 1999. Nutrient uptake by plants under stress conditions. In: Pessaraki, M. (Ed.), Handbook of plant and crop stress. Marcel Dekker, New York. 285-314.

Aliyari, F., Bailey, T.R., Tasdighi, A., Dozier, A., Arabi, M., Zeiler, K., 2019. Coupled SWAT-MODFLOW model for large-scale mixed agro-urban river basins. Environ. Model. Softw. 115, 200–210.

Allaire-leung, S.E., Wu, L., Mitchell, J.P. & Sanden, B.L., 2001. Nitrate leaching, and soil nitrate content as affected by irrigation uniformity in a carrot. Agricultural Water Management, 48.

Almeida, E.R., Favarin, L.J., Otto, R., Pierozan, C., Oliveira, C., Tezotto, T., Lago, C.B., 2017. Effects of nitrogen fertilization on yield components in a corn-palisade grass intercropping system. AJCS 11(03):352-359 (2017). doi: 10.21475/ajcs.17.11.03. pne273.

Amin, M.M., Veith, T.L., Collick, A.S., Karsten, H.D., Buda, A.R., 2017. Simulating hydrological and nonpoint source pollution processes in a karst watershed: a variable source area hydrology model evaluation. Agric. Water Manag. 180, 212–223.

Anand, S., Mankin, K. R., McVay, K. A., Janssen, K.A., Barnes, P. L., and Pierzynski, G. M., 2007. Calibration and validation of ADAPT and SWAT for field-scale Runoff prediction. JAWRA journal of the American water resources association, 43(4),899-910.

Arabi, M., J.R. Frankenberger, B. Engel, and Arnold, J.G., 2008. Representation of agricultural management practices with SWAT. Hydrological Processes 22:3042-3055.

Arheimer, B., Andreasson, J., Fogelberg, S., Johnsson, H., Pers, C. B. & Persson, K., 2005. Climate change impact on water quality: Model results from southern Sweden. Ambio 34, 559–566.

Arnold, J.G., Kiniry, J.R., Srinivasan, R., Williams, J.R., Haney, E.B., Neitsch, S.L., 2013. SWAT 2012 input/output Documentation. Texas Water Resources Institute.

Arnold, J. G., Srinivasan, R., Muttiah, R. S., Williams, J, R.,1998. Large area hydrologic modeling and assessment part I: Model development. Journal of the American Water Resources Association, 1998; 34(1): 73–89. doi: 10.1111/j.1752-1688. 1998. tb05961.x

Arthur, J. D., Wood, A. R., Baker, A. E., Cichon, J. R., Raines, G. L., 2007. Development and Implementation of a Bayesian-Based Aquifer Vulnerability Assessment in Florida. Nat Resour Res, 16(2), 93-107.

Bailey, R., Rathjens, H., Bieger, K., Chaubey, I., Arnold, J.G., 2017.SWATMOD-PREP: Graphical user interface for preparing coupled SWAT-modflow simulations. Journal of the American Water Resources Association. 53(2):400-410. doi:10.1111/1752-1688.12502.

Basche, A., Kaspar, T., Archontoulis, A., Jaynes, D., Thomas J. Sauer, T. and Parklin, T., 2016. Soil water improvements with the long-term use of a winter rye cover crop. Agricultural Water Management, Volume 172, 1 July 2016, Pages 40-50.

Basu, N. B., Jindal, K. E., Schilling, C. F., Takle, E. S., 2012. Evaluation of analytical and numerical approaches for the estimation of groundwater travel time distribution, J. Hydrol., 475, 65–73, doi:10.1016/j.jhydrol.2012.08.052.

Bennett, J.M., Sinclair, T.R., Li Ma, Boote, K.J., 1993. Single leaf carbon exchange and canopy radiation use efficiency of four peanut cultivars. Peanut Science 20, 1–5.

Bennett, P.G.M., Edward, R.E., 2003. Hydrogeologic Investigation of the Floridan Aquifer System Intercession City Osceola County, Florida Technical Publication WS-23 H. South Florida Water Management District.

Beven, K.J., 1989.Changing ideas in hydrology: the case of physically based models J. Hydrol., 105 (1989), pp. 157-172.

Bieger, K., Hörmann, G., and Fohrer. N., 2014. Simulation of streamflow and sediment with the Soil and Water Assessment Tool model in a data scarce catchment in the Three Gorges Region, China. J. Environ. Qual. 43:37–45.

Borisova, T., Hodges, A. W., Stevens, T. J., 2014. Economic contributions and ecosystem services of springs in the lower Suwannee and Santa Fe River Basins of north-central Florida, edited, University of Florida, Food and Resource Economics Department.

Boyer, D.G., and Pasquarell, G.C., 1995. Nitrate concentrations in karst springs in an extensively grazed area 1. JAWRA Journal of the American Water Resources Association, 31(4), pp.729-736.

Boyer, D.G., and Pasquarell, G.C., 1996. Agricultural land use effects on nitrate concentrations in a mature karst aquifer 1. JAWRA Journal of the American Water Resources Association, 32(3), pp.565-573.

Bowen, J.L., Kroeger, K.D., Tomasky, G., Pabich, W.J., Cole, M.L., Carmichael, R.H., Valiela, I., 2007. A review of land-sea coupling by groundwater discharge of nitrogen to New England estuaries: mechanisms and effects Appl. Geochem., 22 2007, pp. 175-191.

Burow, K.R., Nolan, B.T., Rupert, M.G., and Dubrovsky, N. M., 2010. Nitrate in groundwater of the United States, 1991–2003, Environ. Sci. Technol., 44, 4988–4997, 2010.

Butscher, C., Huggenberger, P., 2009. Modeling the temporal variability of karst groundwater vulnerability, with implications for climate change. Environ. Sci. Technol., 43 (6) (2009), pp. 1665-1669

Bush, P. W., and Johnston, R. H., 1988. Ground-Water Hydraulics, Regional Flow, and Ground-Water Development of the Floridan Aquifer System in Florida and in Parts of Georgia, South Carolina, and Alabama, U.S. Government Printing Office, Washington, D.C.

Cerro, I., Antigüedad, I., Srinavasan, R., Sauvage, S., Volk, M., and Sanchez-Perez, J.M., 2014b. Simulating land management options to reduce nitrate pollution in an agricultural watershed dominated by an alluvial aquifer. Journal of Environmental Quality, 43 (1), 67–74. doi:10.2134/jeq2011.0393.

Cibin, R., Chaubey, I., Helmers, M., Sudheer, K.P., White, M., and Arnold, J.G., 2015. Improved Physical Representation of Vegetative Filter Strip in SWAT. 2015.

Chaplot, V., Saleh, A., Jaynes, D.B., 2005. Effect of the accuracy of spatial rainfall information on the modeling of water, sediment, and NO3-N loads at the watershed level.J. Hydrol. 312, 223–234.

Chaubey, I., Chiang, L., Gitau, M.W., Mohamed, S., 2010. Effectiveness of best management practices in improving water quality in a pasture-dominated watershed. Journal of soil and water conservation 65(6):424-437.

Chen, Y., Marek. W.G., Brauer, D. K., and Srinivasan, R., 2017. Assessing the Efficacy of the SWAT Auto-Irrigation Function to Simulate Irrigation, Evapotranspiration, and Crop Response to Management Strategies of the Texas High Plains. Water 2017, 9, 509; doi: 10.3390/w9070509.

Costa, J.E., Heufelder, G., Foss, S., Milham, N.P., Howes, B., 2002. Nitrogen removal efficiencies of three alternative septic system technologies and a conventional septic system. Environ. Cape Cod 5 (1), 15-24.

Coxon, C., 2011. Agriculture and karst. In Karst management (pp. 103-138). Springer, Dordrecht.

Crandall, C.A., Katz, B.G., Hirten, J.J., 1999. Hydrochemical evidence for mixing of river water and groundwater during high-flow conditions, lower Suwannee River basin, Florida, USA. Hydrogeology Journal 7, 454–467.

Dabney, S.M., Delgado, J.A., Meisinger, J.J., Schomberg, H.H., Liebig, M.A., Kaspar, T., 2010. Using cover crops and cropping systems for nitrogen management. In: J.A. Delgado and R.F. Follet, editors, Advances in nitrogen management for water quality. Soil and Water Conserv. Soc., Ankeny, IA. p. 230–281.

Darracq, A., Destouni, G., Persson, K., Prieto, C., Jarsoe, J., 2010. Scale and model resolution effects on the distributions of advective solute travel times in catchments, Hydrol. Processes, 24, 1697–1710.

Daggupati, P., Pai, N., Ale, S., Douglas-Mankin, K. R., Zeckoski, R. W., Jeong, J., Youssef, M. A., 2015. A recommended calibration and validation strategy for hydrologic and water quality models. Trans. ASABE, 58(6), 1705-1719. https://doi.org/10.13031/trans.58.10712.

Dahan, O., Babad, A., Lazarovitch, N., Russak, E. E., and Kurtzman, D., 2014. Nitrate leaching from intensive organic farms to groundwater, Hydrol. Earth Syst. Sci., 18, 333–341, https://doi.org/10.5194/hess-18-333-2014, 2014.

Dakhlalla, O.A., Parajuli, P.B., 2019. Assessing model parameters sensitivity and uncertainty of streamflow, sediment, and nutrient transport using SWAT. Inf. Process. Agric. 6, 61–72.

Davis, A.D., Long, A.J., Wireman, M., 2002. KARSTIC: a sensitivity method for carbonate aquifers in karst terrain. Environ Geol 42:65–72.

De la Monte, S.M., Neusner, A., Chu, J., Lawton, M., 2009. Epidemiological trends strongly suggest exposures as etiologic agents in the pathogenesis of sporadic Alzheimer's disease, Diabetes Mellitus, and Non-Alcoholic Steatohepatitis. J. Alzheimers Dis., 17 (2009), pp. 519-529.

Dosdogru, F., Kalin, L., Wang, R., Yen, H., 2020. Potential impacts of land use/cover and climate changes on ecologically relevant flows. J. Hydrol. 2020, 584, 124654.

Desormeaux, A., Annable, M. D., Dobberfuhl, D. R., Jawitz, J.W., 2019. In situ measurement of nitrate flux and attenuation using a soil passive flux meter. Journal of Environmental Quality, 48(3), 709–716. https://doi.org/10.2134/jeq2018.07.0284.

Destouni, G., Graham, W., 1995. Solute transport through an integrated heterogeneous soil–groundwater system. Water Resources Research, 31 (8) (1995), pp. 1935-1944.

Doerfliger, N., Jeannin, P.Y., Zwahlen, F., 1999. Water vulnerability assessment in karst environments: a new method of defining protection areas using a multi-attribute approach and GIS tools (EPIK method). Environ. Geol., 39 (2) 1999, pp. 165-176.

Doummar, J., Sauter, M., Geyer, T., 2012. Simulation of flow processes in a large-scale karst system with an integrated catchment model (Mike She) – Identification of relevant parameters influencing spring discharge. J. Hydrol. 426–427, 112–123. https://doi.org/10.1016/j.jhydrol.2012.01.021.

Douglas-Mankin, R., Barnes, L., and Devlin, L., 2011. Field-level targeting using SWAT: Mapping output from HRUs to fields and assessing limitations of GIS input data. American Society of Agricultural and Biological Engineers ISSN 2151-0032.

Durden, D., Gordu, F., Hearn, D., Cera, T., Desmarais, T., 2019. NORTH FLORIDA SOUTHEAST GEORGIA GROUNDWATER MODEL (NFSEG V1.1). Technical Publication SJ2019-01.

Eller, K. T., and Katz, B. G., 2017. Nitrogen source inventory and loading tool: An integrated approach toward restoration of water-quality impaired karst springs. Journal of Environmental Management, 196, 702–709. https://doi.org/10.1016/j.jenvman.2017.03.059.

Ellins, K.K., Kincaid, T.R., Hisert, R.A., Johnson, N.A., Davison, C.A., and Wanninkohf, R.H., 1991. Using 222Rn and SF6 to Determine Groundwater Gains and Stream Flow Losses in the Santa Fe River: Hydrogeology of the Western Santa Fe River Basin, Field Trip Guidebook No. 32., Southeastern Geological Society.

EPA, US Environmental Protection Agency. 2016. Ground water and drinking water: Table of regulated drinking water contaminants. <https://www.epa.gov/ground-water-and-drinking-water/table-regulated-drinking-water-contaminants Inorganic (03/20, 2016).

Epelde, A.M., Cerro, I., Sánchez-Pérez, J.M., Sauvage, S., Srinivasan, R., Antiguedad, I., 2015. Application of the SWAT model to assess the impact of changes in

agricultural management practices on water quality. Hydrol. Sci. J., 60 (5) (2015), pp. 825-843, 10.1080/02626667.2014.967692.

Epelde, A.M., Antiguedad, I., Brito, D., Jauch, J., Neves, R., Garneau, C., Sauvage, S., Sánchez-Pérez, J.M., 2016. Different modelling approaches to evaluate nitrogen transport and turnover at the watershed scale. J. Hydrol., 539 (2016), pp. 478-494.

Ercan, M.B., Goodall, J.L., Castronova, A.M., Humphrey, M., Beekwilder, N., 2014. Calibration of SWAT models using the cloud vol 62. doi: https://doi.org/10.1016/j.envsoft.2014.09.002.

Simonne, E.H., Liu, G., and Morgant, B., 2005. Denitrification in Seepage-Irrigated Vegetable Fields in South Florida.

Erisman, J.W., Sutton, M.A., Galloway, J., Klimont, Z., Winiwarter, W., 2008. How a century of ammonia synthesis changed the world. Nat. Geosci. 1, 636–639.

Faramarzi, M., Abbaspour, K.C., Schulin, R., Yang, H., 2009. Modeling blue and green water availability in Iran. Hydrol. Proc. 23 (3), 486–501.

Faramarzi, M., Yang, H., 2010. Analysis of intra-country virtual water trade strategy to alleviate water scarcity in Iran Hydrology and Earth System Sciences, 14 (8) (2010), pp. 1417-1433.

Faulkner, G.L., 1973. Geohydrology of the cross-Florida barge canal area with special reference to the Ocala vicinity. US Geol Surv Water-Resour Inves Rep 1-73, 117 pp.

FDACS, 2015. Water Quality/Quantity Best Management Practices for Florida Vegetable and Agronomic Crops, 2015th Ed., Florida Department of Agriculture and Consumer Services, Tallahassee, Florida.

FDACS, 2018. Status of Implementation of Agricultural Nonpoint Source Best Management Practices. Report to the Governor, the President of the Senate, and the Speaker of the House Pursuant to s. 403.0675(2), Florida Statutes.

FDEP, 2012. BASIN MANAGEMENT ACTION PLAN for the Implementation of Total Daily Maximum Loads for Nutrients Adopted by the Florida Department of Environmental Protection in the Santa Fe River Basin.

FDEP, 2013. Surface Water Quality Standards. Florida Administrative Code, 62-302(62-302), 530-531.

FDEP, 2018. BASIN MANAGEMENT ACTION PLAN for the Environmental Assessment andRestoration Water Quality Restoration Program Florida Department ofEnvironmental Protection in the Santa Fe River Basin. floridadep.gov 2018.

Fenton, O., Mellander, P.E., Daly, K., Wall, D.P., Jahangir, M.M.R., Jordan, P., Hennessey, D., Huebsch, M., Blum, P., Vero, S., Richards, K.G., 2017. Integrated assessment of agricultural nutrient pressures and legacies in karst landscapes. Agric. Ecosyst. Environ. 239, 246–256.

Ferrant, S., Durand, P., E. Justes, J., Probst, J., Sanchez-Perez, M., 2013.Simulating the long-term impact of nitrate mitigation scenarios in a pilot study basin. Agric. Water Manag., 124 (2013), pp. 85-96, 10.1016/j.agwat.2013.03.023.

Ficklin, D.L., Luo, Y.Z., Zhang, M.H., 2013. Watershed modelling of hydrology and water quality in the Sacramento River watershed, California. Hydrol Process 27(2):236–50.

Francesconi, W., Srinivasan, R., Pérez-Miñana, E., Willcock, S.P., and Quintero, M., 2016. Using the Soil and Water Assessment Tool (SWAT) to model ecosystem services: a systematic review. J. Hydrol., 535 2016, pp. 625-636, 10.1016/j.jhydrol.2016.01.034.

Frisbee, A.E., 2007. Nitrate-nitrogen dynamics in tributaries of the Santa Fe river watershed, north-central Florida. A thesis presented to the graduate school of the university of Florida in partial fulfillment of the requirements for the degree of Master of Science. University of Florida. https://ufdcimages.uflib.ufl.edu/UF/E0/01/86/00/00001/frisbee_a.pdf.

Galloway, J.N., Capone, D.G., Boyer, E.W., Howarth, R.W., Seitzinger, S.P., Asner, G.P., Cleveland, C., Green, P., Holland, E., Karl, D.M., Michaels, A.F., Porter, J.H., Townsend, A., Vőrősmarty, C., 2003. Nitrogen cycles: past, present, and future. Biogeochemistry, 70 (2003), pp. 153-226.

Gao, J., Li, F., Gao, H., Zhou, C., Zhang, X., 2015. The impact of land-use changes on waterrelated ecosystem services: a study of the Guishui River Basin, Beijing, China.J. Clean. Prod. 1–8. http://dx.doi.org/10.1016/j.jclepro.2016.01.049.

Gassman, P.W., Reyes, M., Green, C. H., and Arnold. J. G., 2007. The Soil and Water Assessment Tool: Historical development, applications, and future directions. Trans. ASABE 50(4): 1211- 1250.

Gassman, P.W., Sadeghi, A.M., and Srinivasan, R., 2014. Applications of the SWAT Model Special Section: Overview and Insights. J. Environ. Qual. 43:1–8.

Ghaffari, G., Keesstra, S., Ghodousi, J., and Ahmadi. H., 2010. SWAT-simulated hydrological impact of land-use change in the Zanjanrood basin, northwest Iran. Hydrol. Proc. 24(7): 892-903.

Gitau, M. W., Gburek, W. J., and Bishop, P. L., 2008. Use of the swat model to quantify water quality effects of agricultural BMPs at the farm-scale level. American Society of Agricultural and Biological Engineers, Vol. 51(6): 1925-1936.

Graetz, D.A., Love.J., Mackowiak, C.L., Starling, C., Randell, R., 2006. Forage Interim Measure for Nitrogen-based fertilizers for the Suwanee River Basin (SRB) North Florida REC-Suwanee valley.

Grizzetti, B., Bouraoui, F., and De Marsily. G., 2005. Modelling nitrogen pressure in river basins: A comparison between a statistical approach and the physically based SWAT model. Physics and Chemistry of the Earth 30(8-10): 508-517.

Grubbs, J.W., 1998. Recharge Rates to the Upper Floridan Aquifer in the Suwannee River Water Management District, Florida. U.S. Geological Survey Water Resources Investigations Report 97-4283, 30 pp., Reston, Virginia.

Grubbs, J.W., and Crandall, C.A., 2007. Exchanges of Water between the Upper Floridan Aquifer and the Lower Suwannee and Lower Santa Fe Rivers, Florida.U.S. Geological Survey. Professional Paper 1656-C. Reston, Virginia.

Guse, B., Pfannerstill, M., Fohrer, N., 2015. Dynamic modelling of land use change impacts on nitrate loads in rivers. Environ. Process. 2, 575–592.

Haas, H., 2020. Capturing Forest Dynamics in Hydrological Modeling (Master's Thesis). Auburn University, Auburn, AL.

Hamby, D.M.,1994. A review of techniques for parameter sensitivity analysis of environmental meodels. Environ Monit Assess 32:135–154.

Haney, E.B., Haney, R.L., Arnold, J.G., White, M.J., 2018. Comparison of Wheat Yield Simulated Using Three N Cycling Options in the SWAT Model. Open Journal of Soil Science, 2018, 8, 197-211.

Harbaugh, A.W., 2005, MODFLOW-2005, the U.S. Geological Survey modular ground water model and the ground-water flow process: U.S. Geological Survey Techniques and Methods 6-A16.

Harter, T., Davis, H., Mathews, M.C., Meyer, R.D., 2002. Shallow groundwater quality on dairy farms with irrigated forage crops. Journal of Contaminant Hydrology, 55(3–4), 287–315.

Harmel, R.D., and Smith, P.K., 2007. Consideration of measurement uncertainty in the evaluation of goodness-of-fit in hydrologic and water quality modeling. Journal of Hydrol. 337, 326–336.

Harmel, R.D., Smith, P.K., and Migliaccio, K.W., 2010. Modifying goodness-of-fit indicators to incorporate both measurement and model uncertainty in model calibration and validation. Trans. ASABE 53, 55 – 63.

Harrington, D., Maddox, G., Hicks R., 2010. Florida springs initiative monitoring network report and recognized sources of nitrate. Florida Department of Environmental Protection, Tallahassee, Florida.

He, J., Dukes, M.D., Hochmuth, G.J., Jones, J.W., Graham, W.D., 2011. Evaluation of sweet corn yield and nitrogen leaching with CERES-maize considering input parameter uncertainties. Trans. Am. Soc. Agric. Biol. Eng. 54 (4), 1257e1268.

Heffernan, J. B., Cohen, M.J., Frazer, T. K., Thomas, R.G., Rayfield, T. J., Gulley, J., Martin, J.B., Delfino, J. J., and Graham, W. D., 2010. Hydrologic and biotic influences on nitrate removal in a subtropical spring-fed river. Limnol. Oceanogr., 55(1), 2010, 249–263.

Heffernan, J. B., Albertin, A. R., Fork, M. L., Katz, B. G., Cohen, M. J., 2012. Denitrification and inference of nitrogen sources in the karstic Floridan aquifer. Biogeosciences, 9(5), 1671–1690. https://doi.org/10.5194/bg-9-1671-2012.

Henson, W.R., Cohen, M.J., Graham, W.D., 2019. Spatially distributed denitrification in a karst springshed. Hydrological Processes. 2019; 33:1191–1203. https://doi.org/10.1002/hyp.13380.

Hochmuth, G. J., Hanlon, E. A., Hochmuth, B. C., 1992. Responses of pepper, muskmelon, watermelon, and sweet corn to P and K fertilization at Live Oak, Fla. Suwannee Valley REC Research Report 92-28.

Hochmuth, G.J., Hanlon, E.A., 2000. IFAS Standardized Fertilization Recommendations for Vegetable Crops. Circular 1152. University of Florida Institute of Food and Agricultural Sciences, Gainesville, FL.

Hochmuth, G.J., 2000. Management of nutrients in vegetable production systems in Florida. Proc. Soil Crop Sci. Soc. Fla. 59, 11-13.

Hochmuth, G.J., Hanlon, E.A., 2010. Commercial Vegetable Fertilization Principles. SL319. University of Florida Institute of Food and Agricultural Sciences, Gainesville, FL.

Hochmuth, G., Mylavarapu, R., Hanlon, E., 2014. The Four Rs of Fertilizer Management. Soil and Water Science Department, UF-IFAS Extension, SL411, 1-4.

Horton, R., Thompson, M.L., McBride, J.F., 1987. Method of estimating the travel time of noninteracting solutes through compacted soil material. Soil Sci Soc Am J 51:48–53.

Humenik, F.J., Smolen, M.D., Dressing, S.A., 1987. Pollution from nonpoint sources: Where we are and where we should go. Environ. Sci. Technol., 21(8):737-742.

Husic, A., Fox, J., Adams, E., Ford, W., Agouridis, C., Currens, J., Backus, J., 2019. Nitrate pathways, processes, and timing in an agricultural karst system: development and application of a numerical model. Water Resour. Res. 55, 2079–2103.

Hutson, J., Wagenet, R., 1992. LEACHM (Leaching Estimation and Chemistry Model): A Process-Based Model of Water and Solute Movement, Transformations, Plant Uptake and Chemical Reactions in the Unsaturated Zone, Version 3.0, Department of Soil, Crop and Atmospheric Sciences, Cornell University, Ithaca.

Jing, M., Heße, F., Kumar, R., Kolditz, O., Kalbacher, T., Attinger, S., 2019. Influence of input and parameter uncertainty on the prediction of catchment-scale groundwater travel time distributions. Hydrol. Earth Syst. Sci. 2019, 23, 171–190.

Johanson, R., J. I, H. Davis., USERS MANUAL FOR HYDROLOGICAL SIMULATION PROGRAM - FORTRAN (HSPF). U.S. Environmental Protection Agency, Washington, D.C., EPA/600/9-80/015.

Jones, J.W., Hoogenboom, G., Porter, C.H., Boote, K.J., Batchelor, W.D., Hunt, L., Wilkens, P.W., Singh, U., Gijsman, A.J., Ritchie, J.T., 2003. The DSSAT cropping system model. Eur. J. Agron. 18 (3), 235–265.

Kamali, B., Abbaspour, K.C. and Yang, H., 2017. Assessing the Uncertainty of Multiple Input Datasets in the Prediction of Water Resource Components. Water 2017, 9, 709; doi:10.3390/w9090709.

Karki, R., Srivastava, P., Bosch, D. D., Kalin, L., Lamba, J., Strickland, T. C., 2019. Multi-variable sensitivity analysis, calibration, and validation of a field-scale swat model: building stakeholder trust in hydrologic/water quality modeling. trans(asabe).

Kaspar, T. C., Singer, J. W., 2011.The Use of Cover Crops to Manage Soil 2011. Publications from USDA-ARS / UNL Faculty. 1382. http://digitalcommons.unl.edu/usdaarsfacpub/1382.

Katz, B. G., Hornsby, H. D., Bohlke, J. F., Mokray, M. F., 1999. Sources and Chronology of Nitrate Contamination in Spring Waters, Suwannee River Basin, Florida, Report 99-4252 Ed., U.S. Geological Survey, Tallahassee, Florida.

Katz, B. G., Böhlke, J.K., Hornsby, H. D., 2001. Timescales for nitrate contamination of spring waters, northern Florida, USA. Chem Geol 179:167–186.

Katz, B. G., 2004. Sources of Nitrate Contamination and Age of Water in Large Karstic Springs of Florida. Environ. Geol., 46(6-7), 689-706.

Katz, B.G., Griffin D.W., 2008. Using chemical and microbiological indicators to track the impacts from the land application of treated municipal wastewater and other sources on groundwater quality in a karstic springs basin. Environmental Geology 55: 801-21.

Kellman, L.M. and Hillaire-Marcel, C., 2003. Evaluation of nitrogen isotopes as indicators of nitrate contamination sources in an agricultural watershed. Agriculture, ecosystems & environment, 95(1), pp.87-102.

Kiniry, J.R., Arnold, J.G. and Xie, Y., 2002. Application of Models with Different Spatial Scales. In: Lajpat, R.A., Ma, L. and Howell, T.A., Eds., Agricultural System Models in Field Research and Technology Transfer, CRC Press, Boca Raton. https://doi.org/10.1201/9781420032413.ch10.

Kiniry, J.R., Simpson, C.E., Schubert, A.M., Reed, J.D., 2005. Peanut leaf area index, light interception, radiation use efficiency, and harvest index at three sites in Texas. Field Crops Research 91 (2005) 297–306.

Kiniry, J., R., Burson, B.L., Evers, G.W., Williams, J.R., Sanchez, H., Wade, C., Wade, J.W., 2007. Coastal Bermudagrass, Bahiagrass, and Native Range Simulation at Diverse Sites in Texas. Agron. J. 99:450–461 (2007). Modeling doi:10.2134/agronj2006.0119.

Kiniry, J.R., Macdonald, J.D., Armen, R., Watson, B. and Prepas, E.E., 2008. Plant growth simulation for landscape-scale hydrological modelling. Hydrological Sciences–Journal–des Sciences Hydrologiques, 53(5) October 2008.

Kite, G., 2000. Using a basin-scale hydrological model to estimate crop transpiration and soil evaporation J. Hydrol., 229 pp. 59-69.

Knowles, L., O'Reilly, A.M., Adamski, J.C., 2002. Hydrogeology and Simulated Effects of Ground-Water Withdrawals from the Floridan Aquifer System in Lake County and in the Ocala National Forest and Vicinity, North-Central Florida. U.S. GEOLOGICAL SURVEY. Water-Resources Investigations Report 02–4207.

Krueger, E. S., Ochsner, T. E., Porter, P. M., Baker, J. M., 2011. Winter Rye Cover Crop Management influences on Soil Water, Soil Nitrate, and Corn Development. Agron. J. 103:316–323 (2011).

Lam, Q.D., Schmalz, B., and Fohrer, N., 2011. The impact of agricultural best management practices on water quality in a North German lowland catchment. Environmental Monitoring and Assessment, 183, 351–379. doi: 10.1007/ s10661-011-1926-9.

Lassaletta, L., Billen, G., Grizzetti, B., Anglade, J., & Garnier, J., 2014. 50-year trends in nitrogen use efficiency of world cropping systems: The relationship between yield and nitrogen input to cropland. Environmental Research Letters, 9(10), 105011. https://doi.org/10.1088/1748-9326/9/10/105011.

Lenhart, T., Eckhardt, K., Fohrer, N., Frede, H.G., 2002. Comparison of two different approaches of sensitivity analysis Physics and Chemistry of the Earth. Parts A/B/C 27:645–654. doi:https://doi.org/10.1016/S1474-7065(02)00049-9.

Liang, K., Jiang, Y., Qi, J., Fuller, K., Nyiraneza, J., & Meng, F.R., 2020. Characterizing the impacts of land use on nitrate load and water yield in an agricultural watershed in Atlantic Canada. Science of the Total Environment, 729, 138793. https://doi.org/10.1016/j.scitotenv.2020.138793.

Lindsay, J.F., Holliday, D.W., Hulbert, A.G., 1991. Sequence stratigraphy and the evolution of the Ganges–Brahmaputra Delta complex. American Association of Petroleum Geologists Bulletin 75, 1233–1254.

Lin, B., Chen, X., Yao, H., Chen, Y., Liu, M., Gao, L., James, A., 2015. Analyses of land use change impacts on catchment runoff using different time indicators based on SWATmodel.EcologicalIndicators58, 55–63.

Lindgren, G. A., Wrede, S., Seibert, J., and Wallin, M., 2007. Nitrogen source apportionment modeling and the effect of land-use class related runoff contributions, Nordic Hydrol., 38, 317–331, doi:10.2166/nh.2007.015, 2007.

Liu, R., Xu, F., Zhang, P., Yu, W., Men, C., 2016. Identifying non-point source critical source areas based on multi-factors at a basin scale with SWAT. J. Hydrol. 533, 379–388.

Liu, W., Park, S., Bailey, R.T., Molina-Navarro, E., Andersen, H.E., Thodsen, H., Nielsen, A., Jeppesen, E., Jensen, J.S., Jensen, J.B., 2019. Comparing SWAT with SWAT-MODFLOW hydrological simulations when assessing the impacts of groundwater abstractions for irrigation and drinkingwater. Hydrol. Earth Syst. Sci. Discuss. (2019), 10.5194/hess-2019-232.

Loague K. and Corwin D.L., 1998. Regional-scale assessment of non-point source groundwater contamination. Hydrological Processes, 12(6), pp.957–966.

Maddox, G.L., Lloyd, J.M., Scott, T.M., Upchurch, S.B., Copeland. R., 1992.Florida's Ground-Water Quality Monitoring Network Program: Background Hydrogeochemistry. Florida Geological Survey Special Publication 34.

Malagò, A., Pagliero, L., Bouraoui, F., Franchini, M., 2015. Comparing calibrated parameter sets of the SWAT model for the Scandinavian and Iberian peninsulas. Hydrological Sciences Journal , 2015. http://dx.doi.org/10.1080/02626667.2014.978332.

Malik, W., Jiménez-Aguirre, T. M., Dechmi, F., 2020. Coupled DSSAT-SWAT models to reduce off-site N pollution in Mediterranean irrigated watershed. Science of the Total Environment 745 (2020) 141000.

Mapfumo, E., D.S. Chanasyk, and W.D. Willms., 2004. Simulating daily soil water under foothills fescue grazing with the soil and water assessment tool model (Alberta, Canada). Hydrological Processes: 2787 18: 2800.

Marek, G. W., Gowda, P. H., Evett, S. R., Baumhardt, R. L., Brauer, D. K., Howell, T. A., … Srinivasan, R., 2016. Calibration and validation of the SWAT model for predicting daily ET over irrigated crops in the Texas High Plains using lysimetric data. Transactions of the ASABE, 59(2), 611–622.

Marek, G.W., Gowda, P.H., Marek, T.H., Porter, D.O., Baumhardt, R.L., Brauner, D.K., 2017. Modelling long-term water use of irrigated cropping rotations in the Texas High Plains using SWAT. Irrig. Sci. 35 (2), 111–123.

Marella, R.L., 2014. Water withdrawals, use, and trends in Florida, 2010: U.S. Geological Survey Scientific Investigations Report 2015–5088, 59 p.

Maresch, W., Walbridge, M.R., and Kugler, D., 2008. Enhancing conservation on agricultural landscapes: A new direction for the Conservation Effects Assessment Project. J. Soil Water Conserv. 63: 198A–203A.

Martinez-Feria, R.A., Dietzel, R., Liebman, M., Helmers, M, J., Archontoulis, S, V., 2016. Rye cover crop effects on maize: A system-level analysis. Field Crops Research 196 2016 145–159.

Maski, D., Mankin, K. R., Janssen, K. A., Tuppad, P., Pierzynski, G. M., 2008. Modeling runoff and sediment yields from combined in-field crop practices using the Soil and Water Assessment Tool. Journal of Soil and Water Conservation, 63(4), 193–203.

Maupin, M. A., Kenny, J. F., Hutson, S. S., Lovelace, J. K., Barber, N.L., LinseY, K. S., 2014. Estimated use of Water in the United States in 2010, Circular 1405 Ed., U.S. Geological Survey, Reston, Virginia.

McGuire, K. J., and McDonnell, J. J., 2006. A review and evaluation of catchment transit time modelling, J. Hydrol., 330, 543–563, doi:10.1016/j.jhydrol.2006.04.020, 2006.

Meals, D.W., 2001.Water quality response to riparian restoration in an agricultural watershed in Vermont, USA. Water Sci. Technol. 2001 43 175–182.

Meals, D.W., Dressing, S.A., and Davenport, T.E., 2010. Lag time in water quality response to best management practices: A review. J. Environ. Qual. 39: 85–96. doi: https://doi.org/10.2134/jeq2009.0108.

Mechal, A., Wagner, T., Birk, S., 2015. Recharge variability and sensitivity to climate: the example of Gidabo River basin, main Ethiopian rift. J. Hydrology Regional Stud., 4 (2015), pp. 644-660.

Miller, J.A., 1986, Hydrogeologic framework of the Floridan aquifer system in Florida and in parts of Georgia, Alabama, and South Carolina: U.S. Geological Survey Professional Paper 1403-B, 91 p., 33 pis.

Mitteslet, A, R., Storm, D, E., and Stoecker, A.L., 2015. Using SWAT to simulate crop yields and salinity levels in the North Fork River Basin, USA. International journal of agricultural and Biological Engineering, 8(3),110-124.

Mitsch, W.J., Day Jr., J.W., Gilliam, J.W., Groffman, P.M., Hey, D.L., Randall, G.W., Wang, N., 1999. Reducing nutrient loads, especially nitrate-nitrogen, to surface water, groundwater, and the Gulf of Mexico, Topic 5 Report for the integrated assessment on hypoxia in the Gulf of Mexico, NOAA Coastal Ocean Program Decision Analysis Series No.19, NOAA Coastal Ocean Program, Silver Spring, MD.

Moore, E.B., Wiedenhoeft, M.H., Kaspar, T.C. and Cambardella, C.A., 2014. Rye cover crop effects on soil quality in no-till corn silage–soybean cropping systems. Soil Sci. Soc. Am. J., 78 2014, pp. 968-976.

Moloney, C.; Cibin, R.; Chaubey, I., 2015. Using a Single HRU SWAT Model to Examine and Improve Representation of Field-Scale Processes.

Moriasi, D. N., Arnold, G.J., Van Liew, W. M., Bingner, L.R., Harmel, D.R., Veith, L.T., 2007.Model evaluation guidelines for systematic quantification of accuracy in watershed simulations. Transactions of the ASABE Vol. 50(3): 885−900.

Moriasi, D. N., Gitau, M. W., Pai, N. and Daggupati, P., 2012. Hydrologic and water quality models: performance measures and evaluation criteria. Transactions of the ASABE Vol. 58(6): 1763-1785.

Moriasi, D. N., Gitau, M. W., Pai, N., and Daggupati, P., 2015. Hydrologic and water quality models: Performance measures and evaluation criteria, Transactions of the ASABE, 58, 1763-1785, 2015.

Motavalli, P.P., Goyne, K.W. and Udawatta, R.P., 2008. Environmental impacts of enhanced-efficiency nitrogen fertilizers. Crop Management, 7(1), pp.0-0.

Mulla, D.J., Kitchen, N. and David, M., 2004. Evaluating the effectiveness of agricultural management practices at reducing nutrient losses to surface waters.

Mylavarapu, R., Wright, D. and Kidder, G., 2015. UF-IFAS Standardized Fertilization Recommendations for Agronomic Crops. Soil and Water Science Department, UF-IFAS Extension, (SL129), 10/1/2015-8.

Nair, S. S., King, K. W., Witter, J. D., Sohngen, B. L., Fausey, N. R., 2011. Importance of crop yield in calibrating watershed water quality simulation models. J. American Water Res. Assoc. 47(6): 1285-1297.

Neitsch S.L., Arnold J.G., Kiniry J.R., Srinivasan R., Williams J.R., 2004. Soil andWater Assessment Tool Input/Output File Documentation version 2005.Temple, Texas: Grassland, Soil and Water Research Laboratory, USDA-ARS andBlackland Research and Extension Center, Texas A&M University.

Neitsch, S.L., J.G. Arnold, J.R. Kiniry, and J.R. Williams., 2011. Soil and Water Assessment Tool theoretical documentation: Version 2009. USDA– ARS, Grassland, Soil and Water Research Laboratory, Temple, TX; and Blackland

Research and Extension Center, Texas AgriLife Research, Temple, TX. Texas Water Resources Institute Technical Rep. 406, Texas A&M University System, College Station, TX. http://swatmodel.tamu. Edu/documentation/ (accessed 8 Dec. 2012).

Nguyen, V.T. and Dietrich, J., 2018. Modification of the SWAT model to simulate regional groundwater flow using a multicell aquifer, Hydrol. Process. 32, 939–953, https://doi.org/10.1002/hyp.11466, 2018. a, b.

Niraula, R., Kalin, L., Srivastava, P., and Anderson. C.J., 2013. Identifying critical source areas of nonpoint source pollution with SWAT and GWLF. Ecol. Model, 268 2013, pp. 123-133.

Nolan, B.T., Ruddy, B.C., 1996. Nitrate in Ground Waters of the United States - Assessing the Risk; U.S. Geological Survey: Reston, VA, 1996; Fact Sheet FS-092-96.

Nolan, B.T., 2001. Relating nitrogen sources and aquifer susceptibility to nitrate in shallow ground waters of the United States. Groundwater, 39(2), pp.290-299.

NRCS, 2013b. Soil Survey Geographic (SSURGO) Database. U.S. Department of Agriculture. http://websoilsurvey.nrcs.usda.gov.

Obeidat, M., Ahmad, F.Y., Hamouri, N.A., Messadeh, A.M., Athamneh, F.S., 2008. Assessment of nitrate contamination of karst springs, Bani Kanana, northern Jordan. Rev. Mex. Cienc. Geol. 25 (3), 426-437.

Osmond, D.; Meals, D.; Hoag, D.; Arabi, M.; Luloff, A.; Jennings, G.; McFarland, M.; Spooner, J.; Sharpley, A.; Line, D., 2012.Improving conservation practices programming to protect water quality in agricultural watersheds: Lessons learned from the National Institute of Food and Agriculture–Conservation Effects Assessment Project J. Soil Water Conserv. 2012, 67, 122A– 127A.

Panno, S.V., Hackley, K.C., Hwang, H.H. and Kelly, W.R., 2001. Determination of the sources of nitrate contamination in karst springs using isotopic and chemical indicators. Chemical Geology, 179(1-4), pp.113-128.

Parajuli, P., Jayakody, P., Sassenrath, G., Ouyang, Y., Pote, J., 2013. Assessing the impacts of crop-rotation and tillage on crop yields and sediment yield using a modeling approach. Agr. Water Manage. 119, 32–42.

Park, J.Y.; Ale, S.; Teague, W.R., 2017. Simulated water quality effects of alternate grazing management practices at the ranch and watershed scales. Ecol. Model. 2017, 360, 1–13.

Peterson, E.W., Davis, R.K., Brahana, J.V. and Orndorff, H.A., 2002. Movement of nitrate through regolith covered karst terrane, northwest Arkansas. Journal of Hydrology, 256(1-2), pp.35-47.

Panagopoulos, Y., Makropoulos, C., Baltas, E., Mimikou, M., 2011. SWAT parameterization for the identification of critical diffuse pollution source areas under data limitations. Ecol Model 222:3500–3512. doi:10.1016/j.ecolmodel.2011.08.008.

Paul, S., Cashman, M.A., Szura, K., Pradhanang, S.M., 2017. Assessment of Nitrogen Inputs into Hunt River by Onsite Wastewater Treatment Systems via SWAT Simulation. Water 2017, 9, 610.

Pfannerstill, M., Guse, B., and Fohrer, N., 2014. A multi-storage groundwater concept for the SWAT model to emphasize nonlinear groundwater dynamics in lowland catchments. Hydrological Processes, 28 (22), 5599–5612. doi:10.1002/hyp.10062.

Pisinaras, V., Petalas, C., Gikas, G.D., Gemitzi, A., Tsihrintzis, V.A., 2010. Hydrological and water quality modeling in a medium-sized basin using the Soil and Water Assessment Tool (SWAT). Desalination 250, 274–286.

Pittman, J. R., Hatzell, H. H., and Oaksford, E. T., 1997. Spring contributions to water quality and nitrate loads in the Suwannee River during baseflow in July 1995, U. S. Geological Survey WaterResources Investigations Report 97-4152, Reston, VA, 1997.

Pohlert, T., Huisman, J.A., Breuer, L., Frede, H.G., 2005. Modelling of point and diffuse source pollution of nitrate with SWAT in the river Dill, Germany. Adv. Geosci. 5, 7–12.

Pohlert, T., Huisman, J.A., Breuer, L., Frede, H.G., 2005. Evaluation of the soil nitrogen balance model in SWAT with lysimeter data. In: Srinivasan, R., Jacobs, J., Day, D., Abbaspour, K. (Eds.), Proceedings of the 3rd International SWAT Conference, Zurich, Switzerland, July 11–15, pp. 496–508.

Pohlert, T., J. A. Huisman, L. Breuer, and H.G. Freude., 2007. Integration of a detailed biogeochemical model into SWAT for improved nitrogen predictions: Model development, sensitivity, and GLUE analysis. Ecol. Model. 203(3-4): 215-228.

Poikane, S., Kelly, M.G., Salas Herrero, F., Pitt, J.A., Jarvie, H.P., Claussen, U., Leujak, W., Lyche Solheim, A., Teixeira, H., Phillips, G., 2019. Nutrient criteria for surface waters under the European water framework directive: current state-of-the-art, challenges and future outlook. Sci. Total Environ. 695. https://doi.org/10.1016/j.

Pollock, D.W., 1988. Semianalytical computation of path lines for finite-difference models. Ground Water 26: 743-50.

Pollock, D.W., 1994. User's guide for MODPATH/MODPATH-PLOT, version 3: A particle tracking post-processing package for MODFLOW, the U.S. Geological Survey finite-difference ground-water flow model. USGS Open-File Report 94-464. Reston, Virginia: USGS.

Prasad, R., Hochmuth, G.J., 2016. Environmental Nitrogen Losses from Commercial Crop Production Systems in the Suwannee River Basin of Florida. PLoS ONE 11(12): 0167558. doi:10.1371/journal.pone.0167558.

Psaris, A., Chang, H., Winfield, T., Lambrinos, J., 2012. Hydrologic modeling of urbanizing Oregon basins for water-related ecosystem service assessment using SWAT AGU Fall Meeting Abstracts (2012), p. 1480.

Rath, S., Zamora Re, M., Graham, W., Dukes, M., Kaplan, D., 2020. Quantifying nitrate leaching to groundwater from a corn-peanut rotation under a variety of irrigation and nutrient management practices in the Suwannee River Basin, Florida. https://doi.org/10.1016/j.agwat.2020.106634.

Ravbar, N., & Goldscheider, N., 2009.Comparative application of four methods of groundwater vulnerability mapping in a Slovene karst catchment. Hydrogeology Journal, 17, 725e733.

Rayne, T.W., Bradbury, K.R., Muldoon, M.A., 2001. Delineation of capture zones for municipal wells in fractured dolomite, Sturgeon Bay, Wisconsin, USA.Hydrogeol. J. 9, 432–450.

Refsgaard, J.C., Knudsen, J., 1996. Operational validation and intercomparison of different types of hydrological models Water Resources Research, 32 (7) (1996), pp. 2189-2202.

Reed, E.M., Wang, D., Duranceau, S.J., 2018. Evaluating nitrate management in the volusia blue springshed. J. Environ. Eng., 144 (3) (2018), p. 05018001, 10.1061/ (ASCE) EE.1943-7870.0001324.

Rosenau, J.C., Faulkner, G.L., Hendry Jr, C.W. and Hull, R.W., 1977. Springs of Florida (No. 31). Florida Department of Natural Resources: Bureau of Geology.

Saller, S.P., Ronayne, M.J., Long, A.J., 2013. Comparison of a karst groundwater model with and without discrete conduit flow. Hydrogeology Journal 21(7):1555–1566.

Santhi, C., Arnold, J.G., Williams, J.R., Srinivasan, R., 2001. Validation of the SWAT model on a large river basin with point and non point sources. Journal of American Water Resources Association, 37 (5), 1169–1188.

Santhi, C., Srinivasan, R., Arnold, J.G., Williams, J.R., 2006. A modeling approach to evaluate the impacts of water quality management plans implemented in a watershed in Texas. Environ Model Softw 21:1141–1157. doi:10.1016/j.envsoft.2005.05.013.

Scanlon, B. R., Jolly, I., Sophocleous, M., and Zhang, L., 2007. Global impacts of conversions from natural to agricultural ecosystems on water resources: Quantity versus quality, Water Resour. Res., 43, W03437, doi: 10.1029/2006WR005486, 2007.

Schwede, D.B., Lear, G.G., 2014. A novel hybrid approach for estimating total deposition in the United States. Atmos. Environ. 92, 207-220.

Scott, T. M., Means, G. H., Meegan, R. P., Means, R. C., Upchurch, S., Copeland, R. E., Jones, J., Roberts, T., and Willet, A., 2004. Springs of Florida.

Senay, G. B., Bohms, S., Singh, R. K., Gowda, P. H., Velpuri, N. M., Alemu, H., 2013. Operational evapotranspirationmapping using remote sensing andweather datasets: A new parameterization for the SSEB approach. Journal of the American Water Resources Association, 1-2013; 15, http://dx.doi.org/10.1111/jawr.12057.

Sepulveda, N., 2002. Simulation of Ground-Water Flow in the Intermediate and Floridan Aquifer Systems in Peninsular Florida. U.S. GEOLOGICAL SURVEY. Water-Resources Investigations Report 02-4009.

Sepulveda, A. A., Katz, B. G., and. Mahon. G. L., 2006. Potentiometric surface of the Upper Floridan aquifer in the Ichetucknee springshed and vicinity, northern Florida, September 2003.

Shen, Z., Chen, L., Hong, Q., Qiu, J., Xie, H., Liu, R., 2013. Assessment of nitrogen and phosphorus loads and causal factors from different land use and soil types in the Three Gorges Reservoir Area. Sci. Total Environ. 454–455, 383–392.

Shen, Z., Qiu, J., Hong, Q., Chen, L., 2014. Simulation of spatial and temporal distributions of non-point source pollution load in the Three Gorges Reservoir Region. Sci. Total Environ. 493, 138–146.

Shrestha, S., Bhatta, B., Shrestha, M., Shrestha, P.K., 2018. Integrated assessment of the climate and land use change impact on hydrology and water quality in the Songkhram River Basin, Thailand. Sci. Total Environ. 643, 1610–1622.

Shrivastava, V., Graham, W.D., Muñoz-Carpena, R., Maxwell, R., 2014. Insights on geologic and vegetative controls over hydrologic behavior of a large complex basin – global sensitivity analysis of an integrated parallel hydrologic model. J. Hydrol. 519 (B), 2238–2257. http://dx.doi.org/10.1016/j.jhydrol.2014.10.020.

Snider, D. M., Spoelstra, J., Schiff, S. L., and Venkiteswaran. J. J., 2010. Stable oxygen isotope ratios of nitrate produced from nitrification: 18O-labeled water incubations of agricultural and temperate forest soils, Environ. Sci. Technol., 44(14), 5358–5364, doi:10.1021/es1002567.

Sigua, G.C., 2010. Sustainable cow-calf operations and water quality: a review. Agron. Sustain. Dev. 30, 631-648.

Siliang, L., Congqiang, L., Yunchao, L., Zhiqi, Z., Zhihua, Z., 2010. Tracing the sources of nitrate in karstic groundwater in Zunyi, southwest China: a combined nitrogen isotope and water chemistry approach. Environ. Earth Sci. 60 (7), 1415-1423.

Simonne, E., Dukes, M., Hochmuth, G., Hochmuth, B., Studstill, D., Gazula, A., 2006. Monitoring nitrate concentration in shallow wells below a vegetable field. Proc. Fla. State Hort. Soc. 119, 226-230.

Spalding, R.F., Exner, M.E., 1993. Occurrence of nitrate in groundwater—a review. Journal of environmental quality, 22(3), pp.392-402.

Srinivasan, R., Zhang, X., Arnold, J., 2010. SWAT ungauged: hydrological budget and crop yield predictions in the Upper Mississippi River Basin. Trans. ASABE 53, 1533–1546.

Stephens, D.B., Hsu, K.C., Prieksat, M.A., Ankeny, M.D., N. Blandford, T.L., 1998. A comparison of estimated and calculated effective porosity. Hydrogeol J, 6 (1) (1998), pp. 156-165.

Sullivan and Gao, 2016. Assessment of nitrogen inputs and yields in the Cibolo and Dry Comal Creek watersheds using the SWAT model, Texas, USA 1996–2010. Environ. Earth Sci., 75 (9) (2016), pp. 1-20, 10.1007/s12665-016-5546-0.

SWAT. 2019. SWAT: The soil & water assessment tool. <https://swat.tamu.edu/> (8/1, 2019).

Tague, C., 2009.Modeling hydrologic controls on denitrification: sensitivity to parameter uncertainty and landscape representation. Biogeochemistry 2009, 92: 79–90.

Takamatsu, M., Kawasaki, A., Rogers, P.P., Malakie, J.L., 2014. Development of a land-use forecast tool for future water resources assessment: case study for the Mekong River 3S sub-basins. Sustain. Sci. 9, 157–172.

Teshager, A.D., Gassman, P.W., Secchi, S., Schoof, J.T., Misgna, G., 2016. Modeling agricultural watersheds with the Soil and Water Assessment Tool (SWAT): calibration and validation with a novel procedure for spatially explicit HRUs Environ. Manag. 57 (2016), pp. 894-911.

Thayer, P.A., Miller, J.A., 1984. Petrology of lower and middle Eocene carbonate rocks, Floridan aquifer, central Florida: transactions. Gulf Coast Assoc Geol Soc 34:421–434.

Thorup-Kristensen, K., Dresboll, D.B., 2010. Incorporation time of nitrogen catch crops influences the N effect for the succeeding crop. Soil Use Manage. 26 2010, pp. 27-35.

Trang, N.T.T., Shrestha, S., Shrestha, M., Datta, A., Kawasaki, A., 2017. Evaluating the impacts of climate and land-use change on the hydrology and nutrient yield in a transboundary river basin: a case study in the 3S River Basin (Sekong, Sesan, and Srepok). Sci. Total Environ. 576, 586–598.

The Howard T. Odum Florida Springs Institute, 2020.Santa Fe River and Springs Environmental Analysis. Phase 3 – Final Report: Environmental Data.

Ullrich, A., Volk, M., 2009. Application of the Soil and Water Assessment Tool (SWAT) to predict the impact of alternative management practices on water quality and quantity. Agr. Water Manage. 96, 1207–1217.

Upchurch, S. B., Chen, J., Cain, C. R., 2007. Trends of Nitrate Concentrations in Waters of the Suwannee River Water Management District, 2007, SDII Global Corporation Project Number 3017076 Ed., Suwannee River Water Management District, Live Oak, Florida.

Upchurch, S., Chen, J., Cain, C., 2008. Springsheds of the Santa Fe River Basin. Alachua county Department of Environmental Protection, Gainesville, Fl., 93pp.

U. S. Department of Agriculture (USDA). Soil data mart. United State Department of Agriculture. Natural Resources Conservation Service (NRCS); 2005. Link: http://soildatamart.nrcs.usda.gov/Default.aspx.

U. S. Department of Agriculture – National Agricultural Statistics Service (USDA-NASS). Cropland data layer; 2011. Link: http://www.nass.usda.gov/research/Cropland/SARS1a.htm.

U.S. GEOLOGICAL SURVEY Water-Resources Investigations Report,1983, 83-4075; water resources of the Santa Fe River Basin, Florida.

Vallejo, A., Lo´pez-Valdivia, L., Cartagena, M., Tarquis, A., Herna´iz, P., 2004. Denitrification from an irrigated soil fertilized with pig slurry under Mediterranean conditions. Biol Fertil Soils 40:93–100. doi:10.1007/s00374-004-0742-6.

Van Beynena, P.E., Niedzielski, M.A., Bialkowska-Jelinskaa, E., Alsharif, K., Matusick J., 2012. Comparative study of specific groundwater vulnerability of a karst aquifer in central Florida.Appl Geogr 32:868–877.

Van Drecht, G., Bouwman, A. F., Knoop, J. M., Beusen, A. H. W. Meinardi, C. R., 2003. Global modelling of the fate of nitrogen from point and non-point sources in the soils, groundwater, and surface water. Global Biogeochemical Cycles 17: 1115.

Van Meter K., Cappellen V. P., Nandita B. Basu B. N., 2018. Legacy nitrogen may prevent achievement of water quality goals in the Gulf of Mexico, Science 360, 427–430.

Varanou, E., Gkouvatsou, E., and Mimikou, M., 2002. Quantity and quality integrated catchment modeling under climate change with use of soil and water assessment tool model. ASCE J. Hydrologic Eng. 7(3): 228-244.

Vazquez-Amabile, G.G., Engel, B.A., 2005. Use of SWAT to compute groundwater table depth and streamflow in the Muscatatuck River watershed. Transactions of the ASAE, 48 (3) 2005, pp. 991-1003.

Vendramini, J.M.B., Sollenberger, L.E., Dubeux, J.C.B., Interrante, S.M., Stewart, R.L., Arthington, J.D., 2006. Supplementation effects on forage characteristics and performance of early weaned calves grazing rye-ryegrass pastures. Crop Sci. 46:1595-1600.

Vero, E.S., Basu, B.N., Van meter, K., Richards, G.K., Mellander, P., 2017 Review: the environmental status and implications of the nitrate timelag in Europe and North America Hydrogeology Journal · August 2017.

Vesper, D.J., Loop, C.M. and White, W.B., 2001. Contaminant transport in karst aquifers. Theoretical and Applied Karstology, 13(14), pp.101-111.

Vitousek, P. M., Aber, J. D., Howarth, R. W., Likens, G. E., Matson, P. A., Schindler, D. W., Schlesinger, W. H., Tilman, D. G., 1997. Human alteration of the global nitrogen cycle: Sources and consequences. Ecological Applications, 7, 737– 750.

Wang, R., Bowling, L, C., Cherkauer, K, A., 2016. Estimation of the effects of climate variability on crop yield in the Midwest USA. Agricultural and Forest Meteorology 216 (2016) 141-156.

Wang, Y., Jiang, R., Xie, J., Zhao, Y., Yan, D., Yang, S., 2019. Soil and water assessment tool (SWAT) model: A systemic review. In: Guido-Aldana, P.A. and Mulahasan, S. (eds.), Advances in Water Resources and Exploration. Journal of Coastal Research, Special Issue No. 93, pp. 22–0. Coconut Creek (Florida), ISSN 0749-0208.

Wang, R., Luo, Y., Chen, H., Yuan, Y., Bingner, R.L., Denton, D., Locke, M., Zhang, M., 2019. Environmental fate and impact assessment of thiobencarb application in California rice fields using RICEWQ. Sci. Total Environ. 2019, 664, 669–682.

White-Leech, R., Liu, K., Sollenberger, L.E., Woodard, K.R., Interrante, S.M., 2013. Excreta deposition on grassland patches. Crop Sci. 53, 688-703.

Winchell, M., Srinivasan, R., Diluzio, M., Arnold, J., 2013. ArcSwat Interface for SWAT 2012: User's Guide. Blackland Research Center, Texas Agri Life Research.

Williams, J. R., Jones, C. A., Kiniry, J. R., and Spanel, D. A., 1989. The EPIC crop growth model. Transactions of the American Society of Agricultural Engineers, 32(2): 497-511.

Woodard, K.R., Sollenberger, L.E., Graetz, D.A., Chambliss, C.G., Scholberg, J.M., 2006. Verification of Interim BMPs for Nitrogen Fertilization of Hayfields within the Suwannee River Water Management District and Confirmation of Interim BMP for Maximum Nitrogen Fertilization of Hayfields in the Suwannee River Water Management District (Final report for the Florida Department of Agriculture and Consumer Services Projects).

Xia, Y., Mitchell, K., Cosgrove, B., Sheffield, J., Luo, L., ... Lohmann, D., 2012. Continental-scale water and energy flux analysis and validation for North American Land Data Assimilation System project phase 2 (NLDAS-2): 2. Validation of model-simulated streamflow. J. Geophys. Res. Atmos., 117(D3). https://doi.org/10.1029/2011jd016051.

Yang, J., Reichert, P., Abbaspour, K.C., Xia, J., and Yang, H., 2008. Comparing uncertainty analysis techniques for a SWAT application to the Chaohe Basin in China. J. Hydrol. 2008, doi: 10.1016/ j. jhydrol.2008.05.012.

Yang, X., Liu, Q., Fu, G., He, Y., Luo, X., Zheng, Z., 2016.Spatiotemporal patterns and source attribution of nitrogen load in a river basin with complex pollution sources. Water Res., 94 (2016), pp. 187-199.

Yang, Q., Zhang, X., Abraha, M., Del Grosso, S., Robertson, G. P., Chen, J., 2017. Enhancing the soil and water assessment tool model for simulating N_2O emissions of three agricultural systems. Ecosystem Health and Sustainability 3(2):01259.

Yen, H., Bailey, R.T., Arabi, M., Ahmadi, M., White, M.J., Arnold, J.G., 2014.The role of interior watershed processes in improving parameter estimation and performance of watershed models. J Environ Qual 43:1601–1613. doi:10.2134/jeq2013.03.0110.

Young, R.A., Onstad, C., Bosch, D., Anderson, W., 1989. Agnps: A nonpoint-source pollution model for evaluating agricultural watersheds. J. Soil Water Conserv. 1989, 44, 168–173.

Yuan, Y. and Chiang, L.C., 2015. Sensitivity analysis of SWAT nitrogen simulations with and without in-stream processes, Archives of Agronomy and Soil Science, 61:7, 969-987, DOI: 10.1080/03650340.2014.965694.

Zadsar, M., and Azimi, M., 2016. Using SWAT model to investigate the impact of rangeland management practices on the water conservation (a case study: Gorganroud watershed, Golestan, Iran). Journal of Rangeland Science, 6(4), 309– 313.

Zamora, M., Dukes, M, D., Rowland, D., Hensley, D., Graham, W., Hochmuth, B., 2018. Evaluation of water use, water quality and crop yield impacts of corn and peanut irrigation and nutrient BMPs in the spring sheds of Suwannee River Water Management District. Project Final Report FDACS Contract No. 21894.

Zamora-Re, M. I., Dukes, M. D., Hensley, D., Rowland, D., Graham, W. D., 2020. The effect of irrigation strategies and nitrogen fertilizer rates on maize growth and grain yield, accepted pending minor revisions, Irrigation Science.

Zotarelli, L., Scholberg, J. M., Dukes, M. D., Carpena, R, M., 2007. Monitoring of Nitrate Leaching in Sandy Soils: Comparison of Three Methods. J. Environ. Qual. 36:953–962 (2007).

Zotarelli L., Avila L., Scholberg J.M.S., Alves B.J.R., 2009. Benefits of vetch and rye cover crops to sweet corn under no-tillage, Agron. J. 101, 252–260.

Zotarelli, L., Rens, C. Barrett., Cantliffe, D. J., Dukes, M. D., Clark, M., Lands. S., 2013. Subsurface Drip Irrigation (SDI) for Enhanced Water Distribution: SDI—Seepage Hybrid System. HS1217. Gainesville: University of Florida Institute of Food and Agricultural Sciences. http://edis.ifas. ufl.edu/hs1217.

Zhang, Y., Hou, J., Gu, J., Huang, C., Li, X., 2017. SWAT-based hydrological data assimilation system (SWAT-HDAS): Description and case application to river basin-scale hydrological predictions. Journal of Advances in Modeling Earth Systems, 9, 2863–2882.

Zhang, X., Li Ren., and Kong, X., 2016.Estimating spatiotemporal variability and sustainability of shallow groundwater in a well-irrigated plain of the Haihe River basin using SWAT model. Journal of Hydrology 541 (2016) 1221–1240.

BIOGRAPHICAL SKETCH

Sagarika Rath was born and grew up in the city of Bhubaneswar, Odisha, India. She earned a Bachelor of Technology in agricultural engineering from the Odisha Agricultural Institute – Deemed University in 2006 and a master's degree in water resource engineering from Indian Institute of Technology Kharagpur, India in 2008. She has seven years of experience in various water consultancy sector. She joined the University of Florida in August 2016 and received a Doctor of Philosophy in August 2021.